OTS: 60-41,689

JPRS: 5942

28 October 1960

RELIEF MAP OF THE EDGE OF THE MOON ON A GENERAL ZERO REFERENCE LEVEL

By A. A. Nefed'yev

- USSR -

Distributed by:

OFFICE OF TECHNICAL SERVICES
U. S. DEPARTMENT OF COMMERCE
WASHINGTON 25, D. C.

Price: ~~$4.00~~

U. S. JOINT PUBLICATIONS RESEARCH SERVICE
205 EAST 42nd STREET, SUITE 300
NEW YORK 17, N. Y.

OSO: 4812-N

RELIEF MAP OF THE EDGE OF THE MOON ON A GENERAL ZERO REFERENCE LEVEL

News of the Astronomic Engel'gardt Observatory of the Kazan' Order of Red Labor Banner State University imeni V. I. Ul'yanov-Lenin, No 30

/Following is the complete translation of the book by A. A. Nefed'yev entitled "Karty rel'yefa krayevoy zony luny na obshchem zalevom urovne" (English version above), Publication of the Kazan' University, 1958, pages 1-14./

ABSTRACT

The monograph contains an exposition of a method developed by the author for constructing the map of the moon's edge zone on a general zero-reference level.

The maps previously prepared had many substantial shortcomings, particularly because the heights determined from them were referred to different levels.

The moon's maps were plotted by the author from the moon's observations, carried out with the Kazan' heliometer over 50 years (1895-1945) and previously processed for the purpose of deriving the constants of the moon's physical libration.

The monograph is designed for astronomers engaging in investigations of the rotation, motion, and figure of the moon, for teachers, graduate students, college students, and the wide circle of astronomers interested in this problem.

INTRODUCTION

Recently there have been published many works devoted to the investigation of the construction of the surface and of the figure of the moon. Such interest in our satellite is not accidental. The study of the moon is essential for the solution of many astronomic problems. Among these problems are included the study of the rotation of the earth relative to the motion of the moon; observation of the moon to establish systematic errors of the fundamental system of declinations; a solution of geodesic problems, for example the determination of the distances between remote points on the earth's surface, determination of corrections for the dimensions and shape of the earth, etc. To solve the foregoing problem, the moon is the most suitable celestial body, owing to its rapid motion around the earth and the maximum parallax. However, the observation of the moon is connected with many difficulties, including primarily the irregularity of its figure. The geometric figure of the moon differs noticeably from its dynamic figure, considered as a three-axis ellipsoid with the major axis directed towards the earth. In addition, the large mountains and valleys in the moon produce on its edge irregularities which frequently

reach two or three seconds of an arc and their changes, due to the optical libration, introduce systematic errors in the observations. The latter reduce considerably the accuracy of observations. Thus, visual observations of the occultation of stars by the moon are usually carried out with an error of 0.1 second in time, while the photoelectric method makes it possible to note the instant of occultation five times more accurately [94]; corresponding to these quantities will be errors in the determination of distances on earth of 150 and 30 meters. However, it is impossible to realize in practice this accuracy, and one of the principal causes of this are errors introduced in the observation by the irregularities of the moon's edge.

Allowance for irregularities of the moon's edge is also of great significance in the study of the rotation of the moon and in the improvement of the selenographic coordinates of points on the moon's surface.

A study of the moon's relief is in addition of important theoretical significance, since it produces material for judging the physical conditions on the moon both at present and in the past. One can add to it, looking into the future, that in connection with solutions to problems of cosmic navigation, it is necessary to study the moon's surface as a landing place for space ships.

This is why the problem of compilation of maps of the moon's

relief is at present particularly acute. As is well known, such maps were previously made up, but in connection with the discovery in 1934, by A. A. Yakovkin, of the dependence of the moon's radius on the optical libration in latitude, they cannot be considered accurate, since the irregularities are reckoned from different level surfaces. The problem therefore arose of constructing a map of the moon on a general zero-reference level. The difficulty in solving this problem lies in the fact that there is no water on the moon to provide a level surface, as takes place on earth. On the other hand, if the level surface is defined relative to external forms of the relief, the center of such a surface will not coincide with the center of gravity of the moon, in view of the presence of asymmetry in its figure.

As a result, we have decided to consider this difficult problem from the dynamic point of view. In the second chapter of the present book we give for the first time a theoretical solution for this problem. The leveled surface is defined by us as the surface of the level of the gravitational potential of the moon. The center of such a surface will always be the center of gravity of the moon, and irregularities in the moon's edge, defined relative to this surface, can be called barycentric irregularities.

The position of the moon's center of gravity on the celestial sphere is not fixed in any way, since we obtain from observations the position of its center of figure. The

relative placement of these points can be determined only by comparing the observations of the moon with the gravitational theory of its motion in the orbit. This problem is considered by us in detail in the third chapter.

To construct maps, we used the tremendous observation material, obtained with the heliometer of the Engel'gardt observatory over fifty years. The relief of the edge belt of the moon, 15° wide, is presented on eight charts, which are plotted in the selenographic system of coordinates proposed by Mayn. They are described in detail in the fourth chapter.

Corrections for irregularities, taken from our maps, contain the so-called "large relief." Therefore, if the observations of the moons are to be corrected for relief as determined by these maps, its average radius should not depend on the optical libration in latitude, and the correction of the latitude of the moon should reduce in absolute value. An investigation of our maps, which is expounded in the fifth chapter, is evidence that they satisfy completely these conditions. Thus, at the present time we have maps constructed for the first time against a general zero- reference level.

A construction of similar maps has as its final purpose a more accurate determination of the center of gravity of the moon than was possible until now. A correction of observations based on our maps solves this very important problem.

Chapter I

OUTLINE OF THE HISTORY OF INVESTIGATIONS OF THE RELIEF OF THE MOON AND OF ITS FIGURE

1. Determination of Altitudes on the Surface of the Moon

The first attempt at investigating the relief of the moon's surface dates back to antiquity. However, before the invention of the telescope all these investigations were purely speculative in character. Much time and labor, for example, was lost by ancient scientists to explain the overall picture of the moon's surface, visible to the unaided eye. Aristotle thought that the moon's surface is a smooth sphere, which reflects like a mirror the shadows and bright spots of seas and mountains of our earth. The Arabian mathematician of the tenth century, Al-Hazen, suggested that the visible picture of the moon is the consequence of the different reflecting ability of different parts of the moon's surface. However, even then certain scientists have made more accurate guesses regarding the visible appearance of the moon, considering that the picture seen with the unaided eye of the moon's surface depends principally on its relief. These were the view of Democritos and Plutarch.

The first reliable information onthe moon's surface were obtained by Galileo, who detected the mountains and attempted to represent them in a picture. "I-am beyond myself of amazement" he wrote soon after his discovery of the telescope" how I already succeeded in verifying that the moon represents a body similar to the earth." He subsequently engaged in a mathematical solution of the problem of determination of the height of the moon's mountains.

Among the astronomers of the 18th century, basic observations of the surface of the moon were carried out by Hewelius /1/ or Dansig, who made up detailed maps of the moon, published in 1647. He drew the moon at different phases, in order to study better the shape of the mountains and their placement. Hewelis (or Hewelke) gave the lunar formations names of terrestrial geographic places (Apennines, Caucasus, Carpathians, etc.). His contemporary Ricciolli assigned many locations names of famous persons, and later on this custom became universal. A note should also be made of the map by Cassini, which was also based in the same manner on visual estimates and has only historic interest.

In the middle of the 18th century Tobias Meyer prepared a careful map, based on many measurements, which for the first time gave the true relative placement of the moon's mountains.

The second half of the 18th century was distinguished for the construction of large reflecting telescopes, which contribute to further development of observational astronomy. Using one of

the greatest reflecting telescopes of his day, Schroter /2/ made many observations of the moon's mountains and then published his observations in 1791 — 1802, including in his work many illustrations.

In the 19th century many remarkable investigations were made of the moon's surface. It was investigated in great detail. Contributing to this was both the development of instrumental techniques, as well as the improvement of measuring methods. Galileo and Hevelius, in determining the heights of the moon's mountains, used a theoretically correct but practically unsuitable method of measurements. They waited until the first or last quarter of the moon, when the peaks of the mountains on its night side lose the last sun's rays and measured at that instant the distance from the peak to the termination, which in these phases of the moon forms a straight line. Knowing the radius of the moon, the height of the mountain can be calculated by simple trigonometry. However, firstly, it is very difficult to note the last ray incident on the peak of the mountain, and secondly, an incorrect assumption is made here, that this ray is always tangent to the mean surface of the moon. More justified is a method of measuring the shadows of lunar mountains, proposed by Ohlbers, but it does not always give satisfactory results. Knowing the length of the shadow and the height of the sun, it is possible to calculate in principle the height of

the mountain under the condition that the shadow falls on a plane surface. But actually the shadow can fall on a hill or on a valley, and therefore it is necessary to take into account the properties of the landscape, which is very difficult. In addition, if the mountain is very gently sloping (1 — 2°) on the side where the shadow is cast, then when the height of the sun is greater than or equal to 1 or 2°, the mountain produces no shadow. According to an estimate by Schmidt, the error with which the heights of the individual mountains can be determined has an order of 1/155 to 1/34 of their altitude.

Among the lunar maps produced in the past century, one should mention first the Lohrmann map /3/ made up on the principles of topographic surveying. Being an expert in the highly refined geodesic measurements and an expert draftsman, he prepared lunar maps of exceeding duty and accuracy. Lohrmann divided them into 25 parts, of which the first four were published in 1824, and the remaining were published after his death in 1919 by Schmidt. The maps contain 7,178 craters and 99 furrows.

Independent of Lohrmann, Mädler /4/ carried out highly accurate observations of the moon, on the basis of which he made up lunar charts. These were published (in four sheets) in 1836 and differ from Lohrmann's map in having a greater number of details. These maps contain 7,736 craters and 77 furrows.

In 1878 Schmidt /5/ published a lunar map divided, like

Lohrmann's, into 25sections. The scale of the map was twice as large as that of the Lohrmann and Madler maps. It was based on 32 years of observation and contained 32,856 craters and 348 furrows.

Both Madler and Schmidt determined the heights of the lunar mountains by the Ohlbers method, i.e., by measuring the shadow cast by the mountains.

The application of photography to astronomy has made it possible to extend considerably the investigations of the moon's relief, owing to the many advantages of the photographic method over visual observations.

The first work, based on the use of the photographic material, were carried out by Franz and Saunders.

Franz /6/ published in 1901 a list of positions and heights of 150 points, uniformly distributed over the earth's surface. He used five photographs of the moon, obtained near full moon on the refractor of the Lick s observatory. The positions of these third-order points were determined by Franz by correlating them to eight fundamental second-order points, the selenographic coordinates of which were determined relative to the crater Moesting A by means of heliometric measurements /7/. On the other hand, the position of the crater Moesting-A (first-order points) were obtained by Franz from libration observations of the moon /8/. He later on considerably extended his original list, publishing

two similar papers, where the reference points were used the aforementioned points from first to third order. His last list /9/ contains approximately 1400 points. To determine the altitudes, Franz used a stereoscopic method /6/. He compared pairwise five photographs of the moon, obtained at different optical librations. Obviously, the image of the moon visible during the time of one libration, owing to the small rotation of the moon changes during the time of the second libration. The angle of rotation equals the difference between librations. At such a rotation, any point on the moon's surface, for example, any crater, will shift the stronger, the higher it is located, and the farther it is from the moon's center of gravity. This stereoscopic effect can be best measured in the center of the moon's disk, and becomes little noticeable on its edges. On the basis of measuring this effect, it is possible to construct a system of calculations, which gives the heights of the craters above the moon's mean level. Using the heights to determined, Franz constructed a map of the lunar relief and reached the conclusion that the mountainous locations and the locations abundant in craters lie relatively high above the mean level, and the so-called seas are low. He also determined the elongation of the moon towards the earth's direction, which, according to his calculations, amounts to only 1/1000 of the moon's radius, i.e., considerably less than the value obtained by earlier investigators.

Between 1903 and 1911 Saunders /10/ carried out an investiga-

tion of great importance for precision selenography. He determined the positions of almost 2900 objects on the moon's surface relative to the fundamental points of Franz, using photographs obtained at the Lick and Paris observatories.

Speaking of selenographic works performed on the basis of photographic material, we mention also the list of 433 points, published in 1949 by Roth /11/ who used photographs of the moon obtained in 1926 by a graph with the nine inch refractor in Bergedorf. The correlation of the points of this list was carried out by Roth also to the Franz points.

Thus, by now there exists an aggregate of about 4500 points, measured on the moon's disk. Their coordinates are determined in general with accuracy sufficient to serve as reference points for the compilation of a detailed map. All these measurements, however, are burdened with great individual and systematic errors, since they are based on the assumption that the moon is a sphere and they are based on heliometric measurements of nine first and second order points, inaccurately reduced by Franz. At the same time, the third-order points were connected to the latter insufficiently well.

In 1956, Schrutka-Rechtenstamm /89/ again reduced the positions of eight lunar craters earlier determined by Franz /6/, and also recalculated the coordinates of four craters, calculated by Hayn /20/. For this purpose he used the constants

of the physical libration of the moon /68/, determined by him from a reprocessing of the moon's heliometric observations, carried out in Kazan' and in Bamberg (Germany).

Schrutka-Rechtenstamm assumed the following values for the constants

$$I = 1°31'52'' \pm 7''$$
$$f = 0.625 \pm 0.007.$$

The positions of the craters were reduced again by Schrutka-Rechtenstamm to the center of the moon's disk, and not to the center of gravity. He notes that it is most advantageous and most correct to refer the coordinates of the moon's objects to the center of gravity, but in his opinion this problem is not so easy to solve.

As to the determinations of the heights on the moon, then, in Hopmann's evaluation, the only ones worthy of attention at the present time are the measurements of Franz and Ritter. We described the Franz method above. Let us stop now to describe the Ritter method and the results of his investigations of the moon's surface.

In 1934 Ritter /12/ published a paper, in which he attempts to approach the solution of the problem of determining the moon's relief by using the difference in the positions of the observed and theoretical boundary of the shadow. To draw the horizontal lines on the moon, he observed the passage of the terminator through the local elevations and depressions. After determining their positions by connection to the points with

known coordinates, Ritter obtained the observed coordinates ξ_{ob} and η_{ob} of the boundary of the light. Then, using the lunar ephemerides, he calculated the theoretical position of the terminator, i.e., he obtained ξ_c and η_c, assuming the figure of the moon to be a sphere. The height of a point above the sphere was calculated by him from the formula

$$H = \frac{1}{\zeta}\sqrt{\xi^2}(\xi_a - \xi_c). \qquad (1.01)$$

It is easy to see that unlike the Franz method, this method determines more accurately the heights on the edge of the moon and less accurately in the center. Having the values of H, determined from formula (1.01), Ritter then drew a map of isohypses and traced the profiles of the moon's surface. During 70 nights he determined the coordinates of approximately 2,000 points on the moon. The deviations of individual places on the moon's surface from the sphere, according to Ritter's determinations, reach from + 17 to - 14 km, i.e., have twice the value of the heights as measured by Medler, Schmidt, and also as given in Hayn's maps. According to Ritter's maps one can conclude the following regarding the shape of the moon's relief. The south-western region of the moon's surface lies completely above the mean level (sphere) whereas the north-east part is completely below it. In the north-west quarter of the moon's surface the negative deviations predominate. Ritter's data, however, are at the limit of accuracy of his measurements.

The mean error of one value of the altitude amounts in his case to approximately ± 3 km. In addition, his method has many important shortcomings, a basic criticism of which was made, in particular, by A.A. Yakovkin and I. V.Bel'kovich /13/. They indicated that the geometric considerations on which this method is based cannot be considered correct. Actually, the position of the line of the terminator on the moon's surface depends not only on the height of the point located on the terminator, but also on the angle of inclination of the surface element containing this point to the horizontal plane passing through it, or, in other words, on the angle between the normal to the surface of the moon and the radius vector. This angle is zero only when the terminator passes through the peak of the elevation. A calculation made by A. A. Yakovkin and I.V.Bel'kovich indicates that when determining the heights by the Ritter method it is necessary to take into account the inclination of the surface element to the vertical, something Ritter did not do.

It must also be noted that when $\xi = 0$, i.e., in the first and last quarter, formula (101) becomes inapplicable for the calculation of heights.

In a large paper, published in 1952, Hopmann /14/, gave a critical survey of previously performed investigations of the moon's surface. It was noted above that the coordinates of the points of the moon's surface are based on obsolescent data regarding the moon's rotation and an old and not quite complete

theory of its physical libration. Using the constants of the physical libration of the moon, determined by Heyn and serving as a basis for the calculation of physical ephemerides of the moon, Hopmann again reduced the measurements of the positions of 150 points by Franz and calculated the absolute heights of these points above the average level. For this purpose he used the simplified but sufficiently accurate method of Pickering /15/. Let z be the libration in longitude or latitude for an individual plate, z_0 its mean value, derived from five plates; λ_0 and β_0 are the selenographic coordinates of the points obtained by Franz /6/, and x_i the difference in the values of the longitude or latitude for individual plates of relative to their mean, expressed in minutes of the arc. Then the absolute height of the points above the moon's sphere can be obtained from the formula

$$H_i = \frac{x_i}{\cos(\lambda - z_i)\,[\operatorname{tg}(\lambda - z_i) - \operatorname{tg}\lambda]}, \tag{102}$$

where $z_i = z - z_0$, $\lambda = \lambda_0 - z_0$.

An analogous formula will hold also for the latitude β. Thus, Hopmann obtained for each point ten values of H_i and then, taking the average of these, H, he calculated the corrections to the longitudes of Franz's points using the formula

$$\Delta\lambda = H \operatorname{tg}(\lambda - z_i) \tag{1.03}$$

and exactly the same way the corrections for the latitude β.

After a second processing of Franz's measurements, the average error of one value of the altitude, as an average of ten individual values, was found to be ± 2.7 km, of the same order as obtained by Ritter.

From a comparison of the heights of Franz's points with those obtained from Ritter's map, Hopmann derived a correlation coefficient, from the magnitude of which he concluded that the heights do not differ noticeably from each other.

In spite of the fact that the accuracy of the determination of the heights was low, Hopmann made an attempt to calculate the moon's figure. Assuming that the surface of the moon facing us represents an arbitrarily oriented three-axis ellipsoid, he writes the equation of the latter in the form

$$a\xi^3 + b\xi\eta + c\xi\zeta + d\eta^2 + l\eta\zeta + f\zeta^2 = H, \qquad (1.04)$$

where ξ, η, and ζ are the rectangular coordinates of the points, and H are their heights. Using Ritter's observations, Hopmann obtained for the three axes a, b, and c the following deviations from the sphere, + 8.8 km, + 1.1 km, and - 4.7 km respectively. Putting in (1.04) $\xi = 0$, he derived from the same observations the following equation for the edge of the moon,

$$\pm 576 \qquad \pm 1272 \qquad \pm 928 \qquad (1.05)$$

Hopmann concludes from this that the edge of the moon is a circle, accurate to 1:5,000. Assuming this to be true, he obtained the elongation of the moon towards the earth to be 7.3 km. Unlike the generally accepted opinion, it follows from Ritter's measurements that the moon's seas and continents are on the same level.

On the basis of the measurements by Franz and Ritter, Hopmann determined also the coordinates of the direction of the major axis of the moon's ellipsoid. It was found that the major axis deviates greatly from the direction from the moon to the earth. Starting with this, he reached the conclusion that in the south-west part of the surface facing us, there is a convexity, which can be considered as the consequence of a three-axis ellipsoid which is inclined relative to the earth. If it is assumed that on the rear end of the moon there may not be such a convexity, one cannot require that the moon's center of gravity coincides with the center of its figure, which actually does not take place.

Hopmann obtained for the relations of the principal moments of inertia of the moon, from Ritter's measurements, the following values

$$\frac{C-A}{C} = 0.00770, \qquad \frac{C-B}{C} = 0.00330, \qquad f = 0.43. \tag{1.06}$$

At the same time, the theory of tides gives respectively

$$0.0000375, \qquad 0.0000094, \qquad 0.25,$$

which is in clear contradiction with the foregoing figures. On this

basis, Hopmann assumes that the hypothesis that the moon has broken away from the earth is inconsistent, and the moon has more likely been created independently of the earth. As to the irregularities in the moon's figure, the oblateness of its half facing the earth, it must be borne in mind that as the mass of a body is reduced, its deviation from spherical form becomes more noticeable than in a heavy body.

To judge the morphology of the moon's surface, Hopmann and Herman carried out in 1950 measurements of the heights and depths of the craters. A total of about 600 observations were made. The latter consisted of a thorough measurement, in tenths of a crater diameter, of the internal and external shadows from the annular banks, when the object was located near the terminator. Knowing the time of observation and the coordinates of the crater from almanach data of the physical observations of the moon, it was possible to obtain the zenith distance of the sun for the corresponding position of the moon, and then to calculate from the diameter of the crater and the measured length of the shadow the height. The depths of the craters were obtained accurate to ± 0.3 — ± 0.5 km, the heights of the banks were accurate to ± 0.2 — ± 0.3 km. The statistical reduction of the data is evidence that the height of the banks is independent of the diameter of the crater.

From an examination of the maps of the moon's relief, prepared by Mayn and Ritter, Hopmann concludes that the annular shapes

on the moon are insignificant formations. More characteristics are the formations consisting of extensive nests, and also constant wave-like projections. Fifty percent of such formations have an angle of repose of 3° and only in individual regions does it reach 25°. Approximately 3% of the flat localities lie on a hilly landscape.

In 1949 there was published an interesting work by A. V. Khabakov /10/, who considered with great detail and thoroughness the construction of the moon's surface in the geographic aspect. In his research he noted that a study of the morphological features of the moon's relief makes it possible to prove the connection or lack of connection between its forms, and also disclose that these were developed in definite stages, thus casting light on the problem of the endogenous or exogenous origin of the moon's mountains. In Khabakov's opinion, the moon's relief was produced essentially as a result of volcanogenic processes, which were the consequence of an internal multi-phase and prolonged evolution of the physical state of the inside of our satellite.

To conclude this section, we note the work by Schrutka-Rekhtenstamm /17/, published in 1954. In it he publishes a catalog of the measured heights of the moon's mountains. Schrutka-Rekhtenstamm determined them by the Olbers method, i.e., by measuring the length of the shadow cast by the mountain -- a method employed, as is well known, a hundred years ago by Madler

and Schmidt. However, unlike these, he carried out his measurement not visually, but by photography. Schrutka-Rechtenstamm used six maps of the Paris photographic moon atlas /18/, obtained at different phases and librations in latitude. He furthermore chose those reproduced maps, three on which the moon was photographed before full moon, and three after full moon. The libration data were calculated on the basis of Heyn's theory. On each map a total of 16 to 22 points was chosen, for which the exact coordinates were known. Knowing the latter, it was possible to calculate the coordinates of the points relative to the line of the moon's horns and from these the altitude of the sun $h_\odot$. The length of the shadow of a mountain on the map was measured by Schrutka-Rechtenstamm by means of a triangle scale, one side of which was directed along the shadow and perpendicular to the line of the horns, fixed by a rule. Having obtained the length of the shadow in this manner, expressed in parts of the lunar radius, he then obtained the relative heights of the mountains, using the formula

$$H = \frac{a \sin h_\odot}{\sin M} - 2 \sin^2 \frac{i}{2}, \tag{1.07}$$

where

$$\sin \gamma = \frac{a \sin h_\odot}{\sin M} \tag{1.08}$$

and γ is the length of the shadow, measured from the center of the moon. Schrutka-Rechtenstamm determined the heights of a total

of 121-objects. He measured the shadow accurate to 1 mm, corresponding to 300 meters at a lunar diameter of 2 meters on the Paris photographs. Such an accuracy, however, can be attained only if the height of the sun is within $5° < h_{\odot} < 15°$. When $h_{\odot} = 20°$ the error can read 500 meters and more. When the sun is low, the shadows will be long and, falling on other objects, will appear shorter than they actually are. Shorter shadows, corresponding to higher positions of the sun, will give mountain heights subject to greater errors. In addition, as indicated by Schrutka-Rechtenstamm, such measurements are burdened with systematic errors, one source of which is irradiation. Systematic differences have been observed between the heights obtained by Schrutka-Rechtenstamm and those obtained by Schmidt. In order to verify these discrepancies between visual and photographic measurements, Hopmann carried out over ten evenings a series of measurements of the lengths of the shadows, visually with a 27 inch refractor. Comparison of these measurements with the data of Schrutka-Rechtenstamm have shown that the heights measured visually are always less than photographic ones and amount to three quarters of the latter.

This is the situation with the determination of the heights over the entire moon's surface. We see that the measurements are burdened with large individual and systematic errors, and the number of points with known heights is quite insufficient to trace a

detailed topographic map of the moon's surface.

2. Maps and Profiles of the Relief of the Edge Zone of the Moon.

The determination of the positions of the points on the moon's surface, and consequently their heights, the measurements of the moon's coordinates, and also a study of its rotation and of its figure are connected in one manner or another with the observation of the moon's edge. The latter however, is not an exact circle, and its irregularities are quite evident to any observer and vary with the libration of the moon. Their magnitude sometimes reaches more than two seconds of an arc. It is therefore quite obvious that in all observations of the moon, connected with its edge, the errors due to the irregularities of the moon's edge must be taken into account.

The first maps of the relief of the edge zone of the moon were constructed at the beginning of the present century by the German astronomer Hayn. In order to investigate the physical libration of the moon, he used the refractor of the Leipzig observatory for micrometric measurements of the differences of the direct ascensions and declinations between the crater Moesting-A and four other craters, and also connected micrometrically Moesting A with the northern, southern, western and eastern edges of the moon. To obtain corrections for irregularities of the moon's

edge, Hayn /19/ carried out in 1903 special micrometric measurements of the distances between Moesting A and the edge of the moon. Knowing the apparent direct ascent α and declination δ of the moon, and also α_1 and δ_1 of the crater Moesting-A, he compiled trial equations of the form

$$s - s' = dR' - \cos\delta \sin\pi \cdot d(\alpha_1 - \alpha) - \cos\pi d(\delta_1 - \delta). \quad (1.09)$$

for each observation consisting of 18 points of the edge. In these equations π is the position angle of the measured distance s, and s' is the calculated value of the latter. By solving these equations by the method of least squares, the following unknowns were determined: dR' -- correction for the assumed value of the radius of the moon and the coordinates of Moesting-A -- $d(\alpha_1 - \alpha)$ and $d(\delta_1 - \delta)$ relative to the apparent center of the moon. After substituting the obtained values of the unknowns into the trial equations (1.09), the deviations v were obtained, from which dR' were calculated. The differences of those obtained were taken to be the irregularities of the edge. The latter were plotted on a graph, whose abscissas represented the position angle, and graphically smoothed out. A total 154 points was obtained. The changes in the irregularities of the edge with optical libration were established by Hayn from this material only in the position angles 180° -- 200°. After correcting the observations for irregularities in the edge, taken from this profile, he performed a second solution of Eq. (1.09) and after substituting

the obtained values of the unknowns, again obtained the deviations v'. Considering v and v' as random errors of observations, Hayn compared vv with v'v' and reached the conclusion that allowance for irregularities of the edge improves considerably the accuracy of the measurement results. While previously the mean error of one observation was ± 0,82", after correction of the measurements for irregularities of the edge it became ± 0.55".

Having convinced himself with this scanty material that the measurements of the moon must be reduced for irregularities of the edge Hayn /20/ decided in 1907 to plot maps on the basis of greater material, adding to the 1903 observations the heliometric observations of Hartwig of 1877 — 79 and his observation with the refractor, performed in 1898 — 1900. He had at his disposal a total of 500 points. The maps of the moon's edge were plotted by him in a spherical-coordinate system, the positive pole of which is the point of intersection of the first meridian of the moon with its equator; the longitude P was reckoned from the northern pole of the moon in the direction of the court of position angle, and the latitude D was reckoned positive on the side of the observer and reckoned from the equator of a given coordinate system. After calculating P and D, which are functions of the optical libration of the moon, Hayn plotted on them points on the map and drew the lines of equal levels every 0.2". The accuracy of the irregularities taken from this map were

estimated to be ± 0.3".

To test the suitability of these maps and to fill in the gaps in them, Przybyllok made use of 640 ϭcultations of stars by the moon, obtained in 1894 -- 1897 on the refractor of the Berlin Academy and processed by Battermann /21/. The latter has determined with this material the corrections to the coordinates of the moon and to its radius, and also certain terms of the inequalities of the moon's longitude. Przybyllok considered that the residual deviations, which are obtained as a result of substituting in Battermann's equations the most probable values of the unknowns, will be precisely the corrections for the edge. Knowing the position angle of the point on the disk of the moon, in which the ϭcultation took place, he calculated its selenographic coordinates P and D, and then plotted the irregularities he calculated on Hayn's map. It was found that the heights determined by Przybyllok did not supplement the map in the region of the pole, and in many places did not agree with Hayn's heights.

It must be noted, however, that the method of ϭcultation is different in principle from the heliometric method in the form as employed by Hayn. From a processing of the ϭcultation it is possible to obtain the barycentric irregularities of the moon's disk, i.e., the difference between the angle subtended by the directions to a given point of the moon's disk and to the center of gravity of the moon, from the mean value of the apparent

angular radius. By Hayn's method, on the other hand, the irregularities of the edge are calculated relative to the center of the moon's disk. But now we know that the center of gravity and the center of the moon's disk do not coincide.

After becoming convinced that the available material on occultation of stars by the moon does not improve essentially the Hayn map, Przybyllok /22/ decided in 1908 to obtain his own tables for the corrections of the edge. For this purpose, in addition to Battermann's observations, he used 288 heliometric observations of Hartwig and 267 observations of Hayn. After eliminating the unreliable observational material, he had at his disposal 1032 observations of occultations of the star by the moon and heliometric observations. The results of the calculations of the irregularities of the edge were represented by Przybyllok both in the form of tables and in the form of maps. He notes that the overall picture of the moon's relief obtained by him is in satisfactory agreement with the one presented by Hayn's maps, but to draw a detailed profile of the moon there is not enough material. Nevertheless, the consideration of the corrections to the edge, obtained from these maps, gives a noticeable improvement in observation accuracy. Thus, while previously Battermann obtained an average error of one observation of occultation of stars of ± 1.20", after introduction of the corrections the error is reduced to ± 0.80".

The method of occultation is not without faults. As was

shown by Rybka /23/, short-period fluctuations in the motion of the moon can be influence the irregularities of the edge, calculated by this method. In addition, this method does not make it possible to determine the irregularities of the edge in the polar regions of the moon, since, for quite understandable reasons, no occultations of the stars are observed there at all.

In 1939 K. K. Dubrovskiy /24/ again raised the question of using observations of occultation of stars by the moon to calculate irregularities of the moon's profile. However, after Przybyllok's work nobody engaged seriously in application of the occultation method for plotting maps of the moon's relief.

The photographic method was first used and developed for the study of the moon's profile by Hayn /25/. He indicates in one of his works /26/ that he was forced to turn to photography of the moon because he did not have at his disposal either heliometric observations or observations of occultations in an amount sufficient to plot more or less complete maps of the relief. Incidentally, the method of occultation was considered by him in general unsuitable for this purpose. Hayn saw in photography that advantage, that on each plate with a picture of the moon it is possible to measure a large number of heights and the reduction of photographic observations is much simpler than, for example, the reduction of heliometric ones.

Using the refractor of the Leipzig observatory, Hayn obtained

in fifty nights from 1908 through 1912 a total of 100 photographs. On each of these, measuring 6 x 9 cm, there were two pictures of the moon, and also pictures of the stars to orient the plate. The diameter of the moon on the plate amounted to 3 cm. The processing of the photographs consisted of placing near the center of each image of the moon, with the aid of a sharp needle, a marker M, from which the distances Δ to the points on the moon's edge and their position angles π were measured with the aid of a Hopfer coordinate-measuring machine. He then made up trial equations of the form

$$\Delta - R_0 = dR_0 + e\cos\varphi\cos\pi + e\sin\varphi\sin\pi, \qquad (1.10)$$

and after solving these by the method of least squares obtained the coordinates of the centers s of a certain most probable circle, which fits best the point of the moon's edge, and the correction dR_0 to the tentatively assumed value of the radius R_0. Here φ is the position angle of the distance sM = e. Usually Hayn measured on each photograph 45 radii and by equalizing them with the aid of formula (1.10) he obtained a level surface, whose radius was $R_0 + dR_0$. The difference between this and the measured radii was assumed to be the irregularities of the edge. In this way Hayn obtained the heights of 1500 points of the edge.

To investigate the effect of the photographic irradiation, Hayn carried out photometry of the moon's edge. He established that irradiation distorts the measured heights by not more than 0.1". Since this value lies within the accuracy limits of the

measurements of the heights, he disregarded it. Hayn noted that when photographing the moon it is necessary to choose such exposures, at which the bright parts of the moon's surface do not have too large a density, and then it is possible to neglect in most cases the corrections for photographic irradiation.

Having the measured heights, and also their selenographic coordinates P and D, Hayn traced the isohypses every 0.2". The plotting of equal height lines was found to be not an easy task. It was necessary first to establish which measured heights were the most reliable. It was then necessary to visualize the perspective displacement of the mountain in the direction of the line of vision. The isohypses were drawn in such a way that were the observer to be located in the direction of the coordinate axis, they would correspond to the true picture of the relief only in this direction. The great difficulty in the construction of the map was also the fact that the measured points were distributed in the investigated edge zone of the moon very irregularly, in some places they were quite dense, and in the others, to the contrary, there were many gaps. It was particularly difficult to trace the isohypses in mountainous locations, where the number of points was quite insufficient. Hayn remarks that although the observations continued for four years, this time was not enough to obtain photographs under all desirable librations. It was particularly difficult to photography the regions located near the moon's poles. Therefore the regions on the

maps between 175 and 182° and between 359 and 7° in longitude have great gaps.

A very important question is that of the accuracy of the corrections taken from the maps. Each radius of the moon was measured by Hayn twice, and it was therefore possible to calculate its measurement error, which was found to be ± 0.15". Having next the differences between the observed heights and the heights taken from the maps for points with known selenographic coordinates, Hayn calculated the mean error, which we shall call the "smoothing" error. Its value amounted to on the average ± 0.29". It is then obvious that the corrections for the relief, taken from the maps, will have an error of ± 0.25". This is the mean error. In mountainous regions, where it was difficult to draw the isohypses, it will be greater, while in places with gentler topography, its value will be less.

The main purpose that guided Hayn in the construction of the map was to increase the accuracy of the determination of the center of the moon. In the observations of the moon's physical libration by the Bessel method, with a heliometer, one usually measures the distances from the Moesting-A crater to seven points of the edge. The position of the center of the moon, obtained on the basis of these measurements without allowance for the corrections for the irregularities of the edge may be in error by more than one second. If we connect Moesting-A to 18 points, then the

center of the moon could deviate from its true position by one-half second. With 40 measured points of the moon edge, the error in the position of the moon would be one quarter second, whereas with allowance for the irregularities of the edge it is reduced to one eighth of a second. These examples show how important it is to take into consideration the errors of the moon's edge, particularly when one measures a small number of points on the edge. It must also be noted that by introducing corrections for the moon's relief, we get rid of considerable systematic errors, which frequently reach 2".

The weak point in his method was considered by Kayn to be the introduction of a marker near the center of the disk, from which the distances were measured to the moon's edge. But the most important shortcoming of these maps was that the individual photographs of the moon were not interrelated. The point is that in 1934 A. A. Yakovkin has established a dependence of the apparent radius of the moon on the optical libration in latitude. Therefore the centers of the most probable circles, determined from different photographs, will not coincide with each other. Thus, the irregularities taken in different places on the maps, will pertain to different leveled surfaces. Consequently, Kayn's map contained systematic errors and therefore the task he undertook, of more accurate determination of the center of the moon, was not reached in final analysis.

Kayn published his maps in 1914. Forty years later, in 1954,

The French astronomer Weimer /27/ used photographs of the moon, obtained by Loewy and Puiseux in the time from 1894 through 1909 on the large refractor of the Paris observatory, in order to carry out a detailed description of the edge of our satellite. From among the 6,000 photographs obtained by Loewy and Puiseux, only two to 3,000 were retained in the glass library of the observatory, while the others were destroyed by the authors at the very beginning as being of poor quality. The focal distance of the instrument was 18 meters, and therefore the focal image of the moon amounted to 17 cm. Weimer notes that on these photographs of the moon one can see irregularities of the edge even with the unaided eye.

There was no sense of using for this purpose all the photographs that Weimer had at his disposal, if for no other reason than many of them were obtained under the same librations. He therefore decided to trace the profiles of the moon's edge for complete and even librations in longitude and latitude, subject to the condition that the difference in libration between two succeeding photographs was 2°. To satisfy this condition it was necessary to have approximately 150 photographs. Weimer assumes that the interval of 2° he chose between neighboring librations is sufficiently small to have two successive profiles admit of the possibility of interpolating the heights for intermediate values of the librations. He reinforces his criterion by means of the following theoretical arguments.

The height of a mountain HA' on the visible contour of the moon can be calculated from the formula

$$HH' = \frac{r \sin^2 \hat{L}}{2}, \qquad (1.11)$$

where r is the radius of the moon and $\hat{L}$ is the angle made up by this radius, drawn perpendicular to the line of vision, and drawn to the peak of the mountain (see Fig. 1).

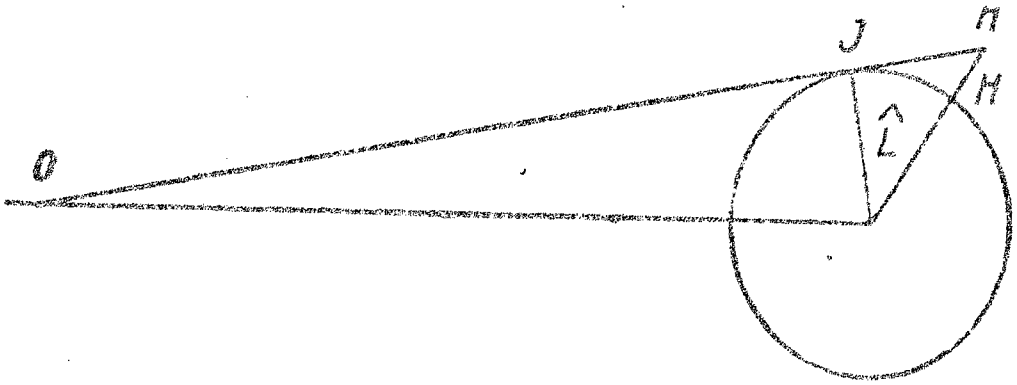

Fig. 1.

Usually the height of the mountains on the moon does not exceed 9 km, and therefore their shift over the moon's surface in the direction of the line of vision, OI, at which they still can still influence the form of the moon's profile, reaches 100 km, or in other words, the maximum value of the angle $\hat{L}$ will not exceed 6°. Let us imagine that the plane of Fig. 1 is the plane of the moon's equator, and then obviously the change in the libration and longitude will exactly correspond to the change in the angle $\hat{L}$. Calculations show that if the libration in longitude is changed by 2°, this will cause a shift in the visible contour over the spherical

surface of the moon by 60 km, and the true height of the mountain will be reduced by 1 km. Consequently, irregularities of the edge up to 1 km in altitude, as shown in one profile, may be lacking on the other profile. This may cause an error in the interpolation of the relief for intermediate librations.

As a consequence of the change in the mean parallax of the moon, the shift of its visible contour reaches in general not more than 2 km, which does not exert a noticeable influence on the true form of the contour.

Changes in the libration may, in addition, cause changes in the relative positions of two objects. The position angle of the mountain can be determined from the formula

$$\operatorname{tg} \Pi = -\operatorname{tg} \lambda \operatorname{cosec} b_0, \qquad (1.12)$$

where λ is the selenographic longitude of the mountain and b_0 is the libration in latitude. A change in λ and b_0 by 6° causes a change in the position angle by 0.6°. Let us assume that these mountains are visible in the apparent contour for all librations, and are located on the moon's equator. Then obviously two mountains may be projected one behind the other under some librations, and they may be seen separately under others, and their position angles may differ by up to 1°. In order to have this effect hardly noticeable in the interpolation of the height, Weimer, as already mentioned, permits the difference between librations of individual profiles to be not greater than 2°. In this

case the position angle of a mountain, shifted over the moon's surface beyond the visible contour by 180 km, changes by a maximum of 0.2°.

To determine the radius of the moon and the coordinates of the center of the moon's disk, Weimer used Hayn's method. On a photograph of the moon near its center, a marker M was placed, from which from 40 to 45 distances Δ were measured to the points of the moon's edges as well as their position angles θ', after which the coordinates of the center of the most probable circle z and its radius R were determined by solving by the method of least squares the trial equations of the form

$$\Delta - R_0 = dR_0 + e\cos\varphi\cos\theta' + e\sin\varphi\sin\theta', \qquad (1.13)$$

where φ is the position angle of the distance zM = e. The most probable circle so determined is called by Weimer the "relative circle." His relative circles, from which he measures the irregularities of the edge, lie on the same sphere. To confirm his conclusions, he refers to the work by Chevalier /28/ and Puiseux /29/, who, when studying the form of the moon's disk, using photographs of the moon, noted that the great irregularities of the edge have a character of continuous formations at large changes in the libration. They explained this by assuming that the mountains and valleys stretch out over several degrees in longitude and therefore they are visible at different librations always in the edge zone. For this reason the concentric

circles, in Weimer's opinion, should not differ greatly from each other. In these discussions Weimer does not consider the existing asymmetry of the moon's disk and consequently his conclusion is incorrect. In addition, he solved Eqs. (1.13) in four versions for one photograph selected by him, using a different numbered points of the edge and covering one half or one quarter of the arc of the moon's countour. Weimer attempts to prove in this manner that the radii and the coordinates of the true center, determined in different versions, will not differ greatly from each other. It appears to us that his optimistic conclusions, on the basis of data that the moon can be considered a sphere, are quite problematic if for no other reason than that they are based on the measurement of only one photograph. In addition, it does not give the average errors of the obtained values of the radii and coordinates of the center, and it is therefore difficult to judge the reliability with which they have been determined. It is known that when the points cover a short arc on the moon's edge, the unknowns of the solution of Eqs. (1.13) are determined with a small weight.

Attempting to prove furthermore that the relative circles of the western and eastern half of the moon do not differ from each other, Weimer compared his moon's profile with the profile obtained by Graff /30/ during the time of the solar eclipse, and the profile drawn by Chevalier /31/ from observations of the moon's eclipse. From such a comparison Weimer concluded that the

principal heights and depressions in these profiles are in satisfactory agreement with each other. Here again in our opinion the material was too small to be able to draw any decisive conclusions.

For the sake of orientation of the photographs, Weimer used 24 craters with exactly known selenographic coordinates. Knowing the latter, and also the libration in longitude and latitude, it is possible to calculate the position angle of the crater relative to the central meridian of the moon, and consequently to orient in the necessary the plates in order to measure the position angles of the points of the moon's edge.

Assuming furthermore that the shape of the moon is an ellipsoid of rotation, Weimer determined its elongation along the direction towards the earth, using for this purpose 72 craters, uniformly distributed along the moon's surface. From the calculations of Weimer, the moon is elongated by 5.8 km towards the earth. The geometric flattening of the moon, which he determined from measurements of the craters, was found to be greatly different from the dynamic flattening, obtained from heliometric observations.

After the coordinates of the true center of the moon's disk were calculated, Weimer proceeded to draw the moon's profiles. The moon's contour could be outlined by three methods: by micrometric measurements, by photoelectric registration, or by optical registration. Weimer decided to use the last method, which in his opinion was the simplest and most accurate.

The method of optical registration consisted of the following. The photographic plate was placed in the measuring apparatus in such a way that the true center of the moon's disk coincided with the center of the rotating circle. The plate was illuminated, so as to be able to see well the moon's edge. Rotating the handle of the dividing head with the left hand, he drew with the right hand on paper the moon's profile. Every 20°, markers were made on the paper tape, which then served to calibrate the abscissa axis.

In order to draw the relative circles, Weimer proceeded in the following manner. From the measured position angles he obtained on the profile those points of the moon's edge, which were used by him to determine the most probable circle. Knowing the heights with respect to this circle, he could, by measuring this height along the scale of the registering apparatus, plot on the tape a series of points which determine the relative line. It was drawn on the graph in the form of a straight line.

The irregularities in the moon's profile were drawn on graphs at a magnification of 24 times. Because of the graininess of the plates and the blurring of the moon's edge, it was possible to distinguish its details, according to Weimer's estimate, within 10 microns, which at this scale of the photograph amounted to 0.1 seconds. This quantity is (in Weimer's opinion) the accuracy of its profiles. He considers it to be . . . . . fully adequate, considering that the errors and positions of the stars reach 0.3

seconds, and the instants of occultation of the stars by the moon are noted with an accuracy not exceeding 0.1 seconds in time. It should be noted, however, that Weimer's estimate of accuracy of his profiles is, it appears to us, purely qualitative and its true value is undoubtedly lower.

The first part of Weimer's atlas /33/, which contains 72 moons profiles for the eastern edge of the moon, was published in 1952 on six large sheets measuring 0.74 by 1.02 meters. The second part of the atlas (for the western edge), which contains the same number of profiles, should be published later. In spite of the fact that Weimer had at his disposal 3,000 photographs, he could not carry out his purpose accurately, namely give the profiles for every even degree of libration in longitude and latitude. Sometimes the actual libration of the photograph deviates up to 1°. Therefore Weimer's graphs contain both ideal librations as well as actual ones, with a count of the physical libration, calculated under the hypothesis that $f = 0.60$ and $I = 1.523°$.

Unlike the Hayn maps, on which the heights are represented as functions of the selenographic coordinates P and D, in the Weimer atlas they pertain to points which are determined by the values of the position angles Π relative to the moon's axis. The positionangles are plotted in steps of 1° along the abscissa axis, and the length of 1° on the graph corresponds to 5 mm. The ordinate axis is so graduated, that the irregularities are

read in an angular measure for an observer located at the mean distance between the earth and the moon. To obtain the angular value of the irregularity of the edge, corresponding to the topocentric parallax p, it is necessary to multiply the value of the irregularity, measure the graph, by p/p_m; the horizontal-equitorial parallax of the moon, p_m, is taken to be 0.9507°.

The heights can be determined from the atlas in general by double interpolation, which undoubtedly makes its use difficult. But the principal shortcoming of Weimer's atlas is the same as that of Heyn's maps. The irregularities of the edge, taken from his graphs, pertain to different level surfaces. Irofa /32/ obtained a considerable coefficient of libration of the moon from observations, in which a correction was introduced for the irregularities of the edge after Weimar's atlas.

Starting with 1946, work was carried out at the Naval Observatory in Washington, under the leadership of Watts, on a study of the relief of the edge zone of the moon. The photographs, used for this purpose, were obtained in Washington, at the Yale-Columbia southern station, in Johannesburg, and at the Lowell observatory in Flagstaff (Arizona). The profile of the moon's edges were traced photoelectrically on a special measuring machine. From the latest communication /34/ concerning the course of the work, it is seen that only 700 photographs were used for the measurements, obtained in 400 nights. The moon's relief is proposed to

be presented in the form of maps. The transition from profiles to maps is scheduled to be concluded by July 1956.

Unfortunately, from the above communications made at different times, nothing can be said in detail regarding the procedure used to plot the maps. In particular, it is known how the main problem of the level surface was solved, something that is mentioned only very briefly in one communication /35/. Weimer, as we have already noted, refused to use photoelectric registration of the moon's edge, considering that this method cannot always reproduce its true profile, and at the same time it is quite cumbersome.

The construction of relief maps of the moon is at the present time a problem which cannot be postponed. It is essential for the solution of many problems connected with the observation of the moon. Kristenson /36/ made a qualitative estimate of the error which can arise in the determination of the instant of contact between the sun and the moon during the time of an eclipse, if one disregards the changes in the profile for different points of observation as a result of the effect of differential libration. This error amounts to 150 meters on the surface of the earth, whereas, according to the calculations of Bonsdorf, it should not exceed 35 meters.

The presently available maps give the overall picture of the moon's profile, while individual minute details of the moon's relief are smoothed out on them. In order to detail the maps

of Hayn, many authors /37/ have compared the irregularities of the moon's edge, obtained by measuring photographs of solar eclipses, with the heights taken from these maps. The discrepancies in heights reach here frequently more than one second of an arc. This is no wonder, however, if one recalls the difficulties with which one encounters in the study of the moon's microrelief.

3. Asymmetry of the Moon's Disk

At present there exists extensive observation material to be able to draw detailed maps of the moon's edge. However, its processing requires much time and labor. At the same time, it is necessary to solve correctly the problem of the level surface. The determination of the latter is connected in turn with investigations of the moon's figure. Observations of the moon indicate that its figure is asymmetrical. The deviation of the figure of the moon's disk from a circle is one of the basic sources of these contradictions found between observed and theoretical positions of the moon in the sky.

One of the first investigators of the moon's figure was Hansen /38/. He considered the moon as a three-axis ellipsoid and from the comparison of the observed positions of the moon with the calculated ones he came to the conclusion that it should be elongated towards the earth by 59 km. These conclusions, however, were refuted even before they were published by the investigations

of Wichmann /39/ on the physical libration of the moon. The elements of rotation of the latter were calculated by Wichmann from heliometric observations of the crater Moesting-A, considering that its radius vector is equal to the mean radius of the moon. Were Hansen's proposition to be correct, then the perspective displacements of the crater Moesting-A would make its observed positions different from the calculated ones by 8", something that did not occur in practice. In fact, as follows from the determination of Kopmann, Wolmer, etc., the moon is elongated towards the earth by 5 -- 7 km.

However, no matter what this elongation might be and the associated removal of the center of gravity from the center of the figure of the moon, it must not be confused with the fact that the center of gravity of the moon does not coincide with the center of its visible disk. To calculate the position of the center of gravity of the moon relative to the center of the figure, Hansen /40/ introduced two coordinates: one in the direction of the radius perpendicular to the plane of the ecliptic, and another one 90° to it. The coordinate in the plane of the ecliptic could have been calculated from observations of large perturbations of the moon's orbit, but in practice this is hardly possible. The second coordinate was determined from the difference in the observed and calculated declinations of the moon. The distance between the center of gravity and the center of the figure of the moon, which owing to libration is variable, can be represented by the following

formula /41/:

$$k_0 + k_1 \sin(l - n), \qquad (1.14)$$

where l -- longitude of the moon and n -- longitude of the ascending node of the moon's orbit on the ecliptic. Hansen, Bettermann /42/ Bakhuyzen /43/, Newcomb /44/ and others determined the distance between these points from meridional observations and observations of occultations, which, from their definitions, range from one tenth to one second of an arc. Here all the investigators agree that the center of gravity is to the north of the center of the figure. A proof of this is also the negative correction for the moon's latitude, determined from a comparison of the meridional observations and the observations of occultations with the gravitational theory of motion of our satellite. Thus, from a large series of observations of occultations, Spencer Jones /45/ found it to be equal to - 0.9 ± 0.04 seconds. Bohme /46/, from a long series of Greenwich meridian observations, found this correction to be 0.51 ± 0.03 seconds. From photographic observations of the positions of the moon, carried out by Hayn, Bohme /47/ found its value to be 0.51 ± 0.10 seconds. We see that the corrections for the latitude of the moon, obtained from different observational material, is determined with great reliability and indicates the presence of asymmetry in the moon's figure, since the calculations of the correction for the latitude are made under the assumption that the moon is a sphere.

Viewing the moon through a telescope, we can readily verify

that its contour is not a circle, but is cut up by valleys and projections. These irregularities of the moon's edge introduce systematic errors in the observations. They can have a periodic character, since because of the optical libration, the same irregularities appear on the edge of the moon after the lapse of a definite time. The literature contains many indications that the moon's observations contain the so-called "limb effect." Thus, Brouwer /48/ concludes from a discussion of meridional observations and observations of occultations, that the noticeable difference between the coefficients of the periodic terms in the moon's longitude, obtained for the eastern and western edges of the moon, is a consequence of the limb effect. The 14-month period in the declinations of the latitudes of the moon were explained by Brown /49/ by the presence of the same effect. Morgan and Pawling /50/, in comparing the Washington and the Greenwich observations of the moon with Brown's theory, have established a dependence of the remaining deviations on the optical libration. Watts et al. /51/, in researches devoted to this problem, indicate effects of similar kind.

We have already noted that in studying the rotation and motion of the moon we observe in one manner or another its edge, and the latter is identified (disregarding the minute relief) with the arc of a circle. However, since A.A. Yakovkin /41/ established the dependence of the apparent radius of the moon on the

Table 1

Series of observations	Instrument	Computer	Value of k
Schluter	Heliometer	Yakovkin	+0.090"
Hartwig (Strasbourg)	"	"	+0.06
Hartwig (Dorpat)	"	Koziel	+0.040±0.014"
Hartwig (Bamberg)	"	Nefed'yev	+0.034±0.008
Krasnov	"	"	+0.057±0.013
Mikhaylovskiy	"	Bel'kovich	+0.07 ±0.02
Barsachiovica	"	Yakovkin	+0.02 ±0.01
Yakovkin	"	"	+0.048±0.006
Bel'kovich	"	Bel'kovich	+0.035±0.009
Nefed'yev	"	Nefed'yev	+0.041±0.012
Drofa	Refractor	Drofa	+0.0115±0.027
Greenwich and Washington observers	Meridian circle	Yakovkin	+0.06
Khabibullin	Photogr. telescope	Khabibullin	+0.070±0.018

optical libration in latitude, such a representation can no longer be considered correct. This dependence was verified with a large amount of observational material. It appeared in all the meridional and micrometric measurements, in the observations of occultations, and in photographic observations of the moon. With this, it takes place both in observations in which corrections have been made for irregularities of the moon's edge, and in that case when the observations were not corrected for the moon's relief. The dependence of the radius of the moon h on the optical libration in latitude b_0 can be represented in the form

$$h = h_0 + kb_0, \qquad (1.15)$$

where k is the coefficient of libration. The agreement between the individual values of the coefficient k, determined from different measurements, is quite satisfactory. This can be illustrated by the data of the following table.

The foregoing values differ somewhat from the coefficient of libration, determined by V. K. Drofa /32/ from micrometric measurements with a double ocular on a refractor. This is apparently explained by the fact that when reducing the observations for irregularities of the edge, he did not use Heyn's map, like all other investigators, but the Weimer moon's profiles. A. D. Korotkova, a student of the Kazan' University, investigated the moon's

relief maps prepared by Przybyllok /22/. In making up this map, use was made essentially of observations of occultations of stars by the moon. The radius of the moon obtained from heliometric observations, corrected for the relief against these maps, was also found to include the libration effect. The latter, according to her calculations, was found to be 0.0228 ± 0.015 seconds. It is quite remarkable that the dependence of the radius on the optical libration in latitude appears in photographic observations just as reliably as in all others. We note only that in this case one must take into account the existing dependence of the moon's radius on the density of the negative, as was shown by I. V.Gavrillov /52/.

The table lists also the coefficient of libration, calculated by A. A. Yakovkin /53/ from meridional observations, carried out at the Greenwich observatory in 1923 — 30. The coefficient was obtained from the condition that the values of the inclination of the lunar equator to the ecliptic, derived from observations of the northern and southern edges of the moon, are not the same. The libration effect was found to be of the same magnitude as obtained by other determinations, although it was derived in an entirely different manner. This proved conclusively that the polar radius depends on the optical libration in latitude. Later on, as we shall see in the third chapter of the present work; A.A. Yakovkin showed that the libration effect depends on the variations of the southern edge of the moon only.

Thus, there are no data to raise any doubt of the presence of the libration effect. However, what is still not clear is the cause of this effect. There have been many statements made on this topic. In the opinion of T. A. Banachiewicz /48, 54/, the Yakovkin effect can be caused by the following factors. We usually measure the eastern or the western half of the moon, which apparently have elliptic forms, and as a result we obtain a different value for the radius. It is also possible that the appearance of ellipticity may be due to irregularities of the moon's edge. Actually, it is known that there are many high mountains on the southern edge of the moon.

The Polish astronomer Koziel /55/ proposes that the appearances of the libration effect are explained by the method used to process the observational material. He used, in the processing of the Dorpat series of heliometric observations made by Hartwig the Krakowian method, proposed by Banachiewicz. When this method is used for the processing, the form of the trial equations is such that one can introduce in them as unknowns the corrections to the radius of the moon, Δh, and the coefficient of libration, k, assuming that they are connected by a linear relation of the type (1.15). With such a processing, Koziel obtained from Hartwig's observations a libration coefficient of zero. He therefore concluded that by joining both edges, when the equalization of the observations gives a certain value for the radius of the moon, the

dependence of this radius on the optical libration in latitude vanishes. The Moon Comission of the International Astronomic Union has expressed a desire /48/ of verifying this and other conclusions made by Kostel through the use of more extensive material. For this purpose I undertook in 1953 a reprocessing of the heliometric observations of the moon, carried out with the Kazan' heliometer from 1938 through 1945 and previously processed by the classical method /56/, by using the Krakovian method. Through simultaneous processing of both edges of the moon are obtained the following result /57/:

$$\Delta h = -0''.15 + 0''.030\, b_0, \qquad \pm 0.04 \pm 0.006, \tag{1.16}$$

that is, the libration coefficient for this case, within the limits of its mean error, is actually zero. Later on I also carried out an exactly similar equalization of the observations, separately for the eastern and western edges of the moon, and found

for the eastern edge	for the western edge
$\Delta h = -0''.37 - 0''.025\, b_0$	$\Delta h = -0''.47 + 0''.035$
$\pm 0.08 \pm 0.011$	$\pm 0.07 + 0.007$

(1.17)

It is seen therefore that the libration term in this case is not eliminated. An analogous result was obtained also in the processing of observations by the ordinary method /56/. The selenographic coordinates of the crater Moesting-A, derived for individual edges,

were found to differ considerably from each other, namely:

for the eastern edge	for the western edge
$\lambda = -5^\circ 8' 13''$	$\lambda = -5^\circ 11' 43''$
$\beta = -3\ 11\ 16$	$\beta = -3\ 12\ 34$ (1.18)

All this indicates once more that the centers of the western and eastern half of the moon do not coincide, in view of the existing asymmetry of the moon's disk. On the other hand, when both edges are simultaneously processed, this effect becomes smoothed out. But since in observations one deals with only one edge of the moon, one cannot disregard the limb effect.

Interesting work on the study of the moon's figure was carried out by I. V. Bel'kovich. By analyzing the observations of the occultations of stars by the moon and the meridional observations, I. V. Bel'kovich /58/ reached the conclusion that the figure of the moon's limb is asymmetrical and that its change takes place, in all probability, in the region of negative librations in latitude. Later, in his large paper devoted to an investigation of the physical libration of the moon, I. V. Bel'kovich /59/, using extensive observational material obtained with the heliometer of the Engel'gardt observatory, concluded that the apparent disk of the moon is "deformed," depending on the values of the optical libration of the moon. With this, in his opinion, the radii of the eastern and western edges of the moon's disk differ from the optical libration in latitude in different ways. In determining the

libration effect for the individual edges, I. V.Bel'kovich /60/ obtained a result which is analogous to ours.

4. On the Determination of the Parameter f.

One of the central problems in the problem of investigating physical libration of the moon is the determination, from observations, of the parameter f and of the inclination I of the moon's equator to the ecliptic. The value of f is a function of the principal moments of inertia of the moon, A, B, and C, and characterizes its dynamic features. Knowing f, we can draw conclusions regarding the figure and internal construction of the moon. The moment of inertia C is the greatest and is directed along the axis of rotation of the moon, while the two others lie in the plane of the lunar equator, of which A is along an axis directed to the point of intersection of the zero meridian with the equator, and B along an axis perpendicular to the preceding one. In order for the rotation to be stable, it is obvious that it is necessary to have $A < B < C$. The value of f should range from zero to unity, it cannot be zero, nor can it be unity. In the former case we would obtain C = B, i.e., the position of the axis of rotation is indeterminate and consequently the rotation will be unstable. In the second case A = B, i.e., the moon will be an ellipsoid of revolution, and Cassini's first law is in this case impossible. We can ascertain theoretically that in the interval between zero and unity, the value of f has several

critical values, at which the first law of Cassini is also excluded. Thus, for example, when f = 0.662 the coefficient of sin 2ω (ω is the distance from the lunar perigee to the ascending node of the moon's orbit) in the expansion of the physical libration in latitude, τ, assumes an infinite value.

From the first German heliometric series of observations of the moon, Wichmann /39/ Hartwig /69/, Franz /8/, and Stratton /62/ obtained a value of the parameter f close to 0.50. After improving the theory of physical libration of the moon, Hayn /19/ in 1904 found it to be 0.85. Later, from processing his own observations with a refractor and the series of observations of Schluter and Hartwig, he obtained a value f = 0.73, which is still the starting point in the calculation of the libration of the moon.

Russian investigators applied much effort and labor to the study of the physical libration of the moon, carrying out large series of observations with a heliometer. A. A. Yakovkin /63/ obtained from the observations of T. A. Banachiewicz a value of f = 0.74, and from his old large series he obtained 0.68 /64/.

In 1948 I. V. Bal'kovich /65/ called attention to the fact that when the value of f is close to critical, the differential equations relative to df become inaccurate. In this case it is necessary to make a second approximation, which consists of the following. Specifying a series of values of f, one compiles several systems of trial equations and then, after solving them by the method

of least squares, one assumes the most probable to be that value of f, for which the sum of the squares of the deviations is the least. With such a solution we obtain two values of this parameter, lying on both sides of the critical value. Thus, I.V. Bel'kovich, by processing his own observations, found for f values of 0.60 and 0.71, while for the series of A. A. Yakovkin he obtained 0.62 and 0.71. I obtained from the heliometric observations of Krasnov and from the processing of the observations of 1938 -- 1945 values of 0.60 and 0.71. The Polish astronomer Koziel /66/, using Hartwig's observations in second approximation, computed in a different manner, obtained exactly the same values for f.

Actually, with the moon's rotation stable, there should be no such duality in the values of f, and the question thus arose of which of the two values is correct. This question was considered in detail by Sh. T. Kabibullin /67/. The question of unique determination of f was solved by him by finding a certain function of f. Such functions are the terms of the longitudinal equations for the determination of the constants of the moon's physical libration, $a_3 \sin g'$ (where g' is the mean anomoly of the sun) and $a_4 \sin 2\omega$. To determine the coefficients a_3 and a_4, Sh. T. Kabibullin used the observations carried out with the heliometer of the Engel'gardt observatory and his own series of photographic observations of the moon. After obtaining the values of the coefficients a_3 and a_4 he calculated from them the value of f and concluded that its true value is 0.60.

This problem was also solved by the Viennese astronomer Schrutka-Rechtenstamm /68/. Taking it into account that the dependence on f of the observed quantities is nonlinear, he separated in the expression for the physical libration in longitude τ the term $k \sin 2\omega$, considering k to be the sixth unknown quantity in the equations for the determination of the constants of the physical libration of the moon. Solving further the problem by the method of approximations, Schrutka-Rechtenstamm made up the difference between the sums of the squares of the deviations, corresponding to two values of f (lying on both sides of his singular point), and the possible minimum $\sum pvv$, and thus solve the problem to which of the two values of f preference should be given. After reprocessing from this point of view the observations of the moon, carried out on the heliometer of the Engel'gardt observatory, as well as Hartwig's series of observations, he, like Kabibullin, reaches the conclusion that the most probable value of this parameter is less than the critical one and is equal to 0.65.

Recently A. A. Yakovkin /95/ proposed a simple and original method of unique determination of f. He separated the largest term $a \sin g'$ in the expansion of the physical libration in longitude τ, and then, by solving by the method of least squares the equations $a \sin g' = l - l_1$, where l is the observed selenocentric longitude of the crater Moesting-A and l_1 the calculated one, he determined the coefficient a. Yakovkin used the same observational material as was

used by Khabibullin, but the value of the parameter f was found by him to be quite different, namely f = 0.69 ± 0.02.

The value of f can be determined also from other considerations. The motion of the perigee Π and of the node Ω of the moon's orbit is due to the action of the sun and the planets. This motion is also influenced by the figure of the earth and of the moon. The latter influence can be represented in the form /69/:

$$\begin{aligned} d\Pi &= +38030'' J' - 100150'' K', \\ d\Omega &= -46050 J' - 23025 K', \end{aligned} \tag{1.19}$$

where

$$J' = \frac{3}{2}\,\frac{2C - A - B}{2M' R_0^2} \quad \text{и} \quad K' = \frac{3}{2}\,\frac{B - A}{M' R_0^2}.$$

Here M' is the mass of the moon and R_0 is its radius. Comparison of the observed displacements of the perigee and the node with the theoretical ones makes it possible to determine J' and K', and then also f. Actually, putting

$$J' + \frac{1}{2} K' = L',$$

we have

$$f = \frac{L' - K'}{L'}. \tag{1.20}$$

It was precisely in this way that Spencer Jones /69/ found for f a value of 0.68. Jeffreys /70/ in 1937 found it to be 0.97, and later in his major work /71/ he obtained f = 0.84 ± 0.08.

We see that there are considerable disagreements in the value of this fundamental constant, obtained by different workers. If f is assumed to be 0.60 and the moon is considered to be a three-axis ellipsoid of homogeneous density, we obtain the following relation between the semi-axis:

$$a : b : c = 1.00062 : 1.00037 : 1. \qquad (1.21)$$

The presence of asymmetry in the figure of the moon raises great difficulties in the study of its rotation and motion. The constants heretofore obtained for the forced physical libration of the moon contain systematic errors, for in their calculation no account is taken of the libration effect in the radius of the moon. A. A. Yakovkin /72/ first derived the elements of rotation of the moon with allowance for the libration effect, which differ considerably from the earlier values. Thus, the parameter f was found to be 0.82, and the inclination I of the moon's equator to the ecliptic was increased by 88 seconds above the value used at the present time. Even greater doubt exists regarding the determination of the magnitude of the free libration of the moon. In investigating the latter, I. V. Bel'kovich /59/ and I /96/ did not obtain a reliable determination, but established fluctuations in the longitude of the crater Mösting-A with a period $\odot$ and $2\odot$. The first of these fluctuations is a consequence of the libration effect of the moon, and the second apparently must be attributed to incorrectly assumed values of f. A. A. Yakovkin /73/ after obtaining preliminary data on the calculation of

the free libration, reached the conclusion that the discrepancy in phases, as obtained by different observers, is due to incorrectly assumed period of free libration. After determining this period, he obtained a value $\gamma = (B - A)/C$, and then calculated the terms of forced libration. Excluding the latter from the observed longitudes, Yakovkin obtained the amplitude of the free libration, which was found to be $52'' \pm 10$ seconds. We believe that a final answer regarding the value of the free libration can be given only after a detailed study of the figure of the lunar disk.

Thus, the investigation of the figure of the moon is at present a very important and urgent problem, with which the mapping of the relief is directly connected with the mapping of the moon's relief relative to a general zero reference level. A theoretical solution of this problem is given in the next chapter.

Chapter II

ON THE ZERO-REFERENCE SURFACE FOR RECKONING HEIGHTS ON THE MOON

5. Formulation of the Problem

The construction of maps and profiles of the relief of the moon's surface should be based on an advantageous choice of the zero-reference surface, from which it is necessary to measure the heights of the points of the relief. To choose such a surface in an undisputed manner is not easy, both in view of the theoretical complexity of the problem and in view of the difficulties connected with the specific nature of observations of the moon. When choosing the level surface one can start with the following premises:

1) Assume the moon to be a sphere and consider deviations from this sphere as irregularities;

2) assume the irregularities of the moon's edge as deviations from an ellipsoid or some initial figure, most closely corresponding to the external appearances of the relief;

3) consider the theoretical figure of the moon corresponding to the hydrostatic equilibrium;

4) consider the deviations of the actual surface relative to the surface of the level of the potential of the moon and the perturbing

potential of the earth.

Obviously, we can consider the moon to be a sphere only in the first approximation, since both observations and theory give evidence that its figure is a three-axis ellipsoid. Thus, for example, Hopmann, using the observations of Ritter, obtained for the three semi-axis a, b, and c the following deviations from a sphere: + 8.8 km, + 1.1 km, and - 4.7 km.

Weimer calculated exactly the same way the figure of the moon from the external shapes of the relief. In analogy with the geoid, he calls this figure a selenoid, which in our opinion is incorrect, for in this case no account is taken of the distribution of the masses inside the moon, and therefore the center of this figure will not coincide with the center of gravity of the moon.

An attempt to represent the figure of the moon by starting out with the conditions of hydrostatic equilibrium of its substance was not crowned with success. The geometric compressions of a three-axis ellipsoid of the moon, calculated on the basis of the hydrostatic theory, differ very greatly from the dynamic ones, obtained from investigations of its physical libration /74/.

It is most advantageous to take as the level surface one of the level surfaces of the potential of the moon's force of gravity, in analogy with the procedure used to determine the figure of the earth. However, in the case of the moon, the gravitational field around it will be also influenced by the earth to a noticeable

degree (the effect of the sun is insignificant). Such a level surface for the moon can be called a selenoid, in analogy with the geoid. Were the moon to have a water shell, like the earth, then the free surface of the water in the lunar oceans would, in the quiet state, be the surface of a selenoid. The absence of water on the moon forces us to choose arbitrarily, within certain limits, some level surface. Thus, for example, one could take that level surface containing a volume equal to the volume of the moon. Then the following condition would hold

$$\int_S H ds = 0, \tag{2.01}$$

where H is the height of the points of the physical surface of the moon relative to the chosen selenoid, and ds is the element of the selenoid surface, over which the integration is carried out. It is obvious that, in practice, condition (2.1) cannot be realized, not only because almost half the moon's surface is inaccessible for observations, but also because on the visible side of the moon, with the exception of the edges of its disk, as noted in the first chapter, too many elevations have been determined, and not reliably at that. One can show, however, that this difficulty is of no principal significance. In fact, let the heights H' determined by us be referred to a certain level surface S'. Knowing the potential of the moon's gravity field by W, we have on the surface S

$$W = C$$

and on the surface S'

$$W = C'.$$

The distance δH of the surface S' from the surface S (see Fig.

2), reckoned along the outward normal to the latter, is

$$\delta H = \frac{C - C'}{g}. \qquad (2.02)$$

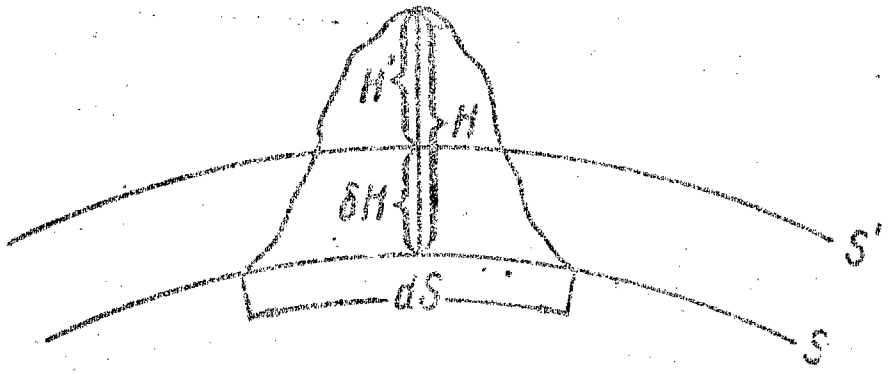

where g is the force of gravity, a quantity which is almost constant in view of the fact that the moon is close to a sphere and rotates slowly. With exactly the same accuracy, i.e., more accurate than 0.001, one can consider δ H to be constant. Since the heights on the moon do not exceed 10 km, then assuming even that δ H can reach so large a value (approximately five seconds as measured from the earth), its fluctuations do not exceed ten meters, i.e., 0.005 seconds as seen from the earth, which is quite insensitive. We obviously have

$$H = H' + \delta H \qquad (2.03)$$

and can consider δ H practically constant.

Therefore, if somehow one succeeds in determining the surface S, the change from the heights H' to the heights H involves no difficulty. For the surface S'

$$\int_{S'} H' ds' = -\Gamma, \qquad (2.04)$$

where Γ represents the excess of volume included inside S', relative to the volume of the moon, or, what is the same, as a consequence of (2.01), relative to the volume S. Comparing (2.01), (2.03) and (2.04) and neglecting quantities of second order in δH, we have

$$\int_{S'} H' ds' = \int_{S} H ds - \delta H \int_{S} ds. \tag{2.05}$$

Bearing in mind that the first integral in the right half of (2.05) vanishes, we obtain

$$\Gamma = 4\pi R_0^2 \delta H, \tag{2.06}$$

where R_0 is the mean radius of the surface S.

6. Hydrostatic Theory of the Figure of the Moon

For further conclusions we must stop to discuss the hydrostatic theory of the figure of the moon. This was developed by Jeffreys /75/ who assumes that the substance of the moon is in hydrostatic equilibrium, as proposed by Clairault in the analysis of the figure of the earth.

We choose the principal axes of inertia of the moon to be the rectangular coordinates x, y, and z. The x axis is directed here approximately towards the earth (see Fig. 3), and the z axis coincides approximately with the moon's axis of rotation. If d is the mean distance between the centers of gravity of the earth T and the moon L, and x, y, and z are the coordinates of an element of mass of the moon dm and r' its distance from the center of the earth, then

$$r' = (d - x)^2 + y^2 + z^2. \qquad (2.07)$$

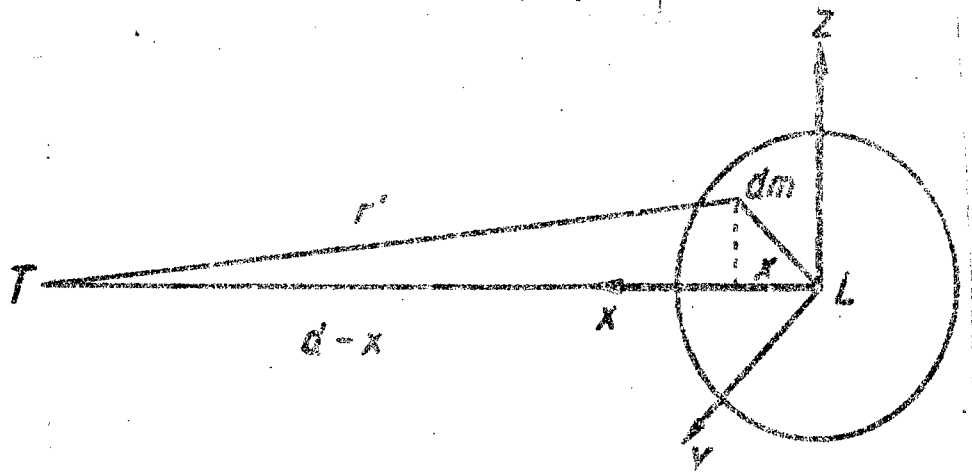

Let us calculate the gravitational potential of the earth ϕ. For this purpose we expand $1/r'$ in powers of the coordinates of the attracted point. We then have

$$\frac{1}{r'} = \frac{1}{\sqrt{(d-x)^2 + y^2 + z^2}} = \frac{1}{d}\,\frac{1}{\sqrt{1 - \frac{2x}{d} + \frac{x^2}{d^2} + \frac{y^2}{d^2} + \frac{z^2}{d^2}}}.$$

Retaining in the expansion terms up to $1/d^4$, we obtain

$$\frac{1}{r'} = \frac{1}{d} + \frac{x}{d^2} + \frac{1}{2d^3}(2x^2 - y^2 - z^2).$$

Thus, at the point with coordinates x, y, z the gravitational potential of the earth is

$$\Phi = \frac{GM}{r'} = \frac{GM}{d} + \frac{GMx}{d^2} + \frac{GM}{2d^3}(2x^2 - y^2 - z^2), \qquad (2.08)$$

where G is the gravitational constant and M is the mass of the earth.

Considering that the moon rotates about an axis perpendicular to the plane of its orbit, uniformly with an angular velocity n, equal to the velocity of its orbital motion around the

earth, we see that this rotation is carried out rigidly about the center of mass of the earth and the moon. We denote by

$$\mu = \frac{M'}{M} \tag{2.09}$$

the ratio of the masses of the moon and the earth, and obtain the distance of the center of mass of the earth-moon system from the origin, i.e., from the center of the moon L.

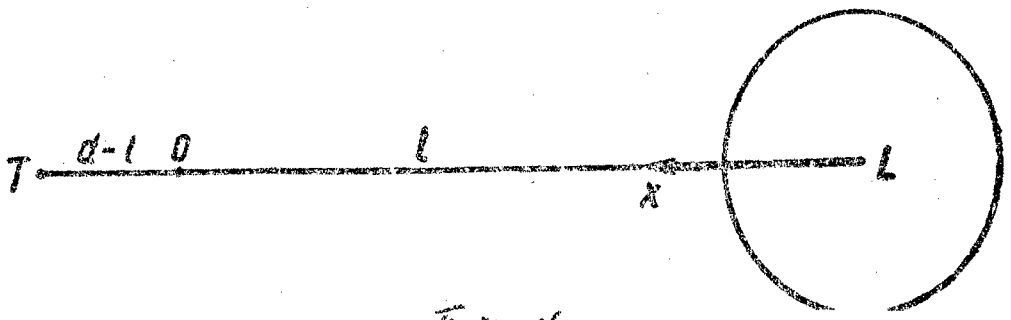

Fig. 4.

From Fig. 4 we have

$$\frac{d-l}{l} = \frac{M'}{M} = \mu,$$

Hence

$$l = \frac{d}{1+\mu}.$$

The rotation of the moon causes a centrifugal-force potential

$$\Omega = \frac{1}{2} n^2 \left[\left(\frac{d}{1+\mu} - x \right)^2 + y^2 \right]. \tag{2.10}$$

Adding it to the potential of the earth, we obtain the total potential

$$\Phi + \Omega = \frac{GM}{d} + \frac{GM\varkappa}{d^2} + \frac{GM}{2d^3}(2x^2 - y^2 - z^2) +$$

$$+ \frac{n^2x^2}{(1+\varkappa)^2} - \frac{n^2dx}{1+\varkappa} + \frac{1}{2}n^2(x^2+y^2).$$

According to Keppler's third law

$$\frac{d^3}{T^2(M+M')} = \frac{G}{4\pi^2}.$$

The angular velocity $n = 2\pi/T$, meaning

$$\frac{4\pi^2 n^3}{M+M'} = G,$$

hence

$$n^2 = \frac{G(M+M')}{d^3} = \frac{GM(1+\varkappa)}{d^3}. \qquad (2.12)$$

We now substitute (2.12) in (2.08), and consequently the terms with x cancel out and we are left with the following expression for the perturbing potential

$$\Phi + \Omega = \frac{GM}{2d^3}(3x^2 - r^2), \qquad (2.13)$$

in which we discard the insignificant terms GM/d and $n^2d^2/2(1+\varkappa)^2$. To take into account the influence of $\beta + \beta_1$ on the moon's figure, we add a term of the form $\lambda(x^2 + y^2 + z^2)$, which by virtue of its symmetry can only cause a small uniform broadening of the figure of the moon. Actually, if we take the latter to be a sphere, then the distance to the surface element on the sphere will be constant

and have a value

$$\rho^2 = x^2 + y^2 + z^2.$$

Consequently, on the sphere $\lambda (x^2 + y^2 + z^2)$ will also be constant and its addition to the potential will cause an increase in the latter by a constant quantity. But henceforth we shall consider only quantities of first order in the compression of the moon (approximately 0.001), and consequently the introduction of the aforementioned term, which appears in second-order quantities, will not influence the determination of its figure. Then expression (2.13) is written in the form

$$\Phi + Q = \frac{GM}{2a^3}(3x^2 - z^2) + \lambda(x^2 + y^2 + z^2). \tag{2.14}$$

The arbitrary factor λ can be chosen such that the entire potential is represented by a harmonic second-order function. For this purpose, obviously, it is necessary to make up the second differential parameter of the expression (2.14) and to determine the value of λ, which will be

$$\lambda = -\frac{GM}{3a^3}.$$

We then obtain

$$\Phi + Q = \frac{1}{6}\frac{GM}{a^3}(3x^2 - 2y^2 - 5z^2), \tag{2.15}$$

and for this expression the Laplace operator really vanishes.

Under the influence of this perturbing potential, the surface of

the moon experiences a deformation, which is also expressed by a harmonic function of second order. The equation of the surface of the level can be written in the form

$$r = R_0(1 + Y_2), \tag{2.16}$$

where Y_2 is a spherical Laplace function and R_0 is the average radius of the moon. In other words, it is a radius of a sphere with a volume equal to the volume of the moon. It can be assumed here that this surface is filled with a homogeneous mass (actually, the moon is almost homogeneous), and apply Laplace's theory of attraction of spheroids /76/. The external potential of the Laplace spheroid on its surface is given in our case by the formula

$$\Phi' = \frac{GM'}{r} + \frac{4\pi\rho R_0^5 Y_2}{5r^3}, \tag{2.17}$$

where ρ is the density of the spheroid (moon). Since the mass of the moon is

$$M' = \frac{4\pi\rho R_0^3}{3},$$

then

$$\Phi' = GM'\left(\frac{1}{r} + \frac{3}{5}\frac{R_0^2 Y_2}{r^3}\right) \tag{2.18}$$

In formula (2.18), which determines the force field of the moon's mass, it is enough to retain spherical functions of second order, which express the ellipticity of the moon. The deviation from ellipticity appears only in spherical functions of third order

and above, which can be determined only from certain effects (say precession) on the earth, but this cannot be done on the moon. However, even third-order terms are already very small, since they are divided by r^4. Thus, the theory of the moon's figure can be constructed up to first-order terms in the correction inclusive, which in practice is quite sufficient.

On the outer surface of the moon's level the sum of the gravitational potentials of the earth and of the moon and of the centrifugal acceleration potential should be constant,

$$\Phi + \Phi' + \Omega = \text{const.} \qquad (2.19)$$

Then on the basis of (2.15), (2.16), and (2.18), accurate to terms of first order inclusive, we have

$$\Phi + \Phi' + \Omega = GM'\left(\frac{1}{R_0} - \frac{1}{R_0}Y_2 + \frac{3}{5}\frac{Y_2}{R_0}\right) + \frac{GM}{6a^3}(7x^2 - 2y^2 - 5z^2) = \text{const}$$

or

$$-\frac{2GM'Y_2}{5R_0} + \frac{GM}{6a^3}(7x^2 - 2y^2 - 5z^2) = 0.$$

From this we determine Y_2 and, substituting in (2.16), we obtain

$$r = R_0\left(1 + \frac{5}{12}\frac{MR_0^2}{M'a^3}\frac{7x^2 - 2y^2 - 5z^2}{R_0^2}\right). \qquad (2.20)$$

Putting successively x, y, $z = R_0$, we obtain the semi-axes of the lunar spheroid, which, with the same accuracy to first order, can

be considered to be an ellipsoid

$$a = R_0\left(1 + \frac{35}{12}\,\frac{MR_0^3}{M'd^3}\right),$$

$$b = R_0\left(1 - \frac{10}{12}\,\frac{MR_0^3}{M'd^3}\right),$$

$$c = R_0\left(1 - \frac{25}{12}\,\frac{MR_0^3}{M'd^3}\right). \qquad (2.21)$$

The principal moments of inertia of a homogeneous ellipsoid are given by the following expressions

$$A = \frac{M'(b^2+c^2)}{5},$$

$$B = \frac{M'(a^2+c^2)}{5},$$

$$C = \frac{M'(a^2+b^2)}{5}.$$

2.

From these we obtain, accurate to the first order in the compression

$$\frac{C-A}{C} = \frac{a^2-c^2}{a^2+b^2} = \frac{(a-c)(a+c)}{a^2+b^2} = \frac{2a(a-c)}{2a^2} = \frac{a-c}{a} = \frac{a-c}{c}$$

and analogously

$$\frac{C-B}{C} = \frac{b-c}{c}.$$

For the moon we shall have

$$\frac{C-A}{C}=\frac{a-c}{c}=\frac{a-c}{R_0}=5\,\frac{M}{M'}\,\frac{R_0^3}{d^3}=0.0000375$$

$$\frac{C-B}{C}=\frac{b-c}{c}=\frac{b-c}{R_0}=\frac{5}{4}\,\frac{M}{M'}\,\frac{R_0^3}{d^3}=0.0000094,$$

(2.2)

where we put $M/M' = 82$, $d/R_0 = 221$. It was said earlier that these values, just as their ratio $(C - B)/(C - A) = f$, do not correspond at all to reality, this being evidence that the moon is far from being in hydrostatic equilibrium, and it does not appear as if it ever was in such an equilibrium in the past /71/.

7. Level Surface of the Moon's Gravitational Potential

It will be our problem to determine the actual gravitational field of the moon. For this purpose we again start with Eq. (2.19), in which $\Phi + \Omega$ is again borrowed from (2.15). However, for Φ', i.e., the moon's gravitational attraction potential, it is necessary to have a general expression for the external potential of a material body.

Let T be the volume of the moon and let ρ be its density. We place the origin of rectangular coordinates in the center of gravity of the moon, O. We denote by ξ, η, and ζ the coordinates of an element of volume of the moon $d\tau$ (see Fig. 5); we denote by x, y, z the coordinates of the attracted point P. We assume that r is always

greater than r'. The moon's potential on the point P is

$$\Phi' = G \int_{\tau} \frac{\rho d\tau}{\Delta} . \tag{2.24}$$

and

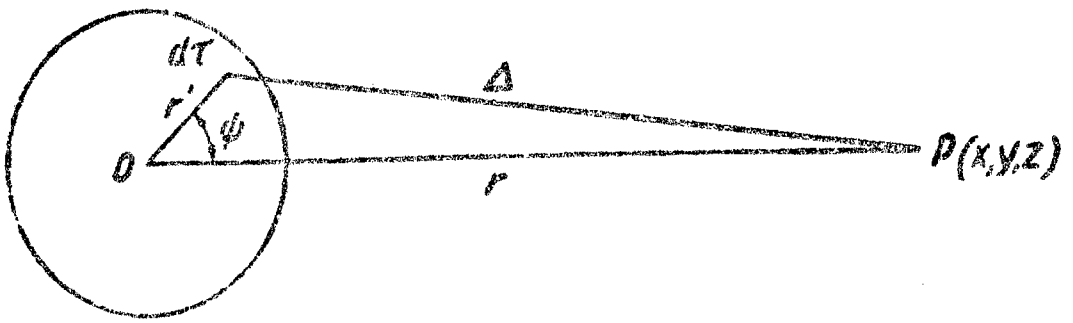

Fig. 5

We furthermore have

$$\Delta^2 = r^2 + r'^2 - 2rr' \cos\psi$$

and consequently

$$\Phi' = G \int_{\tau} \frac{\rho d\tau}{\sqrt{r^2 + r'^2 - 2rr' \cos\psi}} .$$

Let us expand $1/\Delta$ in a series. We have here

$$\frac{1}{\Delta} = \frac{1}{\sqrt{r^2 + r'^2 - 2rr' \cos\psi}} = \frac{1}{r} \frac{1}{\sqrt{1 + \left(\frac{r'}{r}\right)^2 - 2\frac{r'}{r}\cos\psi}} .$$

We employ the expansion of a point potential in Legendre polynomials $P_n(\cos\psi)$ and obtain

$$\frac{1}{\Delta} = \frac{1}{r} \sum_{n=0}^{\infty} \left(\frac{r'}{r}\right)^n P_n(\cos\psi) = \sum_{n=0}^{\infty} \frac{r'^n}{r^{n+1}} P_n(\cos\psi). \tag{2.25}$$

Next, multiplying both halves of the equation by $\varphi\, d\tau$ and integrating for the entire volume T, we obtain

$$\Psi = G\sum_{n=0}^{\infty}\frac{1}{r^{n+1}}\int_T \rho r'^n P_n(\cos\psi)\,d\tau. \tag{2.26}$$

We put

$$G\int_T \rho r'^n P_n(\cos\psi)\,d\tau = Y_n, \tag{2.27}$$

where Y_n is a second-order spherical function.

Since φ' is a harmonic function, every function Y_n will also be harmonic (since they cannot cancel each other out if they are of different order).

Then the main expansion of the potential φ' on an external point P with coordinates x, y, z will have the form

$$\Psi = \sum_{n=0}^{\infty}\frac{Y_n}{r^{n+1}}. \tag{2.28}$$

Let us find now the first coefficients Y_n, corresponding to n = 0, n = 1, and n = 2. We have the following: a) when n = 0, we obtain $P_0(\cos\psi) = 1$, and the corresponding term in φ' will be

$$\frac{G}{r}\int_T \rho P_0(\cos\psi)\,d\tau = \frac{G}{r}\int_T \rho\,d\tau = \frac{GM'}{r},$$

where M' is the moon's mass. b) when n = 1 we have $P_1(\cos\psi) = \cos\psi$, and this gives in the expansion of the potential the following terms

$$\frac{G}{r^2}\int_T \rho r' P_1(\cos\psi)\,d\tau = \frac{G}{r^2}\int_T \rho r' \cos\psi\,d\tau =$$

$$= \frac{G}{r^3}\int_T \rho(x\xi + y\eta + z\zeta)\,d\tau = \frac{Gx}{r^3}\int_T \rho\xi\,d\tau + \frac{Gy}{r^3}\int_T \rho\eta\,d\tau + \frac{Gz}{r^3}\int_T \rho\zeta\,d\tau.$$

The integrals contained here represent coordinates of the center of gravity of the body. And since the origin has been placed at the center of gravity of the moon, then

$$\int_T \rho\xi\,d\tau = \int_T \rho\eta\,d\tau = \int_T \rho\zeta\,d\tau = 0$$

and, thus, there will be no first-order terms in the expansion at all.

c) when n = 2 we have

$$\frac{G}{r^3}\int_T \rho r'^2 P_2(\cos\psi)\,d\tau = \frac{G}{r^5}\int_T \rho r^2 r'^2 P_2(\cos\psi)\,d\tau.$$

It is known that /76, p 231/

$$P_2(\cos\psi) = \frac{3}{2}\cos^2\psi - \frac{1}{2},$$

then

$$\frac{G}{r^5}\int_T \rho r^2 r'^2 P_2(\cos\psi)\,d\tau = \frac{G}{r^5}\int_T \rho\left[\frac{3}{2}(rr'\cos\psi)^2 - \frac{r^2r'^2}{2}\right]d\tau =$$

$$= \frac{G}{r^5}\int_T \rho\left[\frac{3}{2}(x\xi + y\eta + z\zeta)^2 - \frac{(x^2+y^2+z^2)(\xi^2+\eta^2+\zeta^2)}{2}\right]d\tau.$$

Taking outside the integral sign the coordinates of the attracted point, we can reduce the above expression to the following form

$$\frac{G}{r^5}\left[\left(z^2 - \frac{x^2+y^2}{2}\right)\int_T \rho\left(\zeta^2 - \frac{\xi^2+\eta^2}{2}\right)d\tau + 3yz\int_T \rho\eta\zeta\,d\tau +\right.$$

$$+ 3xz\int_\tau \rho\xi\,d\tau + 3xy\int_\tau \rho\xi\eta\,d\tau + \frac{3}{4}(x^2-y^2)\int_\tau \rho(\xi^2-\eta^2)\,d\tau\Big].$$

The integrals $\int \rho\eta\zeta\,d\tau$, $\int \rho\xi\zeta\,d\tau$, $\int \rho\xi\eta\,d\tau$ represent the so-called centrifugal moments, which will vanish when the coordinate axes are taken to be the principal axes of inertia of the moon.

Then we are left with two terms, namely

$$O\Big[\frac{1}{4r^5}(2z^2-x^2-y^2)\int_\tau \rho(2\zeta^2-\xi^2-\eta^2)\,d\tau + \frac{3}{4r^5}(x^2-y^2)\int_\tau \rho(\xi^2-\eta^2)\,d\tau\Big].$$

Let us introduce the principal moments of inertia of the moon, the form of which is

$$\int_\tau \rho(\eta^2+\zeta^2)\,d\tau = A,\quad \int_\tau \rho(\zeta^2+\xi^2)\,d\tau = B,\quad \int_\tau \rho(\xi^2+\eta^2)\,d\tau = C,$$

and obtain

$$\int_\tau \rho(2\zeta^2-\xi^2-\eta^2)\,d\tau = A+B-2C,$$

$$\int_\tau \rho(\xi^2-\eta^2)\,d\tau = B-A.$$

Let us substitute now the results a, b and c in the expansion (2.28), and obtain finally the following expression for the moon's attraction potential

$$\Phi' = GM'\left[\frac{1}{r} + \frac{A+B-2C}{4M'r^3}(2z^2 - x^2 - y^2) + \frac{3(B-A)}{4M'r^3}(x^2 - y^2)\right] + \\ + \sum_{n=3}^{\infty} \frac{Y_n(\lambda,\beta)}{r^{n+1}}, \qquad (2.29)$$

where the last term contains the spherical polynomials $Y_n(\lambda,\beta)$ of higher order, which depend on the selenographic coordinates of the moon λ , β, since ψ' is a function of these coordinates.

It must be noted here above all that the Laplace functions of third order and above appear in the deviations of the selenoid from a normal spheroid, in deviations of wavelike character, which for the most important terms, i.e., the terms of lower order, will include considerable regions of the moon's surface. Even for the earth such deviations of the geoid from a spheroid are known far from reliably, and the only thing that can be stated is that they do not exceed 100 or 150 meters. Their presence in the moon cannot be sensed at all by an observer on earth, in view of the fact that they are multiplied by $1/r$ in high powers. Therefore we are unable to estimate the deviations of the selenoid from a normal spheroid, even were they to be more considerable than on earth (which, incidentally, is quite possible since the moon is not in hydrostatic equilibrium), and we must neglect them. Using (2.15) and (2.29), we write

$$W = \Phi + \Phi' + \Omega = GM'\left[\frac{1}{r} + \frac{A+B-2C}{4M'r^3}(2z^2 - x^2 - y^2) + \right.$$
$$\left. + \frac{3(B-A)}{4M'r^3}(x^2 - y^2)\right] + \frac{GM}{6r^3}(7x^2 - 2y^2 - 5z^2) = \text{const.} \qquad (2.30)$$

which is an equation that determines the sought surface of normal spheroids, which accurate to first order inclusive is a three-axis ellipsoid /74, p 220/. This last surface is taken for the level surface and we shall call it the selenoid henceforth.

We must make here an important qualifying statement. We start out with an expression for the external potential for β', which essentially is incorrect, since the irregularities of the relief of the moon and even large parts of the moon's surface lie outside the limits of the selenoid. But, as is known from theoretical gravimetry, we can imagine these external masses to become condensed and dropped thereby under the surface of the selenoid, returning to the problem of the external gravitational field. This procedure is called the analytic continuation of the potential from outer space inside the attracting masses. However, this causes for a homogeneous moon displacements of the surface of the selenoid by an amount of order $3H^2/2R_0$, where H is the height of the condensed masses above the level of the selenoid. The displacement of the selenoid, even for H = 5 km, can reach only 20 meters, i.e., 0.01" from the earth, which can be neglected without worry.

Eq. (2.30) was obtained without any assumption whatever regarding the

internal distribution of the masses. The factors (A + B - 2C) and (B - A) which enter into this expression are the so-called Stokes constants, since they are harmonic functions. In general, if the body is bounded by the level surface and we expand the potential β' of this body on an external point in powers of its coordinates x, y, and z, then all the expansion coefficients should be Stokes constants, and in this case only they are independent of the internal distribution of the masses.

In order to obtain the figure of our spheroid, we must find such an expression r = f(x, y, z) as a function of the coordinates, but when substituted into (2.30) the condition (2.19) would be satisfied. The principal term of expression (2.30) is 1/r, since the coefficients of the other terms are small, and therefore the deviation of the moon from a sphere is equal to a certain small quantity.

Let us put again

$$r = R_0(1 + Y_2), \tag{2.31}$$

and here, naturally, Y_2 is already another spherical function, not the one in (2.16). We obtain, still with the same accuracy

$$\frac{1}{R_0} - \frac{1}{R_0} Y_2 + \frac{A+B-2C}{4M'R_0^5}(2z^2 - x^2 - y^2) + \frac{3(B-A)}{4M'R_0^5}(x^2 - y^2) +$$

$$+ \frac{M}{6M'd^3}(7x^2 - 2y^2 - 5z^2) = \text{const.}$$

Hence

$$r = R_0\left\{1 + \frac{A+B-2C}{4M'R_0^3}\,\frac{2z^2 - x^2 - y^2}{R_0^2} + \frac{3(B-A)}{4M'R_0^3}\,\frac{x^2 - y^2}{R_0^2} + \right.$$

$$\left. + \frac{MR_0^3}{6M'd^3}\,\frac{7x^2 - 2y^2 - 5z^2}{R_0^2}\right\}.$$

In this expression the unknown terms are $(A + B - 2C)/4M'R_0^2$ and $3(B - A)/4M'R_0^2$. Jeffreys/77/ determined (from the inclination of the lunar equator to the ecliptic) the quantity

$$L' = \frac{3(C-A)}{2M'R_0^2} = 0.0003734 \pm 0.0000016. \qquad (2.33)$$

If we know $f = (c - B)/(C - A)$, * the use of expression (2.32) entails no difficulties. Actually,

$$1+f = \frac{2C-A-B}{C-A}; \quad -(1+f)L' = \frac{3}{2}\frac{A+B-2C}{M'R_0^2};$$

$$1-f = \frac{B-A}{C-A}; \quad (1-f)L' = \frac{3}{2}\frac{B-A}{M'R_0^2}$$

and consequently

$$\frac{A+B-2C}{4M'R_0^2} = -\frac{1}{6}(1+f)L'$$

$$\frac{3}{4}\frac{B-A}{M'R_0^2} = \frac{1}{2}(1-f)L', \qquad (2.34)$$

after which (2.32) gives the figure of the selenoid, and it is nowhere assumed here that the moon is in hydrostatic equilibrium and that its density is homogeneous.

* This quantity is only 0.0002 less than $f = \frac{(C-B)}{(C-A)} \cdot \frac{B}{A}$..

8. Figure of the Selenoid

As can be seen from Section 4 of the first chapter of this work, it is difficult at the present time to fix the exact value of f. Therefore for the calculation that follows we take four selected values of f, namely 0.60, 0.69, 0.71, and 0.82. In this case we obtain

f	$\frac{A+B-2C}{4M'R_0^2}$	$\frac{3(B-A)}{4M'R_0^2}$
0.60	-0.0000996	$+0.0000747$
0.69	-0.0001052	$+0.0000579$
0.71	-0.0001064	$+0.0000541$
0.82	-0.0001133	$+0.0000336.$

Assuming furthermore $M/M' = 82$ and $d/R_0 = 221$, we obtain

$$\frac{MR_0^3}{6M'd^2} = 0.000013.$$

We next calculate the semi-axes a, b, and c of the selenoid (2.32) for the selected values f, successively putting x, y, and z = R_0. For this we consider Fig. 6, which shows the figure of the moon in the form of a three-axis ellipsoid.

At the point α on the end of the semi-axis a we have y = 0, z = 0, x = R_0 + small quantities, and therefore we can put with great accuracy $x^2/R_0^2 = 1$. We then obtain for f = 0.60

$$r = a = R_0[1 - 0.0000996(-1) + 0.0000747(+1) + 0.000013(+7)],$$

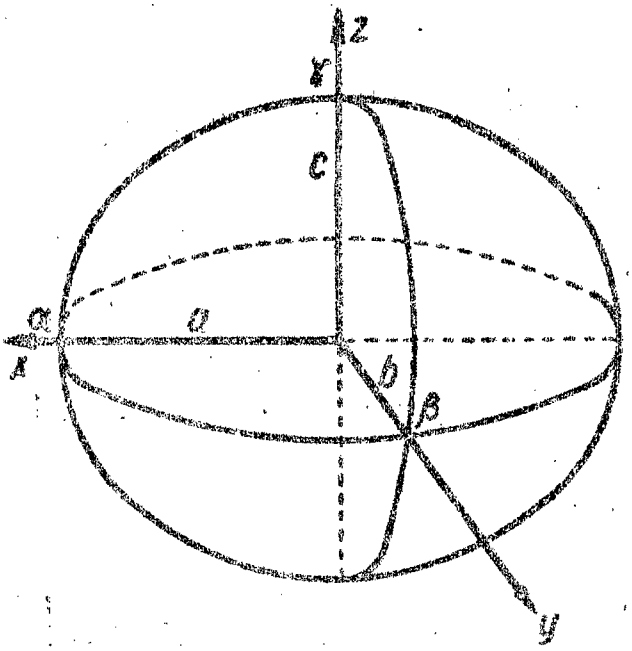

Fig. 6.

or

$$a = R_0(1 + 0.0001834).$$

In order to calculate the semi-axis b, it is necessary obviously to put

$$x = 0, \quad z = 0, \quad y = R_0;$$

We then have

$$b = R_0(1 + 0.0000223).$$

Finally, to calculate semi-axis c, we put $x = 0$, $y = 0$, $z = R_0$, and obtain

$$c = R_0(1 - 0.0002037).$$

Analogously we have calculated the semi-axis of the selenoid for the other values of f; the results are compared in the following

table

f	a/R_0	b/R_0	c/R_0
0.60	1.000183	1.000022	0.999794
0.69	1.000172	1.000045	0.999783
0.71	1.000170	1.000050	0.999781
0.82	1.000156	1.000077	0.999767

This leads to the contractions

f	$\alpha' = \frac{a-b}{R_0}$	$\alpha'' = \frac{a-c}{R_0}$	$\alpha''' = \frac{b-c}{R_0}$
0.60	0.000161	0.000389	0.000228
0.69	0.000127	0.000389	0.000262
0.71	0.000120	0.000389	0.000269
0.82	0.000079	0.000389	0.000310

The differences in the semi-axis are

f	$a-b$	$a-c$	$b-c$
0.60	0.280 км	0.677 км	0.397 км
0.69	0.221	0.677	0.456
0.71	0.209	0.677	0.468
0.82	0.137	0.677	0.540

Were the moon to be a homogeneous liquid, then the deviations of the moon's figure from spheroidal form would be /14/:

$$a - c = 65 \text{ м}, \qquad b - c = 16 \text{ м}.$$

But since, as already noted, the moon is not in hydrostatic equilibrium and in any case is considerably farther from this state than the earth,

It remains to consider the question of what the figure of the selenoid will be when projected on the celestial sphere, or in other words, its visible disk. If the x axis passes to an observed located at an infinite distance, the outline of the selenoid is in the form of an ellipse with semi-axes b and c (see Fig. 6). Since the differences in the semi-axes of the ellipsoid are very small, one can disregard the fact that the observer is actually at a finite distance, since this parallactic effect is much smaller than the effect of libration; at the same time, we see now that it does not influence the oblateness of the disk of the selenoid. Let us first discuss libration in latitude and write the equation of the central meridian of the selenoid, passing through the x axis

$$\frac{x^2}{a^2} + \frac{z^2}{c^2} = 1.$$

We change over to polar coordinates, and then

$$x = r\cos\beta, \quad z = r\sin\beta$$

and consequently

$$\frac{r^2\cos^2\beta}{a^2} + \frac{r^2\sin^2\beta}{c^2} = 1,$$

Hence

$$r^2 = \frac{1}{\frac{\cos^2\beta}{a^2} + \frac{\sin^2\beta}{c^2}}.$$

We next add and subtract $\cos^2\beta/c^2$, and then multiply the numerator

and denominator by c^2, and then obtain

$$r^2 = \frac{c^2}{1-\left(1-\frac{c^2}{a^2}\right)\cos^2\beta}.$$

After extracting the square root and expansion, we obtain

$$r = \frac{c}{\sqrt{1-\left(1-\frac{c^2}{a^2}\right)\cos^2\beta}} = c\left[1+\frac{1}{2}\left(\frac{a^2-c^2}{a^2}\right)\cos^2\beta\right]$$

and finally

$$r = c\left(1+\frac{a-c}{a}\cos^2\beta\right) = c\left(1+\frac{a-c}{R_c}\cos^2\beta\right) = c(1+\varepsilon''\cos^2\beta). \quad (2.35)$$

The polar radius r_p of the visible disk of the selenoid at zero libration is c, since for it $\beta = 90°$. We put $\beta = 90° \pm b_0$, where b_0 is the libration in latitude. If $b_0 = 7°$

$$r_p = c(1+0.015\varepsilon'') = c(1.000058),$$

or

$$r_p = c + 0.010 \text{ km},$$

which shows that r_p does not change noticeably. Since in the case of libration in latitude only the equatorial radius of the disk of the selenoid remains constantly equal to b, we can assume that the libration in latitude hardly influences the figure of the projection of the selenoid on the celestial sphere.

In analysis of the effect of libration in longitude, one must take the equation of the equator of the selenoid, which is obtained analogously (see Fig. 7):

$$r = b\left(1 + \frac{a-b}{b}\cos^2\lambda\right) =$$
$$= b\left(1 + \frac{a-b}{R_0}\cos^2\lambda\right) =$$
$$= b(1 + \alpha'\cos^2\lambda).$$

(2.36)

In the case of zero libration, the equatorial radius r_0 of the disk of the selenoid is equal to b. Let us assume $\lambda = 90° \pm l_0$, where l_0 is the libration in longitude, and let us assume that $l_0 = 8°$, then

$$r_e = b(1 + 0.019\alpha').$$

or for the largest of the values of α' obtained by us, pertaining to $f = 0.60$, we have $r_e = b(1.000031)$ $r_e = b + 0.105$ km.

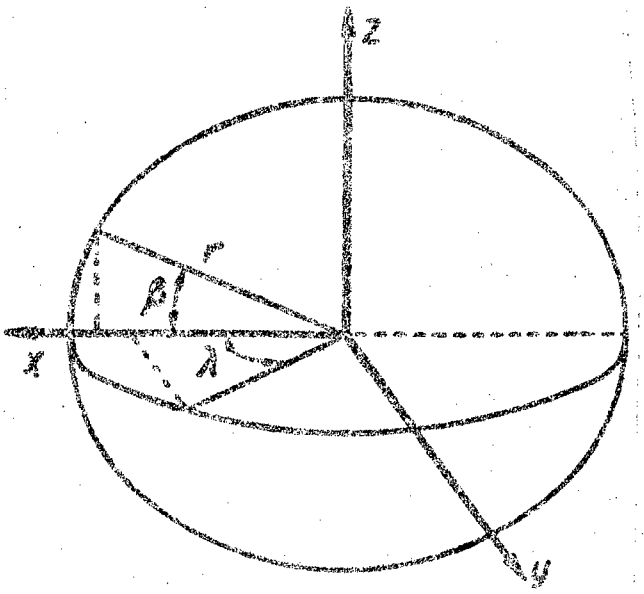

Fig. 7.

It follows therefore as a general conclusion that the disk of the selenoid is practically always an ellipse with semi-axes b and c.

If, for the sake of convenience, we seek heights of points measured on the moon's edge, considering the projection of the selenoid on the celestial sphere to be a circle, then these heights will have to be corrected to refer them to the level surface, and the corrections will depend on the selanographic latitude β, or, what is more convenient, on the position angle p', measured from the axis of rotation of the moon.

In order to obtain a formula for the calculation of the corrections, we shall assume that the projection of the selenoid on the celestial sphere is an ellipse with semi-axes b and c. Let us write the equation of the ellipse

$$\frac{r^2\cos^2\beta}{b^2}+\frac{r^2\sin^2\beta}{c^2}=1,$$

Hence

$$r=c\left[1+\frac{b-c}{R_0}\cos^2\beta\right]=c+\frac{c}{R_0}(b-c)\cos^2\beta.$$

Let us assume $c/R_0 = 1$, and let us add and subtract $(b - c)\sin^2\beta$, and then obtain

$$r=b-(b-c)\sin^2\beta. \qquad (2.37)$$

Let us examine Fig. 8. Let the irregularity A, referred to the circle, have a height H, and let the same irregularity, referred to an ellipse, have the height H'. Then obviously

$$\Delta H = H' - H = b - r. \tag{2.38}$$

Substituting here the value of r, determined from (2.37), we obtain

$$\Delta H = (b - c)\sin^2\beta. \tag{2.39}$$

Bearing in mind that the position angles p' are reckoned in a direction opposite to the direction of the reckoning of the latitude, we can write

$$\Delta H = (b - c)\cos^2 p. \tag{2.40}$$

For our values of f these corrections do not exceed 0.3" and can be readily tabulated. It is important to note that in accordance with what has been said at the beginning, we can add or subtract to or from ΔH, or, what is immaterial, to H itself, a small constant quantity of order H.

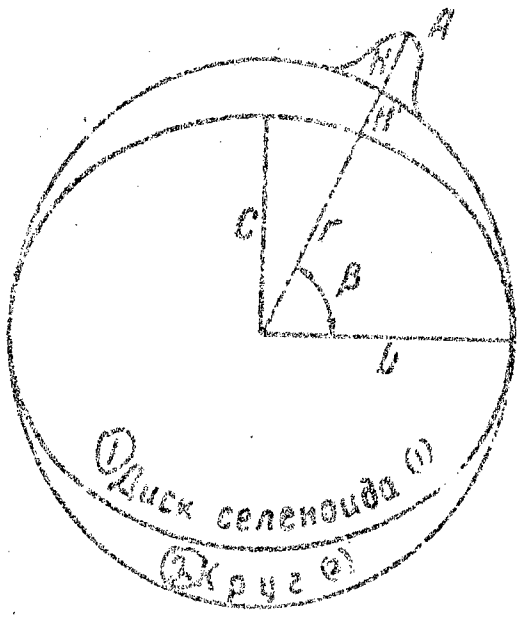

Fig. 8. 1) Disk of selenoid, 2) circle.

Incidentally, if we consider the selenoid to be a sphere, this means that we put in (2.32) $r = R_0$. In this case the harmonic functions of second order, which are included in this equation, will obviously pertain to the relief of the moon. This way, although convenient, can hardly be justified from the theoretical point of view.

To conclude this chapter let us indicate first that the center of the selenoid should coincide with the center of mass of the moon. The position of the projection of the center of the selenoid on the celestial sphere relative to the center of the apparent disk of the moon can be determined only by comparing the observed coordinates of the moon, which are given for the center of the visible disk, with the gravitational theory of motion of the center of mass of the moon. This question will be discussed in the next chapter. Secondly, it must be firmly remembered, that the figure of the selenoid is not the figure of the physical surface of the moon, albeit smoothed. The situation is the same in the case of the earth, in which the continents rise in some places considerably above the geoid. Measurements of the moon's relief performed by Weimer are evidence that on the visible part of the moon one encounters, perhaps overwhelmingly, heights reaching 5 or 6 km (over a certain "level" not defined more accurately). This however does not affect at all

our previous conclusions, which remain fully in force.

We give below a table of the corrections ΔH, calculated with formula (2.40), used to reduce the irregularities of the moon's edge to the level surface of the selenoid.

Table 2

1) Corrections ΔH, 2) for.

p'		1) Поправки ΔH				p'	
		2) для $f=0.60$	2) для $f=0.69$	2) для $f=0.71$	2) для $f=0.82$		
0°	180°	0".20	0".23	0".23	0".21	180°	360°
10	190	0.19	0.22	0.22	0.26	170	350
20	200	0.18	0.20	0.20	0.24	160	340
30	210	0.15	0.17	0.17	0.20	150	330
40	220	0.12	0.13	0.14	0.15	140	320
50	230	0.08	0.09	0.09	0.11	130	310
60	240	0.05	0.05	0.06	0.07	120	300
70	250	0.02	0.03	0.03	0.03	110	290
80	260	0.01	0.01	0.01	0.01	100	280
90	270	0.00	0.00	0.00	0.00	90	270

Chapter III

DETERMINATION OF BARYCENTRIC IRREGULARITIES OF THE MOON'S EDGE

In the preceding chapter we gave for the first time a theoretically complete solution of the problem of the zero surface, from which heights should be measured on the moon. For practical determination of such a surface, it is necessary to solve three problems: 1) to be able to obtain the position of the center of gravity of the moon; 2) to determine the length of one of the principal axes of inertia of the moon; 3) to know the value of the constant f. The third problem has not yet been completely solved, and therefore one cannot calculate definitely the ratio of the semi-axes of the selenoid. This indeterminacy can be avoided by assuming the selenoid to be a sphere and to refer the heights of the moon to this sphere. It appears to us that a solution is advantageous not only from the theoretical aspect, but also from the practical one, since the calculation of irregularities is greatly simplified in this case, and a changeover from a sphere to a three-axis selenoid, after choosing the value of f, is possible by introducing corrections to the height as given in Table 2. It must be emphasized that such a way of mapping the moon's relief could be adopted only after a the theoretical investigation given in the second chapter. Without this investigation it would be

unclear to what extent a sphere is a satisfactory approximation of the level surface. After what has been said, the second problem reduces to a determination of the radius of the sphere which is close to the selenoid. According to our preceding arguments (see p 38 /of source/), the exact value of this radius cannot be determined for the moon in that sense as it can be done for the earth, but there is no need for it. It is merely necessary that the assumed value of the radius be the same constant for all the employed series of observations. As regards the first of the problems formulated above, it must be considered in somewhat greater detail.

The geometric center of either the selenoid or of the sphere we have chosen coincides with the center of gravity of the moon. When projected on the celestial sphere, the center of the figure of the selenoid will also coincide with the projection of the center of gravity. However, the position of the center of gravity is determined only on the basis of the gravitational theory of the moon's motion. The apparent disk of the moon, owing to the presence of mountains on the moon, does not have geometrically regular outlines and it is therefore difficult to offer a rigorous definition for the point that should be called its center. Naturally, from meridional observations and occultation of stars one can obtain the position of the center of the moon's disk, but only in a certain arbitrary and diffused sense, and introduction for correction for the relief did not eliminate this uncertainty, since the heights on the moon are still

referred to a certain surface which is a sphere of variable radius dependent on the optical libration. Actually, Hayn and other investigators determined a certain level for reckoning the heights, in the form of the most probable circle, passing in the best manner through the points of the moons edge. It is quite obvious that the centers and radii of these circles will coincide only in the case when the moon is actually a sphere. However, as soon as this assumption becomes incorrect, the positions thus determined for the visible center of the moons disc and its radii will differ from each other every time, and thus the six heights will be reckoned from different levels. This has led to a situation wherein the observations reduced for irregularities of the edge contain systematic errors, due to the so-called limb effect of the moon. In order to avoid in the future the effect of this error, it is best to refer the heights to a surface, whose center would be the moon's center of gravity. The selenoid surface which we propose as the level surface satisfies precisely this requirement. The position of the center of gravity, however, has not been at all fixed on the moon, and can be determined only by comparison of meridional observations or observation of occultations with the gravitational theory of motion of our satellite. This important question will be discussed in the next section.

9. Determination of the Center of Figure of the Moon Relative to the Center of Gravity

It has been known since Hansen's times that the moon's center of gravity does not coincide with the center of its apparent figure. As a result of the fact that the equator of the moon is only insignificantly inclined to the orbit, one can determine from observation only that component of the distance between these two points, which is located in a direction perpendicular to the plane of the moon's orbit, whereas its projection on the plane of the orbit remains unknown, since it cannot be separated in practice from the irregularities in the moon's longitude.

The fact that the center of gravity does not coincide with the center of figure can be due, obviously, to the fact that the moon is an irregular and inhomogeneous body. If one takes into account the numerous high mountains on the southern hemisphere of the moon, then it may happen, as does on the earth, that there is an internal compensation for the masses of these mountains, or in other words, there is isostasy. Local rises on the southern edge will cause an asymmetry in the moon's disk, and the center of the figure will be shifted to the south relative to the center of gravity, which indeed is observed. As a result of optical libration, the apparent height of these mountains above a certain mean level will change, and this should influence the apparent magnitude of the polar radius of the

moon. The largest apparent height of the mountains will be observed in this case when their base, as a result of libration, is projected on the limb itself.

It has been established from a large amount of observational material (see Table 1) that the moon's apparent radius, reduced to unit distance, can be represented by the empirical formula

$$h = h_0 + 0''.05 b_0, \qquad (3.01)$$

where h_0 is the radius of the moon when the optical libration in latitude, b_0, is equal to zero. This libration variation in the radius was explained by A.A. Yakovkin /41/ by stating that there exists on the spherical moon, in the southern hemisphere, an additional layer around the pole, a layer which extends to the equator, and this layer appears to us to be of variable thickness. According to this hypothesis, the northern hemisphere of the moon is a sphere and its contour appears to us to be a circle of radius R_0, which is independent of optical libration, while the contour of the southern hemisphere is taken to be a semi-ellipse and is given by the equation

$$r = R_0 + a \cos^2 p. \qquad (3.02)$$

Here p is the position angle, reckoned from the northern pole of the moon; the coefficient a is the thickness of the layer above the southern edge, which vanishes for values of p contained between 270° and 90° (through 360°), and is a function of b_0.

Such an idealization of the real edge is undoubtedly highly arbitrary and artificial. It must be stated that the nature of the

Yakovkin layer is not clear. The rapid change in its apparent thickness with oscillations of the libration indicats that it does not extend far along the line of vision and by far does not cover the entire surface of the southern hemisphere. One might think that this is merely local elevation, alternately projecting over the edge of the moon vanishing as a result of libration, and possibly located only in the region of the south pole. We note that there is no need for assuming elevations in the moderate latitudes of the southern hemisphere, since in view of the specific nature of heliometric observations, the determination of the apparent radius of the waning moon is affected in practice only by measurements of the distance in directions from the poles of the moon. No matter what the nature of this elevation, however, our problem consists of finding in practice the position of the center of gravity of the moon relative to the center of its apparent disk. The position of the latter in the celestial sphere is determined from meridional observations, occultations, etc. We are therefore forced to replace temporarily the true profile of the moon by a certain mathematical curve, which would be closer to it than a circle. From this point of view, the Yakovkin contour is a temporary schematization, but one in which still implies that the elevation above the southern pole region is local in character and does not deform exclusively the entire southern hemisphere. We shall not be far from the truth if we assume the Yakovkin hypothesis as a suitable scheme for this profile, which in the past was

replaced during observations by a sphere of variable radius. According to this hypothesis, as we have already said, the moon's contour consists of two curves: its northern half is part of a circle of radius R_0, and its southern half is part of an ellipse with semi-axis R_0 and $R_0 + a$, while the center of gravity of the moon coincides with the center of its northern hemisphere.

Our problem consists now of calculating, on the basis of this hypothesis, the coordinates ξ and η of the center of the figure of the moon relative to the center of gravity. Usually one observes the eastern or the western half of the moon. To obtain an equation for the eastern half of the contour, let us consider Fig. 9. We place the origin of the ξ and η axes at the center of gravity of the moon O, and the origin of the x and y axes at the center of Fig. O'. Then the coordinates of a point on the edge, relative to the center of gravity, will be

$$\begin{aligned} \xi_0 &= R_0 \cos p \\ \eta_0 &= R_0 \sin p, \end{aligned} \tag{3.03}$$

and the coordinates of the same point relative to the axes x and y will be

$$\begin{aligned} x &= (R_0 + \Delta h) \cos p \\ y &= (R_0 + \Delta h) \sin p, \end{aligned} \tag{3.04}$$

where $(R_0 + \Delta b)$ is the radius of the most probable circle. Let us change over from the coordinate system x, y to ξ, η. Then

$$x = \xi_0 - \xi = R_0 \cos p - \xi$$
$$y = \eta_0 - \eta = R_0 \sin p - \eta, \qquad (3.05)$$

where ξ and η, as was already said, are the coordinates of the center of the figure of the moon relative to the center of gravity. From a comparison of Eqs. (3.04) and (3.05) it follows that

$$(R_0 + \Delta R) \cos p = R_0 \cos p - \xi$$
$$(R_0 + \Delta R) \sin p = R_0 \sin p - \eta \qquad (3.06)$$

Let us multiply the first equation of (3.06) by cos p, and the second by sin p and let us add. We then obtain

$$R_0 + \Delta R = R_0 - \xi \cos p - \eta \sin p$$

From this we find for the northern half of the contour the following expression

$$\xi \cos p + \eta \sin p + \Delta R = 0$$
$$0 \leqslant p \leqslant \frac{\pi}{2}. \qquad (3.07)$$

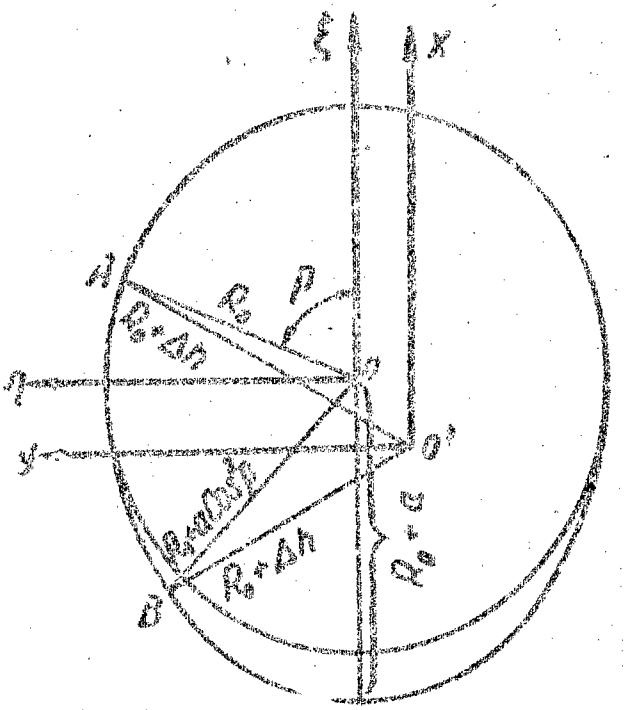

Fig. 9.

Fig

In order to derive an equation for the southern part of the contour, we take the point B on the southern edge of the moon; the distance from this point to the center of gravity will obviously be $(R_0 + a \cos^2 p)$, and the distance to the center of the figure will be $(R_0 + \Delta h)$. Then the coordinates of the point B relative to the center of gravity will be

$$\begin{aligned} \xi_0 &= (R_0 + a\cos^2 p)\cos p \\ \eta_0 &= (R_0 + a\cos^2 p)\sin p. \end{aligned} \tag{3.08}$$

and relative to the center of figure

$$\begin{aligned} x &= (R_0 + \Delta h)\cos p \\ y &= (R_0 + \Delta h)\sin p. \end{aligned} \tag{3.09}$$

Changing again from the coordinate system xy to the system ξ, η

$$\begin{aligned} x &= -\xi_0 + \xi = -(R_0 + a\cos^2 p)\cos p + \xi \\ y &= \eta_0 - \eta = (R_0 + a\cos^2 p)\sin p - \eta. \end{aligned} \tag{3.10}$$

Comparing the right halves of (3.09) and (3.10), we obtain

$$\begin{aligned} (R_0 + \Delta h)\cos p &= (R_0 + a\cos^2 p)\cos p - \xi \\ (R_0 + \Delta h)\sin p &= (R_0 + a\cos^2 p)\sin p - \eta. \end{aligned} \tag{3.11}$$

We next multiply the first equation of (3.11) by cos p and the second by sin p and add, then

$$R_0 + \Delta h = R_0 + a\cos^2 p - \xi\cos p - \eta\sin p$$

and thus, we have for the southern half of the contour

$$\xi\cos p + \eta\sin p + \Delta h = a\cos^2 p$$

$$\frac{\pi}{2} \leqslant p \leqslant \pi. \qquad (3.12)$$

Assuming that the observed points are distributed uniformly over the entire contour and their number is infinite, Yakovkin /72/ obtained by solving (3.07) and (3.12)

$$\begin{aligned} \xi &= -0.42\,a \\ \eta &= -0.56\,a \\ \Delta h &= 0.61\,a. \end{aligned} \qquad (3.13)$$

For the right half of the contour we obtain an analogous result; only the sign of η changes.

Eqs. (3.13) hold for an infinitely large number of points, and generalizing these equations we put

$$\begin{aligned} \xi &= K_\xi\, a \\ \eta &= K_\eta\, a \\ \Delta h &= K_h\, a. \end{aligned} \qquad (3.14)$$

However, one usually observes with the heliometer only a total of seven points of the edge of the moon. To make use of Eqs. (3.14), it is therefore necessary to calculate the values of K_ξ, K_η, and K_h as functions of the position angle p' -- the center of the arc covered by the measurements. Assuming a certain standard distribution of the points of the edge as functions of the position angle, Yakovkin solved (3.07) and (3.12) by the method of least squares, after first substituting in these equations the values of ξ, η, and Δ h from (3.14). He then made up a table of values of K_ξ, K_η, and K_h, in terms

of the argument p', which is given on p 20 of his article /72/.

To calculate coordinates ξ and η we must also know the value of a, which is the difference between the polar and equatorial diameters of the moon's disk. It can be determined only from observation. The radius of the most probable circle from among a large number of observations is determined from formula (3.01). On the other hand, it can be expressed in terms of the quantity a, namely

$$h = R_0 + K_h a.$$

Let us assume for K_h its mean value as given by (3.13); then

$$h = R_0 + 0.61\, a. \tag{3.15}$$

Comparing (3.01) and (3.15), we obtain

$$h_0 + 0''.05\, b_0 = R_0 + 0.61\, a. \tag{3.16}$$

Hayn obtained from measurements made on the Leipzig refractor a difference of + 0.81" between the polar and equatorial diameteters, at an average libration of - 1.8°. Substituting these values of (3.16), we get

$$h_0 - 0''.03 = R_0 + 0.49. \tag{3.17}$$

Eliminating $h_0 - R_0$ from Eqs. (3.16) and (3.17), we obtain the thickness of the layer a for the average parallax

$$a = 0''.96 + 0''.082\, b_0. \tag{3.18}$$

Yakovkin derived, in addition, the value of a from observations of the occultations of stars by the moon in conjunction with heliometric observations. He used a correction of - 0.49" for the latitude of the

moon, obtained by Spencer Jones from observations of occultations. Assuming that this correction is the average value of ξ, and substituting it in (3.13), Yakovkin obtained the following equation

$$-0.42\,\bar{a} = -0''.49. \tag{3.19}$$

where $\bar{a}$ corresponds to the value of a when the libration in longitude is zero. Putting in (3.16) $a = \bar{a}$ and $b_0 = 0$, we obtain

$$0.61\,a = 0.61\,\bar{a} + 0''.05\,b_0.$$

and we can further write

$$0.61\,\bar{a} = (b_0 - R_0)$$

Substituting in (3.19), we obtain still another formula for the determination of a, differing little from (3.18), namely

$$a = 1''.17 + 0''.082\,b_0. \tag{3.20}$$

This circumstance, as emphasized by Yakovkin, is still another independent proof of the fact that the libration effect in the apparent radius of the moon depends only on changes in the southern edge of the moon, since all the conclusions have been made under the assumption that the contour of the moon's hemisphere is represented by the curve $r = R_0 + a\cos^2\varphi$.

We used formula (3.18) to calculate a. Knowing K_ξ, K_η, and a, we calculate ξ and η from formulas (3.14).

The ξ axis was directed along the central meridian of the moon. To go over to the equatorial system, it was necessary to rotate the coordinate axis by an angle C, which is the position angle of the moon's axis relative to the circle of declinations. Then the coordinates

of the center of figure of the moon relative to the center of gravity are determined from the following formulas

$$\Delta x = \xi \cos C - \eta \sin C$$
$$\Delta y = \xi \sin C + \eta \cos C. \qquad (3.21)$$

10. Calculation of Barycentric Irregularities of the Moon's Edge

Observations of the moon with the heliometer of the Engel'gardt observatory have been going on continuously for sixty years. The Kazan' heliometric series of observations are the longest in the world and are of basic significance for the study of the rotation and the figure of the moon. However, until now this extensive observational material was used principally only for derivation of the constants of the physical libration of the moon, which were obtained with a very high degree of accuracy. To calculate the irregularities in the moon's edge and to compile maps of the moon's relief, we used the already processed observations, covering fifty years, and this greatly decreased the amount of computational labor.

Libration observations of the moon consist of measuring distances s from the moon's crater Moesting-A to seven points, located on the illuminated edge of the moon and separated by approximately equal angle distances, and also of measuring their position angles p. The measured values are then subjected to numerous corrections, including those for differential refraction and for irregularities of

the moon's edge, as taken from Hayn's hypsometric maps. This is followed by calculations of the distances h' from the ephemeridal center of the moon to selected points on the edge and their position angles p_0, using the formulas

$$h' \sin p_0 = y_0 + s \sin p$$
$$h' \cos p_0 = x_0 + s \cos p, \qquad (3.22)$$

where x_0 and y_0 are the approximate coordinates of the crater Moesting A. In order to obtain the observed radius of the moon h and the coordinates x and y of Moesting-A relative to the center of the most probable circle, trial equations of the form

$$\Delta x_0 \cos p_0 + \Delta y_0 \sin p_0 - \Delta h = h_0 - h', \qquad (3.23)$$

are setup, their number being equal to the number of points of the edge in the given observation (usually seven or eight points). Solving these equations by the method of least squares one obtains the corrections Δx_0 and Δy_0 to the approximate coordinates x_0 and y_0, and the correction Δh to the ephemeridal radius of the moon.

To calculate the barycentric irregularities of the moon's edge we must know the measured distances h from the center of gravity to the individual points of the moon's edge. However, in processing heliometric observations by formulas (3.22), one calculates the distances h' from a certain assumed center. Therefore, knowing h', we have first calculated h'_0 -- the distance to the points of the edge from the center of the most probable circle, and then, with these obtained, we determine h. To derive the necessary formulas for

the calculation of h'_0, let us examine Fig. 10. The center of the most probable circle O' relative to the ephemeridal (proposed) center will obviously occupy a variety of positions. Assume that it is in the position shown in Fig. 10. It is necessary, however, to note that Δx_0 and Δy_0 will be considered in this case negative. The point is that if upon going from the ephemeridal center to the center of the most probable circle, the coordinates of Moesting-A change by $+\Delta x_0$ and $+\Delta y_0$, then the coordinates of the center of the most probable circle relative to the ephemeridal center will change by $-\Delta x_0$ and $-\Delta y_0$. Let us consider the triangle OKO', in which

side $OK = h'$

side $O'K = h'_0$

side $OO' = \Delta\sigma'$

angle $O'OX = p_0 - 90^0 + \alpha'$

Here p_0 is the position angle h' reckoned from the x axis, directed along the circle of declinations, and α' is the angle between $\Delta\sigma'$ and the y axis. Solving this triangle relative to the side h'_0, we obtain

$$h_0'^2 = h'^2 + \Delta\sigma'^2 - 2h'\Delta\sigma' \cos(p_0 - 90^\circ + \alpha'),$$

or

$$h'_0 = h' \left[1 + \frac{\Delta\sigma'^2}{h'^2} - \frac{2\Delta\sigma'}{h'} \sin(p_0 + \alpha')\right]^{\frac{1}{2}}.$$

Expanding in a series and retaining first-order quantities, we have

$$h_0' = h' - \Delta\sigma' \cdot \sin(p_0 + \alpha'). \tag{3.24}$$

Formula (3.24) has been derived for negative values of Δx_0 and Δy_0. Analogously we can derive formulas for the three other positions of the center of the most probable circle relative to the ephemeridal center. In general we shall have the following formulas for different Δx_0 and Δy_0:

$$\begin{aligned}
h_0' &= h' + \Delta\sigma' \sin(p_0 + \alpha') \quad + \Delta x_0 \\
&\qquad + \Delta y_0 \\
h_0' &= h' + \Delta\sigma' \sin(p_0 - \alpha') \quad - \Delta x_0 \\
&\qquad + \Delta y_0 \\
h_0' &= h' - \Delta\sigma' \sin(p_0 + \alpha') \quad - \Delta x_0 \\
&\qquad - \Delta y_0 \\
h_0' &= h' - \Delta\sigma' \sin(p_0 - \alpha') \quad + \Delta x_0 \\
&\qquad - \Delta y_0
\end{aligned} \tag{3.25}$$

We note that the sign of Δx_0 or Δy_0 as given here, is the one obtained from calculations with formula (3.23). The values of $\Delta\sigma'$ and α' which are contained here can be calculated from the formulas

$$\Delta\sigma' = \sqrt{\Delta x_0^2 + \Delta y_0^2},$$

$$\operatorname{tg}\alpha' = \frac{\Delta x_0}{\Delta y_0}.$$

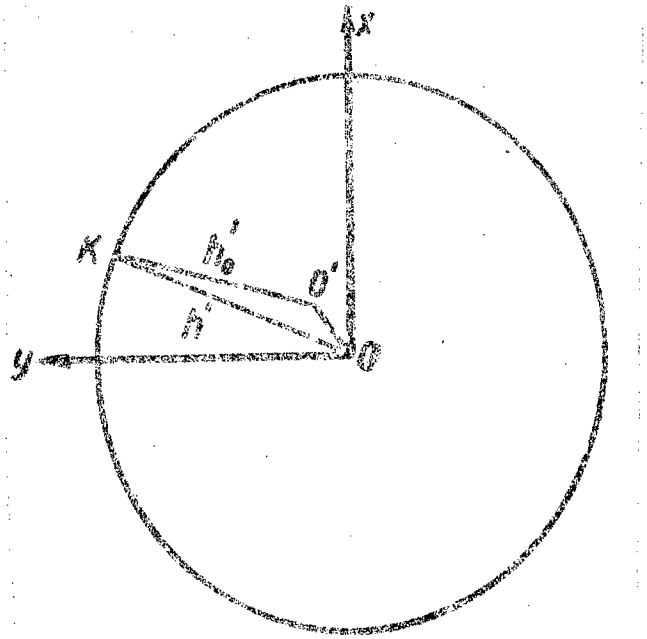

Fig. 10.

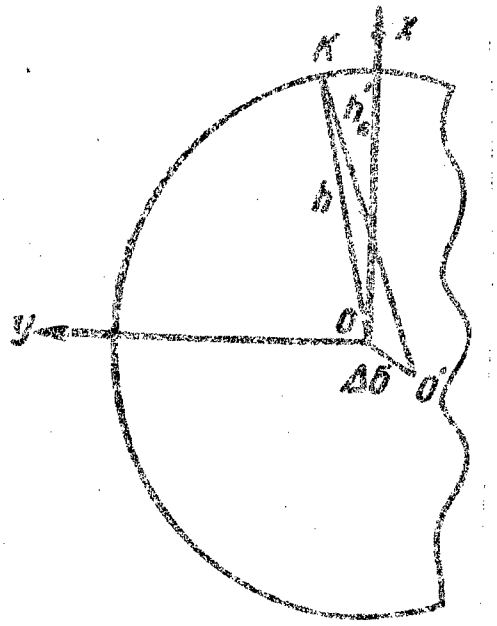

Fig. 11.

We have noted earlier that to obtain the barycentric irregularities of the moon's edge it is necessary to go over from the center of figure to the center of gravity of the moon. When constructing the contour of the moon's profile we started from the fact that the profile is assumed to consist of two parts, the northern half being part of the circle, whereas the southern half is part of an ellipse. The center of gravity should always be on the axis of rotation, and as evidenced by observational data, to the north of the center of figure. The latter, will in addition be shifted relative to the center of gravity in the western or eastern direction, in view of the fact that we always try to draw the most probable circle in such a way, that it fits in the best manner the given profile of the moon. In this case, as can be readily seen, the center of the figure will be shifted relative to the center of gravity for the eastern edge of the moon in a south-west direction, and for the western edge it will be shifted in the south-east direction.

To derive the necessary formulas let us examine Fig. 11, which shows the eastern half of the moon. Let $\Delta\rho$ be the distance between the center of gravity O and the center of the figure O', and let K be a point on the edge of the moon.

Let us place the origin of the rectangular coordinates x and y in the center of gravity of the moon and let us direct the x axis along the circle of declinations, while the y axis is 90° to it. We calculate h, the distance from the center of gravity to the point on the edge

of the moon K, considering that we know h'_0, p_0, and the coordinates Δx and Δy of the center of the figure relative to the center of gravity, these being determined by formulas (3.21). Denoting the angle between $\Delta\delta$ and Δy by α, we obtain from the triangle OO'K

$$h^2 = h_0'^2 + \Delta s^2 - 2h_0'\Delta s\cos(90° - p_0 - \alpha),$$

or

$$h = h_0'\left[1 + \frac{\Delta s^2}{h_0'^2} - \frac{2\Delta s}{h_0'}\sin(p_0 + \alpha)\right]^{\frac{1}{2}}.$$

confining ourselves to first-order quantities in the expansion, we can write, accurate to 0.0005

$$h = h_0' - \Delta s\sin(p_0 + \alpha).$$

(3.26)

For the western half of the moon's disk we obtain analogously

$$h = h_0' + \Delta s\sin(p_0 - \alpha).$$

(3.27)

The quantities $\Delta\delta$ and α are determined from the formulas

$$\Delta s^2 = \Delta x^2 + \Delta y^2$$

$$\operatorname{tg}\alpha = \frac{\Delta x}{\Delta y}.$$

In the calculation of α it is always necessary to take its absolute magnitude value.

Formulas (3.26) and (3.27) contain the position angle

p_0 of the point of the edge relative to the coordinate axis, the origin of which is placed in the center of figure of the moon. However, we have now transferred the origin of the rectangular coordinates to the center of gravity, and therefore the position angle must be suitably corrected. As can be seen from Fig. 10, p_0 should be changed by an angle $OKO' = \pi''$, which can be calculated from the following formula. From the triangle OKO' we have

$$\frac{\Delta\varrho}{\sin\pi''} = \frac{R}{\sin(90^\circ - p_0 - \alpha)} = \frac{R}{\cos(p_0 + \alpha)},$$

or

$$\sin\pi'' = \frac{\Delta\varrho}{R}\cos(p_0 + \alpha)$$

and

$$p = p_0 - \pi''.$$

(3.28)

For the western half of the moon's disk we have

$$\sin\pi'' = \frac{\Delta\varrho}{R}\cos(p_0 - \alpha)$$

and

$$p = p_0 + \pi''.$$

However, calculations show that the angle π'' does not exceed 3.5' in the maximum, and without loss of accuracy we can neglect this correction.

In the second chapter we consider the problem of zero-reference surface, which we chose to be a level surface of the potential of the

moon's gravity. From a theoretical examination of this problem it follows that the figure of the selenoid deviates in general little from a spherical form. Therefore, to simplify the calculations, as indicated at the beginning of this chapter, we can first consider the moon to be a sphere, whose center coincides with the center of gravity and all the deviations from this level surface can be assumed to be the irregularities of the moon's edge. In order to refer these later to a selenoid surface, we can calculate the suitable corrections from formula (2.40), and introduce them in the irregularities we ~~xx~~ determined. We found it most advantageous to assume for this preliminary spherical level surface the radius determined from the given series of libration observations of the moon, and refer to the average parallax and to zero libration in latitude. Assuming such a radius, we thereby exclude the observer's personal error in calculating the irregularities of the moon's edge.. This is very important for unifying and reducing to a single system all the irregularities calculated from different series of observations. Let us denote the radius of the sphere thus determined by r'_0. To be able to compare it with h, calculated from formulas (3.26) and (3.27), it is necessary to reduce r'_0 to the parallax of the moon π, to which pertain the measured values of h, using the formula

$$r_0 = \frac{\pi}{\pi_0} r'_0 . \qquad (3.30)$$

The parallax π was calculated during the processing of the libration observation for the mean Greenwich time of observation of the

moon, r_0, to which all the measured s and p are reduced. Therefore in calculating r_0 we used precisely this parallax.

The values of r_0 so obtained have to be still reduced to the point of observation, by applying the parallactic correction Δr, calculated from the known formula /78/

$$\Delta r = r\left[\cos(\Gamma - \delta)\sin p' + 2\sin^2\left(\frac{p''}{2}\right)\right], \qquad (3.31)$$

where

$$\operatorname{tg}\Gamma = \frac{\operatorname{tg}\varphi' \cos\left(\frac{p''}{2}\right)}{\cos\left(t - \frac{p''}{2}\right)}.$$

Here δ is the declination of the moon and t its hourly angle at the instant of observation, p^{α} and p^{δ} are parallaxes in α and δ, while φ' is the geocentric latitude. This correction was also precisely calculated earlier for the mean green time. It be noted that in (3.31) we should have instead of the ephemeridal value r the value r_0, calculated from (3.30). However, as can be readily seen, this introduces a negligibly small error. After making these corrections, the radius of the level surface becomes

$$h_0 = r_0 + \Delta r. \qquad (3.32)$$

After finding h_0, we calculate the barycentric irregularities of the moon's edge H, using the formula

$$H = h - h_0. \qquad (3.33)$$

We note once more that the irregularities so calculated refer to sphere. But we can changeover without particular difficulty to heights

reckoned from the selenoid level surface, using the numerical data of Table 2.

Chapter IV

MAPS OF THE MOON'S RELIEF AND THEIR ACCURACY

11. The Kazan' Heliometer and Method Employed With It.

In the third chapter we mention that to calculate the irregularities of the moon's relief and to map them, we used the Kazan' heliometric series of observations of the crater Moesting-A. The heliometer of the Engel'gardt observatory was manufactured by Repsold in 1874 and was first intended for observations of the passage of Venus over the sun's disk, in order to determine the solar parallax. The Kazan' heliometer is an instrument of the new type, in which the following structural modifications have been made: the halves of the objective move symmetrically in opposite directions over a cylindrical surface, whose radius equals the focal distance of the objective. There is no lateral displacement of the eyepiece. The entire tube together with the objective box as a whole rotates about the position angle. Readings of the objective scales and of the position dial are with the aid of long-focus microscopes directly from the eyepiece and of the tube. The dimensions of the instrument are as follows: the diameter of the objective 160 mm, focal length 1590 mm. The setting of the instrument is very stable because of an original construction of the column on which the heliometer is mounted.

The coordinates of the pole of the instrument remain almost unchanged over a period of several years, which, as is well known, is very important in positional observations. The relative placements of the different of the instrument remained essentially unchanged over the sixty years of its continuous operation.

An advantage of our heliometer is that it is independent of temperature effects. This is a very important property of the instrument. It frees the observer of frequent refocusing and reducing the readings of the focal scale to a constant reference, since the observations are carried out at a constant focus. Likewise, no dependence of the scale graduation on the temperature has been observed, and consequently, the difficulties involved in the determination of temperature changes in the instrument are eliminated in this case. The value of each scale graduation was determined by the observers with a high degree of accuracy. Thus, for example, in his first series of observations, Krasnov determined it to be

$$51''.8881 \pm 0''.0008.$$

Such high accuracy is due to outstanding optical quality of the instrument and a well worked out method of observations. The images of the stars are obtained in the form of short bright lines (as is usually seen in a heliometer), which stretch perpendicular to the line bisecting the halves of the objective. This contributes greatly to the accuracy of the measurement of distances with the heliometer, for in

this case the stars are arranged by motion of the halves of the objectives on a straight line, which should be parallel to one of the hairs of the cross hair in the field of view of the tube. The cross hair is so oriented, that one hair is strictly parallel to the line bisecting the halves of the objective, and the second is perpendicular to it. To be sure, images of stars in the form of lines make it difficult to estimate parallel positions when measuring position angles, for in this case the images stretch perpendicular to the cross hair, whereas in the measurement of distances they stretch parallel to the latter. But considering that the position dial on our heliometer is read accurate to one half a minute of the hour, this method of observation is suitable also for measurement of position angles. The index of the position dial is usually determined with an error not exceeding $\pm$ 0.1'.

In spite of the fact that our heliometer is small as far as dimensions go, the accuracy of measurements of stellar arcs obtained with it is quite high. Thus, the probable error in one measurement of distance amounts to, under usual mean atmospheric conditions, $\pm$ 0.15" to $\pm$ 0.20". The mean radius of the moon is usually measured with our heliometer with an average error of $\pm$ 0.05". A heliometer similar to ours is described in detail in the book by Ambronn /79/.

To study the physical libration of the moon, one observes the crater Mosting-A. The latter has a very regular configuration,

approaching the circle, so that the center of its figure can be uniquely estimated for different phases of the crater, because the phases of the crater do not affect the observations for most observers. The problem in the observation is the determination of the position of the crater relative to the center of the moon's apparent disk. The method of observation consists of having the observer bisect the crater Maesting-A by the illuminated edge of the moon, and then read the scales connected to the halves of the objective of the heliometer, as well as the micrometer. Two such aimings of the edge on the crater are made before the resetting of the halves of the objective, and two are made after the resetting, for a constant position angle. During the first and last bisections, the time is measured accurate to one second. This method of observation makes the processing of the observations very difficult, for it becomes necessary to reduce measured distances and position angles for each point of the edge of the moon to a certain average instant of one complete observation, consisting, as mentioned above, of measuring distances from the crater to seven or eight points of the edge and of reading the position angles. But it is precisely this method that was used by all the observers with the Kazan' heliometer, in order to guarantee against possible change in the position of the null point of the scales during the time of observation.

To calculate the differential refraction at the beginning and at the end of each observation the temperature and the barometer were

read.

As a whole, the following corrections were introduced in the measured distances a: 1) for run, 2) for errors in scale division, 3) for differential refraction, 4) for motion of the crater over the moon's disk, 5) for changes in the visible radius of the moon, 6) for irregularities in the moon's edge. The following corrections were made to the position angles: 1) for errors in setting, 2) for the error in the index of the position dial and its torsion, 3) for differential refraction, 4) for motion of the crater over the disk of the moon. The calculation of all the foregoing corrections is quite laborious. In our work, however, we used the already reduced values of measured distances and position angles.

In order to judge the accuracy of the observations of the moon without heliometer, we give the magnitude of the error of determining the position of the crater from one observation, which is $\pm$ 0.45", i.e., it amounts to approximately one tenth of the visible diameter of the crater itself. It should be noted that among the astronomical instruments, the heliometer, definitely occupies one of fi the first places as regards accuracy of measurements.

12. Observational Material

Over sixty years, eight series of observations of the moon have been carried out with the Kazan' heliometer. The instrument was first installed in Kazan' and while there two series of observations were

performed, one by A.V. Krasnov in 1895 through 1898, and by A. A. Mikhaylovskiy from 1899 through 1905. The first series remained unprocessed for a long time, since the observation logs were believed lost, but in 1949 they were found and for the next three years they were processed by the author /80/. Krasnov made 112 observations of the crater Moesting-A. He very thoroughly investigated the instrument and determined all its constants. The observations are quite uniformly distributed over the years and cover both positive and negative optical libirations. From among the 112 observations, 57 were made before full moon, four during the time of full moon, and 51 after full moon. Thus, both the western and the eastern edges of the moon were observed equally frequently. Krasnov observed quite persistently. In 1897, for example, he made 52 observations of the moon. These observations, however, were not advantageously distributed with respect to optical librations in longitude and latitude. Negative librations, particularly in latitude, prevail in the main.

The Mikhaylovskiy series covers almost eight years of observations. However, during that time he made only 58 observations of the moon, and almost all these were before full moon (53 observations) and only five of these were of the eastern edge. Initially this series was processed by Volkel /81/, who, however, did not make a complete reduction of the observations and therefore this series was processed again in 1936 by I. V.Bel'kovich /22/ with allowance for all the necessary corrections. The accuracy of the results obtained

was higher than the initial one, but still remain considerably below that with which the constants of the physical libration of the moon were determined from the subsequent series of observations. This is explained, on the one hand, by the small number of observations and on the other hand by the fact that the crater Mosting-A was correlated almost exclusively with the western edge, and the asymmetry of the moon's disk could exert its influence.

In 1908 the heliometer was transferred to the Engel'gardt observatory and in 1910 systematic observations with it were started by T.A. Banachiewicz. This series of observation was carried out from 1910 through 1915 and was processed by A.A. Yakovkin /63/. Of the 130 observations, 76 were carried out before full moon, two during the time of full moon, and 52 after full moon. Almost two thirds of observations were carried out at negative librations in latitude. Owing to the carefully performed observations and their complete and all-sided processing, the elements of rotation of the moon were obtained with a high degree of accuracy. It must be noted that in general all the Kazan' heliometric series have been reduced as rigorously as possible and as thoroughly as possible.

After Banachiewicz left the Engel'gardt observatory, the observations with the heliometer were continued by A. A. Yakovkin. His large series, covering 15 years (1916 — 1931) and containing 251 observations of the moon, were processed in two steps /83/, /64/. In this series, as in the others, the observations are not uniformly

distributed over the edges of the moon. Thus, the western edge was observed 159 times, whereas the eastern one was observed 89 times, while three observations were made during the time of full moon. The number of observations with positive and negative librations in latitude are almost the same. The latter circumstance is of no little importance in mapping the moon's relief, since the possibility of viewing different regions of the edge surface of the moon depends on how strongly the optical libration changes during the time of observation.

Further measurements with the heliometer, starting in 1932 through 1948, were continued by I. V. Bel'kovich. During that time he made 247 observations of the crater Moesting-A, of which 151 observations, carried out from 1932 through 1942, were processed /59/. In this series, the western edge was observed 94 times, the eastern 55 times, and two observations were carried out during full moon. It must be noted that five observations of Bel'kovich were excluded from the processing as being of poor quality (Nos. 1 — 4 and 34). From among the 146 observations, 68 were carried out at positive optical librations in latitude, and 78 at negative ones. In the observations carried out with the Kazan' heliometer, only the Bel'kovich series contains for the eastern edge of the moon a systematic error, which depends on the phase of the crater Moesting-A. The necessary correction for this was introduced by him into the measurements.

In 1938, the author of the present book was enrolled in the

observations with the heliometer and he has been carrying them out to this date. During the 18 years (1938 — 1956) the author has carried out 402 observations of the moon. Of this number, 143 observations, carried out from 1938 through 1945, have been processed /56/. Among these, 79 observations were made before full moon, 61 after full moon, and three during the time of full moon. In this sixth heliometric series, a greater part of the observations was carried out at positive optical librations.

Table 3 shows the number of observations and the measured heights, used in the construction of the maps.

Table 3

1) Series of observations, 2) years, 3) number of observations, 4) number of measured heights,

① Ряд наблюдений	② Годы наблюдений	③ Число наблюдений	④ Количество измер. высо
Krasnov	1895—1898	109	757
Mikhaylovskiy	1898—1905	54	362
Banachiewicz	1910—1915	130	994
Yakovkin	1916—1931	241	1618
Bel'kovich	1932—1942	140	972
Nefed'ev	1938—1945	136	927
Total		810	5630

Comparing the numbers in this table with those given earlier for each series, we see that 35 observations were excluded, since the calculated heights were in strong disagreement with other measurements. The reasons for these were either poor atmospheric conditions, at which the observations were performed, or else, as took place in the series of A.A. Yakovkin, misprints were found in the published data. We did not have an opportunity to correct these mistakes, since we did not have the necessary material for this. In addition, certain observations were excluded by the authors themselves as being of poor quality, but were not designated under the corresponding serial numbers in the published data. As a whole, the heights we used in constructing the maps fill up almost the entire edge belt of the moon. The latter amounts to approximately 6,000 square degrees. Were the observations to be distributed uniformly over all parts of the belt, then in each square degree there would be on the average one height marker. As we shall see below, actually this did not take place.

Speaking further of the material we used, notice must be taken of its significant property, namely homogeneity. All the observations were carried out with one instrument, by one method, and processed by a single procedure. This is particularly important if for no other reason that it frees the observer of additional calculations when unifying the observations of different authors.

We cannot fail to note that a series of data which are

essential in the use of the observational material, were unfortunately not published. These include "parallaxes of the moon in α and δ, topocentric optical libration, the position angle of the moon's axis of rotation, and others. In view of this, in some cases we had to repeat calculations already performed before.

13. Construction of the Maps of the Moon's Relief

In order to proceed to draw the lines of equal height, i.e., the isohypses, much work had to be done on the calculation of the irregularities of the moon's edge. For this purpose, it was necessary to know the measured distances from the center of gravity to the edge of the moon. In the third chapter we indicated the way and gave formulas for such calculations. It was first necessary to calculate, by means of formula (3.25), the distances h'_0 from the center of the most probable circle to the corresponding points of the moon's edge. For this purpose we used the distances h' from a certain ephemeridal center to the measured points of the edge of the moon, which were already calculated during the processing of the libration observations of the moon, and the position angles p_0, which were obtained from the equations

$$\begin{aligned} h' \sin p_0 &= y_0 + s \sin p \\ h' \cos p_0 &= x_0 + s \cos p. \end{aligned} \tag{3.22}$$

Let us make here the following note. In calculating h' from the observations of Krasnov and Nefed'ev, we corrected the measured values

of a for all the corrections, with the exception of the corrections for the irregularities in the moon's edge. The latters were introduced from Hayn's maps directly into the right halves of (3.23). Therefore the values of h' which we calculated from these observations contained the irregularities of the moon's edge. Other observers, on the otherhand, introduced corrections for the relief at an earlier stage of processing, namely in the measured values of s, and consequently the calculated values of h' were obtained in this case from the solution of Eq. (3.22), corrected for irregularities of the edge. But since we need the values of h' corrected for the relief, we had to introduce in all the values of h' thus obtained the errors due to the edge.

In view of the fact that the crater Moesting-A is located close to the center of the moon, it is quite immaterial whether the corrections for relief have been added to s or to h'. Actually, if we differentiate (3.22), we obtain the following relation

$$dh' = ds\cos(p - p_0). \tag{4.01}$$

The difference $(p - p_0)$ can reach 11°; in this case

$$\cos(p - p_0) = 0.98,$$

which is close to unity.

Adding the corrections $\Delta x_0, \Delta y_0$ to the ephemeridal values of the coordinates x_0 and y_0 of the crater Moesting A, obtained by solving (3.23), we calculate h'_0 using (3.25).

In this way obtained h'_0 from the observations of Krasnov,

Banachkiewicz, Bel'kovich, and Nefed'ev. In the processing of the observations of Mikhaylovskiy and Yakovkin we could do so, for we did not have calculated values of Δx_0 and Δy_0. We therefore proceeded in the following manner. Using the published values of the preliminary rectangular coordinates of Hoesting-A, x and y, relative to the center of the moon's disk, we substituted them into (3.22) together with x_0 and y_0, solve these equations, and obtain thereby h'_0 and p_0. This way of calculating h'_0 is naturally cumbersome and much longer than the foregoing method, but in this case it was unavoidable.

We note that the corrections Δx_0 and Δy_0 to the ephemeridal coordinates of the crater Hoesting-A were determined from measurements corrected for the relief by means of Hayn's maps. Thus, the position of the apparent center of the moon's disk was determined sufficiently accurately. Hayn did not make a second approximation (in calculating the height he did not determine the center of the moon with allowance for the errors of the moon's edge), this being a certain shortcoming of his work.

It was next necessary to change-over from the center of the most probable circle to the center of gravity of the moon. For this purpose it was first necessary to calculate the thickness of the hypothetical layer a for the observed librations in latitude d_0, and after this to calculate the coordinates Δx and Δy of the center of the figure of the moon relative to the center of gravity, using (3.21).

Knowing the latter, we then obtain the distances h of the points of the edge to the center of gravity, using (3.26) and (3.27) for their calculation.

Tables 12 -- 17 list each one series of observations of the values of a, b_0, and C -- the position angle of the axis of rotation of the moon, the coordinates Δx and Δy, and also the radius h_0 (for each observation) of the sphere to which we refer the irregularities of the edge. Tables 12, 14, 16 and 17 contain, in addition, the corrections Δx_0 and Δy_0 for the rectangular coordinates of the crater Messing-A, calculated from formula (3.23). These are not given for the observations of Mikhaylovskiy and Yakovkin, for reasons given above.

It was mentioned in the third chapter that when calculating the irregularities of the edge we assumed the radius of the moon r'_0 derived from the particular series of observations. It contains a certain systematic error, which will be present also in the measured values of h. But when calculating the irregularities, when the differences $h - h_0$ are evaluated, this error is eliminated. The average radius of the moon was corrected for the libration change and is given in Table 4.

After reducing the values of r'_0 to the average parallax and to the plane of observation, we calculated the irregularities of the edge H using (3.23).

Вапachiewicz

Table 4

Ряд наблюдений	Средняя либрация по широте	π_0
Краснов	−2".2	15'32".56
Михайловский	+2.3	15 32.48
Банахевич	−1.4	15 32.61
Яковкин	+0.7	15 32.95
Вельнович	−0.1	15 32.35
Нефедьев	+1.5	15 32.21

KEY: 1) Series of observations; 2) average libration in latitude; 3) Krasnov; 4) Mikhaylovskiy; 5) Banachiewicz; 6) Yakovkin; 7) Vel'novich; 8) Nefed'ev.

We found it advantageous to construct the map of the relief of the moon in the selenographic system of coordinates, as was done by Heyn /25/. Let us recall again that the positive pole of such a coordinate system is the point of intersection of the first meridian of the moon with its equator. The longitudes P are measured from the north pole of the moon towards increasing position angles, while the latitudes D are reckoned positive in the direction towards the earth.

The coordinates P and D were calculated in the processing of the libration observations. From these coordinates we obtain the corrections for the irregularities of the moon's edge after Heyn's maps. Usually P and D are calculated accurate to 0.1°. This is quite adequate for our purposes, if we recall that one degree on the Moon's spheroid subtends at the earth an angle of 16".

It must also be noted that in the calculations of P and D we made

use of the position angles p_0, reckoned relative to the center of figure of the moon. However, the origin has now been transferred to the center of gravity of the moon. But this does not influence any way at all significantly the values of P and D. The latter have been calculated from the formulas

$$\begin{aligned} P &= p_0 - C + \Delta_1 + \Delta_2, \\ D &= D_1 + 0''.26, \end{aligned} \tag{4.02}$$

where

$$\begin{aligned} \Delta_1 &= \rho \sin(\Pi - \chi)\left(0''.26 - \frac{1}{2} D_1\right), \\ \Delta_2 &= 0''.0088\ l_0 b_0, \\ \Pi &= p_0 - C, \\ D_1 &= \rho \cos(\chi - \Pi), \\ \operatorname{tg}(180 - \chi) &= \frac{\operatorname{tg} l_0}{\sin b_0}. \end{aligned}$$

We have noted earlier that the transfer of the coordinate axis from the center of figure to the center of gravity of the moon entails a change in p_0 not greater than by 3.5'. As can be seen from (4.02), this error will enter completely into P. But such a change in the coordinate P will be within the limits of the accuracy with which it has been calculated. On the other hand, D remains unchanged at all.

Actually,

$$dD_1 = \rho \sin(\chi - \Pi) \frac{d\Pi}{57^{\circ}} \tag{4.03}$$

and at the maximum values of the quantities contained there,

values ε_φ $d\lambda_1$ do not exceed 0.01°. Therefore, in constructing the maps we have used the previously calculated selenographic coordinates P and D, which has considerably reduced the computational work, which is big enough as is.

Having the calculated values of the height H and their selenographic coordinates P and D, we could proceed to trace the isohypses. Using graph paper, we drew a coordinate grid in a scale of 1°/cm, representing the equator, parallels, and the latitude circle by mutually perpendicular lines. We then spotted on the coordinate grid the points of the moon's edge, relative to the coordinates P and D, and marked each of these by the value of H in tenths of a second of arc. In order to know to which observer the particular points belonged, we spotted them with colored crayons. As can be seen from Table 3, we spotted a total of 5,630 points. The lines of equal levels were drawn every 0.2" in height, and the null isohypses and the isohypses of the elevations were traced by solid lines, while the depressions were shown dotted. The tracing of the isohypses was found to be not a simple problem, since the points were distributed unevenly in the investigated edge belt. Thus, while in the regions of the pole of the moon they were concentrated for certain values of D, and each square degree contained several height markers, in other places to the contrary only one point was contained in an area of 3 or 4°. It was sufficiently easy to display large elevations and depressions, but to figure out the minute relief was sometimes difficult.

However, we adhered from the very beginning to the rule of drawing isohypses only in those places, where there was a sufficient number of points from which an idea could be gained regarding the relief.

14. Description of the Maps

On our maps, the lines of equal level are not isohypses in the usual sense, since, for example, a mountain in the form of a circular cone is represented by a system of strongly stretched oval curves. This happens because usually we measure not the true height of the moon, but its projection on the plane of the picture. Therefore, the isohypses are represented on the map as if the observer were in the direction of the coordinate axis. Consequently, the irregularities obtained from our maps do not give an idea of the true height of the mountain. We cannot say what its actual height is, also because the maps represent a smoothed-out relief. However, in compilation of maps of this kind, such a problem does not arise. It is important merely that the maps represent everytime, for all optical libretions, a lunar profile which is close to reality. The reliability with which the isohypses were drawn depended at least on two conditions, on the uniform distribution and necessary density of points in a given section of the moon's surface, and also on the degree to which the height markers, determined from different series of observations, agreed with each other. The latter condition was satisfied in our case quite well. Where a large elevation or a large

depression was observed, all the points spotted in this region confirmed the fact quite clearly. The relief represented on our maps is in general similar to that traced by Hayn. One cannot speak, however, of any coincidence of isohypses, since our heights are reckoned from a certain common level surface, something which Hayn does not. We therefore cannot make in principle a direct comparison of individual heights, taken from our maps and from those of Hayn, since our corrections for irregularity contain the so-called large relief, which does not enter in Hayn's irregularities.

We have already mentioned that the reliability of drawing the lines of equal heights depends to a considerable extent on how densely the height markers are placed in the given section of the moon's surface. If we consider our maps from this point of view, we can say the following: for values of P between 355 and 5° and for positive D, there was a large, even excessive concentration of points, whereas within these limits of P, but at negative selenographic latitudes, there were so few points, that we refused to draw isohypses. The points were distributed exactly in the same manner at values of P equal to 175 -- 185°, and therefore at negative values of D the maps show a white spot. A similar situation prevails also on Hayn's maps. Apparently these places of the moon are difficult to observe. The distribution of points in individual zones of the edge belt can be seen from the following table:

Table 5

1) Number of points,

P	Δ inclo rotat		P	Δ inclo rotat	
	+ D	− D		+ D	− D
0—10	166	54	180—190	143	75
10—20	65	58	190—200	126	115
20—30	67	31	200—210	92	54
30—40	83	34	210—220	138	79
40—50	48	56	220—230	91	69
50—60	68	51	230—240	128	63
60—70	71	42	240—250	122	81
70—80	62	53	250—260	113	47
80—90	50	38	260—270	115	81
90—100	60	40	270—280	123	61
100—110	76	53	280—290	104	57
110—120	63	41	290—300	119	89
120—130	92	46	300—310	110	50
130—140	64	41	310—320	72	71
140—150	103	36	320—330	142	81
150—160	51	58	330—340	120	38
160—170	62	47	340—350	82	89
170—180	70	33	350—360	136	96
Total Итого...	1374	814	Итого...	2146	1206

From the data of Table 5 we can conclude that at positive latitudes there were more points than at negative ones. This occurs for the following reason. If we look at the maps, we note readily that the entire edge belt from 0° to + 10° in latitude is almost completely filled with points, whereas at negative D one can draw isotypes only from 0° to - 8°, since there were no markers in the remaining part of the belt. There were not enough points in the zones between longitudes 20° — 30°, 205° — 210°, and 330 — 340°

at negative latitudes, and 40° -- 50° at positive latitudes, as well as in the aforementioned zones 175 -- 185° and 355° -- 5°. In all parts of the edge belt, the points were as a whole distributed uniformly. It must also be noted that in the belt covering the western half of the moon, there were more points on the eastern part. The large heights and valleys are represented on our maps with great reliability. They frequently reach in our maps 3 or 4 km. However, these heights and valleys are considerably smaller than those given in the selenographic investigations of Franz, Ritter, Hopmann, and others. In a recently published paper of Benoupe /84/ it is indicated that the amplitude of the height, determined by him by stereoscopic means using two photographs of the moons, reaches 10 km, while the slope of these points is on the average greater than on the earth.

The relief of the moon was represented by us on eight maps. It is drawn in a coordinate system, abscissas of which are the longitudes P and the ordinates are the positive and negative latitudes B. The selenographic coordinates P and D can be read on the map accurate to 0.1°. For convenience in use, the coordinate P is marked every 5°, while D is marked every 2°. In order to be able to pick off from the maps the corrections for relief, it is necessary to calculate the coordinates P and D using formulas (4.02). However, it may be more convenient to represent the coordinates in Krakovian form as given in the papers of Rybka /23/ Banachiewicz /85/ and Koziel /66/. The

heights picked off the maps refer to the average distance of the moon.

15. Concerning the Accuracy of the Maps

To describe the maps it is important to determine the accuracy of the corrections picked off from them for the irregularities H'. This accuracy will apparently depend on the errors which enter into the heliometric measurements, and also on the errors which are connected with drawing the equal-level lines. In order to calculate these errors, it is necessary to recall the method of measuring the irregularities of the moon's edge and the method of mapping the relief. As already mentioned, the heights H calculated from formula (3.33) were subsequently plotted on a coordinate grid, and this was followed by the tracing of the isolypses. Consequently the irregularities picked off the maps will include an error, which we shall call the "smoothing error." This error can be calculated from the formula

$$\varepsilon_{H-H'} = \pm \sqrt{\frac{\sum v^2}{n-1}}, \qquad (4.04)$$

where $v = H - H'$ and n is the number of these differences. The values of v are given for each series in Tables 18 — 23; the brackets contain the differences which were not used in these calculations, since the measured heights deviated greatly from other determinations and were disregarded in constructing the maps.

As can be seen from (3.33), H will contain the error in measuring the radius h. We denote this by ε_y. This latter can be

calculated in the following way. We obtain from observation the measured distances s from the crater Moesting-A to the edge of the moon. The error of the observed s will consist of the error of bisection of the crater by the edge of the moon and the error in reading the scales and the micrometer. In observations, the crater is aimed to the edge twice and two readings are made accordingly of the micrometer. One can therefore calculate the deviations W of the individual values of two readings of the micrometer from their average, and then the error in measurement of s will be

$$\varepsilon_s = \pm \sqrt{\frac{\Sigma W^2}{n-m}}, \tag{4.05}$$

where n is the number of the individual deviations and m is the number of groups. In order to obtain the error of h or h', we turn to Eqs. (3.22). We have the following relation between the errors in the quantities s and h':

$$\varepsilon_{h'}^2 = \frac{\cos p}{\cos p_0} \varepsilon_s^2. \tag{4.06}$$

For a certain standard distribution of seven points over the edge of the moon, the average value of the coefficient cos p/cos p_0 is 0.90. Thus,

$$\varepsilon_{h'} = 0.95 \varepsilon_s = \varepsilon_{H'}. \tag{4.07}$$

If we denote the error of the irregularities taken from the map by $\varepsilon_{H'}$, then, obviously, we can write

$$\varepsilon^2_{H-H'} = \varepsilon^2_H + \varepsilon^2_{H'}$$

and therefore

$$\varepsilon^2_{H'} = \varepsilon^2_{H-H'} - \varepsilon^2_H. \qquad (4.08)$$

The errors ε_H, calculated from (4.08) for the individual series were as follows:

Table 6

① Series of observations	② Ряд наблюдений	ε_H
③ Krasnov	2 Краснов	±0".20
④ Mikhaylovskiy	3 Михайловский	±0.37
⑤ Banachiewicz	4 Банахевич	±0.20
⑥ Yakovkin	5 Яковкин	±0.26
⑦ Bel'kovich	6 Белькович	±0.21
⑧ Nefed'ev	7 Нефедьев	±0.21

On the average we shall have

$$\varepsilon_{H'} = \pm 0".24. \qquad (4.09)$$

From the data given in Table 6 we see that the greatest error is obtained from the observations of Mikhaylovskiy. The constants of the physical libration of the moon, derived from these observations, were also obtained with large average errors. The error in the observations of A. A. Yakovkin was somewhat greater than that from other series. This was due to the fact that in some measurements the calculated irregularities were considerably greater than those obtained from other series. We thought at first that the reason lies

in an incorrectly assumed value of the radius of the moon, but upon more careful examination of the results of the calculations this assumption was found to be incorrect. An impression is gained as if in some cases the observer imagined the relief to be more sharply pronounced than other investigators.

Thus, the accuracy of determination of the heights on the basis of different series is not the same. Therefore, in calculating the average error it would be more correct to calculate its "mean weighted" value, considering the errors $\varepsilon_{H'}$ as certain measured quantities of different weights. Let us assume the approximate mean of these values to be $\varepsilon_0 = 0.20''$ and let the deviations from it be v. Then the weighted average error $\overline{\varepsilon}_{H'}$ is found to be /86/:

$$\overline{\varepsilon}_{H'} = \varepsilon_0 \pm \frac{\sum pv}{\sum p}. \qquad (4.10)$$

The weight p involved here can be calculated from

$$p = \frac{1}{\varepsilon^2_{H'}},$$

and then the error of the irregularities taken from the map will be

$$\overline{\varepsilon}_{H'} = \pm 0''.22. \qquad (4.11)$$

The obtained average error will be greater in those places where the drawing of the isohypses was difficult, and will be less in the places where the relief has been traced with greater reliability.

Hayn assumes the average error of the irregularities taken from his maps to be ± 0.25". Speaking of accuracy of maps, it is necessary

to remember always that both Hayn's maps and those described in the present paper give a smooth relief, and therefore minute details on these may sometimes disappear. This is clearly seen from the following comparison. Bonsdorf and Kirvonen /37/ calculated the average errors m of the moon's profile, determined from the observations of the solar eclipse of 1945 and from Hayn's maps, and obtained the following values:

m (Bonsdorf) = ± 0.10".

m (Lindblad) = ± 0.15.

m (Hayn) = ± 0.28.

It is seen therefore that the profile obtained from the observations of the eclipse is determined more accurately than that obtained from Hayn's maps. In the future when constructing maps it will be possible to use a considerably greater observational material, which undoubtedly will lead to better detailing of the moon's profile. However, even at the present time the accuracy of observations, after correcting them in accordance with the available maps for irregularities of the moon's edge, is considerably increased. Thus, if it is considered that the errors of the edge are random deviations, then the average error of one observation of the moon will amount, as a result of this factor, to ± 0.3". Consequently, allowance for the irregularities of the edge with our maps reduces the average error of

observation of the individual points of the edge by approximately a factor of three. At the same time, in reducing the observations for the relief we get rid of the systematic errors of periodic character. As was already mentioned in the first chapter, certain fluctuations in the moon's motion are apparent and due to the effect of irregularities of the moon's edge on the observations.

S. M. Kosik /88/, using observations of occultations as examples, illustrates how important it is to take into account the irregularities of the moon's edge. The use of Hayn's maps lead to a considerable reduction in the random errors, and the systematic errors manifest themselves in this case more pronouncedly and can be more accurately determined. Such errors, for example, include errors in determination of the time, due to irregularities of the rotation of the earth. S. M. Kosik has shown that to derive a time correction from the observations of the moon, if the relief is taken into account with Hayn's maps, one fifth the observations is necessary than in the case when we wish to obtain the same correction with the same accuracy, but without using the maps.

The average error of the irregularities taken from our maps is found to be the same (if not less) as that obtained with Hayn's maps, in spite of the fact that he used twice as many points. This indicates once more the high accuracy of the heliometric observations.

Chapter V

INVESTIGATION OF MAPS OF THE MOON'S RELIEF

The main purpose of the present work is to be able, when using our maps, to determine the position of the center of gravity of the moon from observations of its edge more accurately than could be done until now. We have already mentioned that earlier determinations of the moon's center of gravity were inaccurate, because of the indeterminacy in the establishment of the zero-level surface from which to reckon the heights. Now, that the zero-level surface has been theoretically derived and has been practically employed in our maps, a more accurate determination of the position of the center of gravity of the moon has become a reality.

In addition, this work has a direct bearing on selenographic investigations. Until now the coordinates of points on the moon's surface were measured relative to the crater Moesting-A, and their heights were reckoned from a certain level, which was determined from external forms of the relief under the assumption that the sum of the height and depressions on the visible surface of the moon is in general close to zero. However, in view of the presence of asymmetry in the figure of the moon, a zero-level surface established in this manner is highly indeterminate and therefore the heights were referred

to everytime to different levels. Now that a level surface has been rigorously derived, this indeterminacy is eliminated. At the same time, a possibility exists of calculating more accurately the coordinates of the crater Messing-A and other points on the moon's spheroid, knowing the position of the center of the moon and its radius. The reduction of the observations on the basis of our maps will permit, in addition, to eliminate the systematic errors in the calculation of the elements of rotation of the moon and its coordinates.

In constructing the maps we set two conditions which they must satisfy:

1) The radius of the most probable circle, corrected for irregularities obtained from our maps, should not depend on the optical libration in latitude;

2) the corrections to the latitude of the moon, calculated from occultations and meridional observations, reduced for irregularities of the edge, should decrease in absolute magnitude and should have a random character.

In the following sections we expound the results of testing the maps from the point of view of satisfaction of the conditions formulated above.

16. Libration Effect in the Radius of the Moon

We have noted earlier that in the irregularities of the moon's edge, determined from our maps, there is contained the so-called "large relief." Consequently, if the observations are corrected for the relief on the basis of these maps, then the libration effect in the apparent radius of the moon should not appear.

In order to verify the extent to which this criterion is satisfied, we again reduce the heliometric observations of the moon for irregularities of the moon's edge, taken from our maps. For this purpose we used three heliometric series: Krasnov's /80/ Nefed'ev's /56/, and Hartwig's as processed by Naumann /90/. We made use for this analysis the series of observations of Krasnov and Nefed'ev because this reduces considerably the computational work, which is very large as it is. The point is, as already mentioned in the preceding chapter, that the corrections for the relief with Hayn's maps were introduced by me in Krasnov's observations and in my own observations directly in the difference $(h_0 - h')$ of the ephemeridal and measured radii of the moon, in other words, in the right halves of the equations

$$\Delta x_0 \cos p_0 + \Delta y_0 \sin p_0 - \Delta k = h_0 - h', \qquad (3.23)$$

whereas in other observation series it was the measured values of s that were corrected for irregularities, and consequently, in order to obtain the three terms of Eqs. (3.23) without corrections for the relief, it would have been necessary to solve (3.22) again, i.e., to

carry out a tremendous computational work. The latter is obviated by using the aforementioned observations of Krasnov and Nefed'ev. Actually, using (hg - h'), uncorrected for irregularities of the edge with Hayn's maps, we have corrected them for the relief with our maps. Obtaining in this way the right halves of the trial Eqs. (3.23) and setting up the normal equations, we solve them by the method of least squares, determining the correction of interest to us for the radius of the moon, Δh. The latter is listed in Tables 7 and 8.

We used the Hartwig heliometric series in this investigation for the following reasons. This series covers a large time interval, namely from 1890 through 1922, and contains 266 observations of the moon. On the average in each observation there were 12 points of the edge. Thus, Hartwig made more than 3,000 measurements. In addition, this large observational material, obtained by Hartwig with the first rate heliometer of the Bamberg Astronomical Observatory, was not used by us in construction of the maps. It was therefore quite desirable to test our maps with this extensive material. At the same time, the observational data and the calculations have been published in detail in Naumann's work, so that the computation work was facilitated.

The correction dR for the moon's radius was determined by Naumann by solving trial equations of the form

$$dR - \sin(\pi + \pi')\cos\delta \cdot d\alpha - \cos(\pi + \pi')\, d\delta = \cos\pi'' \cdot d\Delta', \quad (5.01)$$

where $d\alpha$ and $d\delta$ are the sought corrections for the differences of the direct ascensions of the crater Moesting-A and the center of the moon, and respectively to the difference in the declinations of these points, while dA' are the differences between the observed and the calculated distances from the crater to the points of the moon's edge. The values $dA' \cos \pi''$ are given by Naumann in Table 6 of his work. The position angle $(\pi \div \pi')$ of the observed points of the edge relative to the center of the moon's disk were calculated by us from the formula

$$M = p - \pi''. \tag{5.02}$$

The position angle p of the points of the edge relative to the crater Moesting-A, which enters into this equation, was taken by us from the same Table 6, while the angle π'' at the point of the edge between the directions to the center of the moon and to Moesting-A was calculated by us from the relation

$$\sin \pi'' = \frac{\Delta}{R} \sin (p - \pi). \tag{5.03}$$

The distance Δ and the position angle π of the crater Moesting-A relative to the center of the moon was taken from Table 4 of Naumann's work, and the apparent radius of the moon R was taken from Table 1. After correcting the free terms of the trial Eqs. (5.01) for irregularities of the moon's edge with our maps, we then solve these equations by the method of least squares and determine for each observation the correction dR for the radius of the moon, which together with the values of the optical libration in the latitude

Table 7

Krasnov's Observations

№№	Δh	№№	Δh	№№	Δh
1	— 1.30	44	— 0.74	85	— 1.45
3	— 0.66	45	— 1.17	86	— 0.50
4	— 0.47	46	— 2.18	87	— 1.12
5	— 1.55	47	— 1.93	88	— 1.40
6	— 0.27	48	— 0.77	89	— 1.76
7	— 1.25	49	— 1.29	90	— 1.64
8	— 0.25	50	— 2.21	91	— 1.57
9	+ 0.31	51	— 2.03	92	— 1.60
10	— 1.20	52	— 1.30	93	— 0.86
		53	— 1.62	94	— 1.61
11	— 1.90				
12	— 1.19	54	— 1.96	95	— 1.58
14	— 2.28	55	— 1.11	96	— 1.69
15	— 0.30	56	— 2.19	97	— 1.17
16	— 1.08	57	— 1.77	98	— 1.22
17	— 0.82	58	— 1.66	99	— 0.83
18	— 1.83	59	— 0.59	100	— 1.74
19	— 1.12	61	— 0.87	101	— 1.59
20	— 1.69	62	— 1.94	102	— 1.52
21	— 0.96	63	— 2.24	103	— 1.99
		64	— 1.33	104	— 1.49
22	— 1.12				
23	— 1.40	65	— 1.85	105	— 1.26
24	— 1.43	66	— 1.92	106	— 0.30
25	— 1.08	67	— 0.94	107	— 1.44
27	— 1.17	68	— 1.20	108	— 1.75
28	— 1.61	69	— 1.70	109	— 1.56
29	— 1.32	70	— 1.89	110	— 1.28
30	— 2.08	71	— 1.61	111	— 1.73

31	— 0.62	72	— 1.14	112	— 1.40
32	— 0.69	73	— 0.64		
		74	— 1.45		
33	— 1.66				
35	— 2.81	75	— 1.02		
36	— 1.56	76	— 1.65		
37	— 1.36	77	— 0.84		
38	— 2.99	78	— 1.03		
39	— 2.32	79	— 1.02		
40	— 1.94	80	— 1.02		
41	— 1.63	81	— 1.41		
42	— 0.35	82	— 1.14		
43	— 1.52	83	— 1.99		
		84	— 1.23		

Table 8

Nefed'yev's Observations

№№	Δh	№№	Δh	№№	Δh
3	— 0°34	54	+ 0°26	104	— 0°62
4	+ 0.31	55	— 0.26	105	— 1.16
6	— 0.27	56	— 0.46	106	— 0.79
7	— 0.42	57	— 1.26	107	— 0.42
8	— 0.51	58	— 1.16	108	— 0.31
9	— 0.39	59	— 0.03	109	— 1.00
10	— 0.05	60	— 0.54	110	+ 0.19
11	— 0.84	61	— 1.13	111	— 0.18
12	— 0.02	62	— 0.86	112	— 0.65
		63	— 0.47	113	— 1.03
13	— 1.71				
14	— 0.62	64	— 1.15	114	— 0.80
15	— 0.26	65	— 0.54	115	+ 0.11
16	+ 0.18	66	— 2.05	116	+ 0.75
17	+ 0.23	67	+ 0.16	117	— 1.33
18	— 1.15	68	— 0.57	118	— 0.65
19	+ 0.34	69	— 0.42	119	— 0.73
20	+ 0.15	70	+ 0.60	120	+ 0.20
21	+ 0.99	71	+ 1.35	121	— 0.77

22	— 0.85	72	— 0.03	122	— 1.04
		73	— 1.69	123	— 0.70
23	— 0.32				
24	— 0.57	74	+ 0.20	124	(— 5.43)
25	+ 0.23	75	— 0.69	125	— 1.00
26	— 0.05	76	0.00	126	— 1.73
27	— 0.33	77	— 0.04	127	— 1.00
28	— 0.54	78	— 0.33	128	— 0.38
29	+ 0.67	79	— 0.93	129	— 0.51
30	+ 0.41	80	— 1.16	130	— 0.16
31	— 0.31	81	— 0.65	131	— 0.58
32	— 0.68	82	— 0.68	132	— 0.09
		83	— 0.12	133	— 0.13
33	+ 0.78				
34	— 0.20	84	— 0.98	134	+ 0.24
35	— 0.10	85	+ 1.30	135	— 1.58
36	+ 1.33	86	— 0.50	136	— 0.82
38	+ 0.12	87	— 1.44	137	— 1.47
39	— 0.34	88	+ 0.06	138	— 1.55
40	— 0.23	89	+ 0.13	139	— 0.52
41	+ 1.09	90	— 0.47	140	— 0.56
42	— 0.42	91	+ 0.12	141	— 0.65
43	— 0.41	92	— 0.14	142	— 1.06
		93	— 0.95		
44	— 0.24				
45	— 0.44	94	+ 0.96		
46	+ 0.23	96	— 1.30		
47	+ 1.46	96	— 0.39		
48	+ 0.23	97	— 2.66		
49	— 0.67	98	— 1.10		
50	— 0.74	99	— 0.21		
51	— 0.79	100	— 0.17		
52	— 0.57	101	— 1.96		
53	— 0.42	102	— 1.93		
		103	— 0.46		

Table 9

Hartwig's Observations

M.No.	ΔR	b_0	M.No.	ΔR	b_0
1	+ 0".49	— 4".7	61	+ 0".67	— 4".3
2	+ 0.54	— 5.4	62	+ 0.37	+ 0.4
3	+ 0.86	— 8.2	63	+ 0.62	+ 4.7
4	+ 0.53	+ 4.7	64	+ 1.07	+ 5.2
5	+ 0.96	+ 2.3	65	+ 0.57	— 2.1
6	+ 0.77	— 6.0	66	+ 0.49	+ 7.3

7	+ 0.55	— 2.4	67	+ 0.35	— 3.8		
8	+ 0.01	— 3.4	68	+ 0.50	+ 0.7		
9	+ 0.14	— 5.8	69	+ 0.96	+ 4.8		
10	+ 0.84	— 6.0	70	+ 0.40	+ 5.3		
11	+ 0.29	— 5.8	71	+ 0.62	+ 6.3		
12	+ 1.13	+ 5.3	72	+ 0.30	— 2.4		
13	— 0.38	+ 6.5	73	+ 0.99	— 3.6		
14	— 0.93	+ 5.5	74	+ 0.35	+ 6.9		
15	+ 0.92	— 4.2	75	+ 1.16	+ 7.3		
16	+ 0.74	+ 1.9	76	+ 0.80	+ 5.2		
17	+ 0.78	— 4.9	77	+ 1.07	+ 2.3		
18	+ 0.66	— 5.7	78	+ 0.07	+ 7.3		
19	+ 0.54	— 6.1	79	+ 0.49	+ 6.7		
20	+ 0.54	— 6.1	80	+ 0.88	+ 7.4		
21	+ 1.04	— 2.9	81	+ 0.39	+ 0.1		
22	+ 0.45	— 0.7	82	+ 0.58	— 1.2		
23	+ 0.13	+ 7.1	83	+ 0.96	+ 4.8		
24	+ 0.50	+ 7.3	84	+ 0.51	+ 3.5		
25	+ 0.93	+ 3.6	85	+ 1.03	+ 1.0		
26	+ 0.47	— 0.4	86	+ 0.69	— 0.6		
27	— 0.57	— 3.5	87	+ 0.63	— 2.1		
28	+ 0.87	— 5.7	88	— 0.06	— 3.6		
29	+ 0.33	+ 2.7	89	+ 0.45	— 0.2		
30	+ 0.55	— 2.3	90	+ 0.59	— 1.7		
31	+ 0.77	— 6.2	91	— 0.01	— 3.1		
32	+ 0.35	— 5.6	92	+ 0.61	— 5.7		
33	+ 0.39	— 5.5	93	+ 0.58	+ 4.9		
34	+ 0.09	— 0.1	94	+ 0.44	— 5.8		
35	+ 0.73	— 0.5	95	+ 0.77	— 3.9		
36	+ 0.46	— 5.4	96	+ 0.63	— 5.8		
37	+ 0.80	— 5.9	97	+ 0.83	— 5.9		
38	+ 0.22	— 5.7	98	+ 0.85	— 2.1		
39	+ 0.81	— 3.8	99	+ 0.18	+ 7.3		
40	— 3.20	— 6.3	100	+ 0.60	+ 6.9		
41	+ 0.45	— 3.5	101	+ 0.73	+ 7.1		
42	+ 0.62	— 1.7	102	— 0.32	+ 6.3		
43	+ 0.24	— 0.1	103	+ 0.57	+ 5.4		
44	+ 0.62	— 5.6	104	+ 0.54	+ 4.2		
45	+ 0.71	— 6.0	105	+ 0.84	+ 2.6		
46	+ 0.51	— 3.6	106	+ 0.76	+ 0.1		
47	+ 0.70	— 6.3	107	+ 0.59	— 4.3		
48	+ 0.76	— 4.7	108	+ 5.26	— 4.9		
49	+ 0.48	— 6.0	109	+ 0.94	— 3.9		
50	+ 1.01	+ 7.1	110	+ 0.66	— 4.6		

51	+ 0.71	+ 7.5	111	+ 0.88	— 6.0
52	+ 0.20	+ 0.8	112	+ 0.37	— 3.9
53	+ 0.19	+ 6.2	113	+ 0.65	— 0.5
54	— 0.18	— 4.8	114	+ 0.73	— 4.5
55	+ 0.43	3.8	115	+ 1.18	— 5.5
56	+ 0.69	— 2.7	116	— 0.17	— 3.7
57	+ 0.31	5.8	117	+ 0.63	— 0.1
58	+ 0.69	+ 5.9	118	+ 0.71	— 4.8
59	+ 0.68	+ 7.3	119	+ 0.30	— 5.6
60	+ 0.16	— 5.2	120	+ 0.89	— 3.1
121	+ 0.73	— 4.9	181	+ 0.34	— 2.4
122	+ 0.40	— 5.0	182	+ 0.77	— 3.8
123	+ 0.59	+ 7.4	183	+ 0.35	— 4.8
124	+ 0.65	— 3.0	184	+ 0.78	— 4.6
125	+ 0.79	— 5.3	185	+ 0.46	— 5.3
126	+ 0.53	— 2.7	186	+ 0.71	— 6.1
127	+ 0.25	— 3.6	187	+ 0.79	+ 1.6
128	+ 0.55	— 2.2	188	+ 1.16	+ 0.2
129	+ 0.53	— 3.2	189	+ 0.26	— 1.3
130	+ 0.47	— 4.5	190	+ 0.41	— 5.6
131	+ 0.20	— 5.6	192	+ 0.82	— 3.1
132	+ 0.07	— 6.0	193	+ 0.55	— 1.9
133	+ 0.98	— 6.3	194	+ 0.81	— 5.7
134	+ 0.11	— 0.5	195	+ 0.19	— 5.2
135	+ 0.01	+ 0.4	196	— 0.54	— 5.2
136	+ 0.03	+ 3.5	197	+ 0.12	— 5.6
137	+ 0.22	— 5.4	198	— 0.27	— 6.2
138	+ 0.20	+ 2.7	199	— 0.33	— 6.1
139	+ 0.40	— 5.4	200	+ 0.05	— 6.0
140	+ 0.45	— 0.3	201	+ 0.26	— 5.4
141	+ 0.76	— 4.6	202	+ 0.75	+ 0.5
142	+ 0.58	— 6.0	203	+ 0.56	— 3.9
143	— 1.41	— 5.3	204	— 1.04	+ 4.5
144	+ 0.70	— 6.4	205	+ 0.93	+ 5.5
145	+ 0.83	— 6.3	206	+ 0.65	— 3.5
146	+ 0.80	— 5.8	207	+ 0.35	— 2.1
147	+ 0.42	— 4.9	208	+ 0.58	— 0.4
148	+ 0.47	— 3.6	209	+ 0.55	+ 0.9
149	+ 0.89	— 2.0	210	+ 0.43	+ 2.2
150	+ 0.19	— 0.2	211	+ 0.82	+ 3.9
151	+ 1.03	— 5.2	212	+ 0.17	+ 6.1
152	+ 1.31	+ 2.1	213	+ 0.59	+ 6.6
153	+ 0.61	+ 3.6	214	— 0.12	— 6.6
154	— 0.12	+ 5.4	215	+ 0.22	+ 5.5
155	+ 0.22	+ 6.6	216	+ 0.35	— 0.6
156	+ 0.11	+ 4.3	217	+ 0.66	+ 6.7

157	+ 0.77	+ 7.3	218	— 0.01	+ 7.2
158	+ 0.26	— 3.6	219	+ 0.76	— 4.4
159	+ 0.72	— 4.6	220	— 0.15	— 3.2
160	+ 0.60	+ 0.2	221	+ 0.58	+ 0.4
161	+ 0.08	— 4.6	222	+ 1.05	+ 4.1
162	+ 0.54	— 6.0	223	— 0.25	— 0.5
163	+ 0.82	— 5.8	224	+ 0.46	+ 0.9
164	+ 0.25	— 6.3	225	+ 0.28	+ 5.7
165	+ 0.57	— 5.7	226	+ 0.88	+ 6.6
166	+ 0.47	— 5.0	227	+ 0.22	+ 7.2
167	+ 0.66	— 3.7	228	+ 0.02	+ 7.2
168	+ 1.04	— 2.6	229	+ 0.56	+ 7.3
169	+ 0.48	— 1.1	230	+ 0.57	+ 7.0
170	+ 0.55	— 1.3	231	+ 0.72	+ 6.4
171	+ 0.63	0.0	232	— 1.04	— 1.1
172	+ 0.78	+ 1.6	233	+ 0.32	— 2.5
173	+ 0.13	+ 6.3	234	+ 0.51	— 3.8
174	+ 0.09	+ 2.8	235	+ 0.73	— 4.9
175	+ 0.92	+ 3.9	236	+ 0.62	— 4.9
176	+ 0.24	+ 5.4	237	+ 0.55	+ 2.3
177	+ 0.25	+ 5.4	238	+ 0.77	— 3.5
178	+ 0.53	+ 7.1	239	+ 0.86	— 1.4
179	+ 0.80	+ 5.4	240	+ 0.85	+ 2.6
180	+ 0.07	+ 0.9	241	+ 0.69	+ 4.0
242	+ 0.84	+ 5.3	252	+ 0.13	— 5.8
243	+ 0.02	+ 6.2	253	+ 1.14	— 2.4
244	— 0.10	+ 5.1	254	+ 0.52	— 5.1
245	+ 0.65	+ 6.0	255	+ 0.92	— 2.7
246	+ 0.82	+ 7.0	256	+ 0.30	+ 7.1
247	+ 0.04	+ 7.2	257	+ 1.15	+ 7.0
248	— 0.04	+ 6.6	258	+ 0.69	+ 6.5
249	+ 0.54	+ 3.5	259	+ 0.82	+ 2.8
250	+ 0.70	— 5.6	261	+ 1.05	— 0.8
251	+ 0.22	— 5.8	262	+ 0.95	— 4.6
			263	+ 0.09	— 1.8
			264	+ 1.44	— 2.5
			265	+ 1.41	— 5.9
			266	+ 0.58	— 1.8

b_0 are listed in Table 9.

After obtaining the values of Δh and ΔR, we then broke them down into groups in accordance with the optical libration in latitude, and calculated in each group the mean weighted values, which are listed in Table 10.

Table 10

1) Krasnov's observations, 2) Nefed'ev's observations, 3) Hartwig's observations.

(1) Наблюдения Краснова		(2) Наблюдения Нефедьева		(3) Наблюдения Гартвига	
b_0	Δh	b_0	Δh	b_0	ΔR
−5°7	−1″32	−5°1	−0″44	−5°8	+0″53
−4.0	−1.46	−3.9	−0.33	−4.1	+0.55
−2.1	−1.40	−2.2	−0.36	−2.1	+0.64
−0.1	−1.25	+0.3	−0.54	0.0	+0.50
+2.1	−1.27	+2.1	−0.56	+2.3	+0.67
+4.6	−1.39	+4.2	−0.55	+4.2	+0.65
+6.7	−1.55	+6.7	−0.30	+6.6	+0.47

Assuming that a linear relation should exist between the apparent radius of the moon and the optical libration in latitude, we made up trial equations of the form

$$\Delta h = \Delta h_0 + k b_0 \qquad (5.04)$$

and solved them by the method of least squares. The results of this solution are listed in Table 11.

Table 11

1) Series of observations, 2) after introduing corrections for the irregularities of the edge, 3) with Hayn's maps, 4) with Nefed'ev's maps, 5) Krasnov, 6) Nefed'ev, 7)Hartwig.

1) Ряд наблюдений	2) После внесения поправок за неровности края	
	3) по картам Гайна	4) по картам Нефедьева
Краснов 5)	$\Delta h_0 = -1''.38 \pm 0''.06$ $k = +0.057 \pm 0.013$	$\Delta h_0 = -1''.38 \pm 0''.041$ $k = -0.008 \pm 0.010$
Нефедьев 6)	$\Delta h_0 = -0.51 \pm 0.05$ $k = +0.031 \pm 0.013$	$\Delta h_0 = -0.44 \pm 0.046$ $k = -0.004 \pm 0.011$
Гартвиг 7)	$dR_0 = +0.46 \pm 0.034$ $a = +0.034 \pm 0.038$	$dR_0 = +0.57 \pm 0.034$ $k = +0.0006 \pm 0.0080$

In addition, we calculated the libration coefficient k in Hartwig's series for the case when these observations were corrected for irregularities of the edge with Hayn's maps, using for this purpose the data given by Naumann in Tables 4 and 7; his value is given in Table 11. For comparison we give also the coefficients k, calculated from the observations of Krasnov and Nefed'ev introduing in them corrections for the relief by Hayn's maps.

It is seen from Table 11 that in all series there appears a clearly pronounced dependence of the radius of the moon on the optical libration in latitude, when the corrections for irregularities of the edge were taken from Hayn's maps. In the case of reduction of observations with our own maps, the coefficient of libration is zero. The very sensitive methods which we used to test our maps leads to the conclusion that the correction of observations for the relief, as done

with these maps, excludes the systematic errors in the radius of the moon, due to the lunar effect. Thus, the irregularities of the edge are referred to us to a barycentric sphere of constant radius.

We have already noted that the presence of asymmetry in the moon leads to the fact that the centers of the eastern and western halves of the moon do not coincide and that the coefficient of libration is found to be different when it is determined separately for each edge of the moon. When reducing the observations for irregularities with our maps, this does not take place, as can be illustrated with an example of processing of a series of heliometric observations of the moon /56/. If the irregularities are taken from Hayn's maps, the libration effect in the radius, for individual edges, was found to be

For the western edge = + 0.083".

For the eastern edge = - 0.018.

At the same time, when the observations were corrected for relief with our maps, the values of k were found to be accordingly:

For the western edge = + 0.014".

For the eastern edge = - 0.013.

This example shows again that the average radius and the center of the moon, are determined more reliably when the observations are reduced with our maps than heretofore.

17. Correction of the Latitude of the Moon.

The fact that the latitude of the moon, obtained from occultation of stars by the moon, differs from the value given by Brown's tables is, as is well known, due to several causes. Thus, for example, the flattening of the earth, was assumed by Brown to be 1/294, whereas to calculate the geocentric coordinates of the observer when reducing the moon's observations it is necessary to use a flattening value of 1/297, corresponding to the international spheroid. Furthermore, the latitude of the moon is influenced by the correction for the equinox of the catalog FK_3, obtained from modern meridional observations. Finally, Woolard /91/ established an error in Brown's tables and, in order to exclude it, the tabulated latitude must be increased by

$$\Delta\beta = +0''.26\cos(n - 10^\circ)\cos(2D - F + 270^\circ), \tag{5.05}$$

where $F = l - n$ is the difference between the mean longitude of the moon, l, and the mean longitude of the moon's node, n, while D is the difference between the mean longitudes of the moon and the sun. The sum of the aforementioned corrections of the orbital latitude of the moon can be represented by the following formula

$$\begin{aligned}\Delta\beta = &+0''.25\sin(F + n) + 0''.02\cos(F + n) + \\ &+0''.11\sin(F - n) - 0''.03\cos(F - n).\end{aligned} \tag{5.06}$$

As shown by Murray /92/ on the basis of an analysis of observations of occultations, the presence of these errors in the

latitude of the moon is confirmed and is expressed in general by means of terms with arguments $(F \pm n)$.

In addition to the foregoing terms, the correction to the moon's latitude includes terms with arguments ℓ and F and a constant quantity of value - 0,64", namely - 0.64" - 0.42" sin $(\ell - 8^{\circ})$ - 0.26" sin F + 0.08" cosF. It is assumed that the main cause of these last terms is the systematic effect of the irregularities of the moon's limb and the asymmetry in the figure of the moon.

Consequently, if the observation used to determine the correction to the latitude of the moon is subjected to a correction for irregularities of the moon's edge, taken from our maps, the correction to the latitude should diminish in magnitude.

To test our maps from this point of view, we used the Polish observations of occultations of stars by the moon, processed by Rybka /23/. This series covers the time from September 1901 through December 1922 and contains 199 observations of occultations. Rybka corrected his observations for irregularities of the edge with Hayn's maps and calculated the coefficients of the trial equations, in which the unknowns were the corrections $d\alpha$ and $d\delta$ to the equatorial coordinates of the moon. The trial equations in his case were of the form

$$s - \Delta = -a \cdot d\alpha - b \cdot d\delta + c \cdot dt + d \cdot p + e \cdot \varepsilon, \qquad (5.07)$$

in which s is the measured angular distance between the star and the center of the moon, and Δ the calculated distance, while dt, p, and ε

express the total effect of errors in s, due to errors in geocentric coordinates of the observer and errors in the positions of the stars. The errors in the coordinates of the center of the moon will be due to inaccuracy of the lunar tables, errors in determining the time, and the fact that the geometric center of the moon does not coincide with the center of gravity.

In the aforementioned work, Rybka gives the free terms of the trial equations, corrected for irregularities of the moon's edge with Hayn's maps, and also the selenographic coordinates P and D. He did not solve Eqs. (5.07), however. Their solution by the method of least squares was carried out in two versions, namely: with introduction for relief with Hayn's maps, and with our maps. We have obtained the following values for the unknowns:

	With Hayn's maps	with Nefed'ev's maps
$da =$	$+ 3''.86$	$+ 3''.29$
$d\delta =$	$- 0.86$	$- 0.39$
$dt =$	$+ 14.2$	$+ 15.3$
$p =$	$- 0.47$	$- 0.17$
$s =$	$+ 0.59$	$+ 0.58$

Using these data, we calculated the correction for the moon's latitude by the formula

$$\Delta B = \frac{[1 + (v\alpha)]\, d\delta - (v\delta)\, da}{[1 + (v\alpha)][1 + (\beta\delta)] - (v\delta)(\beta\alpha)}, \qquad (5.08)$$

where $(v\alpha)$, $(v\delta)$, $(\beta\alpha)$, and $(\beta\delta)$ are coefficients which we

interpolated for the mean longitude and latitude of a given series using Newcomb's tables /93/. It was found that this correction, determined from observations reduced with our maps, were decreased in absolute magnitude by 0.32" compared with those values which were obtained as a result of introducing corrections for irregularities of the moon's edge with Hayn's maps.

Thus, our maps satisfy fully the two conditions formulated above and consequently they are constructed for a common zero-reference level. Their use makes it possible to obtain the coordinates of the point for which the ephemerids of the moon have been compiled.

CONCLUSION

One of the most interesting and at the same time most complicated problems in celestial mechanics is the question of the study of the moon's rotation, which has engaged the attention of astronomers for more than 100 years. A large contribution to the solution of this delicate problem was introduced by the Kazan' astronomers, who carried out long series of observations of the moon with a heliometer, covering in the whole a time of more than 60 years. Starting with 1949, the photographic method has been used at the Engel'gardt observatory successfully for the study of this problem.

In view of the closeness of the moon and of the many details on its surface, it is possible to derive from observation the laws of its rotation with exceeding accuracy. At the same time, the same

circumstance considerably complicates the processing of the observational material, since all the irregularities in the structure of the moon exert a substantial influence on the observations. In all the meridional and heliometric measurements of the moon, and also in the determinations of the instants of occultations we observe in one form or another the edge of the moon which is covered with many irregularities. The German astronomer Mayn paid serious attention to the matter of excluding from the observations the errors due to irregularities of the moon's edge. For this purpose he made up maps of the moon's relief. However, it was found out later that both these maps, and the profiles of the moon's edge published by the French astronomer Weimer, have a major shortcoming which lies, as is well known, in the fact that the irregularities of the edge are referred in them to different leveled surfaces.

The present work is the first attempt at constructing maps of the moon's relief against a common level surface. The main results of this work are as follows:

1. A theoretical solution has been obtained for the problem of the level surface from which to reckon heights. This surface was determined by us in the form of a three-axis ellipsoid (see Eq. (2.30)), and was called, in analogy with the earth, a selenoid. The center of the selenoid is the center of gravity of the moon.

2. Using the hypothesis of A.A. Yakovkin regarding the figure of the moon's disk, we calculated the relative placement of the center

of figure and of the center of gravity of the moon as a function of the optical libration, and gave formulas for calculating the irregularities relative to the level surface.

3. Maps were constructed for the relief of the moon from heliometric observations, carried out with the heliometer of the Engel'gardt observatory over a period of fifty years.

4. An investigation was made of the maps, leading to the conclusion that they have been constructed against the common zero-reference level.

Thus, after correcting the observations for irregularities, with the aid of these maps, we exlude the systematic errors connected both with the micro relief and with the large-scale relief of the moon. It mustn't be forgotten however, when using these maps, that they show the smoothed relief. Therefore, for example, in reducing individual instants of occultation for irregularities of the edge we cannot always accomplish the desired purpose. However, in a large scale processing of occultation, as was undertaken in his day by Buttermann or by Newcomb, introduction of corrections for irregularities will undoubtedly improve the results. This pertains also to the reduction for irregularities of the edge of both meridional and heliometric or photographic observations of the moon. The latter are being particularly extensively engaged at the present time. The plan of the International Geophysical Year provides for setting up photographic observations of the moon simultaneously with the stars

and to correct them for irregularities of the edge it is again necessary to have exact maps of the moon's relief. This again emphasizes the urgency of the problem under consideration here.

The moon's relief is very highly varied and complicated, and therefore its representation on maps with all details is a very difficult task. One must have for this purpose extensive observational material. It will be possible later on to detail our maps, by making use of additional material. For this purpose it is quite desirable to process the 96 observations performed on the heliometer of the Engel'gardt observatory by I. V. Bel'kovich from 1943 through 1948 and the 260 observations of the authors of this book, obtained over an eleven year period (1946 — 1956). This will give approximately 2500 points of the edge zone of the moon. In addition, their exist heliometric observations carried out abroad by Schluter, Wichmann and Hartwig, the use of which can yield more than 5,000 points. However, the calculation of the barycentric irregularities of the edge with the aid of this last material entails great computational work, since the necessary data have not been published for this purpose.

The heights obtained from heliometric observations can be considered as reference points on the moon's surface. To detail the maps further one can subsequently make use of photographic material.

Astronomic Observatory imeni Engel'gart,
May 1957.

BIBLIOGRAPHY

1. J. Hevelii. Selenographia sea descriptio lunae... Danzig. 1647.
2. J. H. Schroter. Selenotopographische Fragmente... Bde I, II, 1791, 1802.
3. W. H. Lohrmann. Topographie der sichtbaren Mondoberfläche. 1824.
4. J. H. Mädler. Mappa selenographica. 1837.
5. J. Schmidt. Charte der Gebirge des Mondes. 1878.
6. J. Franz. Ortsbestimmung von 150 Mondkratern. Mitteil. Sternw. Breslau. I, 19
7. J. Franz. Die Figur des Mondes. Astr. Beob. Königsberg. Bd. 38, 1899.
8. J. Franz. Die Konstanten der physischen Libration des Mondes. Astr. Bec
Königsberg. Bd. 38, 1899.
9. J. Franz. Die Randlandschaften des Mondes. Neva Acta Leopoldina. Bd. 9
Hall. 1913.
10. S. A. Saunder. The determination of selenographic positions and the measu
ment of lunar photographs. Memoirs Royal Astr. Soc. Vol. LX. Part. I. London. 19
11. H. Roth. Ortsbestimmung von 443 Punkten über Albedo auf einer Vollmondau
nahme. Mitteil. der Wiener Sternwarte. Bd. 4, Nr. 7. Wien, 1949.
12. H. Ritter. Versuch einer Bestimmung von Schichtlinien auf dem Mon
AN 252. S. 157. 1934.
13. A. Jakowkin und L. Belkowitsch. Zur Frage nach der Bestimmu
der Mondfigur vermittelst Terminatorbeobachtungen. AN 258, S. 305, 1935.
14. J. Hopmann. Selenodätische Untersuchungen. Mitteil. der Univ.— Stern
Wien. Bd. 6, № 3, 1952.
15. W. H. Pickering. A photographic Atlas of the Moon. Annals of the Ha
Coll. Observ. Bd. 51, № 1, 1903.

16. A. V. Khabakov. Ob osnovnykh voprosakh istorii razvitiya poverkhnosti Luny /On the Main Problems in the History of Development of the Moon's Surface/, 1949.

17. G. Schrutka-Rechtenstamm. Relative Höhenbestimmungen auf dem Monde mittels des Pariser Mondatlasses und visueller Messungen am Fernrohr. Sitz.-Akad. Wien Math.-naturw. Kl. Abt II. 163, 179, 1954.

18. M. Loewy, P. Puiseux. Atlas photographique de la Lune. Paris. 1910
19. F. Hayn. Selenographische Koordinaten II. Sächsische Akad. d. Wiss. Le
zig. 1904.
20. F. Hayn. Selenographische Koordinaten III. Sächsische Akad. d. Wiss. Le
zig. 1907.
21. H. Battermann. Beiträge zur Bestimmung der Mondbewegung... Beobachtu
sergebnisse der Königl. Sternwarte zu Berlin, Heft IV. 1902
22. E. Przybyllok. Das Profil der Randpartien des Mondes. Mitteil. d. Ste
warte Heidelberg. XI. 1908.
23. E. Rybka. Occultations of stars by the Moon, observed in Cracow, Wars
and Lwow from 1901 to 1922. Acta Astr. Ser a, Vol. I. p. 90.

24. K. K. Dubrovskiy. On the Question of the Study of the Moon's Profile. Uch. zap. Gor'kovskogo un-ta /Science Notes, Gor'kiy Univ./ No 6, 1939

25. F. Hayn. Selenographische Koordinaten IV. Sächsische Akad. d. Wiss. Leipzig. 1914.

26. F. Hayn. Beobachtungen des Mondes. Vierteljahrschrift der Astron. Gesellschaft 48. Jahrgang, Heft 3, p 231.

27. T. Weimer. Recherches sélénographiques: allongement du Sélénoide: libration physique; profils lunaires. Paris, 1954.

28. S. Chevalier. Ann. Obs. Zô-zé. t. X. 1915.

29. P. Puiseux et B. Jekhowsky. Bull. Astron. t. 25. 1918.

30. K. Graff. Ableitung des Mondprofils während der Finsterniss aus den Aufnahmen mit dem 20-m Rohr. Astr. Abhandl. der Hamburger Sternwarte in Bergedorf, Bd. III, № 1, 1913, p. 53.

31. S. Chevalier. Diamètreet forme du disque lunaire. Bull. Astron. Tome XXXIV, Paris. 1917.

32. V. K. Drofa. Determination of the Constants of the Moon's Physical Libration with the 10" Refractor of the Kiev Astronomical Observatory. Abstract of Dissertation, 1955.

33. T. Weimer. Atlas de profils Lunaires. Paris, 1952.

34. Draft Reports International Astronomical Union. Cambridge. 1955. p. 150.

35. Transactions of the International Astronomical Union. Vol. VIII. Cambridge. 1954, p. 219.

36. H. Kristeason. The lunar contours at the total solar eclipse of 1954 June 30. Arkiv för astronomi utgivet av K. Svenska Vetenskaps-Akademien. Bd. 1. Häfte 5. Stockholm 1954. S. 411.

37. K. Graff. Das Mondprofil während der ringförmigen Sonnenfinsterniss, 1912 April 17. AN Bd. 192. № 4587, 1912.

S. Fujinami, T Ina, S. Kawai. On the profile of the Moon's silhouette, as observed in the partial Eclipse of February 14 th 1953. Publ. of the Astron. Society of Japan. Vol. 6, № 2, 1954.

38. P. A. Hansen. Sur la Figure de la Lune. Mém. Royal Astr. Soc. 24, 1856.

39. M. Wichman. Erster Versuch zur Bestimmung der physischen Libration des Mondes aus Beobachtungen mit dem Heliometer. AN №№ 619, 621, 628, 630, 631.

40. P. A. Hansen. MN 15, p. 13 et Mem. RAS 24.

41. A. A. Yakovkin. The Radius and the Form of the Moon. Byulleten' AOE /Bulletin, Astr. Observ. in. Engel'gardt/ No 4, 1934.

42. H. Battermann. Beitrag zur Bestimmung der Mondbahn und Mondhalbmessers. Beob.-Ergebn. der König. Sternwarte zu Berlin. № 13, 1910.

43. S. Bakhuyzen. Investigation into the empirical terms in the mean Longitude. Proceed. Acad. Wiss. Amsterdam. XIV. 2 part, 1912.

44. S. Newcomb. Researches on the Motion of the Moon, part II. Astr. Papers of the Amer. Ephem. 9, 1912.

45. H. Spencer Jones. A Revision of Newcomb's Occultation Memoir. MN Vol. 90, 1, 1929.

46. E. W. Brown. The mean latitudes of the Moon and Sun. MN 74, 158, 1914.

47. S. Böhme. Bearbeitung der Aufnahmen von F. Hayn zur Ortbestimmung des Mondes. AN Bd 256, № 6141, 1935.

48. Transactions of the International Astronomical Union. Vol. VII.

49. E. Brown. The Motion of the Moon. MN Vol. 93.

50. H. R. Morgan, J. Pawling. Irregularities in the Moon's limbs from transi circle observations. AJ 41, № 16.

51. C. B. Watts, A. N. Adams and S. M. Bestul. Washington meridian observations of the moon, 1933—1944. AJ 51, № 1155, 1945.

52. I. V. Gavrilov. On the Dependence of the Moon's Radius on the Density of Negatives in Photographic Observations. ATs AN SSSR, No 175, 1956. /Astr. Circular, Acad. Sci. USSR/

53. A. A. Yakovkin, Inclination of Moon's Orbit and the Libration Effect. Publ. Kiev Astron. Observ. No 4, 1953.

54. T. Banachiewicz. Sur la détermination du profil de la Lune. Acta Astron Sér. c, Vol. 5, 1952

55. K. Koziel. O efekcie Jakowkina Sprawozdania polskiego towarzystwa Astronomicznego. Zeszyt III. 1951.

56. A. A. Nefed'yev. Physical Libration of the Moon. Izv. astr. observ. im. Engel'gardta /News, Astr. Observ. im. Engel'gardt/ No 26, 1951.

57. ——, On the Problem of the Libration Effect in the Moon's Radius. ATs AN SSSR No 147, 1954.

58. I. V. Bel'kovich, On the Question of the Limb Effect in the Observations of the Moon. Byull. AOE, No 10, 1936.

59. ——, Physical Libration of the Moon, Izv. AOE, No 24, 1949.

60. ——, On the Asymmetry of the Moon's Disc. ATs AN SSSR No 83, 1949.

61. E. Hartwig, Beitrag zur Bestimmung der physischen Libration des Monde aus Beobachtungen am Strassburger Heliometer. Karlsruhe, 1880.

62. F. Stratton. The Constants of the Moon's physical Libration. Mem. of th Royal Astr. Soc. Vol. 59, p. IV, 1908.

63. A. A. Yakovkin, Constants of the Physical Libration of the Moon. Publ. de l'Obs. Astr. Engelhardt de l'Univ. de Kasan, No 13, 1928.

64. ——, Rotation and Figure of the Moon, part II., Izv. AOE, No 23, 1945.

65. I. V. Bel'kovich. On the Questions of the Values of the Moments of Inertia of the Moon. ATs AN SSSR No 81, 1948.

66. K. Koziel. The Moon's Libration and Figure... Acta Astr. Sér. a Vol. 4 1948—1949.

67. Wh. T. Khabibullin, On the Determination of the parameter f of the Physical Libration of the Moon, Byull. ITA /Bull. Inst. Theoret. Astron./ vol. VI, No 4, 1955.

68. O. Schrutka-Rechtenstamm. Zur physischen Libration des Monde Sitz.-Ber. Akad. Wien. Abt. II, 164, 323, 1955 = Mitt. Sternwarte Wien 8, 151.

69. H. Spencer Jones. The mean motion of the lunar Perigee and node an figure of the Moon. MN Vol. 97, № 5, 1937.

70. H. Jeffreys. On the figure of the Earth and Moon. MN Vol. 97, № 1, 193

71. H. Jeffreys. The Earth. Cambridge. 1952.

72. A. A. Yakovkin. Experience in determining the Constants of Physical Libration of the Moon with Allowance for Changes in its Profile. Publ. Kiev Astr. Obs. No 3, 1950.

73. ——, Reality of the Free Libration of the Moon. Tr. 10 Astronometricheskoy konferentsii /Works of the Tenth Astronometric Conference/, 1954.

74. M. F. Subbotin. Kurs nebesnoy mekhaniki /Course of Celestial Mechanics/ vol III, p. 213, Gostekhizdat 1949.

75. H. Jeffreys. Certain hypotheses as to the internal Structure of the Earth and Moon. Mem of the RAS. Vol. LX, part VI, p. 190, 1915.

76. N. I. Idel'son. Teoriya potentsiala /Theory of the Potential/ ONTI, 1936, p. 249.

77. H. Jeffreys. The Figures of the Earth and Moon. MN. Geophys. Suppl. Vol. 5. № 7, 1948, p. 285.

78. K. Graff. Formeln und Hilfstafeln zur Reduktion von Mondbeobachtungen und Mondphotographien. Veröff. d. Königl. Astr. Rech.-Inst. zu Berlin. № 14, 1901, S. 5.

79. L. Ambronn. Handbuch der Astronomischen Instrumentenkunde. Bd 2, S. 565, Berlin. 1899.

80. A. A. Nefed'yev. Constants of the Moon's Physical Libration, Derived from Heliometric Observations by A. V. Krasnov, Izv. AOE, No 29, 1953.

81. M. Wilkel. Beitrag zur Bestimmung der Konstanten der Libration des Mondes. Tr. astr. observ. Kazanskogo un-ta, /Works of the Astr. Obs. of the Kazan' Univ./ vol XVII, 1908.

82. I. V. Bel'kovich. Constants of the Physical Libration of the Moon. Byull. AOE, No 10, 1936.

83. A. A. Yakovkin, Rotation and Figure of the Moon, part I, Izv. AOE, No 21, 1939.

84. M. Albert Senoaque. Sur le sphéroïde lunaire., C. r Acad. Sci. 1956, 242, № 19.

85. T. Banachiewicz. Tables selénographiques dans le système équatorial. Cracovie. 1949.

86. N. I. Idel'son. Sposob naimen'shikh kvadratov /Method of Least Squares/, 1932.

87. R. A. Hirvonen. Determination of the inner contact moments from the 1945 Solar eclipse pictures. Veröff. d. Finnisch. Geodät. Inst. № 46. 1955.

88. S. M. Kosik. On Allowance for the Irregularities of the Moon's Edge in processing of observations of Occultations of Stars by the Moon. Byull. Tashkentskoy astr. observ. /Bull. Tashkent Astr. Obs./ No 10, 1938.

89. G. Schrutka-Rechtenstamm. Neureduktion der acht von J. Franz und der vier von F. Haya gemessenen Mondkraterpositionen. Sitz.-Ber. Akad. Wien. Abt. II, 165, 97, 1956 = Mitt. Sternwarte Wien.

90. H. Naumann. Selenographische Koordinaten. V, Heft VII. Veröff. d. Univers.—Sternwarte zu Leipzig, 1939.

91. E. W. Woolard. AJ 57, 38, 1951.

92. C. A. Murray. The Moon's observed latitude from occultations 1932—1953. MN Vol. 116, № 5, 1956.

93. S. Newcomb. A compendium of spherical astronomy. 1906, p. 432.

94. H. Saudig. Sonnenfinsternissbeobachtungen zur Bestimmung der Erdfigur. Allgem. Vermessungs-Nachr. № 1, 1955.

95. A. A. Yakovkin. Duality of Solution of the Problem of the Physical Idbration of the Moon and the Choice of the True Solution. Afs AN SSSR No 178, 1957.

Table 12

Krasnov's Measurements

1) Observation number

№№ obsn.	a	b_0	C	Δx_0	Δy_0	Δx	Δy	h_0
1	0'91	− 19.3	− 21.9	− 0'01	− 0'42	− 0'45	− 0'15	858'52
3	0.96	− 0.19	− 21.8	− 0.26	− 0.06	− 0.54	− 0.22	889.83
4	0.93	− 0.35	− 21.8	− 0.30	+ 0.18	− 0.54	− 0.22	891.20
5	0.83	− 1.69	− 22.0	− 1.53	− 1.54	− 0.49	− 0.25	894.34
6	0.64	− 3.93	− 20.1	− 0.07	+ 0.32	− 0.35	− 0.14	906.28
7	1.30	+ 4.15	− 15.5	− 0.37	+ 1.21	− 0.40	+ 0.75	868.38
8	0.93	+ 0.27	− 21.5	− 0.28	+ 0.96	− 0.52	− 0.29	888.32
9	0.85	− 1.27	− 22.0	− 0.65	− 0.24	− 0.40	− 0.07	892.35
10	0.55	− 5.01	− 18.5	+ 0.22	− 1.38	− 0.32	− 0.15	912.65
11	0.47	− 5.93	− 11.7	+ 0.81	− 0.91	− 0.25	− 0.18	926.87
12	0.68	− 3.37	− 21.2	− 0.08	− 0.16	− 0.49	− 0.17	900.93
14	0.51	− 5.44	+ 3.1	+ 0.57	− 0.34	− 0.21	− 0.25	951.74
15	1.03	+ 0.89	− 20.7	+ 0.97	+ 1.33	− 0.28	+ 0.44	891.25
16	0.80	− 1.95	− 22.1	+ 0.54	+ 2.19	− 0.19	+ 0.48	898.56
17	0.50	− 5.66	− 14.3	+ 1.33	+ 0.67	− 0.24	− 0.14	924.27
18	0.71	− 3.07	− 21.5	+ 0.89	+ 1.39	− 0.16	+ 0.44	902.95
19	0.68	− 3.83	− 20.9	+ 0.14	+ 1.70	− 0.15	+ 0.49	907.35
20	0.65	− 3.76	− 21.4	+ 0.64	+ 1.04	− 0.14	+ 0.40	902.98
21	0.46	− 6.12	− 12.8	+ 1.01	+ 1.24	− 0.16	+ 0.26	937.29
22	0.55	− 5.04	+ 2.7	+ 0.65	+ 0.27	− 0.07	+ 0.01	967.66
23	0.63	− 3.96	+ 6.8	+ 0.46	− 1.15	− 0.24	− 0.24	978.36
24	0.46	− 6.12	− 15.2	+ 1.10	+ 0.39	− 0.14	+ 0.26	924.37
25	0.58	− 4.58	+ 5.8	+ 0.91	+ 0.42	− 0.28	+ 0.19	977.32
27	1.38	+ 3.67	+ 22.2	− 0.02	+ 0.06	− 0.29	− 0.78	992.37
28	0.41	− 6.29	− 7.7	+ 0.99	− 0.18	− 0.18	+ 0.22	935.30
29	0.55	− 5.42	+ 3.6	+ 0.23	+ 0.62	− 0.26	+ 0.25	967.94
30	0.65	− 3.83	+ 9.2	− 0.25	+ 2.13	− 0.34	+ 0.27	983.99
31	0.75	− 2.57	+ 13.6	+ 0.26	0.00	− 0.40	+ 0.25	991.37
32	1.21	+ 3.03	+ 22.0	− 1.22	+ 1.48	− 0.23	− 0.75	1009.85
33	0.75	− 2.52	+ 12.5	− 1.04	+ 1.21	− 0.40	+ 0.30	976.18
36	0.84	− 1.52	− 21.0	+ 0.79	+ 3.56	− 0.18	+ 0.52	898.03
37	0.50	− 5.67	− 18.3	+ 0.05	+ 0.05	− 0.27	− 0.12	890.18
38	0.48	− 5.91	− 14.8	+ 0.49	− 0.86	− 0.27	− 0.16	895.94
39	0.60	− 4.43	− 0.6	+ 1.14	− 0.59	− 0.26	− 0.30	910.94
40	0.65	− 3.43	+ 5.2	+ 0.51	− 0.71	− 0.27	− 0.35	924.73
41	0.76	− 2.16	+ 10.0	+ 0.20	− 1.06	− 0.29	− 0.36	933.56
42	0.79	− 2.13	+ 10.3	− 0.01	− 0.35	− 0.27	− 0.43	937.47

43	0.58	— 4.64	— 22.1	+ 2.05	+ 2.74	— 0.13	+ 0.36	891.52
44	0.49	— 5.76	— 12.0	— 1.21	+ 1.02	— 0.17	— 0.03	901.47
45	0.59	— 4.54	— 2.0	+ 0.47	+ 0.47	— 0.28	— 0.27	912.22
46	0.67	— 3.53	+ 3.3	+ 0.06	— 1.67	— 0.28	— 0.31	917.45
47	0.77	— 2.27	+ 8.8	+ 0.46	— 1.22	— 0.30	— 0.41	929.94
48	0.46	— 6.04	— 17.2	+ 2.07	+ 1.26	— 0.14	+ 0.26	896.56
49	0.75	— 2.54	+ 7.1	+ 0.22	+ 0.61	— 0.30	— 0.39	930.89
50	0.77	— 2.26	+ 20.6	— 0.40	— 0.90	— 0.15	— 0.48	966.93
51	0.50	— 5.56	— 8.0	+ 1.17	+ 2.26	— 0.19	+ 0.25	911.11
52	0.73	— 2.75	+ 5.6	— 0.68	+ 0.86	— 0.35	+ 0.33	931.25
53	0.85	— 1.36	+ 19.5	+ 0.04	+ 0.15	— 0.44	+ 0.34	943.45
54	1.01	+ 0.64	+ 15.1	— 0.72	+ 1.35	— 0.55	+ 0.37	960.48
55	1.13	+ 2.09	+ 18.6	— 0.52	— 0.03	— 0.66	+ 0.36	975.02
56	0.87	— 1.04	+ 9.6	— 0.49	+ 0.74	— 0.46	+ 0.32	927.17
57	1.03	+ 1.61	+ 17.1	— 1.05	— 0.46	— 0.62	+ 0.38	959.24
58	1.11	+ 1.87	+ 17.4	— 1.16	+ 0.29	— 0.63	+ 0.36	959.57
59	1.25	+ 3.48	+ 20.2	— 1.75	+ 1.05	— 0.38	+ 0.01	975.15
61	1.43	+ 5.76	+ 22.2	— 0.52	+ 1.09	— 0.85	+ 0.37	960.95
62	1.56	+ 7.31	+ 21.9	— 1.54	0.00	— 0.90	+ 0.49	985.40
63	1.57	+ 7.39	+ 21.9	— 1.47	+ 0.07	— 0.92	+ 0.48	985.04
64	1.58	+ 7.61	+ 19.6	— 1.27	+ 0.51	— 0.89	+ 0.52	993.85
65	0.89	— 0.80	— 17.4	— 0.04	+ 0.85	— 0.50	— 0.30	947.84
66	0.77	— 2.26	— 20.1	+ 1.04	+ 1.62	— 0.45	— 0.22	933.13
67	0°35	— 0°18	— 15.7	+ 0°77	+ 1°68	— 0°52	— 0°35	960°07
68	0.93	— 0.37	— 15.9	+ 0.08	+ 2.15	— 0.50	— 0.33	959.67
69	0.82	— 1.73	— 19.6	+ 1.02	+ 2.07	— 0.47	— 0.26	947.26
70	0.81	— 1.88	— 19.1	+ 0.46	+ 0.79	— 0.47	— 0.24	947.78
71	0.70	— 3.17	— 21.2	+ 0.85	+ 1.67	— 0.41	— 0.21	934.42
72	0.66	— 3.27	— 21.3	+ 0.85	+ 1.53	— 0.40	— 0.21	935.09
73	0.50	— 5.56	— 22.4	+ 0.90	+ 1.17	— 0.29	— 0.14	911.03
74	0.49	— 5.76	— 22.4	+ 0.64	+ 0.05	— 0.29	— 0.13	912.38
75	0.45	— 5.90	— 21.2	+ 0.91	+ 1.53	— 0.28	— 0.13	901.90
76	0.47	— 6.00	— 21.1	+ 0.97	+ 1.43	— 0.28	— 0.12	903.89
77	0.47	— 5.94	— 15.8	+ 0.71	+ 1.03	— 0.26	— 0.15	893.12
78	0.76	— 3.47	— 21.5	+ 1.40	+ 1.42	— 0.14	+ 0.11	931.94
79	0.53	— 5.23	— 22.7	+ 1.45	+ 1.33	— 0.31	— 0.12	914.27
80	0.52	— 5.35	— 22.7	+ 1.66	+ 1.22	— 0.30	— 0.10	915.69
81	0.72	— 2.98	— 20.8	+ 1.17	+ 1.87	— 0.18	+ 0.42	927.00
82	0.69	— 3.26	— 21.0	+ 1.31	+ 2.65	— 0.17	+ 0.41	928.26
83	0.62	— 4.17	— 22.3	+ 1.46	+ 2.29	— 0.15	+ 0.38	920.70
84	0.60	— 4.39	— 22.4	+ 1.52	+ 2.23	— 0.15	+ 0.35	921.29
85	0.54	— 5.09	— 22.6	+ 1.43	+ 1.61	— 0.14	+ 0.28	914.43
86	0.51	— 5.48	— 22.3	+ 1.67	+ 0.83	— 0.03	— 0.05	906.05
87	0.49	— 5.76	— 20.8	+ 1.22	+ 1.29	— 0.27	— 0.07	909.56
88	0.57	— 4.75	— 10.4	+ 0.83	+ 1.53	— 0.30	— 0.21	893.25
89	0.62	— 4.14	— 22.0	+ 1.60	+ 3.04	— 0.13	+ 0.39	921.19

90	0.59	— 4.47	— 22.2	+ 1.37	+ 2.05	— 0.13	+ 0.36	918.77
91	0.54	— 5.08	— 22.7	+ 1.50	+ 2.96	— 0.12	+ 0.34	919.87
92	0.53	— 5.21	— 22.7	+ 1.85	+ 3.05	— 0.11	+ 0.33	919.09
93	0.50	— 5.60	— 22.8	+ 1.71	+ 1.98	— 0.11	+ 0.31	910.18
94	0.49	— 5.71	— 22.8	+ 1.63	+ 3.93	— 0.11	+ 0.30	910.78
95	0.47	— 5.98	— 21.9	+ 2.01	+ 2.76	— 0.11	+ 0.29	903.44
96	0.46	— 6.13	— 21.8	+ 2.11	+ 3.00	— 0.11	+ 0.27	903.35
97	0.45	— 6.17	— 21.8	+ 1.36	+ 1.57	— 0.12	+ 0.26	902.32
98	0.50	— 5.59	— 17.4	+ 0.62	+ 1.84	— 0.14	+ 0.28	891.48
99	0.54	— 5.10	— 13.4	+ 0.86	+ 1.52	— 0.13	+ 0.26	892.38
100	1.14	+ 2.25	+ 15.0	— 0.07	— 0.74	— 0.36	— 0.61	907.89
101	1.37	+ 4.97	+ 20.6	— 1.94	— 0.98	— 0.32	— 0.66	927.95
102	0.47	— 5.94	— 18.3	+ 1.70	+ 3.27	— 0.13	+ 0.29	898.28
103	0.47	— 5.99	— 17.8	+ 1.98	+ 1.45	— 0.14	+ 0.26	895.62
104	0.52	— 5.40	— 14.8	+ 2.02	+ 2.68	— 0.16	+ 0.30	894.73
105	0.95	— 0.07	+ 7.8	— 0.31	+ 0.95	— 0.48	+ 0.40	904.92
107	1.48	+ 6.30	+ 22.6	— 1.75	+ 0.15	— 0.60	— 0.48	949.70
108	1.15	+ 2.34	+ 13.6	— 0.80	— 0.52	— 0.62	+ 0.42	916.49
109	1.37	+ 4.94	+ 20.0	— 1.10	— 1.16	— 0.79	+ 0.44	938.44
110	1.46	+ 6.05	+ 22.1	— 1.38	— 1.69	— 0.85	+ 0.45	950.53
111	1.47	+ 6.23	+ 22.1	— 1.94	— 0.66	— 0.86	+ 0.45	950.81
112	1.36	+ 4.85	+ 19.0	— 1.31	— 1.14	— 0.79	+ 0.41	925.96

Table 13

Mikhaylovskiy's observations

№№ nadir.	a	b_0	C	Δx	Δy	h_0
1	1"59	+ 7"35	+ 22"8	— 0"25	+ 0"47	964"58
2	1.57	+ 7.46	+ 21.3	— 0.69	+ 0.49	979.19
3	1.26	+ 3.66	+ 12.1	— 0.66	+ 0.51	893.87
4	1.44	+ 5.83	+ 18.2	— 0.81	+ 0.49	897.65
5	1.58	+ 7.52	+ 22.2	— 0.93	+ 0.47	892.84
6	1.49	+ 6.49	+ 24.2	— 0.88	+ 0.41	885.55
7	1.42	+ 5.50	+ 24.5	— 0.86	+ 0.39	890.73
8	1.33	+ 4.49	+ 23.7	— 0.80	+ 0.37	939.74
9	0.95	— 0.13	+ 13.6	— 0.52	+ 0.34	895.70
10	0.53	— 5.24	— 11.0	— 0.20	+ 0.27	938.35
11	0.53	— 5.20	— 22.8	— 0.30	— 0.09	967.66
12	0.46	— 6.04	— 14.7	— 0.15	+ 0.24	932.70
13	1.47	+ 6.19	+ 23.3	— 0.89	+ 0.40	927.98

14	1.27	+ 3.84	+ 24.7	— 0.75	+ 0.35	913.11
15	1.40	+ 5.41	+ 24.3	— 0.84	+ 0.39	923.16
16	1.31	+ 4.21	+ 24.8	— 0.81	+ 0.35	913.57
17	0.69	— 3.31	— 24.2	— 0.17	+ 0.38	946.92
18	0.56	— 4.82	— 20.9	— 0.17	+ 0.27	916.76
19	1.53	+ 7.01	— 1.4	— 0.62	+ 0.77	982.79
20	1.55	+ 7.19	— 0.7	— 0.67	+ 0.79	978.08
21	1.44	+ 5.80	+ 20.8	— 0.82	+ 0.46	989.36
22	0.75	— 2.55	+ 18.0	— 0.22	— 0.42	924.39
23	0.91	— 0.58	+ 22.5	— 0.51	+ 0.28	933.31
24	0.79	— 2.02	+ 19.6	— 0.45	+ 0.17	923.46
25	1.19	+ 2.80	+ 24.9	— 0.72	+ 0.26	951.02
26	0.94	— 0.29	+ 23.1	— 0.55	+ 0.24	929.40
27	0.63	— 4.05	+ 12.3	— 0.32	+ 0.18	905.16
28	0.48	— 5.90	— 4.2	— 0.21	+ 0.23	889.99
29	1.56	+ 7.28	— 0.9	— 0.69	+ 0.68	991.82
31	1.55	+ 7.15	+ 6.5	— 0.76	+ 0.70	975.70
32	1.55	+ 7.19	+ 7.2	— 0.77	+ 0.68	972,90
33	1.49	+ 6.45	+ 12.2	— 0.81	+ 0.59	986.48
34	1.49	+ 6.47	+ 13.3	— 0.81	+ 0.57	982.22
35	1.40	+ 5.37	+ 17.4	— 0.81	+ 0.48	995.25
36	1.40	+ 5.35	+ 18.1	— 0.81	+ 0.47	994.51
37	0.54	— 5.15	+ 13.2	— 0.19	— 0.27	949.57
38	1.42	+ 5.61	+ 16.4	— 0.80	+ 0.46	978.06
40	1.19	+ 2.83	+ 23.3	— 0.71	+ 0.32	988.87
42	1.05	+ 1.09	+ 24.9	— 0.64	+ 0.28	986.67
43	0.91	— 0.58	+ 24.7	— 0.55	+ 0.24	986.43
44	0.78	— 2.17	+ 23.0	— 0.44	+ 0.15	980.55
45	1.52	+ 6.80	— 15.8	— 0.84	— 0.52	909.34
46	0.69	— 3.33	— 16.5	— 0.22	+ 0.38	898.36
47	0.78	— 2.22	— 19.7	— 0.21	+ 0.46	892.80
48	0.79	— 2.10	— 20.3	— 0.22	+ 0.46	891.36
49	0.89	— 0.81	— 22.7	— 0.21	+ 0.54	890.68
50	1.54	+ 7.07	— 1.8	— 0.64	+ 0.79	955.00
51	1.54	+ 7.06	— 0.5	— 0.67	+ 0.75	934.96
52	1.48	+ 6.40	+ 5.4	— 0.71	+ 0.65	951.22
54	1.30	+ 4.13	+ 16.0	— 0.72	+ 0.44	982.59
55	1.16	+ 2.48	+ 20.5	— 0.68	+ 0.35	997.82
56	0.94	— 0.27	+ 24.4	— 0.55	+ 0.17	1002.08
57	0.97	+ 0.14	+ 24.0	— 0.58	+ 0.24	979.44
58	0.84	— 1.44	+ 24.8	— 0.51	+ 0.20	990.50

Table 14

Banachiewicz's observations

№ № набл.	a	b_0	C	Δx_0	Δy_0	Δx	Δy	h_0
1	1'40	+ 5'36	— 22'6	+ 0'39	+ 1'20	— 0'78	— 0'42	968"15
2	1.31	+ 4.25	— 21.4	— 0.18	+ 1.34	— 0.77	— 0.37	972.98
3	1.41	+ 5.50	— 22.7	+ 0.34	+ 1.34	— 0.77	— 0.40	975.54
4	1.41	+ 5.44	— 22.7	+ 0.57	+ 1.12	— 0.61	— 0.41	976.86
5	1.33	+ 4.46	— 21.9	— 0.62	+ 0.67	— 0.79	— 0.37	979.89
6	1.32	+ 4.38	— 21.8	— 1.29	— 0.87	— 0.76	— 0.32	982.02
7	1.29	+ 4.08	— 20.0	— 0.13	+ 1.19	— 0.75	— 0.39	983.00
8	1.21	+ 3.02	— 19.8	— 0.32	+ 0.31	— 0.69	— 0.32	984.47
9	1.09	+ 1.57	— 16.9	— 0.37	+ 1.61	— 0.61	— 0.37	981.80
10	1.50	+ 6.62	— 19.1	+ 0.66	+ 1.43	— 0.35	+ 0.76	953.93
11	1.43	+ 5.75	— 22.6	— 0.76	+ 1.08	— 0.27	+ 0.77	962.31
12	0.85	— 1.40	— 9.6	+ 0.26	— 0.18	— 0.44	— 0.31	984.97
13	0.84	— 1.50	— 9.3	+ 0.22	— 0.06	— 0.43	— 0.36	987.53
14	1.47	+ 6.26	— 21.2	— 0.72	+ 1.51	— 0.30	+ 0.90	970.87
15	1.04	+ 0.97	— 16.3	— 0.50	+ 1.87	— 0.58	— 0.34	1008.12
16	1.03	+ 0.86	— 16.1	— 1.61	+ 2.67	— 0.57	— 0.31	1010.73
17	1.01	+ 0.66	— 15.8	+ 0.28	+ 2.33	— 0.53	— 0.24	1013.22
18	0.88	0.98	— 11.4	— 0.90	+ 0.81	— 0.46	— 0.33	1008.16
19	0.87	— 1.13	— 11.1	— 0.45	+ 1.64	— 0.45	— 0.36	1010.03
20	1.02	+ 1.53	— 17.8	— 0.35	+ 0.18	— 0.31	+ 0.63	1013.55
21	0.82	— 1.76	— 9.2	— 1.25	+ 0.47	— 0.42	— 0.33	1013.45
22	0.67	— 3.56	— 2.7	— 0.38	+ 1.31	— 0.31	— 0.23	1009.42
23	0.66	3.61	— 2.4	— 0.64	+ 1.55	— 0.31	— 0.28	1010.92
24	0.51	5.10	+ 4.4	+ 0.76	+ 2.68	— 0.22	— 0.24	999.61
25	0.46	— 5.05	+ 10.2	+ 0.70	+ 1.83	— 0.18	— 0.22	982.95
26	0.42	— 5.64	— 15.2	+ 0.15	+ 0.62	— 0.14	— 0.20	965.11
27	0.57	— 4.78	— 0.1	+ 0.45	+ 0.87	— 0.25	+ 0.28	978.63
28	0.47	— 6.01	+ 21.5	— 0.77	+ 0.53	— 0.26	+ 0.07	949.77
29	0.47	— 5.95	+ 21.5	+ 0.17	+ 2.17	— 0.25	+ 0.08	950.31
30	0.48	— 5.89	+ 21.6	+ 1.09	+ 1.71	— 0.26	+ 0.08	948.11
31	0.54	— 5.16	+ 22.4	— 0.12	+ 2.22	— 0.04	— 0.02	939.52
32	0.55	— 5.03	+ 22.4	+ 0.91	+ 1.05	— 0.07	— 0.02	938.92
33	0.51	5.48	+ 22.2	— 0.61	+ 1.45	— 0.30	+ 0.12	936.53
34	0.52	5.41	+ 22.2	— 0.19	+ 1.42	— 0.30	+ 0.12	935.48
35	0.41	— 6.35	+ 20.1	— 0.97	+ 0.31	— 0.25	+ 0.14	944.36
37	0.67	3.46	+ 21.8	— 9.30	— 1.23	— 0.39	+ 0.19	915.99
38	0.61	— 3.40	+ 21.8	+ 0.89	+ 1.63	— 0.40	+ 0.16	913.99
39	0.79	— 2.07	+ 20.4	— 8.63	+ 2.16	— 0.47	+ 0.21	906.62
40	0.66	3.64	+ 22.0	— 1.01	+ 1.57	— 0.40	+ 0.18	917.77

41	1.42	+ 5.63	— 21.0	— 0.31	- 0.07	— 0.32	+ 0.88	921.18
42	1.42	+ 5.58	20.9	— 0.60	+ 0.92	— 0.33	+ 0.88	922.09
44	1.24	+ 3.26	— 22.1	— 1.98	— 0.61	— 0.26	+ 0.79	952.93
44	1.22	+ 3.14	- 22.1	— 1.09	+ 0.45	— 0.30	+ 0.71	953.57
45	1.09	— 1.54	— 20.9	— 0.27	+ 1.30	— 0.29	+ 0.34	969.47
46	1.26	+ 3.70	- 22.2	— 0.42	- 0.28	— 0.26	+ 0.90	935.55
47	0.68	— 2.44	— 11.3	+ 0.12	+ 2.19	— 0.24	+ 0.37	998.61
48	0.66	— 3.65	- 10.6	+ 1.19	+ 0.97	— 0.23	+ 0.36	1000.21
49	0.96	+ 0.03	— 21.2	+ 0.17	+ 11.45	0.56	— 0.27	915.51
50	0.84	— 1.42	— 19.6	— 1.19	+ 15.27	— 0.49	- 0.25	926.90
51	1.10	— 1.72	— 22.0	+ 1.46	+ 0.10	— 0.65	— 0.33	904.04
52	1.09	+ 1.04	- 22.0	+ 0.17	+ 0.58	— 0.65	— 0.28	905.52
53	0.98	+ 0.26	— 21.6	+ 0.19	+ 15.84	— 0.58	— 0.27	912.06
54	0.85	- 1.44	- 20.1	- 1.15	— 0.42	— 0.50	— 0.25	923.67
55	0.64	— 3.97	— 14.8	— 0.85	— 0.77	- 0.35	— 0.22	940.19
56	0.54	— 5.17	10.3	0.60	+ 1.49	— 0.28	— 0.20	954.23
57	0.42	- 6.54	— 1.1	+ 1.66	— 0.31	— 0.16	— 0.20	962.50
58	0.42	— 6.57	- 0.8	+ 1.22	+ 1.12	— 0.19	— 0.20	966.12
59	0.92	0.54	— 21.0	+ 0.18	+ 0.48	— 0.24	+ 0.52	925.85
60	0.49	— 5.71	+ 13.9	+ 0.69	- 0.84	— 0.27	+ 0.17	996.88
61	0.50	— 5.67	— 14.1	+ 1.15	— 0.52	— 0.27	+ 0.15	995.45
62	0°57	— 4°71	+ 17°6	+ 0°18	— 0°30	— 0°33	+ 0°18	1006°16
63	0.59	— 4.51	+ 17.9	+ 1.22	+ 0.25	— 0.34	+ 0.17	1005.62
64	0.79	— 2.08	+ 21.3	— 0.10	+ 0.32	— 0.47	+ 0.22	997.19
65	0.88	— 1.95	+ 21.4	— 0.93	+ 1.21	— 0.47	+ 0.22	994.87
66	0.92	— 0.48	+ 21.9	+ 0.70	— 0.05	— 0.54	+ 0.27	997.23
67	0.93	— 0.47	+ 21.9	+ 0.45	— 0.33	— 0.55	+ 0.27	997.50
68	0.94	— 0.30	+ 21.9	— 1.61	+ 0.22	— 0.55	+ 0.29	996.69
69	0.94	— 0.25	+ 21.9	+ 0.43	+ 1.40	— 0.55	+ 0.28	995.70
70	1.06	+ 1.28	+ 21.4	— 0.95	+ 0.09	— 0.59	+ 0.34	992.67
71	1.07	+ 1.33	+ 21.4	— 0.40	+ 0.48	— 0.61	+ 0.34	992.96
72	1.21	+ 3.05	+ 19.5	— 1.13	— 0.39	— 0.55	— 0.30	984.40
73	0.76	— 2.43	+ 20.8	— 0.47	+ 0.68	— 0.44	+ 0.23	982.25
74	0.77	— 2.37	+ 20.9	+ 0.10	+ 0.87	— 0.46	+ 0.21	980.79
75	0.89	— 0.80	+ 21.8	— 0.08	— 0.86	— 0.52	+ 0.22	982.82
76	0.96	— 0.75	+ 21.8	— 0.08	— 0.94	— 0.53	+ 0.24	981.81
77	1.09	+ 0.56	— 21.7	+ 0.09	+ 1.13	— 0.59	— 0.27	891.61
78	0.89	— 0.83	— 21.9	— 0.42	+ 0.87	— 0.52	— 0.26	892.57
79	0.76	— 2.22	— 21.3	+ 0.84	+ 2.01	— 0.46	— 0.21	898.29
80	0.68	— 3.44	— 20.9	— 0.26	+ 1.09	— 0.39	— 0.21	903.78
81	0.91	— 0.57	— 21.9	+ 0.66	+ 1.30	— 0.53	— 0.22	890.77
82	0.80	— 1.96	— 21.6	— 0.65	+ 0.48	— 0.47	— 0.22	893.89
83	0.47	— 6.02	— 13.3	+ 0.52	+ 0.50	— 0.25	— 0.16	913.92
84	0.49	— 5.73	— 14.6	— 1.06	+ 0.16	— 0.26	— 0.14	909.58
85	0.49	— 5.77	— 14.7	+ 0.19	+ 0.95	— 0.26	- 0.13	911.85

86	0.45	— 6.26	+ 6.1	+ 0.73	+ 1.11	— 0.18	— 0.24	950.07
87	0.53	— 5.29	— 17.1	+ 0.33	— 2.16	— 0.17	+ 0.26	911.26
88	0.53	— 5.28	— 16.9	— 0.11	+ 0.19	— 0.17	+ 0.28	915.08
89	0.52	— 5.26	— 16.6	— 0.01	— 6.19	— 0.17	+ 0.27	916.06
90	0.56	— 4.92	+ 11.2	— 0.92	+ 0.37	— 0.21	— 0.22	973.75
91	0.55	— 4.82	+ 11.9	+ 0.08	+ 0.55	— 0.20	— 0.20	977.91
92	0.42	— 6.53	— 12.2	+ 0.44	— 1.97	— 0.15	— 0.24	917.57
93	0.45	— 6.26	+ 3.0	— 0.49	— 1.16	— 0.21	+ 0.19	959.57
94	0.76	— 2.41	+ 17.9	— 0.44	+ 0.36	— 0.42	+ 0.24	985.93
95	1.04	+ 0.93	+ 21.8	+ 0.27	— 0.35	— 0.62	+ 0.31	1007.26
96	1.05	+ 1.03	+ 21.8	— 0.56	— 0.26	— 0.59	+ 0.32	1008.34
97	1.05	+ 1.14	+ 21.8	+ 0.47	+ 0.52	— 0.59	+ 0.32	1008.04
98	1.19	+ 2.86	+ 21.9	— 1.37	+ 0.05	— 0.6[illegible]	— 0.38	1012.31
99	1.26	+ 3.70	+ 21.5	— 0.79	+ 1.13	— 0.71	+ 0.40	1004.07
100	1.12	+ 1.95	+ 22.0	— 0.90	— 1.08	— 0.49	+ 0.06	977.0[illegible]
101	0.54	— 5.07	— 21.6	+ 1.92	+ 1.90	— 0.12	+ 0.28	897.61
102	0.64	— 3.85	+ 8.3	+ 0.08	— 0.22	— 0.33	+ 0.22	932.67
103	0.65	— 3.76	+ 8.6	— 0.48	— 0.17	— 0.33	+ 0.22	932.94
104	1.00	+ 1.61	+ 20.7	+ 2.22	— 0.79	— 1.03	— 0.30	970.32
105	1.10	+ 1.74	+ 20.8	— 2.04	— 0.27	— 0.70	— 0.27	972.74
106	0.58	— 4.53	+ 4.1	+ 0.10	— 0.75	— 0.28	+ 0.25	914.57
107	0.58	— 4.58	+ 4.3	+ 0.58	— 1.06	— 0.28	+ 0.26	913.34
108	0.67	— 3.51	+ 8.9	— 0.34	— 0.31	— 0.25	+ 0.26	926.90
109	0.68	— 3.46	+ 9.0	+ 1.15	— 2.44	— 0.36	+ 0.27	926.60
110	0.79	— 2.13	+ 13.3	— 0.24	— 1.61	— 0.43	+ 0.27	940.36
111	0.79	— 2.04	+ 13.5	+ 0.18	— 2.75	— 0.43	+ 0.27	939.96
112	0.80	— 1.98	+ 13.6	— 0.31	— 0.18	— 0.44	+ 0.26	939.15
113	0.90	— 0.72	+ 16.8	+ 0.93	— 0.37	— 0.50	+ 0.32	953.60
114	0.91	— 0.62	+ 17.0	+ 0.35	— 0.60	— 0.51	+ 0.32	954.52
115	1.03	+ 0.99	+ 19.7	+ 0.58	— 0.06	— 0.60	+ 0.34	966.83
116	1.04	+ 0.93	+ 19.7	— 0.51	+ 0.06	— 0.60	+ 0.34	967.57
117	1.04	+ 1.02	+ 19.8	+ 0.49	— 1.20	— 0.61	+ 0.30	968.74
118	1.05	+ 1.15	+ 19.9	— 0.19	— 1.96	— 0.61	+ 0.30	968.78
119	1.02	+ 0.76	+ 19.9	— 0.36	+ 1.20	— 0.60	+ 0.33	949.07
120	1.25	+ 3.51	+ 22.1	— 0.58	— 1.20	— 0.74	+ 0.37	981.10
121	1.25	+ 3.55	+ 22.1	— 0.46	— 0.61	— 0.74	+ 0.37	981.91
122	1.26	+ 3.61	+ 22.2	— 0.82	— 7.98	— 0.74	+ 0.35	982.60
123	1.44	+ 5.85	+ 21.1	+ 1.63	— 0.45	— 0.71	+ 0.26	1062.64
124	0.76	— 2.20	— 21.2	+ 0.75	+ 0.76	— 0.42	— 0.23	949.28
125	0.61	— 4.29	— 22.2	+ 0.97	+ 0.13	— 0.35	— 0.18	937.85
126	0.60	— 4.36	— 22.3	— 0.31	+ 0.54	— 0.36	— 0.12	938.77
127	0.53	— 5.35	— 22.4	+ 1.99	+ 0.37	— 0.28	— 0.08	936.04
128	0.52	— 5.41	— 22.4	+ 1.16	+ 1.33	— 0.30	— 0.13	927.72
129	0.41	— 6.65	— 19.6	+ 1.07	+ 0.43	— 0.24	— 0.10	969.05
130	0.41	— 6.66	— 19.5	+ 0.99	+ 1.20	— 0.24	— 0.13	969.61

Table 15

Yakovkin's observations

№ № наб.	a	b_0	C	Δx	Δr	h_0
1	0".49	— 5".7	— 22".8	— 0".23	— 0".03	963.93
2	0.48	— 5.8	— 21.0	— 0.27	— 0.11	949.37
3	0.48	— 5.9	— 20.9	— 0.23	— 0.04	951.20
4	0.51	— 5.5	— 23.0	— 0.12	+ 0.31	959.04
5	0.49	— 5.7	— 23.0	— 0.11	+ 0.29	958.92
6	0.48	— 5.8	— 23.0	— 0.11	+ 0.29	955.24
7	0.48	— 5.8	— 22.5	— 0.13	+ 0.25	952.43
8	0.47	— 6.0	— 22.4	— 0.13	+ 0.24	952.13
9	0.49	— 5.7	— 20.9	— 0.15	+ 0.23	942.98
10	0.48	— 5.8	— 20.7	— 0.15	+ 0.25	944.89
11	0.48	— 5.9	— 20.5	— 0.15	+ 0.21	944.24
12	0.52	— 5.4	— 17.7	— 0.03	+ 0.01	935.90
13	0.57	— 4.7	— 13.4	— 0.28	— 0.11	927.61
14	0.58	— 4.6	— 13.2	— 0.27	0.10	926.76
15	0.76	— 2.5	— 3.5	— 0.37	0.30	909.42
16	0.50	— .6	— 23.0	— 0.11	+ 0.29	956.74
17	1.19	+ 2.8	+ 13.8	— 0.39	— 0.65	894.27
18	0.53	— 5.3	— 16.5	— 0.17	+ 0.29	924.91
19	0.98	+ 0.2	+ 5.2	— 0.48	— 0.41	899.23
20	1.01	+ 0.6	+ 22.0	— 0.71	— 0.34	899.57
22	1.30	+ 4.1	+ 16.3	— 0.72	+ 0.44	895.92
23	1.30	+ 4.2	+ 16.5	— 0.72	+ 0.46	895.80
24	1.33	+ 4.5	+ 16.8	— 0.76	+ 0.43	892.93
25	1.45	+ 6.0	+ 21.4	— 0.84	— 0.45	899.65
26	1.47	+ 6.2	+ 21.5	— 0.86	+ 0.40	900.90
27	1.48	+ 6.4	+ 21.7	— 0.87	+ 0.45	899.81
28	1.52	+ 6.8	+ 22.8	— 0.87	+ 0.46	904.10
29	1.52	+ 6.8	+ 22.9	— 0.89	+ 0.45	904.94
30	1.56	+ 7.3	+ 23.3	— 0.80	— 0.07	913.11
31	1.57	+ 7.4	+ 23.3	— 0.78	+ 0.17	911.65
32	1.40	+ 5.4	+ 18.5	— 0.76	+ 0.48	895.36
33	1.45	+ 6.4	+ 21.0	— 0.86	+ 0.45	897.13
34	1.53	+ 6.9	+ 22.5	— 0.90	+ 0.45	903.19
35	0.56	— 4.9	— 20.7	— 0.50	— 0.05	1007.15
36	0.51	— 5.5	— 22.7	0.29	— 0.10	1001.87
37	0.49	— 5.7	— 22.8	— 0.28	— 0.09	1000.91
38	0.48	— 5.9	— 23.4	— 0.28	— 0.10	990.94
39	0.47	— 6.0	— 23.4	— 0.27	— 0.09	991.67
40	0.48	— 5.9	— 22.7	— 0.28	— 0.10	978.70

41	0.53	— 5.3	— 29.6	— 0.31	— 0.16	963.58
42	0.60	— 4.5	— 17.5	— 0.34	— 0.17	947.[illegible]
43	0.60	— 4.5	— 17.3	— 0.34	— 0.16	940.2[illegible]
44	0.64	— 4.9	— 18.5	— 0.29	+ 0.29	1011.[illegible]
45	0.62	— 4.2	— 19.1	— 0.18	+ 0.28	1011.4[illegible]
46	0.54	— 5.1	— 21.6	— 0.07	+ 0.12	1013.0[illegible]
47	0.53	— 5.2	— 21.9	— 0.21	— 0.01	1013.17
48	0.50	— 5.6	— 23.2	— 0.27	— 0.07	1018.20
49	0.57	— 4.7	— 20.5	— 0.16	+ 0.32	1004.83
50	0.58	— 4.9	— 20.6	— 0.16	+ 0.30	1005.11
51	0.53	— 5.3	— 22.6	— 0.13	+ 0.30	1007.[illegible]
52	0.51	— 5.5	— 22.[illegible]	—0.14	+ 0.25	1008.3[illegible]
53	0.98	+ 0.2	— 0.6	— 0.44	— 0.46	926.31
54	1.09	+ 1.6	+ 4.9	— 0.45	— 0.52	914.[illegible]
55	0.58	— 4.6	— 19.2	— 0.15	+ 0.34	985.9[illegible]
56	0.57	— 4.8	— 19.4	— 0.15	+ 0.33	985.21
57	0.53	— 5.3	— 21.8	— 0.13	+ 0.30	991.96
58	0.51	— 5.5	— 22.0	— 0.13	+ 0.29	993.06
59	0.49	— 5.7	— 23.3	— 0.11	+ 0.30	995.81
60	0.48	— 5.8	— 23.4	— 0.12	+ 0.26	997.41
61	0.49	— 5.7	— 23.3	— 0.13	+ 0.26	996.57
62	0°53	— 5°2	— 21°7	— 0°16	+ 0°19	992°77
63	0.66	— 3.7	— 16.6	— 0.22	+ 0.32	970.52
64	1.26	+ 3.7	+ 9.9	— 0.66	+ 0.48	908.86
65	1.27	+ 3.8	+ 10.2	— 0.66	+ 0.53	910.18
66	1.36	+ 4.9	+ 14.3	— 0.73	+ 0.52	902.39
67	1.37	+ 5.0	+ 14.6	— 0.74	+ 0.51	903.36
68	1.44	+ 5.8	+ 17.9	— 0.79	+ 0.49	896.61
69	1.29	+ 4.0	+ 9.4	— 0.66	+ 0.47	910.88
70	1.55	+ 7.2	+ 23.5	— 0.84	+ 0.43	889.30
71	1.51	+ 6.7	+ 21.0	— 0.29	— 0.81	891.04
72	1.45	+ 6.0	+ 16.1	— 0.81	+ 0.50	905.27
73	1.46	+ 6.1	+ 16.4	— 0.82	+ 0.48	901.89
74	1.47	+ 6.2	+ 16.5	— 0.82	+ 0.50	899.08
75	1.55	+ 7.2	+ 21.7	— 0.91	+ 0.48	893.13
76	1.56	+ 7.5	+ 23.3	— 0.93	+ 0.47	889.84
77	1.47	+ 6.2	+ 22.0	— 0.78	— 0.11	891.92
78	1.57	+ 7.4	+ 21.1	— 0.89	+ 0.49	895.19
79	1.42	+ 5.6	+ 23.7	— 0.81	+ 0.42	891.37
80	1.48	+ 6.3	+ 24.2	— 0.89	+ 0.40	896.09
81	0.48	— 5.8	— 21.8	— 0.26	— 0.12	949.61
82	0.49	— 5.7	— 21.0	— 0.12	+ 0.01	955.26
83	0.52	— 5.4	— 23.2	— 0.30	— 0.11	953.43
84	0.51	— 5.5	— 22.4	— 0.19	— 0.01	964.91
85	0.49	— 5.7	— 19.6	— 0.15	+ 0.24	930.23
86	0.48	— 5.8	— 19.8	— 0.15	+ 0.25	956.86

87	0.99	+ 0.4	— 15.3	— 0.55	— 0.36	987.94
88	0.52	— 5.4	23.6	— 0.13	+ 0.28	978.09
89	0.52	— 5.4	— 23.6	— 0.13	+ 0.27	978.63
90	0.51	— 5.5	— 23.7	— 0.13	+ 0.27	977.60
91	0.81	— 1.8	— 21.2	— 0.47	— 0.22	1006.70
92	0.82	— 1.7	— 20.9	— 0.48	— 0.24	1005.94
93	1.55	+ 7.2	+ 20.0	— 0.36	— 0.96	956.88
95	1.55	+ 7.2	+ 10.8	— 0.81	+ 0.61	964.36
96	1.56	+ 7.3	+ 15.2	— 0.84	+ 0.58	965.29
97	1.57	+ 7.4	+ 15.4	— 0.86	+ 0.57	963.03
98	1.56	+ 7.3	+ 15.4	— 0.86	+ 0.34	957.14
99	1.47	+ 6.2	+ 24.1	— 0.86	+ 0.42	939.36
100	1.28	+ 3.9	+ 23.9	— 0.23	— 0.76	919.89
101	1.27	+ 3.8	+ 23.8	— 0.97	— 0.35	918.52
102	1.58	— 7.6	+ 18.5	— 0.90	+ 0.53	956.73
103	1.58	+ 7.6	— 18.7	— 0.90	+ 0.48	952.24
104	1.31	+ 4.3	+ 24.3	— 0.78	+ 0.37	917.76
105	0.48	— 5.8	— 15.2	— 0.26	— 0.13	897.53
106	0.49	— 5.7	— 17.8	— 0.26	— 0.03	903.89
107	0.52	— 5.4	— 21.1	— 0.30	— 0.11	912.15
108	0.60	— 4.4	+ 23.8	— 0.16	+ 0.31	932.97
109	0.60	— 4.4	— 23.9	— 0.16	+ 0.31	934.03
110	0.80	— 1.9	— 24.3	— 0.46	— 0.14	953.25
111	0.82	— 1.7	— 24.2	— 0.19	+ 0.49	958.36
112	0.82	— 1.7	— 24.1	— 0.18	+ 0.50	959.92
113	1.09	+ 1.6	— 18.9	— 0.29	+ 0.64	986.57
114	0.90	— 0.7	— 23.3	— 0.21	+ 0.54	966.53
115	1.40	+ 5.4	— 4.4	— 0.51	+ 0.71	1013.86
116	1.13	+ 2.1	— 18.2	— 0.31	+ 0.67	967.40
117	1.53	+ 7.0	+ 17.8	— 0.80	+ 0.52	934.11
118	1.53	+ 7.6	+ 18.1	— 0.88	+ 0.51	994.44
119	1.30	— 6.6	+ 21.0	— 0.87	+ 0.47	976.27
120	1.21	+ 3.1	+ 24.8	— 0.72	+ 0.33	956.69
121	1.08	+ 1.5	+ 23.7	— 0.64	+ 0.32	946.95
122	0.96	0.0	+ 21.2	— 0.56	+ 0.27	933.14
123	0°53	— 5°2	— 17°6	— 0°16	+ 0°17	887°87
124	0.56	— 4.5	— 20.8	— 0.18	0.00	889.93
126	0.65	— 1.4	— 24.9	— 0.48	— 0.11	905.31
127	1.54	+ 7.1	+ 4.1	— 0.64	+ 0.51	996.84
128	1.54	+ 7.1	+ 4.5	— 0.64	+ 0.50	998.73
129	1.27	+ 3.8	+ 23.6	— 0.66	+ 0.27	1013.91
130	1.26	+ 3.7	+ 23.8	— 0.66	+ 0.29	1015.30
131	0.83	— 1.6	+ 22.1	— 0.47	+ 0.25	984.99
132	1.44	+ 5.9	— 16.3	— 0.78	— 0.36	998.00
133	1.19	+ 2.8	— 23.9	— 0.25	+ 0.73	994.64

134	1.19	+ 2.8	− 23.8	− 0.25	+ 0.73	895.37
135	1.20	+ 2.9	− 23.6	− 0.24	+ 0.62	891.87
136	1.52	+ 6.8	− 9.7	− 0.74	− 0.64	918.61
137	1.53	+ 6.9	+ 7.8	− 0.58	− 0.81	945.64
138	1.53	+ 6.9	+ 8.0	− 0.56	− 0.83	946.77
139	1.53	+ 6.9	+ 8.2	− 0.56	− 0.81	946.66
140	1.47	+ 6.2	+ 12.9	− 0.48	− 0.84	951.53
141	1.38	+ 5.1	+ 16.4	− 0.36	− 0.86	967.30
142	1.44	+ 5.9	− 15.8	− 0.38	+ 0.73	913.65
143	1.44	+ 5.9	− 15.6	− 0.38	+ 0.85	912.35
144	1.55	+ 7.2	− 2.1	− 0.64	+ 0.81	942.55
145	1.55	+ 7.2	− 1.7	− 0.65	+ 0.80	941.20
146	1.52	+ 6.8	+ 6.4	− 0.71	+ 0.68	956.79
147	1.48	+ 6.4	+ 10.0	− 0.76	+ 0.62	964.18
148	1.49	+ 6.5	− 19.0	− 0.87	− 0.48	894.89
149	1.49	+ 6.5	− 18.8	− 0.83	− 0.36	895.70
150	1.19	+ 2.8	− 24.9	− 0.30	+ 0.54	903.76
151	1.30	+ 4.1	− 24.4	− 0.68	− 0.27	899.05
152	1.39	+ 5.2	− 22.8	− 0.79	− 0.42	895.46
153	1.47	+ 6.2	− 20.2	− 0.84	− 0.49	893.25
154	1.52	+ 6.8	− 0.4	− 0.56	− 0.29	900.95
155	0.89	− 2.0	+ 24.8	− 0.41	+ 0.07	979.66
156	0.98	+ 0.3	+ 23.0	− 0.56	+ 0.29	957.42
157	0.96	+ 0.2	+ 23.2	− 0.59	+ 0.27	954.56
158	0.80	− 2.0	+ 24.7	− 0.48	+ 0.22	947.89
159	0.66	− 3.3	+ 24.5	− 0.41	+ 0.18	962.99
160	0.48	− 5.8	+ 14.2	− 0.27	+ 0.15	973.29
161	1.43	+ 6.3	− 23.4	− 0.59	− 0.42	925.47
162	1.48	+ 6.3	− 23.3	− 0.89	− 0.41	925.96
163	1.54	+ 7.1	− 21.2	− 0.90	− 0.46	913.30
164	1.53	+ 7.0	− 21.0	− 0.87	− 0.48	914.93
165	1.58	+ 7.6	− 13.9	− 0.87	− 0.60	898.25
166	1.58	+ 7.5	− 13.7	− 0.86	− 0.58	900.02
167	0.97	+ 0.1	− 19.0	− 0.25	+ 0.60	964.09
168	1.11	+ 1.8	− 22.3	− 0.26	+ 0.67	957.63
169	1.44	+ 5.9	− 24.0	− 0.23	+ 0.05	932.12
170	1.44	+ 5.8	− 23.9	− 0.81	− 0.42	931.95
171	1.51	+ 6.7	− 22.1	− 0.89	− 0.46	922.16
172	1.57	+ 7.4	− 15.3	− 0.85	− 0.54	906.12
173	0.61	− 4.3	+ 24.4	− 0.36	+ 0.14	943.81
174	0.83	− 1.6	+ 22.1	− 0.50	+ 0.24	913.36
175	0.83	− 1.6	+ 22.3	− 0.50	+ 0.25	910.14
176	0.72	− 2.9	− 23.8	− 0.43	+ 0.20	924.19
177	0.72	− 2.9	+ 24.0	− 0.43	+ 0.29	922.18
179	0.57	− 4.8	+ 8.4	− 0.22	− 0.28	987.64
180	0.49	− 5.7	+ 20.3	− 0.29	+ 0.13	964.38

181	0.48	— 5.8	+ 18.4	— 0.28	+ 0.14	900.85
182	0.94	— 0.2	— 11.8	— 0.50	— 0.35	1006.83
183	1.09	+ 1.6	— 17.2	— 0.62	— 0.37	1003.09
184	1.23	+ 3.3	— 21.3	— 0.71	— 0.36	993.80
185	1.52	+ 6.8	— 24.4	— 0.91	— 0.40	957.76
186	1.53	+ 7.0	— 24.0	— 0.89	— 0.43	952.30
187	1.58	+ 7.5	— 22.2	— 0.94	— 0.44	938.27
188	0.73	— 2.8	— 1.7	— 0.27	+ 0.33	994.94
189	0.87	— 1.1	— 8.5	— 0.33	+ 0.45	1002.72
190	1.02	+ 0.7	— 14.7	— 0.31	+ 0.60	1005.74
191	1.16	+ 2.5	— 19.5	— 0.57	— 0.16	1004.39
192	0.81	— 1.8	— 5.5	— 0.32	+ 0.43	984.60
193	0.83	— 1.6	+ 17.7	— 0.48	+ 0.29	895.77
194	0.53	— 5.2	+ 24.1	— 0.31	+ 0.14	898.32
195	0.49	— 5.7	+ 23.7	— 0.29	+ 0.12	906.48
196	0.50	— 5.6	+ 19.9	— 0.29	+ 0.12	821.38
197	0.61	— 4.3	+ 12.2	— 0.29	+ 0.13	842.62
198	0.62	— 4.2	+ 11.7	— 0.28	+ 0.12	841.79
199	0.71	— 3.0	+ 6.5	— 0.29	— 0.30	852.21
200	1.28	+ 3.9	— 17.9	— 0.63	— 0.12	895.99
201	1.35	+ 4.7	— 19.7	— 0.28	+ 0.72	902.96
202	0.84	— 1.5	+ 12.9	— 0.28	— 0.46	896.34
203	1.55	+ 7.2	— 21.0	— 0.34	+ 0.97	872.02
204	1.22	+ 3.2	— 6.1	— 0.46	+ 0.66	948.64
205	0.48	— 5.8	+ 23.4	— 0.28	+ 0.10	893.78
206	0.49	— 5.7	+ 23.5	— 0.11	— 0.29	892.62
207	0.47	— 6.0	+ 23.6	— 0.28	+ 0.09	891.26
208	0.54	— 5.3	+ 20.9	— 0.10	— 0.02	891.89
209	0.65	— 3.8	+ 15.6	— 0.20	— 0.36	898.18
210	0.49	— 5.7	+ 23.2	— 0.29	+ 0.12	896.37
211	0.48	— 5.8	+ 22.9	— 0.29	+ 0.11	898.17
212	0.53	— 5.3	+ 21.5	— 0.31	+ 0.12	892.03
213	0.63	— 4.0	+ 16.1	— 0.33	+ 0.14	899.83
215	0.54	— 5.1	+ 20.0	— 0.31	+ 0.15	894.38
216	0.60	— 4.4	+ 17.3	— 0.35	+ 0.16	899.69
217	0.62	— 4.2	+ 17.1	— 0.35	+ 0.18	898.74
218	1.57	+ 7.4	— 23.2	— 0.93	— 0.44	980.59
220	0.82	— 1.7	— 15.0	— 0.44	— 0.31	1098.97
221	0.51	— 5.5	+ 19.8	— 0.30	+ 0.15	928.04
222	0.38	— 7.1	+ 22.9	— 0.22	+ 0.08	913.22
223	0.49	— 5.7	+ 23.0	— 0.27	+ 0.08	905.63
224	0.48	— 5.9	+ 21.5	— 0.29	+ 0.13	920.59
226	0.48	— 5.9	+ 22.9	— 0.29	+ 0.11	949.20
227	0.85	— 1.4	+ 14.1	— 0.47	+ 0.30	933.19

228	1.55	+ 7.2	— 21.9	— 1.33	+ 0.44	— 0.25	951.76
229	1.48	+ 6.4	— 22.9	— 0.73	— 0.25	— 0.30	964.31
230	1.20	+ 2.9	— 15.3	— 0.64	— 0.30	— 0.43	983.12
231	0.94	— 0.3	— 5.5	— 0.45	— 0.43	+ 0.80	976.70
232	1.34	+ 4.6	— 19.8	— 0.23	+ 0.80	+ 0.80	996.56
233	1.30	+ 4.2	— 19.5	— 0.33	+ 0.80	+ 0.80	994.29
234	0.87	— 1.1	— 6.7	— 0.34	+ 0.46	+ 0.46	998.57
235	0.87	— 1.1	— 6.0	— 0.35	+ 0.49	+ 0.49	1000.35
236	0.76	— 2.5	— 0.6	— 0.33	+ 0.37	+ 0.37	1003.67
237	0.74	— 2.7	+ 0.2	— 0.31	+ 0.36	+ 0.36	1006.00
238	0.85	— 1.4	+ 19.4	+ 0.04	— 0.01	— 0.01	913.01
239	0.56	— 5.0	+ 22.5	— 0.32	+ 0.19	+ 0.19	939.18
241	1.05	+ 0.9	+ 13.9	— 0.55	+ 0.29	+ 0.29	896.19
243	0.48	— 5.8	+ 10.3	— 0.66	— 0.01	— 0.01	1021.95
244	0.40	— 6.1	+ 14.3	— 0.25	+ 0.16	+ 0.16	985.18
246	0.48	— 5.8	+ 18.2	— 0.28	+ 0.15	+ 0.15	988.04
247	0.50	— 4.9	— 5.2	— 0.24	— 0.13	— 0.13	959.92
248	0.61	— 4.0	— 7.6	— 0.32	— 0.21	— 0.21	955.54
249	1.09	+ 1.6	+ 20.6	— 0.63	+ 0.26	+ 0.26	995.76
250	1.21	+ 3.6	+ 16.0	— 0.72	+ 0.43	+ 0.43	987.49

Table 16

Bel'kovich's observations

№№ набл.	a	b_0	C	Δx_0	Δ_{10}	Δx	Δy	h_0
6	0°56	— 1°87	12°3	— 0°03	— 0°03	— 0°30	+ 0°19	946°92
7	0.58	— 4.66	12.6	+ 0.04	+ 0.61	— 0.31	+ 0.19	944.96
8	0.65	— 3.64	16.2	+ 0.21	— 0.33	— 0.35	+ 0.20	962.64
9	0.78	— 2.19	19.2	— 1.97	+ 0.66	— 0.44	+ 0.20	977.67
11	1.02	+ 0.78	338.5	— 0.05	— 1.20	— 0.60	— 0.29	916.57
12	0.79	— 2.07	338.5	+ 0.41	+ 1.54	— 0.45	— 0.18	901.00
13	0.93	— 0.31	338.2	— 0.31	+ 0.82	— 0.53	— 0.18	912.93
14	0.70	— 3.14	339.1	+ 0.26	+ 1.33	— 0.41	— 0.16	900.90
15	0.62	— 4.15	340.7	+ 0.59	+ 0.80	— 0.35	— 0.16	896.23
16	0.86	— 1.20	338.0	+ 0.39	+ 0.91	— 0.50	— 0.30	906.32
17	1.15	+ 2.30	340.1	+ 0.30	+ 1.66	— 0.28	+ 0.72	917.27
18	1.02	+ 0.75	338.6	+ 0.54	+ 1.61	— 0.24	+ 0.62	910.57
19	0.72	— 2.93	338.6	— 0.06	— 0.25	— 0.17	+ 0.45	893.60
20	0.54	— 5.16	5.0	+ 0.01	— 0.04	0.22	— 0.34	908.83
21	0.45	— 6.19	348.0	+ 1.28	+ 0.36	— 0.16	+ 0.25	896.64
22	0.45	— 6.19	348.3	+ 1.00	+ 0.62	— 0.16	+ 0.25	896.70
23	0.49	— 5.77	0.5	+ 0.08	+ 0.91	— 0.22	+ 0.20	907.01
24	0.47	— 6.01	358.6	+ 0.65	+ 0.25	0.21	+ 0.22	904.12
25	0.69	— 3.28	11.8	— 0.14	+ 0.39	— 0.35	+ 0.25	919.57
26	1.18	+ 2.66	21.9	— 0.44	— 0.20	— 0.65	+ 0.36	972.26

27	1.52	+6.87	18.1	−0.24	−0.28	−0.36	−0.86	994.22
28	0.79	−2.05	9.6	−0.12	−0.09	−0.42	+0.29	897.34
29	0.80	−1.54	9.8	−0.49	−0.02	−0.41	+0.26	896.22
30	1.01	+0.55	16.8	−0.47	−0.71	−0.56	+0.29	906.15
31	0.97	+0.07	15.5	−0.07	−0.20	−0.54	+0.32	904.72
32	0.97	+0.16	15.6	−0.05	−0.18	−0.51	+0.33	905.39
33	1.12	+1.96	18.8	−0.53	−0.31	−0.02	+0.25	911.62
35	1.07	+1.38	17.5	−0.39	−0.16	−0.60	+0.34	906.84
36	1.09	+1.54	17.6	−0.29	−0.78	−0.62	+0.37	906.14
37	1.31	+4.23	21.2	−0.59	+0.08	−0.78	−0.40	911.51
38	1.57	+7.43	19.5	+0.02	−0.85	−0.90	+0.51	961.63
39	0.95	−0.15	382.7	+0.07	+0.82	−0.53	−0.26	977.75
40	1.14	+2.22	349.0	+0.01	+0.68	−0.60	−0.45	1002.28
41	1.04	+1.07	346.4	+0.04	+0.92	−0.33	+0.61	989.05
42	1.03	+0.89	346.2	+0.05	+0.93	−0.32	+0.59	989.39
43	0.90	−0.73	342.3	−0.42	−0.27	−0.24	+0.54	993.51
44	0.69	−0.53	342.2	+0.05	+0.78	−0.24	+0.53	994.08
45	0.48	−5.91	343.1	+1.28	+1.42	−0.15	+0.25	937.96
46	0.47	−5.92	343.2	+1.34	+1.46	−0.15	+0.25	917.59
47	0.47	−5.93	343.3	+1.35	+2.30	−0.14	+0.25	936.71
48	0.46	−6.08	341.9	+1.84	+2.65	−0.12	+0.25	910.26
49	1.05	+1.14	12.4	−1.16	+0.14	−0.56	−0.39	895.81
50	1.05	+1.22	12.5	−0.90	+0.86	−0.58	+0.36	896.02
51	1.55	+7.19	22.4	+0.08	+6.08	−0.27	−0.90	903.41
52	1.56	+7.26	22.4	−0.85	+0.45	−0.26	−0.89	904.24
53	1.46	+6.66	22.2	−0.23	−0.71	−0.87	+0.44	896.54
55	1.55	+7.18	19.1	+0.13	−0.38	−0.36	−0.78	919.25
56	1.37	+4.93	19.8	−0.10	−0.50	−0.78	+0.35	894.12
57	1.01	+0.57	351.1	−0.62	−0.21	−0.38	+0.53	963.65
58	1.00	+0.46	351.0	+0.73	+0.72	−0.35	+0.57	958.88
59	0.52	−5.33	337.2	+1.19	+0.81	−0.30	−0.10	1005.12
60	0.52	−5.39	337.2	+0.75	+1.67	−0.30	−0.10	1015.01
61	0.48	−5.86	337.0	+2.51	+3.25	−0.27	−0.08	936.33
62	0.77	−2.29	343.6	−0.01	−1.05	−0.25	+0.41	1000.36
63	0.55	−4.98	337.7	+0.49	+0.89	−0.06	+0.03	1014.13
64	0.49	−5.68	339.7	+2.13	+2.25	−0.29	−0.12	902.89
65	0.63	−4.06	337.7	+0.06	+1.43	−0.33	−0.19	959.59
66	0.62	−4.09	347.9	+0.55	+1.25	−0.33	−0.19	960.54
67	0.69	−3.33	341.5	+0.15	+0.12	−0.17	+0.41	992.49
68	0.68	−3.45	341.4	−0.26	+0.53	−0.18	+0.10	991.64
69	0°61	−4°31	346°2	+1°47	−0°25	−0°32	−0°23	979°51
70	0.72	−2.98	343.0	−0.05	+0.97	−0.21	+0.43	971.82
71	0.71	−3.07	342.9	−0.05	−0.62	−0.17	+0.42	971.48
72	0.51	−5.47	337.5	−0.10	−0.29	−0.13	+0.29	988.93
73	0.58	−4.63	343.8	+0.39	+1.40	−0.19	+0.32	967.49
74	0.76	−2.38	352.8	−0.17	+0.05	−0.28	+0.41	989.75
76	1.44	+5.80	20.1	−0.47	−0.32	−0.31	−0.87	896.41

77	1.44	+ 5.85	20.2	— 0.49	+ 0.76	— 0.31	— 0.85	899.55
78	1.23	+ 3.32	11.4	— 0.85	+ 2.12	— 0.65	+ 0.48	919.27
79	1.24	+ 3.41	11.6	— 0.73	+ 2.10	— 0.66	+ 0.48	918.09
80	1.24	+ 3.46	11.6	— 0.67	+ 2.53	— 0.65	+ 0.36	917.33
81	1.34	+ 4.61	15.5	0.91	+ 1.15	— 0.74	+ 0.46	908.97
82	1.35	+ 4.71	15.6	— 0.43	+ 1.13	— 0.75	+ 0.49	907.91
83	1.52	+ 6.87	22.0	+ 0.25	— 0.38	— 0.49	— 0.56	887.22
84	1.58	+ 7.59	23.1	+ 0.07	— 0.26	— 0.94	+ 0.43	892.45
85	1.46	+ 5.01	18.5	+ 0.25	— 1.29	— 0.80	+ 0.50	895.57
86	0.58	— 4.66	340.6	— 0.41	— 0.69	— 0.33	— 0.14	959.28
87	0.57	— 4.72	340.5	— 0.52	— 0.81	— 0.39	— 0.15	961.06
88	1.48	— 6.57	19.7	+ 1.65	— 0.77	— 0.77	+ 0.22	893.58
89	0.88	— 1.26	352.3	+ 0.27	+ 0.05	— 0.33	+ 0.47	949.20
90	0.85	— 1.36	352.1	+ 0.04	— 1.43	— 0.31	+ 0.46	949.55
91	0.49	— 5.78	336.4	+ 1.24	+ 1.14	— 0.30	— 0.11	985.91
92	0.48	— 5.81	336.4	+ 0.89	+ 0.53	— 0.24	— 0.10	987.38
93	0.46	— 5.87	336.4	+ 0.93	+ 1.32	— 0.28	— 0.16	988.29
94	0.71	— 4.09	347.0	+ 0.72	— 1.00	— 0.23	+ 0.39	954.77
95	0.51	— 5.44	339.0	+ 0.04	— 0.85	— 0.13	+ 0.28	989.02
96	1.14	+ 2.16	1.8	— 0.35	0.00	— 0.48	— 0.57	984.49
97	1.14	+ 2.19	2.0	— 0.70	+ 1.21	— 0.48	— 0.59	985.77
98	0.64	— 3.94	340.6	+ 0.75	— 0.43	— 0.15	+ 0.39	981.48
99	1.27	+ 3.75	6.8	— 0.96	+ 1.49	— 0.62	— 0.54	960.62
100	1.55	+ 7.19	22.3	— 0.11	— 0.26	— 0.31	— 0.82	924.61
101	1.35	+ 4.79	10.3	— 0.95	+ 0.77	— 0.70	+ 0.54	951.44
102	1.36	+ 4.86	10.5	— 1.37	+ 1.14	— 0.69	+ 0.57	950.75
103	1.54	+ 7.11	23.9	+ 0.48	— 0.19	— 0.54	— 0.54	904.40
104	1.54	— 7.12	24.0	+ 0.33	— 0.41	— 0.94	— 0.68	903.06
105	1.43	+ 5.71	22.0	0.08	+ 0.31	— 0.28	— 0.89	892.84
106	1.35	+ 4.71	19.5	+ 0.13	— 0.11	— 0.33	— 0.83	889.01
107	1.52	+ 6.50	17.9	— 1.51	+ 0.25	— 0.82	+ 0.31	934.12
108	1.55	+ 7.25	20.9	— 0.93	— 0.46	— 0.92	+ 0.49	923.19
109	1.56	— 7.30	20.9	0.28	— 0.36	— 0.90	+ 0.46	902.90
110	1.37	+ 5.10	20.4	0.31	+ 0.11	— 0.12	— 0.55	888.24
111	1.59	+ 7.68	22.7	+ 0.59	+ 0.13	— 0.91	+ 0.47	915.99
112	1.57	+ 7.47	23.8	— 0.68	+ 0.01	0.94	— 0.45	908.58
113	1.58	+ 7.50	23.8	— 0.51	+ 0.12	— 0.95	+ 0.46	907.29
114	0.94	— 0.22	346.8	— 0.31	+ 1.05	— 0.50	— 0.35	989.32
115	0.91	— 0.19	347.0	0.44	+ 0.77	— 0.51	— 0.34	989.80
116	0.95	— 0.18	347.0	— 0.74	+ 0.90	— 0.52	— 0.34	989.82
117	1.08	+ 1.41	352.1	0.27	+ 0.43	— 0.56	— 0.46	981.50
118	1.08	+ 1.42	352.3	+ 0.03	— 0.61	0.56	— 0.44	983.25
120	1.31	— 4.30	3.1	— 0.98	+ 0.59	— 0.49	— 0.63	983.93
121	0.46	— 0.05	336.6	— 0.05	— 0.30	— 0.11	+ 0.26	951.37
122	0.51	— 5.49	335.8	— 0.15	+ 0.16	— 0.10	+ 0.31	970.74

124	1.39	+ 5.19	6.5	− 1.50	+ 0.95	− 0.52	− 0.73	932.61
124	1.28	+ 3.89	22.1	+ 0.38	− 0.35	− 0.29	− 0.78	921.27
125	1.28	+ 3.90	22.0	− 0.43	+ 1.22	− 0.28	− 0.81	922.37
126	1.52	+ 6.82	24.1	− 0.74	− 0.60	− 0.89	+ 0.43	941.42
127	1.28	+ 3.85	22.2	− 0.48	+ 0.39	− 0.76	+ 0.38	912.60
128	1.01	+ 1.01	15.6	− 0.21	+ 1.99	− 0.58	+ 0.34	897.24
129	0.59	− 4.51	351.3	+ 0.07	+ 0.77	− 0.24	+ 0.29	887.28
130	0.58	− 1.69	353.2	0.32	+ 0.27	− 0.23	+ 0.29	887.32
131	0°50	− 5°59	344°3	+ 0°24	− 0°07	− 0°12	+ 0°18	893.71
132	0.49	− 5.72	340.7	+ 0.12	− 0.05	− 0.20	− 0.03	899.39
133	0.55	− 4.36	338.3	+ 0.62	− 0.47	− 0.33	− 0.12	912.49
134	0.62	− 4.19	335.5	+ 0.88	+ 0.16	− 0.37	− 0.12	921.44
135	1.01	+ 1.03	343.7	− 0.18	+ 0.78	− 0.58	− 0.35	957.26
136	1.05	+ 1.05	343.9	− 0.18	+ 0.85	− 0.58	− 0.35	959.41
137	1.54	+ 7.11	9.2	− 1.55	− 1.68	− 0.79	+ 0.62	984.61
138	1.55	+ 7.16	9.3	− 0.85	− 0.85	− 0.79	+ 0.61	984.16
139	1.41	+ 5.45	18.3	− 0.34	− 0.01	− 0.81	+ 0.47	946.09
140	0.64	− 3.91	342.6	+ 0.69	+ 1.00	− 0.37	− 0.20	935.71
141	0.60	− 4.37	15.2	+ 0.38	− 0.01	− 0.30	+ 0.11	1000.44
142	0.60	− 4.40	15.0	− 0.72	+ 0.29	− 0.30	+ 0.12	999.33
143	0.55	− 4.09	356.0	+ 0.68	+ 1.95	− 0.29	− 0.23	968.69
144	0.56	− 1.02	337.0	+ 0.58	+ 0.11	− 0.20	+ 0.51	922.06
145	0.52	− 5.46	14.3	+ 0.34	+ 0.43	− 0.17	− 0.24	1001.04
146	0.52	− 5.37	14.1	+ 0.37	+ 0.13	− 0.17	− 0.24	1001.[illegible]
147	0.55	− 4.94	16.6	− 0.07	+ 0.30	− 0.32	+ 0.15	983.02
148	0.56	− 5.57	8.0	+ 0.50	+ 0.05	− 0.25	+ 0.17	1004.04
149	0.90	− 0.75	340.2	+ 0.59	+ 1.43	− 0.52	− 0.25	986.51
151	0.53	− 5.25	0.2	− 0.23	+ 2.08	− 0.24	− 0.24	982.39

Table 17

Nefed'yev's observations

Obs. №	a	b_0	C	Δx_0	Δy_0	Δx	Δy	h_0
3	0°62	− 4°21	335°6	+ 0°15	− 1°37	− 0°36	− 0°12	923°54
4	0.79	− 3.12	336.0	+ 0.15	− 0.25	− 0.42	− 0.19	931.25
5	0.81	− 1.80	337.7	− 0.25	− 1.16	− 0.48	− 0.23	941.76
6	0.93	− 0.32	340.8	− 1.14	− 1.48	− 0.53	− 0.25	952.85
7	0.48	− 5.82	341.7	+ 0.61	+ 1.31	− 0.15	+ 0.24	900.96
8	1.18	+ 2.63	349.1	− 1.26	− 1.05	− 0.62	− 0.48	967.79
9	1.56	+ 7.32	15.4	− 0.12	− 0.30	− 0.45	− 0.54	976.34
10	1.04	+ 0.92	342.7	− 0.30	− 0.01	− 0.32	+ 0.54	978.87
11	1.04	+ 0.94	342.9	− 0.45	+ 0.87	− 0.32	+ 0.56	981.23
12	1.31	+ 4.32	352.6	− 1.02	− 0.01	− 0.50	+ 0.66	968.64

13	1.32	+ 4.44	352.9	— 0.94	+ 2.15	— 0.51	+ 0.64	967.25
14	1.41	+ 5.51	24.4	— 1.19	+ 0.24	— 0.83	— 0.31	989.85
15	1.41	+ 5.53	24.4	— 1.50	— 0.99	— 0.78	— 0.39	989.40
17	1.17	+ 2.59	23.4	— 0.12	+ 0.48	— 0.22	+ 0.73	970.39
18	1.57	+ 7.46	18.3	— 0.25	+ 1.24	— 0.90	+ 0.50	978.93
19	1.53	+ 6.94	21.8	— 1.26	— 1.53	— 0.88	+ 0.47	978.91
20	1.45	+ 5.98	24.1	— 0.57	— 0.22	— 0.86	+ 0.41	973.80
22	0.76	— 2.47	335.3	— 0.43	— 0.62	— 0.45	— 0.19	901.87
23	0.52	— 5.38	339.7	+ 0.16	+ 1.26	— 0.14	+ 0.30	899.77
24	0.52	— 5.40	339.6	+ 0.09	+ 0.43	— 0.14	+ 0 29	896.22
25	0.76	— 2.39	335.2	— 0.99	+ 0.07	— 0.16	+ 0.45	901.06
26	0.76	— 2.38	335.2	— 0.52	+ 0.52	— 0.18	+ 0.45	901.92
27	1.00	+ 0.48	337.5	— 0.31	+ 0.95	— 0.27	+ 0.52	917.53
28	1.44	+ 5.83	353.9	— 1.76	+ 0.04	— 0.54	+ 0.76	963.09
29	1.51	+ 7.07	6.6	— 1.85	— 0.70	— 0.66	+ 0.64	991.29
30	1.54	+ 7.08	12.2	— 1.14	— 0.75	— 0.92	— 0.11	996.98
31	1.50	+ 6.54	357.3	— 1.31	— 0.15	— 0.62	+ 0.76	959.51
32	1.54	+ 7.11	3.6	— 2.36	+ 0.33	— 0.71	+ 0.73	976.43
33	1.53	+ 6.97	15.3	— 1.78	— 1.51	— 0.80	+ 0.57	1004.11
34	1.51	+ 6.74	17.8	— 1.58	— 1.36	— 0.86	+ 0.52	997.87
35	1.51	+ 6.74	18.0	— 1.97	— 0.46	— 0.87	+ 0.52	986.21
36	1.43	+ 5.76	21.9	— 1.28	— 2.32	— 0.83	+ 0.45	1008.26
38	1.37	+ 5.05	23.4	— 1.09	— 1.03	— 0.81	+ 0.39	996.92
39	1.29	+ 4.06	24.5	— 0.73	— 0.99	— 0.78	+ 0.31	984.70
40	1.02	+ 0.76	23.7	— 1.25	+ 0.27	— 0.61	+ 0.28	989.68
41	0.64	— 3.86	11.4	+ 0.29	+ 0.10	— 0.20	— 0.18	971.23
42	0.52	— 5.31	345.3	+ 0.26	+ 1.71	— 0.16	+ 0.30	909.17
43	0.64	— 3.89	338.9	— 0.03	+ 1.25	— 0.16	+ 0.37	899.08
44	1.15	+ 2.35	337.3	— 0.62	+ 0.54	— 0.27	+ 0.69	893.72
45	0.99	+ 0.32	24.9	— 0.88	— 0.19	— 0.60	+ 0.24	1005.98
46	0.55	— 4.05	349.8	+ 0.36	+ 0.76	— 0.28	— 0.19	968.61
47	0.55	— 1.94	349.6	+ 1.16	+ 1.34	— 0.29	— 0.21	968.14
48	0.62	— 4.10	344.5	+ 0.81	+ 0.08	— 0.34	— 0.18	953.85
49	0.62	— 4.10	344.4	+ 0.61	— 0.80	— 0.32	— 0.24	953.83
50	0.71	— 2.99	340.4	— 0.32	— 0.93	— 0.41	— 0.21	938.59
51	0.51	— 5.48	5.8	— 0.89	+ 1.85	— 0.25	+ 0.22	986.19
52	0.60	— 4.46	346.6	+ 0.35	+ 0.23	— 0.33	— 0.18	962.93
53	0.79	— 2.64	338.4	+ 0.79	— 0.59	— 0.47	— 0.21	938.40
54	0.91	— 0.65	336.1	+ 0.60	+ 1.50	— 0.55	— 0.26	926.02
55	1.22	+ 3.23	335.8	— 0.96	+ 2.34	— 0.24	+ 0.77	900.94
56	1.21	+ 3.02	335.4	— 0.29	+ 1.86	— 0.23	+ 0.76	903.38
57	1.21	+ 3.00	335.5	+ 0.36	+ 2.62	— 0.30	+ 0.70	903.69
58	1.41	+ 5.46	13.0	— 0.73	— 1.49	— 0.47	— 0.77	909.11
59	0.85	— 1.38	24.8	— 0.61	+ 0.02	— 0.52	+ 0.20	972.27
60	0.85	— 1.39	24.8	— 0.32	+ 0.22	— 0.52	+ 0.19	971.97
61	0.52	— 5.41	352.5	— 0.43	— 3.07	— 0.26	— 0.22	967.52
62	1.15	+ 2.36	21.5	— 1.46	— 0.37	— 0.68	+ 0.31	933.98
63	1.15	+ 2.36	21.6	— 0.98	— 1.15	— 0.68	+ 0.35	933.61
64	0.94	— 0.30	24.6	+ 0.33	— 0.63	— 0.56	+ 0.25	944.72
65	0.93	— 0.33	24.6	— 0.10	— 0.49	— 0.56	+ 0.22	944.10

66	0°61	— 4°28	21°0	— 0°78	+ 2°22	— 0°35	+ 0°16	989°80
67	0.61	— 4.28	20.9	+ 0.18	+ 0.22	— 0.35	+ 0.17	989.75
68	0.63	— 3.98	351.0	— 0.37	— 0.81	— 0.33	— 0.27	994.05
69	0.51	— 5.47	13.8	— 1.09	+ 1.46	— 0.28	+ 0.17	995.05
70	0.60	— 4.35	358.2	+ 0.36	+ 1.40	— 0.21	— 0.08	1005.49
73	1.04	+ 0.92	337.0	+ 0.53	— 0.49	— 0.62	— 0.30	974.39
74	1.04	+ 0.95	337.0	+ 0.83	+ 0.91	— 0.62	— 0.28	974.12
75	0.97	+ 0.14	338.4	+ 0.09	+ 0.81	— 0.24	+ 0.59	977.89
76	0.97	+ 0.18	338.3	— 0.14	+ 0.38	— 0.22	+ 0.61	977.60
77	1.24	+ 3.41	335.2	— 0.03	+ 0.69	— 0.73	— 0.34	957.01
78	1.24	+ 3.43	335.1	+ 0.50	+ 0.80	— 0.74	— 0.34	957.35
79	1.58	+ 7.54	348.6	— 1.00	— 0.43	0.85	— 0.63	901.44
80	1.58	+ 7.51	348.7	— 1.01	— 0.70	— 0.84	— 0.60	902.16
81	1.06	+ 1.18	336.6	— 0.39	+ 0.38	— 0.22	+ 0.67	960.52
82	1.49	+ 6.43	339.0	— 0.40	+ 0.76	— 0.84	— 0.47	927.81
83	1.49	+ 6.43	339.1	— 0.37	+ 1.29	— 0.86	— 0.46	928.10
84	1.57	+ 7.39	346.8	— 1.15	+ 0.26	— 0.85	— 0.60	909.36
85	1.56	+ 7.36	346.9	— 1.10	+ 0.54	— 0.82	— 0.61	909.57
86	1.57	+ 7.40	351.6	— 0.74	+ 0.21	— 0.79	— 0.64	901.92
87	1.57	+ 7.38	351.7	— 1.28	+ 0.31	— 0.80	— 0.60	902.44
88	1.56	+ 7.32	349.4	— 0.72	0.00	— 0.81	— 0.55	904.12
89	1.56	+ 7.20	349.6	— 0.43	+ 0.53	— 0.82	0.64	904.96
90	1.54	+ 7.13	354.5	— 0.55	— 0.07	— 0.74	— 0.70	897.39
91	1.54	+ 7.09	354.6	— 0.21	— 0.27	— 0.75	0.69	898.64
92	1.53	+ 6.94	0.5	— 1.31	+ 0.95	— 0.66	— 0.74	897.11
95	1.35	+ 4.70	10.7	— 0.11	— 1.43	— 0.49	— 0.70	896.03
96	1.26	+ 3.61	15.0	— 0.30	— 1.96	— 0.38	— 0.71	897.08
97	1.25	+ 3.49	335.2	+ 0.46	+ 4.25	— 0.24	+ 0.79	941.29
98	1.55	+ 7.15	342.0	— 0.62	+ 2.24	— 0.40	+ 0.95	908.31
99	1.56	+ 7.13	342.1	— 0.73	+ 1.25	— 0.42	+ 0.94	909.44
100	1.18	+ 2.66	16.4	— 0.62	— 0.13	— 0.36	— 0.66	891.82
101	1.36	+ 4.89	7.5	— 1.92	+ 1.66	— 0.66	+ 0.59	896.52
102	1.36	+ 4.88	7.5	— 1.31	+ 2.35	— 0.66	+ 0.59	896.03
103	1.04	+ 1.00	20.2	— 1.01	+ 0.69	— 0.60	+ 0.34	963.85
104	1.04	+ 0.97	20.2	+ 0.26	— 0.40	— 0.61	+ 0.33	964.36
105	1.07	+ 1.35	19.0	— 0.89	— 0.26	— 0.63	— 0.35	901.45
106	1.07	+ 1.34	19.1	— 0.41	— 0.25	— 0.62	+ 0.35	900.72
107	0.68	— 3.39	24.6	— 0.94	+ 1.29	— 0.41	+ 0.17	914.35
108	0.68	— 3.39	24.6	— 0.33	+ 1.42	— 0.41	+ 0.18	913.45
109	0.54	— 5.17	22.1	— 0.04	+ 0.88	— 0.32	+ 0.15	940.46
110	0.50	— 5.65	12.0	— 0.85	+ 1.22	— 0.27	+ 0.17	967.79
111	1.17	+ 2.61	337.8	— 0.42	+ 0.50	— 0.69	— 0.35	996.19
112	0.81	— 1.86	349.6	+ 0.30	+ 0.01	— 0.28	+ 0.44	1000.33
113	1.57	+ 7.43	345.0	— 0.74	+ 1.84	— 0.87	— 0.57	935.15
114	1.43	+ 5.68	4.2	— 0.56	— 0.60	— 0.59	— 0.71	904.74
115	1.13	+ 2.02	339.1	— 0.46	— 0.32	— 0.28	+ 0.66	985.29

116	1.56	+ 7.34	345.1	− 1.77	− 0.34	− 0.42	− 0.59	950.17
117	1.08	+ 1.41	14.4	− 0.86	− 0.18	− 0.36	− 0.60	896.28
118	0.96	+ 0.04	18.1	− 0.98	− 0.36	− 0.25	− 0.58	894.66
119	1.46	+ 6.10	353.7	− 1.39	+ 3.09	− 0.54	+ 0.79	924.35
120	0.71	− 3.10	28.4	− 0.42	+ 0.24	− 0.19	− 0.36	890.75
121	0.48	− 5.87	21.6	− 1.05	+ 2.04	− 0.29	+ 0.13	900.78
122	0.48	− 5.84	21.4	+ 0.42	+ 0.95	− 0.28	+ 0.12	909.36
123	0.68	− 3.37	3.7	− 0.53	+ 1.53	− 0.33	+ 0.30	918.13
125	0.75	− 2.51	0.3	+ 0.01	+ 1.96	− 0.34	+ 0.35	944.94
126	1.01	+ 0.59	348.6	− 0.05	+ 1.58	− 0.34	+ 0.51	976.73
127	1.01	+ 0.64	348.3	+ 0.64	+ 0.51	− 0.35	+ 0.53	977.51
128	1.50	+ 6.60	335.9	− 0.61	+ 1.47	− 0.78	− 0.32	1009.96
129	1.50	+ 6.58	335.6	+ 0.01	+ 1.41	− 0.78	− 0.36	1010.44
130	1.57	+ 7.40	339.2	− 0.56	+ 1.47	− 0.92	− 0.49	995.88
131	1°56	+ 7°35	339°3	− 0°21	+ 1.70	− 0°90	− 0°50	995°66
132	0.76	− 2.38	18.8	− 0.88	+ 0.32	− 0.21	− 0.44	914.15
133	0.77	− 2.36	18.9	− 0.58	− 0.91	− 0.22	− 0.42	912.67
134	1.35	+ 4.81	352.6	− 1.32	+ 3.26	− 0.49	+ 0.75	958.11
135	1.35	+ 4.77	352.7	− 1.30	+ 4.05	− 0.48	+ 0.75	956.87
136	1.15	+ 2.35	2.1	− 1.05	+ 3.24	− 0.54	− 0.52	943.24
137	0.55	− 5.05	23.4	− 0.67	+ 2.47	− 0.33	+ 0.14	899.32
138	0.55	− 5.04	23.4	− 0.14	+ 2.19	− 0.32	+ 0.14	899.00
139	0.62	− 4.09	13.0	− 0.45	− 0.77	− 0.22	− 0.29	893.89
140	1.52	+ 6.78	340.9	− 1.59	+ 0.06	− 0.84	− 0.50	1005.61
141	1.51	+ 6.72	340.1	− 1.78	+ 0.91	− 0.84	− 0.59	1006.33
142	1.45	+ 5.94	342.8	− 0.75	+ 0.34	− 0.81	− 0.51	989.42
143	1.44	+ 5.86	341.0	− 1.05	+ 5.33	− 0.79	− 0.48	1000.69

Table 18

Krasnov's Observations

№№ набл.	P	D	H	H − H'	№№ набл.	P	D	H	H − H'
1	154°5	− 3°4	+ 14	0	10	19°2	+ 3°1	+ 2	+ 4
	127.9	− 4.5	+ 12	+ 8		0.3	+ 5.3	+ 5	+ 5
	101.6	− 4.6	− 6	− 4					
	74.7	− 3.7	0	+ 1	11	1.0	+ 6.1	+ 6	+ 8
	47.6	− 1.9	− 7	− 1		29.7	+ 2.2	− 11	− 3
	20.0	+ 0.4	− 4	− 1		59.0	− 2.4	− 4	+ 2
	2.6	+ 1.9	− 6	+ 1		89.4	− 6.4	+ 15	+ 7
						120.6	− 8.5	0	0
3	153.7	− 0.9	+ 21	+ 5		152.6	− 8.1	+ 2	+ 2
	124.9	− 1.7	+ 15	+ 8		173.6	− 6.4	− 16	− 16
	95.9	− 2.0	− 2	+ 1					
	66.0	− 1.8	− 10	− 6	12	172.6	− 3.5	− 14	+ 6

	34.9	− 0.9	− 3	− 1
	2.8	+ 0.3	+ 3	+ 7
	9.0	+ 0.1	+ 1	+ 1
4	354.5	+ 0.9	+ 8	+ 14
	26.4	− 0.6	− 5	− 2
	57.7	− 1.7	+ 2	+ 2
	88.0	− 2.3	+ 6	+ 2
	117.3	− 2.2	+ 6	+ 8
	146.3	− 1.5	+ 3	+ 9
	169.1	− 0.6	0	+ 6
5	3.4	+ 1.7	− 4	+ 3
	34.9	− 0.5	− 13	− 8
	65.7	− 2.5	− 19	− 13
	96.1	− 3.6	− 10	− 4
	126.2	− 3.7	+ 3	− 7
	156.1	− 2.8	+ 4	− 4
	182.8	− 1.2	− 7	− 2
6	1.9	+ 4.0	− 1	+ 7
	31.4	+ 0.6	− 3	+ 1
	61.2	− 3.0	− 1	+ 3
	91.4	− 5.7	+ 17	+ 16
	122.1	− 6.8	+ 7	+ 5
	152.8	− 5.9	+ 24	+ 14
7	185.8	+ 4.1	+ 10	+ 11
	211.5	+ 2.4	+ 6	+ 8
	239.5	0.0	+ 2	+ 10
	269.8	− 2.4	− 1	+ 8
	301.6	− 4.2	+ 3	+ 1
	333.9	− 4.7	− 5	− 1
8	191.3	+ 0.7	+ 20	+ 13
	163.1	+ 0.2	0	+ 1
	135.8	− 0.2	+ 5	+ 5
	108.7	− 0.5	− 10	+ 8
	80.9	− 0.7	+ 9	+ 12
	51.9	− 0.6	+ 9	(+ 21)
	21.5	− 0.3	+ 7	+ 10
9	3.3	+ 1.4	+ 3	+ 10
	33.8	− 0.0	0	+ 7
	63.4	− 1.4	− 4	+ 1
	92.4	− 2.2	+ 15	+ 13
	120.8	− 2.5	+ 11	+ 10
10	170.8	− 5.7	− 19	+ 2
	139.6	− 7.4	− 1	− 1
	108.7	− 7.0	− 23	+ 3
	78.1	− 4.6	+ 4	+ 6
	45.4	− 0.9	− 9	− 3

	144.7	− 4.4	− 3	+ 2
	117.3	− 4.3	− 6	− 6
	90.0	− 3.1	+ 4	+ 4
	63.0	− 1.2	− 11	− 5
	35.8	+ 1.0	− 9	− 5
	8.2	+ 3.1	− 1	− 2
	352.7	+ 4.0	− 4	+ 1
14	173.8	− 5.8	− 20	− 6
	142.6	− 7.4	− 11	− 11
	142.6	− 7.4	− 10	− 10
	111.6	− 6.8	− 25	+ 1
	81.3	− 4.3	+ 1	0
	51.7	− 0.6	− 6	+ 6
	22.8	+ 3.2	− 16	− 11
	3.4	+ 5.4	− 6	+ 2
15	183.7	+ 1.1	+ 11	+ 2
	234.0	0.0	− 10	+ 2
	260.9	− 0.6	− 6	− 15
	238.9	− 1.0	+ 6	+ 6
	208.1	+ 0.6	− 6	− 2
16	183.9	− 1.6	− 4	+ 4
	208.9	− 0.6	+ 3	+ 6
	234.6	+ 0.6	− 6	+ 6
	260.8	+ 1.7	+ 5	− 1
	287.3	+ 2.5	− 11	+ 2
	313.9	+ 2.9	+ 1	− 7
	340.1	+ 2.7	+ 3	+ 5
	357.6	+ 2.2	− 3	+ 6
17	159.6	− 6.6	+ 12	+ 13
	128.7	− 6.7	+ 21	+ 1
	95.3	− 5.0	+ 10	+ 12
	65.9	1.9	+ 9	− 13
18	356.6	+ 2.4	− 6	− 2
	330.1	+ 3.0	− 25	− 1
	303.2	+ 2.9	− 6	− 2
	276.2	+ 2.3	− 11	− 2
	249.1	− 1.3	− 5	− 5
	222.4	0.0	0	− 5
	185.2	− 0.6	− 8	− 2
19	189.2	− 3.0	− 6	+ 4
	216.4	− 0.9	+ 6	+ 8
	243.6	+ 1.5	− 2	− 1
	271.1	+ 3.6	− 16	+ 4
	298.4	+ 4.9	− 8	− 2
	325.4	+ 5.2	− 21	− 8
	353.6	+ 4.4	+ 3	+ 3

20	346°.5	+ 4°.7	− 4	− 2
	320.3	+ 5.4	− 14	− 4
	293.7	+ 5.0	− 10	− 6
	266.9	+ 3.5	− 24	− 2
	240.2	+ 1.4	− 9	− 3
	213.7	− 1.0	− 1	+ 1
	188.0	− 3.0	− 15	− 2
21	193.5	− 4.3	+ 26	(+ 32)
	220.8	− 0.4	+ 4	+ 5
	247.6	+ 3.6	0	+ 4
	273.8	+ 6.8	+ 2	+ 8
	299.6	+ 8.6	+ 4	+ 8
	325.3	+ 8.8	− 4	+ 4
	350.4	+ 6.5	+ 2	0
22	57.4	− 0.4	+ 3	+ 3
	30.5	+ 2.6	+ 1	+ 8
	3.6	+ 5.1	+ 1	+ 9
	336.2	+ 6.5	− 3	+ 3
	308.4	+ 6.6	+ 24	(+ 22)
	280.0	+ 5.1	+ 4	+ 8
	251.4	+ 2.4	+ 13	+ 3
	242.5	+ 1.5	+ 5	+ 7
23	346.8	+ 4.8	− 2	+ 1
	16.5	+ 3.3	+ 4	+ 2
	45.6	+ 1.0	− 6	− 2
	74.3	− 1.4	0	+ 3
	103.0	− 3.5	− 11	− 2
	132.2	− 4.6	+ 2	0
	149.8	− 4.6	+ 8	+ 2
24	0.5	+ 6.4	+ 1	+ 1
	334.0	+ 8.6	− 8	− 1
	307.1	+ 9.1	− 8	− 4
	281.0	+ 7.7	+ 2	+ 8
	252.5	+ 4.6	+ 15	+ 5
	224.6	+ 0.5	+ 2	+ 2
	196.0	− 3.9	+ 7	+ 2
	187.8	− 5.0	− 14	+ 4
25	198.7	− 2.5	+ 10	+ 8
	229.1	+ 1.0	− 1	+ 4
	259.4	+ 4.3	+ 13	+ 6
	289.6	+ 6.4	+ 3	+ 10
	319.4	+ 7.0	− 5	+ 8
	349.0	+ 5.7	+ 2	+ 7
	12.4	+ 3.7	+ 6	+ 2

29	192°.1	− 3°.2	+ 5	+ 1
	229.2	+ 1.1	+ 1	+ 3
	247.7	+ 5.1	− 6	− 4
	274.8	+ 7.9	+ 1	− 1
	301.9	+ 9.1	− 6	− 3
	328.8	+ 8.3	− 18	− 4
	355.0	+ 6.0	0	+ 4
30	352.4	+ 4.9	− 11	− 6
	324.8	+ 7.0	− 18	− 10
	297.2	+ 7.6	− 12	− 7
	269.7	+ 6.6	− 29	− 7
	242.1	+ 4.1	− 5	− 5
	214.5	+ 0.7	+ 1	+ 1
	188.8	− 2.6	− 16	− 6
31	192.4	− 1.2	+ 30	+ 14
	220.1	+ 1.4	+ 5	+ 10
	248.0	+ 3.7	+ 10	+ 13
	276.2	+ 5.3	+ 15	(+ 21)
	304.6	+ 5.6	+ 6	+ 3
	332.9	+ 4.7	0	+ 13
	1.3	+ 2.7	+ 2	+ 8
32	15.6	− 2.4	+ 9	+ 13
	47.3	− 1.1	− 2	+ 6
	76.8	+ 0.4	+ 4	+ 6
	104.0	+ 1.9	+ 3	+ 11
	129.8	+ 2.9	+ 29	(+ 27)
	155.4	+ 3.4	+ 28	+ 9
	181.9	+ 3.3	+ 22	+ 9
33	191.0	− 0.9	+ 14	+ 4
	218.3	+ 2.7	− 12	− 8
	245.4	+ 5.7	− 3	+ 3
	272.7	+ 7.5	− 6	+ 1
	300.1	+ 7.7	− 5	− 1
	328.0	+ 6.2	− 25	− 2
	349.6	+ 4.1	− 6	0
36	350.5	+ 1.0	− 9	− 16
	321.8	− 1.2	− 21	− 10
	292.8	− 3.2	− 12	− 14
	263.7	− 4.2	− 7	− 7
	234.9	− 4.2	− 18	− 2
	207.3	− 3.1	− 5	− 1
	183.7	− 1.5	− 6	+ 1
37	353.8	+ 6.0	+ 4	+ 3
	17.7	+ 5.2	− 1	− 5

27	170.1	+ 4.6	+ 4	+ 10
	144.8	+ 5.2	+ 6	+ 2
	120.4	+ 4.8	− 7	− 4
	95.3	+ 3.6	+ 5	+ 3
	68.2	+ 1.6	− 2	+ 4
	38.5	− 0.9	0	+ 2
	5.9	− 3.3	0	− 1
28	358.5	+ 6.8	− 1	− 2
	332.6	+ 9.4	− 14	− 6
	306.6	+ 10.3	− 2	− 2
	280.6	+ 9.1	0	+ 6
	254.0	+ 6.1	+ 2	− 3
	227.2	+ 1.7	0	0
	199.5	− 3.1	+ 9	+ 6
39	10.1	+ 3.0	− 8	− 11
	35.0	+ 0.8	− 16	− 11
	60.1	− 2.2	− 16	− 10
	85.5	− 4.8	− 2	− 4
	111.3	− 6.4	− 31	− 5
	137.4	− 6.7	− 16	− 10
	170.7	− 5.0	− 24	− 2
40	5.7	+ 3.1	− 4	− 2
	32.7	− 0.2	− 14	− 10
	59.4	− 3.3	− 15	− 9
	86.6	− 5.7	− 2	− 4
	115.0	− 6.8	− 4	+ 3
	142.1	− 6.2	− 11	− 5
	172.6	− 4.0	− 24	− 3
41	152.7	− 4.6	+ 13	+ 1
	127.2	− 6.2	+ 2	− 6
	101.1	− 6.5	− 4	− 4
	74.9	− 5.4	− 5	− 3
	48.7	− 3.2	− 6	− 4
	22.5	− 0.2	− 7	− 1
	5.4	+ 1.5	− 7	− 6
42	5.1	+ 1.8	+ 1	+ 3
	29.6	− 1.1	− 1	0
	54.5	− 3.9	− 15	− 3
	79.4	− 5.8	+ 6	+ 11
	103.8	− 6.6	− 7	− 7
	128.5	− 6.2	+ 10	− 5
	152.1	4.7	+ 15	+ 3
	172.4	− 2.7	− 5	+ 12

	41.0	+ 3.6	− 15	− 11
	64.0	+ 1.5	− 7	+ 3
	87.1	− 0.9	0	− 4
	110.7	− 3.1	− 27	− 2
	135.1	− 4.8	+ 2	+ 2
	158.0	− 5.5	0	+ 1
38	157.8	− 6.2	− 8	− 6
	131.8	− 5.7	− 1	− 5
	106.6	− 4.1	− 24	+ 2
	82.0	− 1.6	− 11	− 8
	58.0	+ 1.1	− 19	− 13
	34.2	+ 3.6	− 14	− 11
	10.4	+ 5.6	− 2	− 3
	51.4	− 1.3	− 14	− 6
	26.6	+ 1.3	− 17	− 11
	10.0	+ 2.9	− 10	− 13
47	4.7	+ 2.1	− 6	− 3
	29.9	− 0.4	− 6	− 4
	55.4	− 2.9	− 11	− 3
	80.4	4.7	− 4	+ 2
	105.8	− 5.5	− 27	− 2
	130.7	− 5.3	+ 3	− 1
	155.4	− 4.1	+ 2	− 6
	171.7	− 2.8	− 21	− 3
48	0.0	+ 6.3	+ 7	+ 5
	337.8	+ 6.2	+ 9	+ 9
	312.0	+ 5.0	+ 8	+ 5
	286.2	+ 2.8	− 2	+ 7
	259.4	0.0	+ 11	− 1
	232.3	− 2.7	− 3	+ 7
	197.9	− 5.2	0	+ 6
49	3.2	+ 2.6	− 4	− 3
	28.1	+ 0.5	− [illegible]	− 2
	53.9	− 1.7	− 12	− 4
	78.3	− 3.4	+ 5	+ 6
	103.0	− 4.5	− 10	0
	128.0	− 4.7	+ 5	+ 3
	152.3	− 4.0	+ 21	+ 8
	170.8	− 3.0	− 15	+ 1
50	169.5	− 2.5	− 8	0
	148.0	− 3.2	− 2	0
	125.2	− 3.4	+ 16	+ 8

43	191.2	− 4.7	− 11	− 2		102.2	− 3.1	− 2	+ 2		
	217.8	− 4.6	+ 1	+ 5		77.5	− 2.1	− 2	+ 5		
	246.0	− 4.4	+ 2	+ 4		52.0	− 0.7	− 15	− 3		
	274.7	− 1.3	− 14	+ 1		25.0	+ 1.1	− 10	− 4		
	302.2	+ 1.1	− 14	− 4		12.6	+ 1.9	− 7	− 10		
	328.8	+ 3.2	− 26	− 1							
	354.4	+ 4.7	+ 2	+ 1	51	201.3	− 3.5	− 3	− 7		
						227.6	− 0.4	− 10	− 6		
44	137.1	− 5.7	+ 1	+ 6		253.5	+ 2.6	− 1	− 3		
	112.0	− 4.3	− 25	+ 1		279.4	+ 5.2	− 12	− 8		
	88.3	− 2.1	+ 6	+ 2		304.4	+ 6.8	− 13	− 15		
	64.6	+ 0.4	+ 3	+ 3		328.4	+ 7.2	− 25	− 8		
	41.0	+ 3.0	− 3	0		353.1	+ 6.3	− 9	− 6		
	17.9	+ 5.0	+ 8	+ 4							
	354.9	+ 6.3	+ 7	+ 5	52	347.7	+ 4.3	− 9	− 5		
	329.5	+ 6.5	− 9	+ 10		323.2	+ 6.3	− 15	− 5		
	322.4	+ 6.4	− 3	+ 13		298.5	+ 7.2	− 12	− 8		
						274.4	+ 6.8	− 9	− 3		
45	1.9	+ 4.7	− 7	+ 1		248.8	+ 5.2	− 11	− 12		
	26.0	+ 2.5	− 10	− 2		224.7	+ 2.8	− 6	− 4		
	50.0	0.0	0	+ 1		197.9	− 0.2	+ 3	− 3		
	74.8	− 2.6	0	+ 1		169.2	− 1.4	− 7	− 7		
	98.4	− 4.0	− 7	− 5							
	124.1	− 5.7	− 4	− 2	53	191.0	+ 0.2	+ 19	+ 1		
	149.3	− 5.8	+ 2	+ 2		215.0	+ 2.9	+ 3	− 1		
	171.9	− 4.9	− 18	+ 4		240.8	+ 5.2	+ 2	0		
						263.1	+ 6.6	− 4	+ 5		
46	150.8	− 5.2	+ 5	− 2		288.2	+ 6.9	− 5	+ 3		
	125.4	− 5.7	− 16	− 15		313.1	+ 6.0	+ 3	− 1		
	101.0	− 5.1	− 4	− 2		348.0	+ 3.0	− 6	0		
	76.0	− 3.5	− 22	− 18							
54	347.6	+ 1.0	− 10	− 2	63	344.0	− 5.6	− 19	− 8		
	321.8	+ 3.6	− 12	− 4		314.3	− 1.6	− 9	− 13		
	295.9	+ 5.8	− 9	− 6		284.9	+ 2.8	− 10	− 2		
	270.9	+ 6.7	− 15	+ 3		258.2	+ 6.3	− 5	− 6		
	245.6	+ 6.5	− 1	+ 1		232.8	+ 8.4	− 12	− 11		
	223.0	+ 5.2	− 13	− 11		209.7	+ 9.0	− 8	− 14		
	199.5	+ 3.0	0	− 1		187.9	+ 8.2	+ 17	+ 2		
	190.5	+ 2.1	+ 11	− 5							
					64	342.9	− 6.2	− 8	0		
55	189.2	+ 3.3	+ 10	0		307.5	− 2.0	− 1	+ 3		
	211.9	+ 5.1	+ 4	+ 2		274.3	+ 2.7	− 16	0		
	235.8	+ 6.3	− 1	+ 2		243.1	+ 6.4	− 12	− 10		
	259.5	+ 6.4	+ 9	+ 1		214.9	+ 8.2	− 4	− 4		
	284.6	+ 5.4	− 5	+ 9		188.7	+ 8.2	+ 19	0		
	310.6	+ 3.3	+ 10	+ 6		163.3	+ 8.0	+ 15	0		
	337.0	+ 0.0	+ 2	+ 5							
	353.3	− 1.2	+ 4	+ 9	65	11.0	+ 2.4	0	− 2		
						37.4	+ 5.2	− 13	− 11		

							32.4	+ 6.3	− 21	− 6			
							84.4	+ 7.3	− 15	− 6			
							105.9	+ 6.8	− 5	− 1			
							127.5	+ 5.3	+ 4	− 5			
							150.6	+ 3.0	+ 11	+ 1			
							167.0	+ 1.0	− 3	− 5			
56	198.0	+ 1.7	+ 6	− 6									
	221.3	+ 4.1	+ 1	+ 3									
	244.6	+ 6.9	− 12	− 6									
	283.4	+ 7.9	+ 2	0									
	317.8	+ 6.3	− 6	− 7									
	343.5	+ 3.5	− 11	− 11									
	354.0	+ 2.2	− 9	− 5									
						66	164.5	0.0	− 1	− 1			
57	348.4	+ 0.2	− 8	0			139.7	− 3.1	− 5	− 4			
	422.1	+ 3.6	− 9	0			117.2	+ 5.5	+ 2	+ 2			
	296.0	+ 6.3	− 7	+ 4			95.3	+ 7.0	− 1	+ 1			
	271.3	+ 7.7	− 9	+ 1			73.6	+ 7.6	− 8	− 6			
	233.6	+ 7.2	− 3	− 1			50.9	+ 7.1	− 8	+ 2			
	210.5	+ 5.9	− 3	− 1			26.2	+ 5.4	− 3	0			
	188.9	+ 3.9	+ 3	− 5			10.5	+ 3.8	− 4	− 7			
58	157.7	+ 3.2	+ 8	− 2		67	14.7	+ 1.9	+ 9	+ 4			
	210.4	+ 5.8	− 2	− 6			41.6	+ 4.1	− 2	+ 2			
	243.0	+ 7.6	− 9	− 8			66.2	+ 5.4	− 4	+ 2			
	256.1	+ 8.2	− 2	0			89.0	+ 5.8	+ 1	+ 1			
	280.9	+ 7.5	− 11	− 5			111.2	+ 5.4	+ 6	+ 2			
	406.0	+ 5.5	− 5	− 12			133.4	+ 4.2	+ 6	+ 4			
	362.3	− 2.2	− 20	− 2			157.0	− 2.3	+ 21	+ 11			
	353.4	− 0.7	− 6	0			172.4	− 0.8	− 2	+ 3			
59	332.8	− 2.3	− 4	0		68	173.1	+ 0.5	+ 5	+ 10			
	325.5	+ 1.4	− 21	5			145.5	+ 3.0	+ 1	+ 2			
	299.4	+ 4.8	− 8	− 2			120.1	+ 4.7	− 2	+ 5			
	273.3	+ 7.2	− 5	− 1			95.5	+ 5.6	+ 10	+ 11			
							71.0	+ 5.5	+ 11	+ 15			
61	351.5	− 4.5	− 5	+ 5			48.7	+ 4.2	− 6	− 2			
	325.3	− 0.3	− 3	+ 5			13.8	+ 1.9	+ 10	+ 4			
	301.2	+ 3.9	− 1	+ 1									
	270.6	+ 7.0	− 10	+ 5		69	14.6	+ 3.5	+ 9	+ 1			
	245.8	+ 8.9	− 4	+ 4			43.4	+ 5.7	+ 2	+ 6			
	223.5	+ 9.2	− 5	+ 1			69.5	+ 6.5	− 4	+ 3			
	191.6	+ 7.2	+ 20	+ 3			91.6	− 6.1	+ 7	+ 13			
	176.8	+ 7.8	+ 14	+ 4			118.8	+ 4.7	+ 6	+ 6			
							144.5	+ 2.4	+ 1	+ 3			
62	188.3	+ 8.2	− 1	(− 19)			164.1	− 0.2	+ 1	+ 1			
	209.1	+ 8.9	− 23	(− 29)									
	232.0	+ 8.3	− 23	(− 21)		70	164.4	0.0	− 4	− 4			
	256.5	+ 6.4	− 17	− 13			138.3	+ 2.8	− 3	0			
	282.6	+ 3.4	− 16	− 10			113.9	+ 4.9	− 7	− 5			
	309.6	0.9	− 1	− 7			66.4	+ 6.4	− 8	− 2			
	319.8	5.0	+ 7	+ 12			40.3	− 5.5	− 6	− 2			
							11.3	+ 3.3	− 1	− 4			
71	696	+ 491	− 4	− 2		79	490	+ 588	0	+ 8			
	24.9	+ 6.3	− 2	0			33.6	+ 6.9	− 1	+ 3			
	59.9	+ 7.1	− 10	0			60.6	+ 6.4	− 10	+ 2			
	84.1	+ 6.6	− 8	+ 1			86.5	+ 4.7	+ 4	+ 3			

	107.6	+5.1	+1	+1
	132.2	+2.6	+7	+3
	149.5	+0.6	+11	+4
	170.1	−1.8	−8	0
72	169.1	−1.8	+1	+6
	139.9	+1.6	−7	−1
	113.8	+4.4	+2	+4
	88.3	+6.3	−5	−5
	62.6	+7.0	−12	+1
	35.3	+6.4	−1	−1
	10.6	+4.6	+3	+1
73	0.8	+5.9	−2	+1
	30.0	+7.2	−4	0
	56.7	+6.8	−12	+4
	81.7	+5.2	−5	+2
	107.1	+2.6	−6	−3
	134.0	−0.6	+4	+2
	169.2	−4.5	−10	+8
74.	170.1	−4.7	−20	+2
	139.7	−1.5	−16	−1
	111.6	+1.9	−15	−11
	84.7	+4.8	−13	−8
	59.1	+6.6	−14	−4
	31.5	+7.2	−12	−8
	2.8	+6.2	−10	−3
75	4.0	+6.4	−2	+6
	33.2	+7.1	−2	+2
	60.2	+6.2	−11	+1
	86.4	+4.1	−1	−3
	112.9	+1.1	−3	+2
	141.8	−2.3	−13	0
	171.1	−5.0	−20	+2
76	171.6	−5.2	−23	−1
	140.7	−2.3	−19	−1
	112.4	+1.0	−6	0
	85.2	+4.1	−3	−1
	59.1	+6.2	−16	−4
	32.2	+7.1	−6	−2
	3.1	+6.4	−8	−2
77	7.2	+6.3	−3	+3
	36.1	+5.8	+6	+4
	64.0	+4.0	−12	−2
	91.4	+1.3	0	+6
	119.6	−1.6	+8	+3
	149.6	−4.2	+12	+6
	169.2	−5.4	−16	+8

	113.2	+2.0	−1	+1
	141.2	−1.2	−13	−2
	158.7	−3.1	+19	+3
80	158.9	−3.3	+15	0
	132.2	−0.4	−2	−5
	108.5	+2.3	−7	−3
	88.1	+4.4	−3	−6
	65.4	+6.1	−14	−8
	42.1	+6.9	0	+4
	17.3	+6.6	+3	−1
	355.8	+5.4	+1	+6
81	196.6	−4.4	−1	+5
	217.2	−5.5	−1	+2
	248.6	−6.0	−2	+1
	280.6	−4.6	−11	+2
	312.2	−1.8	+3	−2
	342.5	+1.4	−8	−4
	353.4	+2.6	−2	+2
82	355.9	+3.2	−1	+3
	327.3	+0.2	−17	−4
	296.2	−2.9	−13	−9
	265.0	−5.1	+3	−1
	232.6	−5.8	−13	−4
	202.8	−4.7	−3	0
	189.4	−3.7	−11	+4
83	187.0	−4.5	−20	−7
	214.5	−6.0	+2	+4
	243.9	−6.1	−6	−1
	273.1	−4.6	−8	0
	301.8	−1.8	−8	−4
	329.7	+1.3	−29	−5
	359.8	+4.4	−4	−4
84	2.2	+4.8	−8	0
	335.5	+2.3	−6	0
	307.4	−0.8	−2	+2
	278.2	−3.8	−12	+1
	248.3	−5.7	−5	−1
	218.7	−6.1	−2	0
	190.4	−4.9	−5	+6
85	193.2	−5.7	+2	−2
	222.6	−6.5	+1	+1
	253.6	−5.4	+6	+6
	284.0	−2.8	−11	+6
	313.2	+0.5	0	−6
	340.5	+3.6	+2	0
	5.7	+5.8	−8	−1
	13.3	+6.2	+7	+4

78	46.5	+6.0	− 5	+ 2	86	248.3	−5.5	0	+ 1		
	21.8	+5.2	+ 9	+ 10		281.3	−2.6	− 6	+ 14		
	354.2	+3.3	+ 10	+ 9		309.4	+0.7	+ 13	+ 10		
	325.8	+0.5	− 1	+ 13		331.0	+3.7	+ 5	+ 11		
	294.2	−2.8	+ 7	+ 5		25.6	+6.0	− 6	− 2		
	262.9	−4.8	+ 14	+ 10		47.8	+6.9	− 3	− 1		
	231.7	−5.6	+ 2	+ 9							
86	69°1	+6.9	+ 2	+ 10		256°1	−7°3	− 4	− 4		
	90.1	+4.2	+ 10	+ 13		278.6	−4.8	− 25	(− 24)		
	103.8	+2.6	+ 7	+ 11		305.3	−1.2	− 17	− 13		
87	149.3	−3.2	+ 14	+ 4		333.2	+2.7	− 14	− 10		
	123.5	−0.4	+ 4	+ 2		355.1	+6.5	− 9	− 5		
	99.0	+2.4	0	+ 5	95	350.1	+5.9	− 2	+ 1		
	74.7	+4.8	+ 1	+ 2		353.1	+5.6	− 6	0		
	51.1	+6.3	− 11	0		327.1	+2.5	− 26	− 4		
	26.2	+6.8	0	+ 4		299.5	−1.3	− 6	− 4		
	359.7	+6.0	+ 5	+ 4		270.7	−4.9	− 9	− 3		
	347.1	+5.2	− 2	+ 1		241.2	−7.2	− 4	+ 7		
88	2.7	+5.0	− 3	+ 5		211.4	−7.5	− 6	− 2		
	31.2	+4.1	− 16	+ 8		186.9	−6.3	− 16	− 4		
	58.9	+2.3	0	+ 4	96	187.3	−6.4	− 15	− 1		
	86.8	+0.1	+ 4	0		215.3	−7.5	+ 1	+ 1		
	114.6	−2.1	− 10	+ 6		244.5	−6.7	− 6	− 2		
	143.0	−3.8	− 7	0		274.1	−4.1	− 13	− 7		
	161.6	−4.4	− 11	+ 1		302.6	−0.5	− 4	+ 2		
	171.8	−4.5	− 21	+ 1		330.6	+3.2	− 27	− 3		
89	348.0	+3.1	− 9	− 3		353.9	+5.9	− 4	− 6		
	320.8	−0.4	− 17	− 7	97	0.6	+6.5	0	0		
	291.3	−4.0	− 12	− 7		337.7	+4.2	0	0		
	261.4	−6.5	0	− 2		311.1	+0.8	+ 5	+ 6		
	231.9	−7.2	− 8	− 1		282.3	−3.0	− 6	+ 14		
	207.7	−6.0	− 13	− 8		252.9	−6.0	+ 7	+ 9		
	190.2	−4.9	− 10	+ 2		223.4	−7.4	− 4	− 4		
90	187.5	−4.9	− 14	+ 2		192.0	−6.6	− 14	+ 5		
	215.6	−6.7	− 3	− 1	98	1.4	+5.9	− 5	− 2		
	244.4	−6.6	− 12	− 8		334.2	+3.9	− 3	+ 7		
	274.0	−5.1	− 2	+ 7		304.6	+0.7	− 1	+ 3		
	303.4	−2.0	− 5	0		274.5	−2.6	− 11	0		
	331.6	+1.6	− 20	+ 2		243.6	−5.2	0	+ 4		
	355.8	+4.3	− 7	− 5		212.4	−6.2	0	+ 1		
91	347.7	+3.3	− 4	− 9		195.7	−6.0	+ 12	+ 6		
	320.2	−0.1	− 16	− 9	99	197.1	−5.2	+ 3	+ 6		
	290.8	−4.2	− 11	− 4		226.7	−4.6	+ 8	+ 6		
	260.8	−7.2	+ 2	+ 2		257.3	−2.6	+ 6	+ 6		

	230.7	− 8.1	− 1	+ 5
	201.8	− 7.0	− 4	+ 2
	187.8	− 5.7	− 18	+ 1
92	187.8	− 5.8	− 18	+ 1
	215.4	− 7.7	− 2	− 2
	244.7	− 7.8	− 10	− 6
	273.9	− 5.9	− 3	+ 4
	301.4	− 2.6	− 9	− 6
	328.6	+ 1.4	− 25	− 2
	351.0	+ 4.4	− 6	− 1
93	351.1	+ 4.9	− 3	+ 4
	324.2	+ 1.2	− 9	+ 1
	295.8	− 2.9	− 6	− 4
	266.9	− 6.2	+ 7	+ 5
	236.3	− 8.0	− 9	+ 3
	206.8	− 7.6	+ 3	+ 9
	189.5	− 6.2	− 15	+ 5
94	192.7	− 6.7	− 9	− 3
	221.1	− 8.0	− 10	− 10
102	355.1	+ 3.6	+ 1	+ 4
	329.1	+ 3.3	− 26	− 2
	301.6	− 0.2	− 4	+ 3
	273.7	− 3.5	− 6	+ 3
	244.3	− 6.1	− 2	+ 2
	215.7	− 7.0	+ 1	+ 2
	188.3	− 6.2	− 15	+ 4
103	193.5	− 6.3	+ 6	+ 2
	221.3	− 6.4	+ 2	+ 2
	249.6	− 4.9	− 3	+ 5
	279.7	− 1.9	− 3	+ 14
	308.5	+ 1.6	+ 3	+ 5
	335.6	+ 4.4	− 10	− 3
	358.5	+ 6.2	0	0
104	351.6	+ 5.2	− 4	+ 2
	324.2	+ 2.9	− 12	− 1
	295.6	− 0.1	− 3	− 6
	266.4	− 3.0	+ 2	− 6
	237.1	− 5.2	− 7	+ 5
	207.5	− 5.9	+ 3	+ 8
	188.4	− 5.5	− 26	0
	201.6	− 1.6	− 15	+ 5
105	189.3	+ 0.6	+ 15	+ 2
	186.4	+ 0.5	+ 7	+ 3

	287.0	0.0	+ 2	0
	316.3	+ 2.7	+ 12	+ 6
	344.7	+ 4.7	+ 8	+ 6
	11.4	+ 5.6	+ 5	+ 3
100	157.6	+ 0.3	+ 19	+ 1
	131.4	− 2.2	+ 4	+ 2
	102.7	− 4.4	− 6	+ 1
	73.3	− 5.5	+ 1	+ 4
	42.9	− 5.0	− 3	+ 1
	11.4	− 3.0	− 10	− 2
	8.7	− 2.8	− 3	− 1
	90.5	− 5.0	+ 12	+ 9
101	11.5	− 8.0	− 10	− 2
	45.4	− 8.0	− 15	− 9
	78.9	− 7.2	− 2	− 2
	109.6	− 4.4	− 28	− 2
	133.5	− 0.4	− 12	− 2
	165.0	+ 3.4	+ 6	+ 2
	93.8	− 6.1	+ 10	+ 6
108	190.0	+ 3.9	+ 8	+ 0
	218.9	+ 5.1	+ 7	+ 11
	242.5	+ 5.9	+ 2	+ 2
	267.6	+ 5.4	− 12	+ 10
	293.7	+ 4.0	+ 6	+ 12
	319.7	+ 1.8	− 4	+ 2
	346.7	0.8	− 4	+ 4
109	347.2	− 3.3	3	+ 3
	319.0	+ 0.4	2	0
	292.3	+ 3.9	+ 11	+ 17
	266.6	+ 6.5	− 15	+ 5
	241.8	+ 7.8	+ 7	+ 7
	216.7	+ 7.8	+ 5	+ 8
	191.8	+ 6.3	− 22	+ 4
110	182.8	+ 6.6	+ 26	+ 2
	204.9	+ 8.2	+ 11	+ 9
	228.0	+ 8.6	0	(+ 22)
	252.1	+ 7.6	+ 10	+ 3
	279.0	+ 5.0	− 7	− 2
	306.2	+ 1.3	− 8	+ 9
	329.6	− 2.1	− 10	+ 1
	341.8	− 3.7	− 1	+ 4
111	341.0	− 3.9	− 5	+ 1
	311.4	+ 0.6	− 2	− 1

Table 19

Mikhaylovskiy's Observations

№№ набл.	P	D	H	H − H'	№№ набл.	P	D	H	H − H'
1	4896	− 6?1	− 10	− 4	9	354?1	+ 0?6	− 7	0
	317.7	− 0.7	− 1	+ 5		299.8	+ 2.2	− 19	− 10
	287.5	+ 4.7	− 15	+ 4		272.6	+ 2.5	− 26	− 6
	257.3	+ 8.9	− 7	− 5		245.9	+ 2.2	− 11	− 10
	233.1	+ 10.4	− 2	+ 4		219.3	+ 1.6	− 8	− 6
	209.2	+ 10.4	+ 8	+ 6		195.6	+ 1.2	− 10	− 8
	185.2	+ 8.7	+ 2	− 14					
					10	284.4	− 2.4	− 11	− 9
2	182.0	+ 8.0	+ 15	0		260.6	+ 0.9	− 13	− 7
	205.1	+ 9.3	+ 2	+ 1		236.4	+ 4.0	− 7	− 3
	229.6	+ 9.6	− 6	− 6		212.0	+ 6.4	− 12	− 2
	256.9	+ 7.6	− 1	+ 2		187.4	+ 7.5	− 4	− 6
	284.9	+ 4.1	− 15	+ 1		162.4	+ 7.3	− 21	− 9
	315.4	− 0.9	+ 7	− 3		137.2	+ 5.8	− 4	+ 2
	11.0	− 8.2	− 15	− 15					
					11	151.2	− 6.0	+ 10	+ 4
3	186.0	+ 3.6	+ 7	− 1		124.1	− 5.6	− 3	+ 1
	215.9	+ 3.4	+ 5	+ 1		97.4	− 3.9	− 5	0
	234.8	+ 2.6		+ 3		71.4	− 1.4	− 5	− 3
	254.9	+ 1.5		− 7		45.9	+ 1.4	− 3	+ 2
	274.8	+ 0.2	− 14	+ 2		20.7	+ 3.9	− 1	+ 2
	294.8	− 1.1	+ 1	− 3		355.4	+ 5.7	− 1	+ 3
	314.6	− 3.0	+ 6	− 2					

4	198.2	+ 6.5	+ 9	− 5
	218.5	+ 6.2	+ 1	+ 3
	240.0	+ 5.1	+ 6	+ 2
	287.0	+ 0.7	− 7	− 6
	314.2	− 2.0	0	− 3
	338.0	− 4.3	− 7	− 3
5	343.5	− 7.3	− 5	+ 4
	314.7	− 6.0	+ 14	+ 8
	286.4	− 3.1	0	+ 11
	259.5	+ 0.4	+ 12	0
	234.4	+ 3.6	+ 8	+ 12
	211.2	+ 6.0	+ 13	+ 9
	189.8	+ 7.5	+ 27	+ 9
6	182.5	+ 6.6	+ 17	− 5
	204.5	+ 4.4	+ 14	+ 12
	239.4	− 0.1	− 2	+ 9
	266.5	− 3.7	+ 9	0
	295.3	− 6.4	− 5	− 2
	324.9	− 7.5	0	+ 2
	354.2	− 6.6	− 8	0
7	183.1	+ 5.7	+ 26	+ 3
	207.3	+ 3.8	+ 4	+ 8
	233.9	+ 1.0	− 8	+ 4
	262.8	− 2.2	− 1	− 6
	293.5	− 4.9	− 6	+ 1
	325.1	− 6.2	− 6	− 6
8	351.8	− 4.4	− 17	− 7
	316.7	− 4.0	− 8	− 18
	281.7	− 2.1	− 29	− 9
	218.2	+ 0.5	− 12	− 15
	217.0	+ 3.0	− 6	− 8
	188.4	+ 4.5	+ 3	− 6
17	203.0	− 0.5	− 1	− 3
	229.2	+ 2.5	− 4	− 1
	255.4	+ 5.1	− 4	− 4
	281.7	+ 6.6	− 9	− 3
	308.1	+ 5.9	+ 7	+ 6
	334.6	+ 5.8	− 9	+ 1
	350.9	+ 4.5	− 6	+ 1
18	224.6	+ 1.2	+ 4	+ 1
	251.1	+ 4.6	+ 17	+ 7
	277.4	+ 7.1	+ 5	+ 3

12	357.0	+ 6.8	− 11	− 6
	331.2	+ 9.4	− 19	− 7
	305.0	+ 10.2	− 7	− 5
	279.1	+ 9.1	− 17	− 14
	252.8	+ 6.1	− 3	− 4
	226.1	+ 1.8	− 20	− 17
	198.2	− 3.0	− 11	− 5
13	187.8	+ 5.6	+ 12	+ 1
	211.6	+ 2.6	− 11	− 9
	237.2	− 1.1	− 20	− 4
	265.0	− 4.8	− 3	− 9
	294.4	− 7.4	− 11	− 6
	324.6	− 8.0	− 20	− 12
	354.2	− 6.5	− 13	− 5
14	351.5	− 4.3	− 2	+ 7
	321.1	− 6.0	+ 9	+ 12
	290.1	− 5.9	− 7	+ 2
	259.7	− 4.1	+ 7	+ 2
	231.8	− 1.3	+ 1	+ 11
	204.1	+ 1.7	3	+ 1
	179.8	+ 4.1	+ 26	+ 10
15	187.2	+ 4.8	+ 11	0
	210.0	+ 1.6	+ 4	+ 8
	235.2	− 2.2	− 15	− 1
	262.5	− 5.8	+ 1	− 2
	291.4	− 8.1	− 10	0
	320.9	− 8.2	+ 2	+ 6
16	351.7	− 4.8	− 11	+ 1
	323.3	− 6.9	− 9	− 1
	294.1	− 7.2	− 1	+ 4
	265.3	− 5.7	+ 6	+ 2
	237.8	− 2.9	− 6	+ 8
	212.1	+ 0.4	− 3	− 3
	188.7	+ 3.5	+ 11	+ 1
26	189.6	− 1.0	+ 7	+ 7
	215.0	− 3.4	− 2	+ 2
	242.2	− 5.1	− 10	− 2
	270.7	− 5.6	− 14	− 8
	299.5	− 4.7	+ 6	+ 4
	327.9	− 2.6	− 14	− 2
	354.9	0	− 14	− 6
27	199.5	− 5.0	− 6	− 2
	228.0	− 5.7	+ 6	+ 4
	257.6	− 4.9	+ 5	+ 3

	303.6	+ 8.1	0	0
	329.6	+ 7.6	− 10	+ 4
	355.5	+ 5.6	− 22	− 18
19	198.3	+ 8.0	+ 6	− 1
	227.8	+ 7.5	+ 4	+ 6
	260.0	+ 4.8	+ 5	− 3
	295.1	− 0.3	− 6	− 6
	332.6	− 4.4	− 12	− 2
20	186.9	+ 7.8	+ 8	− 4
	209.7	+ 8.2	+ 9	+ 3
	234.1	+ 7.3	− 9	− 7
	260.5	+ 4.9	+ 10	+ 2
	319.0	− 2.9	0	− 6
	350.3	− 4.3	− 10	+ 2
21	353.0	− 5.8	− 14	− 2
	319.8	− 5.9	+ 1	+ 1
	286.6	− 4.0	− 12	− 2
	254.8	− 0.8	− 5	− 11
	225.2	+ 2.5	− 3	0
	195.1	+ 5.0	+ 9	− 5
	173.5	+ 6.3	− 9	− 9
22	57.0	+ 5.8	+ 14	(+ 22)
	84.1	+ 5.4	− 15	− 7
	110.4	+ 4.0	− 9	− 7
	137.5	+ 1.7	− 8	− 5
	166.9	− 3.1	+ 10	+ 6
23	191.9	− 1.4	+ 20	+ 4
	218.1	− 3.4	+ 7	+ 11
	246.1	− 4.7	+ 2	+ 2
	275.1	− 4.8	− 1	+ 5
	304.4	− 3.7	+ 6	+ 6
	332.9	− 1.6	− 8	+ 7
24	23.2	+ 4.1	− 29	(− 25)
	352.8	+ 1.6	− 17	− 11
	320.2	− 1.4	− 18	− 14
	285.8	− 4.1	− 41	(− 31)
	250.8	− 5.2	− 16	− 8
	216.8	− 4.4	− 15	− 11
	185.0	− 2.2	− 25	− 11
25	198.8	+ 1.0	+ 12	+ 2
	222.1	− 1.7	0	+ 1
	247.2	− 4.2	− 6	− 1
	273.7	− 5.9	− 6	+ 2
	300.9	− 6.3	+ 4	0
	328.0	− 5.3	− 17	− 3
	354.2	− 3.2	− 2	+ 3

	287.3	− 2.7	− 1	+ 7
	316.2	+ 6.2	+ 6	− 2
	343.8	+ 3.0	− 6	− 2
	9.8	+ 5.0	+ 1	+ 1
28	199.2	− 6.4	− 18	− 12
	226.1	− 6.2	− 13	− 9
	253.5	− 5.5	− 4	− 3
	280.9	− 1.8	− 24	− 4
	307.5	+ 1.3	− 12	− 11
	333.0	+ 4.1	− 12	+ 12
	357.2	+ 6.0	− 6	0
29	349.8	− 7.1	− 1	+ 4
	317.4	− 0.9	+ 14	+ 6
	285.8	+ 4.2	0	+ 14
	258.1	+ 7.9	+ 18	+ 18
	231.6	+ 9.7	+ 8	+ 10
	207.0	+ 9.6	+ 16	+ 10
31	351.8	− 6.1	− 16	− 4
	316.2	− 1.5	+ 5	− 5
	288.5	+ 3.4	− 15	− 5
	259.6	+ 7.2	0	− 8
	232.8	+ 9.1	− 10	− 10
	208.0	+ 9.2	+ 5	− 1
	164.5	+ 7.9	+ 13	+ 1
32	351.0	− 6.0	− 2	+ 10
	319.0	− 1.3	+ 4	+ 2
	288.7	+ 3.6	− 10	0
	260.3	+ 7.3	+ 12	+ 4
	233.9	+ 9.3	+ 4	+ 2
	209.5	+ 9.4	+ 15	+ 9
	186.3	+ 8.1	+ 8	− 6
33	186.0	+ 7.2	+ 20	+ 2
	209.3	+ 8.0	+ 8	+ 2
	234.0	+ 7.6	+ 6	+ 6
	260.6	+ 5.7	+ 13	+ 5
	289.0	+ 2.3	− 2	+ 7
	319.2	− 1.8	+ 9	+ 13
	350.4	− 5.4	− 8	+ 4
34	185.3	+ 7.2	+ 1	− 15
	208.9	+ 8.2	+ 1	− 5
	233.5	+ 7.9	− 7	− 5
	260.8	+ 5.9	− 4	− 12
	289.7	+ 2.5	− 15	− 9
	320.4	− 1.8	− 18	− 15
	352.3	− 5.6	− 15	− 3

35	188°.4	+6°.0	+17	+5	45	187°.6	−2°.3	−14	−2
	211.6	+6.2	+1	−3		218.3	−3.5	−6	−2
	236.4	+5.4	−5	−2		250.8	−3.6	−9	−7
	262.7	+3.5	−8	−2		284.0	−2.4	−20	−7
	290.7	+0.8	−6	−3		316.9	−0.7	−12	(−21)
	320.0	−2.2	−1	−1		348.6	+1.7	−9	−1
	350.0	−4.6	−11	+1		19.4	+3.4	−8	−12
36	187.2	+6.0	+10	0	46	357.5	+3.4	+2	+2
	211.0	+6.5	+9	+5		332.5	+0.9	−19	+3
	236.2	+5.9	−3	0		305.1	−1.8	+4	+8
	263.1	+4.9	+15	−7		278.7	−4.2	−2	+10
	291.8	+1.3	+3	+1		251.0	−5.6	+7	+9
	321.7	−1.9	−11	−1		223.7	−5.6	0	+1
	352.4	−4.6	−3	+6		197.3	−4.4	+8	+10
37	152.3	−1.2	+12	0	47	358.8	+2.6	−16	−12
	126.3	+2.7	−2	−4		331.9	+4.2	−35	(−18)
	102.6	+5.8	−10	−10		303.5	+5.1	−8	−4
	79.8	+7.9	−9	9		274.4	+4.7	−23	−11
	56.6	+8.8	−19	−15		245.4	+3.2	−16	−14
	32.0	+8.3	−7	−5		217.4	+1.1	−12	−12
	5.2	+6.1	−10	−3		190.7	−1.1	−4	+4
38	353.1	−5.0	−4	+4	48	359.5	+2.3	−7	−4
	323.6	−2.4	−19	−9		333.3	+0.3	−22	−6
	294.6	+0.8	+2	+2		306.0	−1.7	−11	+7
	267.1	+3.7	−20	+2		277.8	−3.4	−17	−7
	241.0	+5.8	+5	+4		249.8	−4.2	−1	+7
	216.7	+6.7	−3	−2		222.4	−3.1	−7	−5
	193.8	+6.5	+17	+3		195.1	−2.8	−2	−3
40	190.5	+3.1	+10	−4	49	0.8	+1.1	−14	−14
	214.3	+2.9	+8	+8		332.8	−0.1	−23	−1
	239.4	+2.1	+1	+6		303.7	−1.2	−9	−3
	265.9	+1.0	−14	+6		274.1	−2.0	−18	−6
	293.4	−0.4	−2	0		245.0	−2.2	−6	−4
	321.6	−1.6	−8	+2		216.7	−1.8	−8	−4
	349.7	−2.5	−7	−2		190.1	−0.3	+4	−6
42	352.9	−6.9	+1	+5	50	349.8	−5.7	−16	−4
	324.3	−0.9	−12	−2		317.2	−0.9	−11	(−21)
	295.2	−0.7	0	−4		285.1	+4.0	−22	−8
	266.5	−0.2	−20	−6		257.0	+7.6	−5	−1
	238.6	+0.4	−1	+11		230.1	+9.3	−10	−7
	211.9	+0.9	+4	+4		205.3	+9.2	−3	−5
	186.7	+1.3	+7	−1		181.4	+7.5	+22	+8
43	359.1	+0.8	−13	−9	51	290.8	+4.8	−5	+1
	330.0	−0.2	−32	−13		264.6	+6.5	−8	0

	209.9	— 1.2	— 4	— 2		240.2	+ 16.8	+ 6	+ 6
	269.5	— 1.6	— 19	— 7		217.3	+ 10.8	— 1	+ 5
	239.6	— 1.7	— 20	— 6		195.6	+ 9.3	+ 13	0
	210.9	— 1.2	+ 2	+ 2					
	183.8	— 0.4	— 2	+ 4	52	191.6	+ 8.2	+ 10	— 8
						214.4	+ 10.1	0	— 1
44	187.6	— 2.3	— 9	+ 1		238.2	+ 10.4	+ 7	+ 7
	218.3	— 3.5	— 7	— 7		263.5	+ 8.9	+ 1	+ 3
	250.8	— 3.6	— 7	+ 1		289.8	+ 5.5	— 11	— 3
	284.0	— 2.4	— 16	+ 2		319.6	+ 0.5	— 10	— 8
	316.9	— 0.7	— 2	— 12		350.1	— 4.8	— 6	+ 6
	348.6	+ 1.7	— 16	— 8					
54	357.7	— 3.0	— 13	— 6		304.3	+ 3.7	+ 1	+ 1
	321.7	+ 0.9	— 15	+ 3		330.4	+ 2.5	— 17	+ 7
	292.8	+ 4.4	— 5	+ 1		356.5	+ 0.8	— 11	— 7
	265.2	+ 6.8	— 19	— 2					
	238.9	+ 7.7	— 4	— 4	57	351.7	+ 0.8	— 2	+ 4
	214.0	+ 7.2	— 12	— 14		324.8	+ 3.1	— 11	+ 1
	190.2	+ 4.4	+ 16	+ 4		298.1	+ 6.5	— 3	+ 3
						271.8	+ 5.3	— 16	+ 2
55	352.8	— 1.6	+ 4	+ 9		246.1	+ 4.9	+ 3	+ 9
	333.3	+ 1.3	— 2	+ 8		221.2	+ 3.7	+ 4	+ 6
	288.3	+ 3.8	+ 13	(+ (9)		196.8	+ 1.9	+ 13	+ 5
	266.3	+ 5.4	— 9	+ 13					
	239.5	+ 5.3	+ 6	0	58	355.5	+ 2.0	+ 1	— 4
	213.8	+ 5.1	— 1	2		327.5	+ 3.5	— 16	+ 14
	189.0	+ 4.2	+ 18	+ 6		280.5	+ 4.2	+ 8	+ 14
						271.3	+ 4.0	— 16	+ 1
56	204.2	+ 1.6	— 3	+ 1		244.0	+ 3.9	+ 14	+ 14
	228.3	+ 3.0	— 3	— 2		217.0	+ 1.4	+ 10	+ 10
	253.1	+ 4.0	— 5	— 3		190.5	— 0.5	+ 25	+ 9
	278.5	+ 4.2	0	+ 4					

Table 20

Kanachkewicz's Observations

№ № наб.	P	D	H	H — H'	№ № наб.	P	D	H	H — H'
1	170.7	+ 5.9	+ 1	+ 2		128.2	+ 2.1	+ 1	— 2
	158.1	+ 4.8	+ 9	+ 3		147.7	+ 3.2	— 1	— 1
	145.7	+ 3.6	+ 10	+ 10		169.2	+ 3.9	— 11	0
	132.5	+ 2.2	+ 1	— 1					
	119.5	+ 0.6	+ 6	0	9	170.6	+ 2.8	— 12	— 1
	105.7	— 1.1	— 25	0		149.5	+ 2.7	+ 20	+ 11

	76.2	−4.3	−5	+1			128.4	+2.4	+11	−6			
	32.6	−6.6	−2	+2			106.1	+1.7	−13	−5			
							33.6	+0.3	−4	−1			
2	4.6	−4.9	+1	+1			60.6	−0.2	−10	−4			
	38.2	−5.0	+2	+2			34.3	−1.3	−9	−3			
	70.3	−3.5	+3	+1			6.1	−2.0	−6	−4			
	96.5	−1.2	+3	0									
	126.8	+1.5	+15	+7		10	182.6	+8.0	+1	−15			
	152.6	+3.7	+16	+4			202.7	+9.5	−2	−2			
	168.8	+4.8	+1	+4			224.1	+9.9	−20	−16			
							236.7	+8.0	−13	−9			
3	158.2	+7.0	+25	(+23)			262.0	+4.8	−21	−11			
	157.2	+5.8	+4	−4			309.0	+3.4	−10	−7			
	146.4	+4.0	−3	−3									
	124.9	+1.6	+10	+6		11	179.8	+6.8	+6	−3			
	100.2	−1.2	−8	−1			230.5	+7.6	+3	−4			
	77.6	−3.9	+5	−6			222.8	+7.9	−14	−11			
	51.8	−6.0	−7	−2			246.2	+6.8	−2	0			
	27.8	−6.7	−6	−4			258.2	+1.0	−2	0			
							315.2	−1.3	+7	0			
4	11.0	−6.4	−6	+2									
	39.7	−6.5	0	0		12	3.1	+1.0	−1	+5			
	67.1	−5.0	−12	−5			25.7	+2.4	−1	+7			
	91.5	−2.6	+7	+5			52.6	+3.4	−17	−2			
	118.4	+0.6	+6	+2			75.2	+3.8	+2	+3			
	137.9	+2.9	+4	+3			96.9	+3.7	+4	+1			
	157.7	+4.9	+16	+7			117.7	+3.1	+2	0			
	162.6	+6.6	+22	+1			139.2	+2.1	−5	0			
							159.4	+1.0	+18	+2			
5	170.4	+5.2	−8	−4									
	149.4	+4.0	+11	+1		13	172.3	0.0	−6	−1			
	128.1	+2.3	+1	−15			148.7	+1.4	+6	+1			
	105.7	+0.1	−32	−15			126.7	+2.6	+3	0			
	81.0	−2.3	−8	−4			105.5	+3.5	−1	−1			
	56.8	−4.0	−13	−4			82.2	+3.8	−3	0			
	29.6	−5.2	−14	−6			62.3	+3.7	−10	−1			
	3.1	−5.1	−16	−14			39.1	+3.1	−5	−2			
							14.2	+1.9	0	−7			
6	3.2	−5.0	−12	−10									
	28.2	−5.1	−8	−6		14	345.6	−5.2	−11	+1			
	55.5	−4.1	−20	−12			317.0	−0.7	+6	−4			
	81.0	−2.3	−8	−6			289.8	+3.6	−9	0			
	104.7	−0.1	−30	−14			264.6	+7.2	−8	+2			
	127.0	+2.0	+2	−4			240.0	+9.2	+7	+7			
	148.4	+3.7	+5	0			196.4	+8.9	+15	+2			
	169.6	+5.0	−15	−11			180.8	+7.5	+15	+4			
7	169.6	+4.0	−3	−2		15	171.4	+2.1	−4	+2			
	128.1	+2.4	+15	−2			149.0	+2.1	+21	+16			
	105.2	+1.0	−17	−6			127.1	+1.8	+19	+9			

	58.6	−2.1	−11	−5
	32.5	−3.3	−6	−2
	4.8	−3.7	−2	−3
8	2.8	−3.5	−14	−12
	30.1	−3.3	−4	−1
	56.4	−2.2	−11	−5
	81.1	−0.8	−10	−7
	104.2	+0.7	−23	−10
16	78°5	+0°4	+4	+2
	101.3	+1.0	−5	−2
	123.9	+1.6	+10	+2
	145.2	+1.9	0	+6
	167.4	+2.0	+6	+5
17	2.7	−1.0	+4	+2
	29.5	−0.7	+3	+5
	54.8	−0.2	−4	+4
	78.8	+0.4	+4	+2
	101.6	+0.9	−2	+4
	123.7	+1.3	+7	+1
	145.8	+1.5	0	+5
18	169.3	+0.5	−15	−3
	146.4	+1.4	−5	0
	124.5	+2.1	+5	0
	102.9	+2.6	−6	−2
	81.1	+2.7	−4	−1
	58.5	+2.5	−7	−4
	34.6	+1.8	−11	−9
	7.4	+0.7	+1	+1
19	169.1	+0.2	−8	+4
	145.0	+0.8	−6	0
	123.0	+1.3	+8	+8
	102.3	+1.6	−4	+2
	80.5	+1.7	+2	+2
	57.9	+1.6	−2	+3
	34.0	+1.3	−4	−1
	8.7	+0.8	+6	+5
20	196.9	+3.1	+13	+6
	220.4	+3.7	−7	−4
	245.1	+3.7	0	+1
	270.9	+3.0	−26	−4
	279.6	+1.8	−2	+4
	322.3	+0.3	−13	+1
	352.3	−1.5	−5	0
21	169.0	−0.4	−1	+6
	145.6	+0.4	−6	+1

	105.1	+1.2	−7	+3
	82.6	+0.5	+5	+3
	58.9	−0.3	+8	+7
	33.7	−1.0	+4	+4
	7.2	−1.5	+5	+9
16	2.7	−1.4	+1	−1
	29.2	−0.9	+6	+7
	54.5	−0.3	−4	+4
24	350°5	+4°8	+4	+3
	24.1	+6.7	−6	−2
	46.7	+7.4	−1	+3
	67.9	+7.1	−8	0
	88.5	+5.9	+3	+3
	109.2	+4.0	−4	−2
	130.8	+1.5	+9	−2
	154.0	−1.5	+25	+6
25	152.3	1.4	+18	+6
	129.1	+2.2	+18	0
	107.9	+5.3	+8	+5
	87.7	+7.5	−1	−1
	67.8	+8.9	−5	+1
	47.3	+9.2	−6	−2
	25.3	+8.3	−3	0
	1.4	+6.1	−2	+2
26	0.8	+8.6	5	−3
	24.2	+9.2	−1	+1
	45.9	+10.3	−16	−12
	66.1	+10.1	−16	−2
	85.7	+8.8	−6	0
	105.4	+6.4	+4	+6
	125.3	+3.1	+3	+1
	150.1	−1.1	+14	+1
27	355.5	+4.4	−1	−3
	330.6	+3.5	−21	+3
	304.0	+2.0	−4	0
	276.7	0.0	12	−2
	249.1	−2.0	+2	+3
	221.8	−3.4	−2	−1
	195.0	−4.0	+13	+1
	185.4	−4.0	−18	−6
28	193.8	−6.3	+7	+2
	222.2	−7.3	+2	+2
	251.7	−6.4	+10	+12
	281.2	−6.1	−13	−3
	309.9	−0.2	+5	−3

	123.9	+ 1.1	+ 11			338.6	+ 3.5	+ 1	+ 3		
	101.2	+ 1.8	+ 5	+ 6		2.6	+ 6.6	− 13	− 6		
	79.1	+ 2.1	− 1	+ 5		19.2	+ 7.1	+ 6	+ 2		
	56.2	+ 2.2	− 1	+ 1							
	32.3	+ 2.0	− 6	+ 2							
	7.1	+ 1.4	+ 7	− 3							
				+ 6	29	193.0	− 6.1	− 2	0		
						216.0	− 7.0	− 1	0		
22	354.4	+ 2.8	+ 5	+ 5		244.5	− 6.5	− 9	− 6		
	19.4	+ 4.2	+ 5	+ 6		273.9	− 5.3	− 12	− 3		
	43.0	+ 4.9	− 5	− 1		302.8	− 1.0	− 1	+ 5		
	65.3	+ 4.9	+ 5	+ 11		330.4	+ 2.5	− 20	+ 4		
	87.0	+ 4.2	+ 10	+ 6		356.5	+ 5.3	− 9	− 5		
	107.9	+ 3.0	+ 6	+ 3		19.8	+ 7.0	0	− 4		
	129.6	+ 1.3	+ 36	(+ 21)	30	19.1	+ 6.6	− 2	− 2		
	152.5	− 0.6	+ 23	+ 13		355.0	+ 5.0	− 1	+ 2		
						328.8	+ 2.2	− 35	− 11		
23	169.3	− 2.0	− 3	+ 4		301.1	− 1.2	− 4	+ 1		
	146.1	0.0	− 10	− 4		272.4	− 4.3	− 6	− 3		
	121.6	+ 1.9	0	+ 6		243.0	− 6.3	− 2	+ 4		
	99.9	+ 3.4	− 3	− 1		214.9	− 6.6	− 5	− 4		
	78.7	+ 4.5	− 4	+ 3		188.8	− 6.1	− 7	− 1		
	56.8	+ 5.1	− 13	− 2							
	34.1	+ 4.9	− 4	0							
	9.9	+ 3.9	− 5	− 7							
31	72.6	+ 6.8	− 4	0		226.0	− 3.3	− 8	− 6		
	51.1	+ 7.3	− 10	+ 2		198.0	− 2.0	+ 11	− 5		
	26.9	+ 6.9	− 6	− 2		169.0	− 1.7	− 8	− 6		
	4.8	+ 5.3	− 8	9							
	339.1	+ 2.6	− 9	− 7	40	355.1	+ 2.4	− 10	− 7		
	311.6	− 0.7	+ 1	− 6		326.8	− 1.2	− 15	− 4		
	282.7	− 4.0	− 16	0		297.5	− 4.5	− 4	− 2		
	253.2	− 6.2	+ 2	+ 3		279.5	− 6.0	− 14	− 5		
						249.1	− 7.1	− 3	− 1		
32	59.7	+ 6.7	− 9	+ 1		219.5	− 6.1	− 4	− 2		
	37.8	+ 6.6	− 6	− 2		191.6	− 3.8	− 1	+ 2		
	14.4	+ 5.6	+ 4	− 2							
	349.2	+ 3.6	+ 2	+ 8	41	184.8	+ 7.2	+ 8	− 6		
	322.3	+ 0.6	− 9	+ 6		205.4	+ 8.7	− 1	− 3		
	294.6	− 2.5	+ 2	− 1		227.3	+ 9.0	− 5	− 3		
	264.8	− 5.0	+ 3	− 1		250.6	+ 8.9	− 2	− 8		
	235.4	− 6.2	− 13	− 1		275.5	+ 5.6	− 8	− 2		
						302.0	+ 1.9	− 16	− 1		
33	186.0	− 5.4	− 14	+ 6		329.8	− 2.3	− 8	− 6		
	216.0	− 7.0	+ 3	+ 4		351.8	5.3	− 13	− 1		
	245.4	− 6.9	− 5	− 3							
	275.0	− 4.9	− 7	− 1							
	304.8	− 1.6	+ 6	+ 11	42	345.1	− 4.3	− 16	− 4		
	330.4	+ 1.7	− 25	− 1		317.6	− 0.2	− 4	− 10		
	358.3	+ 5.0	− 6	− 3		291.0	+ 3.8	− 20	− 14		
	3.2	+ 5.4	− 9	− 1		265.5	+ 6.9	− 16	+ 1		
						241.2	+ 8.7	− 4	− 2		

34	2.9	+5.2	−6	+2
	347.5	+3.7	−5	0
	320.8	+0.5	−8	+3
	292.4	−3.0	+2	+1
	263.0	−5.7	+4	+1
	233.5	−6.9	0	+11
	204.6	−6.2	−2	+4
	190.6	−5.3	−6	+2
35	356.7	+5.4	−6	−2
	329.9	+1.9	−26	−4
	301.7	−2.2	−11	−7
	272.2	−5.9	−12	−2
	241.9	−7.9	11	0
	212.1	−7.8	2	0
	187.6	6.1	22	−5
37	357.3	+2.6	−3	0
	302.2	−3.4	−5	−3
	272.8	−5.4	−10	0
	243.1	−6.0	−5	0
	214.2	−5.2	−2	0
	187.5	−3.1	−12	+2
	214.2	−5.2	0	+2
38	3.2	+3.1	4	+3
	337.0	+0.4	−5	1
	308.7	−2.5	+5	+4
	279.3	−4.8	−12	0
	249.6	−5.8	+3	+6
	220.7	−5.3	+3	+4
	193.0	−3.4	+14	+5
39	2.4	+1.7	−8	−2
	355.3	−0.7	−19	−12
	336.9	−3.6	−3	−1
	277.7	−4.4	−13	−3
	248.4	−4.7	−17	−9
47	180.2	−1.9	−17	−7
	210.9	+0.7	−1	0
	235.6	+3.3	−14	−7
	260.2	+5.3	+2	−6
	285.1	+6.4	−14	−2
	310.0	+6.4	−7	−3
	335.1	+5.2	−16	−8
	0.2	+3.1	−6	−3
48	189.7	−1.8	−2	0
	214.4	+1.0	+1	+1

	218.0	+9.1	−9	−5
	198.8	+8.3	−4	−10
43	189.8	+5.2	+8	−2
	210.2	+6.9	0	−4
	233.3	+7.7	−11	−10
	257.1	+7.3	−3	+1
	282.1	+5.6	−10	+2
	308.3	−2.7	+7	+4
	325.4	−0.9	−12	−6
	348.3	−2.4	−12	−8
44	353.2	−2.8	+1	+6
	328.0	+0.5	−10	+6
	298.8	+4.2	−5	+2
	273.2	+6.4	−5	+1
	248.6	+7.7	0	−2
	225.3	+7.6	+1	+3
	202.9	+6.3	+2	+2
45	351.6	−1.1	−17	−12
	213.4	−5.4	−6	−8
	236.7	+6.5	−3	0
	260.8	+6.6	+4	−2
	285.9	+5.5	−11	+3
	311.6	+3.3	+6	−1
	336.5	+0.4	−6	−2
46	187.0	+5.6	+12	+2
	208.1	+7.7	+8	+2
	230.1	+6.9	+2	+5
	253.1	+8.8	+8	+2
	277.5	+7.3	+10	+6
	303.0	+4.3	−3	+1
	329.6	+0.3	−27	+2
	346.1	−2.7	−2	+3
54	1.8	+0.7	−10	−7
	27.6	−2.0	−10	−3
	53.6	−4.2	−18	−8
	79.4	−5.6	−10	−6
	104.1	−5.8	−23	−3
	130.0	−4.6	+2	−1
	154.3	−3.0	+10	−4
55	171.4	−3.8	−23	−1
	146.1	−6.4	−3	−1
	120.6	−6.8	+5	+3
	94.3	−6.3	+11	+3

	230.9	+ 3.7	− 2	0
	263.6	+ 5.8	− 17	− 1
	288.6	+ 6.8	− 8	− 1
	313.5	+ 6.6	0	− 4
	336.4	+ 5.3	− 5	− 3
	356.8	+ 3.7	+ 1	+ 1
49	1.8	− 0.8	+ 1	− 1
	28.5	− 3.6	− 4	0
	55.2	− 5.5	− 7	+ 2
	81.7	− 6.2	+ 8	+ 5
	107.6	− 5.6	0	(+ 26)
	132.7	− 3.9	+ 1	− 1
	156.9	− 1.4	+ 8	+ 2
	173.6	+ 0.4	+ 4	+ 8
50	173.0	− 1.2	+ 3	+ 12
	148.8	− 3.9	+ 2	0
	124.0	− 5.9	− 2	− 1
	97.4	− 6.8	− 8	− 8
	70.8	− 6.2	− 11	− 7
	44.3	− 4.2	+ 1	+ 5
	18.9	− 1.3	− 5	− 4
	2.1	+ 0.6	− 8	− 4
51	179.2	+ 2.6	+ 8	+ 1
	156.6	+ 1.0	+ 16	+ 6
	134.0	− 1.0	+ 3	+ 1
	110.5	− 2.7	− 22	+ 1
	86.1	− 4.0	+ 7	+ 4
	60.4	− 4.6	− 4	0
	43.8	− 4.5	− 4	0
	6.4	− 2.8	+ 2	+ 2
52	2.9	− 2.4	0	0
	20.4	− 3.5	− 3	− 1
	47.5	− 4.6	− 4	0
	73.6	− 4.5	+ 2	+ 5
	99.0	− 3.7	− 4	− 2
	122.6	− 2.1	0	− 2
	148.6	0.0	+ 9	+ 5
	168.4	+ 1.8	− 5	− 1
53	358.5	− 0.7	− 7	− 4
	24.8	− 2.9	− 2	− 1
	51.3	− 4.4	− 4	+ 2
	77.3	− 4.9	− 5	− 2
	102.8	− 4.4	− 10	− 2
	127.5	− 3.1	+ 10	+ 1
	151.3	− 1.2	+ 21	+ 4
	173.4	+ 0.8	− 6	− 2

	69.5	− 4.6	− 6	− 5
	44.1	− 1.9	+ 3	+ 1
	19.1	+ 2.2	− 4	− 2
	1.0	+ 3.4	− 11	− 0
56	172.9	− 5.0	− 22	0
	147.1	− 6.9	+ 8	+ 2
	121.1	− 7.4	+ 2	0
	96.0	− 6.4	0	− 1
	69.8	− 4.1	− 4	− 5
	45.0	− 1.0	− 5	− 2
	20.2	+ 2.3	− 2	+ 2
	1.8	+ 4.5	− 6	+ 2
57	173.0	− 6.0	− 13	+ 4
	146.3	− 6.8	+ 3	+ 1
	120.7	− 6.2	+ 8	+ 0
	95.6	− 4.4	− 2	0
	71.2	− 1.7	+ 6	+ 5
	47.4	+ 1.2	0	+ 6
	23.7	+ 4.0	− 4	0
	5.0	+ 5.7	− 4	+ 4
58	1.8	+ 6.1	+ 10	+ 14
	27.1	+ 3.7	0	+ 1
	50.7	+ 0.9	− 2	+ [illegible]
	74.5	− 2.1	+ 5	+ [illegible]
	99.8	− 4.7	+ 17	(+ 19)
	124.2	− 6.5	+ 10	+ 8
	149.9	− 6.9	+ 9	+ 6
	173.2	− 6.1	− 14	+ 7
59	5.8	− 0.3	− 8	− 3
	339.4	+ 2.0	− 7	− 5
	313.3	+ 3.9	+ 5	− 2
	287.4	+ 5.0	− 17	− 4
	261.9	+ 5.2	− 5	− 3
	237.1	+ 4.4	− 8	− 4
	213.0	+ 3.0	− 5	− 3
	189.3	+ 1.1	+ 11	− 3
60	0.5	+ 5.4	− 7	− 5
	335.9	+ 7.0	− 6	0
	311.2	+ 7.4	− 3	0
	285.3	+ 6.4	− 12	0
	261.0	+ 4.3	+ 5	− 1
	235.6	+ 1.4	8	+ 1
	210.0	− 1.8	− 3	− 2
	188.0	− 4.2	− 14	+ 4
61	196.4	− 3.3	+ 8	+ 6
	222.0	− 0.2	+ 3	0
	247.5	+ 2.9	+ 1	+ 5

61	272°6	+ 5°5	− 10	+ 1
	298.0	+ 7.1	− 4	+ 2
	322.9	+ 7.4	− 3	+ 8
	347.4	+ 6.4	− 4	0
	2.2	+ 4.5	− 6	+ 2
62	184.5	− 3.5	− 19	− 5
	210.2	− 1.7	+ 2	+ 3
	236.1	+ 0.6	− 6	+ 6
	262.2	+ 2.7	− 15	− 13
	289.1	+ 4.4	− 5	+ 7
	314.0	+ 5.2	+ 2	− 4
	339.3	+ 5.0	+ 1	0
	4.2	+ 4.0	− 14	− 8
63	190.3	− 3.0	− 4	+ 2
	215.9	− 1.0	+ 2	+ 4
	241.8	+ 1.3	− 5	− 3
	267.6	+ 3.4	− 24	− 2
	293.5	+ 4.9	0	+ 5
	319.3	+ 5.4	− 17	− 12
	344.7	+ 4.9	+ 1	− 1
	5.4	+ 3.9	− 13	− 8
64	0.1	+ 1.7	− 5	− 3
	332.4	+ 2.2	− 24	− 6
	306.3	+ 2.3	− 2	− 4
	279.1	+ 1.9	− 9	− 4
	252.0	+ 1.2	+ 8	+ 6
	225.5	+ 0.3	− 5	− 2
	199.7	− 0.6	+ 11	+ 4
	183.1	− 1.1	− 6	− 2
65	183.8	− 1.0	− 12	− 8
	[illegible]	− 0.2	− 12	− 8
	233.8	+ 0.7	− 19	− 7
	259.9	+ 1.5	0	− 8
	287.0	+ 2.1	− 21	− 9
	314.0	+ 2.3	− 13	(− 21)
	340.8	+ 2.0	− 11	− 7
	1.8	+ 1.6	− 11	− 6
66	359.0	− 0.1	− 4	0
	331.6	− 0.2	− 23	− 4
	303.8	− 0.1	− 4	+ 4
	281.3	− 0.1	− 15	0
	251.3	+ 0.2	+ 5	+ 5
	183.0	+ 0.6	+ 11	+ 4
67	182.9	+ 0.6	+ 22	+ 15
	207.1	+ 0.4	− 9	− 5

69	180°2	+ 0°7	+ 16	+ 13
	204.4	+ 0.7	+ 7	+ 11
	229.9	+ 0.6	0	+ 7
	256.5	+ 0.4	+ 5	+ 8
	284.2	+ 0.2	− 5	+ 5
	312.1	0.0	+ 14	− 10
	339.9	− 0.1	+ 7	+ 5
	2.3	− 0.2	+ 4	+ 3
70	351.7	− 2.2	− 5	0
	322.3	− 2.6	− 11	− 1
	293.3	− 2.2	+ 3	+ 1
	264.5	− 1.3	− 10	− 2
	237.0	0.0	− 11	+ 1
	210.6	+ 1.2	− 1	− 1
	195.2	+ 2.2	− 4	− 5
	172.4	+ 2.7	− 8	− 1
71	353.0	− 2.2	− 3	+ 1
	324.5	− 2.7	− 14	− 4
	295.5	− 2.4	− 7	− 6
	266.7	− 1.5	− 7	− 1
	239.0	− 0.2	− 7	+ 3
	212.7	+ 1.2	− 4	0
	189.1	+ 2.2	+ 6	− 1
	171.8	+ 2.5	− 17	− 5
72	307.7	− 4.6	− 2	− 1
	277.8	− 3.3	− 10	+ 2
	249.0	− 1.2	− 5	− 5
	221.8	+ 1.2	− 3	− 3
	195.8	+ 3.2	+ 7	+ 1
	173.5	+ 4.5	− 7	− 3
	151.5	+ 5.2	+ 19	+ 3
	131.1	+ 5.2	+ 12	+ 2
73	183.4	− 1.5	− 10	− 3
	208.0	− 0.7	− 3	+ 1
	233.7	+ 0.3	− 14	− 2
	260.2	+ 1.4	+ 5	− 2
	287.0	+ 2.2	− 22	− 10
	314.0	+ 2.6	− 6	− 14
	340.6	+ 2.5	− 6	− 3
	358.6	+ 2.1	− 12	− 9
74	353.1	+ 2.2	− 8	− 2
	325.6	+ 2.6	− 32	− 9
	299.3	+ 2.4	− 11	− 1
	272.8	+ 1.8	− 29	− 7
	246.2	+ 0.9	+ 6	+ 6

	233.0	+0.4	−5	+6
	260.1	+0.3	+16	+6
	287.9	+0.1	0	+3
	315.9	0.0	+13	+5
	343.7	−0.1	−1	+3
	2.8	−0.1	+2	+4
[illegible]	1.5	−0.2	−5	−7
	334.6	−0.1	−6	+3
	306.9	0.0	−5	−1
	278.8	+0.2	−15	−1
	251.3	+0.4	+4	−3
	224.8	+0.5	−3	−2
	199.4	+0.6	+5	−2
	170.7	+0.7	+1	−1
	293°6	+0°7	−4	−2
	321.2	+0.6	−21	−7
	348.5	+0.5	−9	−1
	358.4	+0.4	−8	−4
77	170.0	+1.3	−12	−6
	147.0	+0.6	−8	−2
	124.5	−0.1	+7	+5
	101.4	−0.8	−8	−4
	78.2	−1.3	−4	0
	53.7	−1.6	−10	−2
	28.1	−1.5	−3	−2
	3.0	−1.1	−4	−6
78	3.3	+0.1	−4	0
	29.8	−1.0	+6	+7
	56.1	−1.8	−7	0
	79.7	−2.3	+2	+2
	103.6	−2.2	−14	−2
	127.0	−1.8	+18	+7
	150.2	−1.0	+20	+6
	172.6	−0.1	+1	+5
79	2.5	+1.5	−4	+2
	28.3	−0.4	−1	+1
	53.5	−2.1	−7	+1
	78.4	−3.3	−1	0
	112.7	−3.9	−31	−5
	127.2	−3.7	+11	+2
	151.4	−2.9	+24	+8
	173.3	−1.6	−7	+4
80	4.2	+2.5	−5	0
	29.6	+0.1	−7	−2
	54.6	−2.3	−14	−2

	220.1	−0.2	−3	−1
	194.8	−1.1	−1	−4
75	357.3	+0.4	−12	−8
	329.2	+0.6	−29	−5
	302.6	+0.7	−7	+3
	274.9	+0.7	−20	−4
	247.7	+0.6	−6	−1
	221.3	+0.4	−2	−2
	195.1	+0.2	−4	−4
76	188.6	+0.2	+6	+3
	213.1	+0.4	−1	0
	239.0	+0.7	−6	+2
	265.3	+0.7	−27	−9
	4°5	−0°2	0	+6
	21.4	+3.1	−3	+1
	359.8	+5.6	+4	+2
84	354.5	+5.7	+6	+6
	18.5	+3.5	−5	−5
	43.1	+0.8	−9	−5
	67.3	−2.9	−2	+1
	91.9	−4.5	+11	+7
	116.9	−6.1	0	−1
	142.4	−6.5	−6	0
	169.2	−5.5	−13	+5
85	351.1	+6.0	−2	+4
	15.2	+3.0	+10	+2
	39.2	+1.3	+6	+4
	63.3	−1.7	−4	0
	87.9	−4.3	+7	+6
	113.0	−6.1	−20	0
	138.5	−6.7	−4	+5
	162.8	−6.9	−13	+7
86	2.0	+5.7	−6	0
	25.7	+2.5	−2	+6
	49.8	−0.6	0	+1
	74.4	−4.0	+2	+3
	99.6	−6.6	−2	−2
	125.6	−7.8	+3	+1
	151.8	−7.4	+6	0
	173.2	−6.1	−19	−3
87	359.0	+4.8	−9	−9
	334.9	+5.8	−5	+4
	310.6	+5.8	−1	+3
	286.2	+4.8	−14	9

	79.6	−4.2	−4	0		251.4	+3.0	0	−4		
	104.6	−5.2	−13	+6		236.4	+0.7	−18	−6		
	129.6	−5.2	+4	0		211.0	−1.8	0	0		
	154.5	−4.3	+15	+8							
	172.4	−3.0	−17	+1	88	139.7	−2.9	+4	0		
						225.3	−0.3	−3	1		
81	358.6	+0.1	−	1		251.1	+0.3	+2	4		
	23.4	−0.6	−	6		276.6	+4.5	−1	5		
	48.9	−1.2	−	1		302.0	+5.9	−4	0		
	73.4	−1.4	−	0		327.2	+6.2	−24	7		
	97.2	−1.4	−	5		352.9	−5.4	−6	0		
	120.4	−0.8	+10	6		4.5	+4.6	−10	2		
	143.3	−0.6	−	4							
	166.3	0.0	+	7	89	4.5	+4.8	−7	+1		
						341.8	+6.2	+3	+1		
82	2.8	+1.4	−	4		317.0	+6.7	−5	−8		
	28.4	−0.1	−	3		291.7	+6.0	−1	+5		
	54.4	−1.5	−	17		266.2	+4.1	−22	0		
	78.1	−2.5	−	6		240.5	+1.5	−2	+1		
	103.2	−3.0	−	12		214.9	−1.4	−2	+2		
	126.2	−3.0	+11	0		197.6	−3.2	0	+3		
	150.0	−2.4	+12	1							
	172.6	−1.4	−	5	90	151.8	−5.2	+13	+2		
						126.1	−5.2	+7	+5		
83	173.6	−5.7	−	12		101.3	−4.2	+11	+13		
	147.3	−7.4	+10	2		77.1	−2.4	−7	−7		
	121.2	−7.5	+	3		54.1	−0.3	−9	0		
	95.3	−6.1	+	5		29.1	+1.2	−2	+5		
	70.1	−3.6	+	4		4.9	+3.6	−3	+3		
						340.4	+5.5	+2	0		
91	337°2	+5°7	+	2		239°4	+3°7	+6	+7		
	1.2	+4.4	−	8		214.7	+4.2	+2	+2		
	25.4	+2.5	−	11		191.5	+4.1	+17	+7		
	49.5	+0.1	−	10		168.2	+3.4	−31	(−19)		
	73.6	−2.2	+	4							
	97.9	−4.1		0	99	349.6	−3.7	0	+10		
	122.6	−5.2	−	1		326.4	−1.6	+1	+6		
	147.6	−5.4		0		302.3	+0.8	+10	+10		
						280.2	+3.1	−12	+10		
92	358.6	+6.6	+	2		259.3	+4.7	+14	+9		
	335.0	+8.6	+	4		235.0	+5.3	+7	+7		
	311.0	+9.2	+	4		212.1	+5.2	+17	+6		
	286.8	+8.4	−	8		176.8	+4.6	+22	(+20)		
	262.3	+6.0	+	7							
	237.6	+2.6	+	5	100	351.9	−1.5	−10	−5		
	212.4	−1.4	+	6		328.7	+1.1	−7	+3		
	189.1	−4.7	−	10		306.6	+3.5	−3	+3		
						278.4	+5.1	−22	0		
93	191.3	−4.1	−	12		245.1	+5.7	−7	−1		
	216.7	−0.5	+	1							

	241.9	+ 3.3	− 8	− 9
	266.9	+ 6.4	− 27	− 5
	291.4	+ 6.4	− 7	− 2
	315.7	+ 8.9	− 4	− 4
	339.9	+ 7.9	− 5	− 9
	3.7	+ 5.6	− 14	− 6
94	356.5	+ 2.5	− 2	+ 2
	330.3	+ 5.2	− 20	− 3
	305.7	+ 6.8	+ 2	− 2
	280.8	+ 7.2	− 10	− 4
	256.1	+ 6.4	+ 6	− 10
	231.8	+ 4.6	− 13	− 5
	207.8	+ 1.8	− 6	− 4
	189.0	− 0.5	+ 2	− 6
95	355.2	− 1.2	− 3	+ 2
	327.6	+ 0.8	− 10	− 4
	300.6	+ 2.6	+ 3	+ 4
	274.0	+ 3.9	− 14	+ 2
	248.2	+ 4.4	− 4	− 2
	223.4	+ 4.1	− 3	− 1
	199.6	+ 3.2	+ 4	+ 4
	183.6	+ 2.2	+ 26	+ 4
96	183.7	+ 2.3	+ 21	+ 5
	207.1	+ 3.6	− 2	− 2
	231.1	+ 4.4	− 5	− 1
	256.2	+ 4.4	− 3	+ 1
	282.2	+ 3.7	− 10	− 3
	306.9	+ 2.2	0	0
	336.0	+ 0.1	0	+ 4
97	185.6	+ .4	− 4	− 2
	208.9	+ 3.7	− 11	− 11
	232.9	+ 3.5	− 19	− 15
	256.0	+ 4.5	− 11	− 12
	284.2	+ 3.6	− 15	− 6
	311.0	+ 2.0	− 10	− 12
	338.1	+ 0.1	− 15	− 11
98	338.2	− 2.3	+ 1	+ 3
	309.7	− 0.5	+ 5	− 1
	292.9	+ 0.7	− 3	− 1
	265.6	+ 2.4	− 20	+ 1

101	182.2	− 4.7	− 22	− 2
	215.4	− 5.2	− 15	− 12
	243.7	− 4.4	− 12	− 8
	272.2	− 2.5	− 23	− 12
	300.2	+ 0.1	− 14	− 8
102	194.1	− 1.9	+ 15	+ 7
	219.6	+ 0.6	+ 1	+ 3
	244.8	+ 3.1	0	0
	270.1	+ 5.0	− 20	+ 2
	295.5	+ 6.0	0	+ 2
	320.7	+ 5.9	− 13	0
	345.9	+ 4.7	0	− 1
	10.7	+ 2.7	+ 2	− 1
103	358.3	+ 3.7	− 6	− 4
	334.6	+ 5.3	− 12	− 3
	309.1	+ 6.2	− 1	− 1
	283.8	+ 5.8	− 14	0
	255.6	+ 4.4	+ 4	0
	233.4	+ 2.3	− 14	− 12
	209.4	− 0.3	− 2	+ 2
104	89.2	− 4.6	− 7	− 10
	112.3	− 3.3	− 38	− 12
	135.8	− 1.4	− 23	(− 23)
	156.6	+ 0.7	+ 1	− 15
	181.1	+ 2.8	− 17	(− 22)
	204.0	+ 4.4	− 11	− 12
	227.5	+ 5.4	− 7	− 4
	252.0	+ 5.6	+ 10	0
105	277.2	+ 4.9	− 5	+ 1
	239.0	+ 5.8	+ 10	+ 4
	215.1	+ 5.1	− 6	− 6
	192.1	+ 3.7	+ 3	− 7
	169.6	+ 1.8	− 5	+ 1
	146.9	− 0.4	− 4	+ 1
106	196.3	− 2.2	+ 5	+ 7
	216.4	+ 0.4	+ 6	+ 6
	241.3	+ 3.6	+ 2	+ 1
	266.1	+ 6.1	− 19	+ 2
	290.8	+ 7.5	2	+ 4

106	318.5	+ 7.6	+ 11	+ 4
	338.8	+ 6.5	0	+ 2
	353.1	+ 5.3	− 6	− 4
107	351.4	+ 5.2	− 4	+ 2
	326.9	+ 7.2	− 13	+ 1
	302.2	+ 7.6	+ 2	+ 6
	277.5	+ 6.9	+ 3	0
	252.9	+ 5.0	+ 12	+ 2
	228.2	+ 2.2	+ 3	+ 4
	203.3	− 1.1	− 4	− 4
	190.2	− 2.7	+ 6	+ 1
108	190.7	− 2.5	+ 5	+ 5
	215.4	− 0.8	− 2	− 2
	239.8	+ 3.3	− 2	− 4
	264.2	+ 6.4	− 17	− 1
	288.8	+ 7.8	− 9	− 3
	313.6	+ 7.8	− 2	− 7
	338.6	+ 6.5	− 6	− 4
	356.1	+ 4.8	− 6	− 6
109	357.2	+ 3.6	+ 3	+ 1
	331.2	+ 6.1	− 2	+ 15
	307.4	+ 7.5	+ 10	+ 8
	262.6	+ 7.5	− 2	+ 4
	258.0	+ 6.3	+ 6	+ 6
	233.6	+ 3.9	+ 2	+ 7
	209.3	+ 0.9	+ 3	+ 7
	189.9	− 1.5	+ 8	+ 6
110	189.4	− 0.2	− 4	− 15
	213.2	+ 2.8	− 5	− 3
	237.5	+ 5.3	− 10	− 6
	261.5	+ 7.0	− 7	− 8
	285.1	+ 7.4	− 14	− 6
	311.1	+ 6.6	− 6	− 3
	336.3	+ 4.6	− 20	− 14
	1.8	+ 1.7	− 8	− 2
111	350.0	+ 3.4	− 5	+ 2
	324.7	+ 6.3	− 13	− 4
	299.5	+ 8.0	− 3	+ 1
	274.8	+ 8.3	+ 4	+ 1
	250.4	+ 7.2	+ 5	0
	226.4	+ 4.8	− 2	+ 1
	202.5	+ 1.7	+ 5	+ 8
112	195.9	+ 0.9	+ 1	+ 2
	219.7	+ 3.8	− 9	− 5

114	341.0	+ 2.6	− 2	+ 1
	315.3	+ 5.3	− 2	− 10
	290.9	+ 6.9	− 12	− 6
	265.1	+ 7.3	− 14	0
	240.9	+ 6.4	− 3	− 2
	217.2	+ 4.5	− 2	+ 2
	193.6	+ 1.9	− 6	− 5
115	255.2	− 0.8	− 6	0
	328.5	+ 2.3	− 24	0
	302.3	+ 5.0	− 5	− 1
	276.8	+ 6.6	+ 2	+ 1
	252.0	+ 7.0	+ 4	4
	228.2	+ 6.2	− 4	− 1
	204.9	+ 4.5	− 1	− 3
	183.2	+ 2.2	+ 21	+ 4
116	193.0	+ 3.3	− 11	(− 19)
	215.9	+ 5.5	− 12	− 8
	239.4	+ 6.8	− 8	9
	263.8	+ 7.0	− 21	11
	289.9	+ 6.0	− 21	13
	314.8	+ 3.8	− 5	− 13
	341.2	+ 0.9	− 3	− 6
117	348.5	0.0	− 4	+ 4
	321.9	+ 3.1	− 10	0
	295.9	+ 5.6	− 1	+ 2
	270.5	+ 7.0	− 15	+ 3
	246.0	+ 7.1	− 2	0
	222.4	+ 6.0	− 3	− 1
	199.4	+ 4.1	+ 6	+ 3
118	187.6	+ 2.9	+ 13	+ 4
	210.2	+ 5.2	+ 9	+ 5
	233.4	+ 6.8	+ 3	+ 5
	257.2	+ 7.4	+ 28	(+ 2)
	282.1	+ 6.7	− 19	− 9
	306.8	+ 4.8	+ 8	0
	334.2	+ 1.8	− 10	0
	358.5	− 1.2	− 6	2
119	354.5	− 0.2	− 7	− 1
	329.6	+ 3.6	− 27	− 3
	301.9	+ 6.8	− 8	4
	277.0	+ 8.5	− 3	− 5
	253.6	+ 8.7	+ 2	− 4
	229.8	+ 7.5	− 12	− 8
	207.2	+ 5.3	− 9	− 11
	184.6	+ 2.2	+ 10	+ 4

	243.5	+ 6.2	− 8	− 4								
	267.6	+ 7.6	− 10	+ 8	120	352.6	− 3.1	− 6		0		
	292.2	+ 7.7	− 6	− 3		325.3	+ 0.7	− 14	−	4		
	317.2	+ 6.4	+ 6	+ 2		298.3	+ 4.3	− 7	−	1		
	342.4	+ 4.0	− 1	+ 1		272.6	+ 6.9	− 11	−	3		
	356.4	+ 2.0	− 6	− 3		248.0	+ 8.2	− 2	−	3		
						224.7	+ 8.1	− 4	−	5		
113	344.0	+ 2.2		0		202.4	+ 6.8	− 5	−	5		
	327.0	+ 4.1	− 29	+ 1		182.9	+ 4.9	+ 34	+	9		
	301.4	+ 6.2	−	6								
	276.3	+ 7.1	+ 5	+ 3	121	191.7	+ 5.9	+ 20	+	6		
	251.8	+ 6.8	+ 4	− 5		213.9	+ 7.7	+ 3	+	1		
	227.8	+ 5.3	− 1	+ 3		236.6	+ 8.4	+ 3	+	2		
	204.2	+ 3.0		0		260.6	+ 7.8	+ 15	+	7		
	184.0	+ 0.7	+ 13	+ 9								
121	285?8	+ 5?8	− 2	+ 12		30?5	+ 6?6	− 9		0		
	312.1	+ 2.6	+ 7	+ 4		71.9	+ 6.3	− 2	+	5		
	339.4	− 1.3	+ 2	0		92.4	+ 5.3	0	+	6		
						113.1	+ 3.6	− 2		0		
122	346.4	− 2.2	− 10	− 6		134.8	+ 1.4	+ 6	+	4		
	318.8	+ 1.7	− 7	− 7		157.9	− 1.2	+ 20	+	4		
	292.3	+ 5.2	− 4	+ 2								
	265.5	+ 7.5	− 13	+ 4	127	356.4	+ 4.5	+ 10	+	8		
	242.2	+ 8.4	− 11	+ 7		21.1	+ 6.4	+ 14	+	14		
	219.0	+ 8.0	− 1	+ 2		43.8	+ 7.2	+ 5	+	10		
	198.8	+ 6.4	+ 7	+ 1		65.2	+ 6.9	+ 2	+	8		
						85.9	+ 5.8	+ 5	+	9		
123	156.6	+ 4.9	+ 16	+ 2		106.5	+ 4.0	+ 9	+	13		
	177.5	+ 6.8	− 7	− 11		128.0	+ 1.6	+ 21	+	5		
	198.7	+ 7.8	+ 8	− 1		151.0	− 1.2	+ 27	+	8		
	221.1	+ 7.8	+ 5	+ 6								
	245.0	+ 6.5	− 3	+ 3	128	164.2	− 2.6	− 4	+	2		
	270.7	+ 3.9	− 14	+ 7		138.8	0.0	− 2	+	5		
	298.1	+ 0.4	+ 10	+ 6		117.5	+ 2.6	+ 13	+	7		
	326.6	− 3.3	− 24	− 11		96.4	+ 4.8	+ 12	+	4		
						75.8	+ 6.3	+ 6	+	8		
124	182.6	− 2.3	− 22	− 10		54.9	+ 7.1	− 5	+	3		
	157.6	0.0	+ 19	+ 1		32.9	+ 6.9	0	+	4		
	134.9	+ 2.1	+ 5	+ 3		9.4	+ 5.7	+ 1		0		
	113.6	+ 3.9	− 2	0								
	92.9	+ 5.1	− 5	+ 1	129	1.1	+ 6.3	− 4	−	2		
	72.0	+ 5.7	− 8	− 2		24.3	+ 7.3	− 9	−	5		
	50.3	+ 5.5	− 13	− 5		46.5	+ 7.2	− 9	−	5		
	27.1	+ 4.6	− 5	0		67.8	+ 6.1	− 12	−	4		
						88.7	+ 4.3	−	−	3		
125	170.9	− 2.3	− 10	+ 2		110.2	+ 1.8	− 7	−	1		
	146.6	+ 0.3	0	+ 5		132.7	− 1.0	+ 1	−	1		
	124.4	+ 2.7	+ 2	− 2		156.9	− 3.8	− 2	−	2		
	103.3	+ 4.7	− 5	− 2	130	176.4	− 5.1	− 20	+	2		

	82.7	+6.0	−18	−9		145.1	−2.6	−10	−4
	61.9	+6.6	−23	−7		121.7	+0.3	−10	−4
	39.9	+6.3	−11	−7		99.7	+2.9	−9	−7
	16.5	+5.1	+1	+1		78.5	+5.2	−12	−4
						57.4	+6.7	−15	0
126	3.4	+4.2	−3	+5		35.8	+7.4	−8	−6
	27.8	+5.9	−6	−2		12.9	+7.0	+1	+1

Table 21

Yakovkin's Observations

№№ набл.	P	D	H	H − H'	№№ набл.	P	D	H	H − H
1	1?9	+6?2	−6	−1		257?1	−1?8	+2	+1
	43.4	+9.0	−6	−1		267.9	−5.2	−2	−7
	60.1	+4.7	−12	−5		238.2	−7.2	−25	−13
	117.7	−3.8	+2	+2		268.9	−7.3	−9	−3
						195.8	−3.2	+5	+6
2	155.0	−2.2	+32	+11					
	130.5	+1.5	+21	+9	10	263.0	−7.1	−8	−2
	108.0	+4.7	0	+1		232.0	−7.4	−17	−9
	86.7	+7.0	+7	+8		251.7	−5.7	+18	+14
	68.7	+8.6	−8	0		291.0	−2.4	−9	−5
	48.2	+9.1	−2	+3		310.1	+1.3	−18	−14
	26.4	+8.4	−6	−3		345.7	+4.7	0	+4
						10.5	+6.9	+3	+3
3	358.6	+6.0	+8	+7					
	22.6	+8.2	+13	+15					
	44.6	+9.0	−7	−2	11	14.9	+7.2	+13	+12
	65.3	+8.6	−9	−2		350.5	+5.3	−8	−2
	85.3	+7.3	+6	−13		324.2	+2.3	−23	−12
	104.2	+5.2	+26	+18		287.5	−4.8	+11	+4
	126.9	+2.0	+26	(+22)		238.1	−7.0	−21	−9
						269.0	−7.3	−8	−2
4	352.9	+5.2	−11	−7					
	326.8	+2.6	−44	(−21)	12	228.0	−7.0	−19	−7
	299.2	−0.7	+1	+1		267.6	−5.1	+11	+6
	270.6	−3.9	−16	−9		296.7	−1.9	+4	+3
	241.5	−6.1	−23	−12		324.7	+1.7	−19	−6
	212.9	−6.7	+1	+2		351.1	+4.8	−3	+3
	190.6	−5.9	−33	(−20)		16.6	+6.9	+10	+6
						38.5	+7.7	−2	+2
5	192.8	−6.2	−8	−5		60.0	+7.4	−13	−12
	221.0	−6.6	−2	−2		80.7	+6.2	−14	−4
	250.1	−5.4	−3	+1					

	279.1	− 2.8	− 23	− 6	13	145.3	− 0.9	− 10	− 1
	307.3	+ 0.5	− 5	− 1		122.2	+ 1.8	− 4	+ 1
	334.3	+ 3.7	− 13	− 3		101.3	+ 4.0	+ 12	+ 8
	359.8	+ 5.9	− 4	− 6		80.5	+ 5.8	− 9	− 1
						59.6	+ 6.8	− 26	− 16
6	169.2	− 6.1	− 50	(− 39)		37.8	+ 6.9	− 11	− 8
	217.3	− 6.7	− 10	− 9		14.4	+ 6.0	+ 10	+ 5
	246.2	− 5.5	− 9	− 5		349.5	+ 4.0	− 7	− 1
	275.1	− 3.6	− 21	− 12					
	303.4	+ 0.4	− 8	0	14	345.1	+ 3.7	− 2	0
	330.5	+ 3.5	− 67	(− 43)		11.3	+ 5.7	− 2	− 4
	356.1	+ 5.9	− 4	+ 2		34.7	+ 6.7	− 11	− 8
	2.7	+ 6.3	− 19	− 13		56.8	+ 6.6	− 25	− 9
						77.6	+ 5.7	− 15	− 7
7	194.4	− 6.6	+ 8	+ 2		98.7	− 4.0	− 16	− 10
	223.0	− 7.2	− x	− 7		120.1	+ 1.8	0	+ 1
	252.5	− 6.1	0	+ 2		142.8	− 0.7	− 32	(− 26)
	281.8	− 3.2	− 26	− 9					
	310.2	+ 0.4	+ 1	− 7	15	154.3	+ 0.4	+ 27	+ 11
	336.2	+ 3.7	− 17	− 12		131.6	+ 1.4	+ 4	− 2
	3.0	+ 6.3	− 14	− 8		109.9	+ 2.9	+ 6	+ 1
						88.7	+ 4.0	0	− 2
8	4.4	+ 6.6	− 10	− 4		45.0	+ 4.7	− 26	(− 22)
	339.2	+ 4.3	+ 1	0		21.4	+ 3.9	− 12	− 7
	312.5	+ 1.0	− 6	− 4		2.2	+ 2.9	− 10	− 3
	284.3	− 2.6	− 19	− 3					
	255.2	− 5.6	+ 26	(+ 22)	16	201.6	− 6.9	− 1	− 2
	225.9	− 7.1	− 19	− 16		230.5	− 7.2	− 1	+ 4
	197.4	− 6.9	− 4	+ 1		260.2	− 5.7	+ 13	+ 9
						289.4	− 2.6	− 7	− 3
9	15.8	+ 7.2	+ 6	+ 3		317.6	+ 1.1	0	− 4
	351.3	+ 5.2	− 11	− 5		344.3	+ 4.4	+ 12	+ 10
	325.0	+ 2.9	− 36	(− 21)		340.8	+ 5.0	− 9	− 3
17	16[illegible]3	+ 2[illegible]8	- 24	− 10		30[illegible]2	− 2[illegible]1	+ 19	+ 6
	147.4	+ 2.1	+ 3	+ 5		338.2	− 4.7	− 9	− 5
	125.5	+ 1.1	+ 17	+ 15		351.3	− 5.4	− 8	+ 4
	101.2	− 0.1	− 26	− 18					
	79.8	− 1.2	+ 1	+ 5	26	352.2	− 5.6	− 15	− 3
	58.0	− 2.2	− 10	− 1		329.4	− 3.1	+ 4	+ 3
	36.8	− 2.6	+ 4	+ 5		289.6	+ 0.2	− 17	− 13
	11.4	− 2.7	− 22	− 14		260.4	+ 3.4	+ 15	+ 8
						233.0	+ 5.7	− 2	+ 1
18	356.2	+ 5.1	− 5	− 2		207.8	+ 6.7	− 2	− 5
	328.8	+ 1.6	− 44	(− 20)		184.1	+ 6.6	+ 34	(+ 20)
	300.6	− 2.5	− 9	− 7					
	271.0	− 6.0	− 14	− 7	27	186.0	+ 6.9	+ 14	0
	240.8	− 7.9	− 16	− 6		208.6	+ 7.1	+ 6	+ 2
	208.9	− 7.6	− 15	− 9		258.9	+ 4.0	+ 15	+ 9
	191.0	− 6.2	− 30	− 16		286.7	+ 0.9	0	+ 3
						314.3	− 2.3	+ 20	+ 16

19	196.8	−0.5	0	−1
	221.1	−2.0	−1	0
	246.8	−3.1	−2	+2
	275.6	−3.4	−21	−10
	306.6	−2.8	+5	+9
	335.3	−1.5	−11	−6
	354.2	−0.3	−3	+3
20	283.1	+1.6	−12	−4
	246.3	+5.3	−7	−3
	231.7	+6.4	−3	0
	205.5	+7.1	−3	−7
	186.7	+6.8	+15	+3
	165.7	+5.7	+26	+14
	144.8	+3.8	+4	+2
	125.4	+1.4	+14	−9
22	353.0	−3.8	−2	+5
	324.1	−3.3	−16	−7
	295.2	−1.8	+6	+4
	267.0	+0.1	−20	−5
	240.2	+1.9	−3	−2
	216.9	+3.4	+8	+4
	191.4	+4.2	+11	+2
23	188.5	+4.4	+6	−5
	211.9	+3.8	−9	−8
	236.8	+2.5	−14	−7
	263.4	+0.6	−17	(−26)
	291.3	−1.4	−1	+2
	320.0	−3.0	−2	−4
	348.9	−3.9	−16	−6
24	352.8	−4.1	−6	+1
	335.5	−3.7	−14	−8
	306.6	−2.2	+2	+6
	278.3	−0.1	−15	−2
	251.1	+2.0	+11	−2
	225.4	+3.6	−11	−8
	201.5	+4.5	−5	−5
	195.0	+4.6	+16	+6
25	182.8	+6.4	+42	(+23)
	205.8	+6.5	+6	+3
	229.2	+5.6	−2	+1
	254.3	+3.7	+11	+9
	281.1	+0.9	−17	−4

	346.4	−5.4	−18	−6
28	343.0	−5.4	−17	−6
	312.1	−2.1	+12	+10
	281.8	+1.7	−16	−8
	255.3	+4.8	−9	−8
	226.9	+7.0	−2	0
	202.3	+7.6	+4	+1
	179.3	+7.0	+15	+7
29	180.2	+6.9	+23	+15
	203.2	+7.7	+11	+11
	227.7	+7.1	+6	+4
	254.3	+5.1	+10	+7
	282.7	+1.8	−19	−4
	313.0	−2.2	+16	+15
	344.4	−5.5	−8	+4
30	137.4	+3.0	−10	−7
	160.0	+5.8	−23	−18
	182.2	+7.7	+17	0
	205.0	+8.5	−4	−6
	255.5	+5.9	−10	−8
	283.7	+2.4	−21	−15
	313.8	−2.0	+6	+4
31	315.9	−2.1	+20	+12
	284.6	+2.5	−5	+1
	255.3	+6.3	+7	+8
	229.3	+8.3	−2	+1
	203.4	+8.7	+10	+9
	180.1	+7.7	0	−8
	157.1	+5.5	+17	+5
32	189.6	+5.7	+8	−4
	213.0	+5.3	−19	−11
	240.2	+3.8	+5	+2
	268.5	+1.4	−36	−18
	299.0	−1.4	+4	+4
	329.8	−3.9	−23	−10
33	352.7	−5.8	−15	−3
	320.7	−3.2	+1	0
	289.9	+0.3	−11	−7
	260.7	+3.6	+8	+1
	233.4	+5.9	−7	−4
	208.2	+7.0	−12	−16
	188.6	+6.3	+30	+10

34	182.3	+ 7.3	+ 31	+ 13	42	358.0	+ 4.5	− 4	− 1
	205.7	+ 7.6	− 1	− 4		36.3	+ 8.6	− 19	− 4
	230.8	+ 7.6	− 5	− 4		61.7	+ 9.4	− 25	− 16
	258.2	+ 4.7	+ 10	+ 9		85.4	+ 8.6	− 18	− 10
	287.4	+ 1.1	− 9	− 3		109.0	+ 5.4	− 5	− 5
	318.5	− 2.9	+ 16	+ 9		134.1	− 2.9	− 1	− 3
	350.6	− 6.1	− 24	− 12		155.6	− 0.6	+ 17	+ 5
35	354.8	+ 5.0	0	+ 2	43	154.2	− 0.4	+ 30	+ 9
	20.9	+ 5.3	+ 1	+ 1		129.6	+ 3.5	+ 41	(+ 21)
	45.9	+ 4.7	− 22	− 16		104.0	+ 6.8	+ 1	+ 5
	69.9	+ 3.2	0	− 6		81.3	+ 8.7	− 14	− 4
	93.7	+ 1.3	+ 1	+ 3		58.2	+ 9.3	− 18	− 2
	118.0	− 0.8	− 6	− 6		33.3	+ 8.4	− 14	− 8
						5.8	+ 5.6	− 9	− 2
36	150.2	− 3.4	+ 2	− 4	44	202.5	− 3.0	+ 13	+ 11
	125.6	− 0.6	+ 19	+ 9		230.3	− 1.3	− 22	− 12
	100.6	+ 2.1	− 6	− 2		259.1	+ 0.8	+ 16	+ 4
	82.5	+ 4.4	− 1	+ 7		287.6	+ 2.8	− 13	0
	59.6	+ 6.1	− 17	− 11		316.3	+ 4.1	+ 22	+ 14
	36.0	− 6.8	0	− 2		344.0	+ 4.5	+ 6	+ 4
	0.9	+ 5.9	− 3	0		18.2	− 3.7	+ 1	− 1
37	0.1	+ 6.0	− 2	− 2					
	25.0	+ 6.9	− 8	− 4	45	350.3	+ 4.7	− 11	− 5
	50.9	+ 6.5	− 32	(− 22)		321.8	+ 4.5	− 14	− 6
	74.8	+ 5.0	0	0		292.4	+ 3.2	− 12	− 6
	98.6	+ 2.7	− 10	− 4		262.7	+ 1.1	− 6	− 1
	123.4	− 0.1	− 3	− 4		233.5	− 3.1	− 8	− 7
	153.1	− 3.4	+ 44	(+ 32)		17.8	+ 3.9	+ 16	+ 12
38	134.8	− 2.9	+ 26	+ 6	46	305.2	+ 2.4	+ 4	+ 4
	128.9	+ 0.6	+ 32	+ 17		336.0	+ 4.5	− 13	− 6
	105.4	+ 3.8	+ 10	+ 6		6.9	+ 5.4	− 11	− 5
	83.1	+ 6.2	− 15	− 6		35.2	+ 4.9	− 5	− 2
	60.9	+ 7.7	− 23	− 15		62.3	+ 3.4	− 17	− 7
	37.9	+ 8.1	0	+ 5		89.0	+ 1.3	− 3	− 3
	6.6	+ 6.7	+ 1	+ 7		116.2	− 1.2	− 14	− 6
39	3.3	+ 6.6	− 3	+ 3	47	141.0	− 4.0	− 35	− 17
	29.9	+ 8.0	− 8	− 3		107.8	− 1.5	− 47	(− 28)
	54.1	+ 7.9	− 13	− 5		80.9	+ 1.4	− 2	− 4
	77.3	+ 6.6	+ 6	+ 11		54.3	+ 3.5	− 31	− 11
	100.3	+ 4.2	+ 6	+ 5		26.9	− 4.8	− 18	− 14
	124.4	+ 1.0	+ 21	+ 19		356.2	+ 5.0	− 8	− 5
	150.5	− 2.5	+ 48	(+ 30)		327.9	+ 3.1	− 48	(− 24)

40	154.2	− 2.2	+ 28	+ 10	48	348.1	+ 5.1	+ 4	+ 9		
	128.2	+ 1.8	+ 25	+ 9		14.0	+ 6.5	+ 16	+ 14		
	105.2	+ 5.0	+ 8	+ 2		38.8	+ 6.5	− 15	− 11		
	83.3	+ 7.4	− 21	− 11		62.1	+ 6.3	− 18	− 2		
	61.7	+ 8.8	− 30	(− 20)		85.0	+ 3.8	+ 5	+ 7		
	39.0	+ 8.9	− 11	− 6		108.6	+ 1.4	− 22	− 12		
	7.0	+ 6.9	− 10	− 4		153.6	− 3.3	+ 38	(+ 20)		
41	155.2	− 1.4	+ 31	+ 11	49	2.1	+ 4.9	− 10	− 2		
	129.6	+ 2.7	+ 26	+ 6		325.4	+ 5.3	− 13	− 6		
	106.9	+ 6.0	− 10	− 7		307.7	+ 5.1	+ 23	(+ 19)		
	85.5	+ 9.1	− 19	− 12		279.5	+ 2.8	+ 4	+ 6		
	64.1	+ 9.4	− 21	− 7		251.0	+ 0.5	+ 16	+ 11		
	41.9	+ 9.2	− 14	− 9		222.4	− 2.0	+ 8	+ 8		
	18.3	+ 7.7	+ 2	− 2		200.8	− 3.1	+ 15	+ 12		
50	208.9	− 385	+ 6	+ 8	58	283.2	− 4.2	− 4	− 1		
	230.2	− 1.4	− 12	− 2		224.6	− 2.0	− 22	− 13		
	257.6	+ 1.1	+ 5	− 1		255.4	+ 0.5	+ 1	+ 5		
	285.1	+ 3.4	− 1	+ 10		283.9	+ 2.9	− 10	− 8		
	312.1	+ 5.0	+ 16	+ 13		305.3	+ 4.8	+ 12	+ 4		
	338.6	+ 5.5	+ 8	+ 11		327.4	+ 5.8	− 46	(− 27)		
	4.2	+ 5.0	− 6	+ 2		354.0	+ 5.9	+ 4	+ 2		
51	195.5	− 5.0	+ 25	+ 17	59	197.8	− 5.2	− 2	+ 3		
	223.5	− 4.9	− 2	0		223.5	− 4.0	− 4	− 3		
	252.1	− 1.6	+ 17	+ 15		249.9	− 1.9	+ 5	+ 6		
	280.5	+ 1.0	− 10	+ 2		276.2	+ 6.7	− 20	− 9		
	308.5	+ 3.4	+ 22	(+ 20)		302.6	+ 3.1	+ 10	+ 14		
	335.4	+ 5.0	− 14	− 7		327.2	+ 4.9	− 46	(− 27)		
	1.3	+ 5.6	− 11	− 7		351.2	+ 5.8	− 8	− 2		
52	14.0	+ 5.7	+ 4	− 1	60	358.0	+ 6.1	+ 1	− 1		
	305.6	+ 5.7	+ 3	− 8		334.2	+ 5.4	− 12	− 3		
	321.2	+ 3.9	− 16	− 8		309.4	+ 3.8	+ 18	+ 14		
	220.7	+ 3.3	+ 1	− 5		281.7	+ 1.4	− 21	− 11		
	231.7	− 3.3	− 15	− 8		254.6	− 1.4	+ 18	+ 17		
	261.2	− 5.0	+ 3	− 6		227.1	− 3.6	+ 4	+ 2		
						198.8	− 5.2	− 7	− 3		
53	9.2	+ 1.3	+ 4	− 2	61	199.1	− 5.6	− 8	− 2		
	39.2	+ 4.9	− 15	− 14		228.5	− 5.0	− 6	− 6		
	65.2	+ 7.1	− 29	− 14		254.9	− 3.1	+ 22	+ 16		
	90.8	+ 7.8	− 14	− 12		282.9	− 0.4	− 15	0		
	114.3	+ 7.2	− 7	− 5		310.2	+ 2.5	+ 4	+ 1		
	138.4	+ 5.4	− 3	− 6		336.5	+ 4.7	+ 4	0		
	161.6	+ 2.8	+ 7	− 5		7.8	+ 6.2	− 6	0		

54	11.0	− 0.1	− 2	− 1	62	25.6	+ 6.5	− 18	− 14
	40.9	+ 3.5	− 5	− 1		356.4	+ 5.3	− 2	+ 2
	67.6	+ 5.9	− 6	+ 1		325.3	+ 2.6	− 40	(− 23)
	91.8	+ 7.0	+ 3	+ 1		292.3	− 1.0	− 2	0
	114.8	+ 7.1	+ 1	+ 3		259.0	− 4.3	+ 1	− 3
	137.8	+ 6.0	+ 8	+ 5		223.7	− 6.0	− 4	− 3
	155.9	+ 4.5	+ 29	+ 9		222.6	− 6.0	− 3	− 2
55	350.7	+ 5.3	− 13	− 7	63	345.5	+ 2.7	− 7	− 3
	323.0	+ 5.6	− 17	− 7		316.1	− 0.3	+ 17	+ 8
	295.5	+ 5.9	− 2	+ 1		285.3	− 3.2	+ 6	+ 6
	267.6	+ 3.2	− 43	(− 21)		253.8	− 5.2	+ 13	+ 13
	239.6	+ 0.6	− 13	− 7		222.5	− 5.6	+ 4	+ 4
	211.6	− 2.0	− 7	− 6		202.5	− 5.0	− 3	0
	201.6	− 2.9	+ 12	+ 8					
56	199.6	− 3.2	+ 6	+ 3	64	359.0	− 1.3	− 18	− 6
	224.5	− 0.9	− 2	− 6		319.4	− 6.0	+ 2	+ 1
	249.3	+ 1.6	+ 7	+ 7		283.7	− 5.9	− 14	− 8
	274.2	+ 3.8	− 26	− 9		256.8	− 4.2	+ 4	+ 9
	299.9	+ 5.4	− 7	− 1		230.4	− 1.5	− 18	− 8
	323.2	+ 6.0	− 12	− 3		204.0	+ 1.5	− 12	− 8
	347.2	+ 5.6	− 4	− 1		197.2	+ 2.2	+ 22	+ 10
57	353.2	+ 6.1	− 4	− 1	65	169.3	+ 3.2	+ 2	− 9
	329.2	+ 5.6	− 40	− 18		212.1	+ 0.8	− 7	− 6
	304.6	+ 4.5	+ 3	0		236.8	− 1.9	− 35	(− 19)
	279.4	+ 2.6	− 1	+ 1		262.1	− 4.3	− 16	(− 20)
	253.9	+ 0.2	+ 3	+ 1		318.6	− 5.9	− 1	− 5
	228.3	− 2.2	− 22	− 18		290.9	− 5.8	− 22	− 13
	202.3	− 4.1	+ 1	+ 3		349.9	− 4.3	− 17	− 5
66	345.6	− 5.5	− 15	− 3		245.3	− 1.3	− 1	+ 1
	315.5	− 6.2	+ 7	− 2		223.7	+ 1.6	+ 22	(+ 19)
	289.1	− 5.3	− 6	+ 9		200.9	+ 4.6	+ 4	+ 2
	273.0	− 4.2	0	+ 8					
	235.9	− 0.5	− 15	− 3	75	190.9	+ 6.9	+ 31	+ 15
67	194.8	+ 4.1	+ 25	+ 17		211.9	+ 5.1	0	− 3
	216.8	+ 1.9	+ 15	+ 12		234.1	+ 2.4	− 12	− 2
	241.2	− 0.8	+ 3	+ 8		258.2	− 1.0	+ 16	+ 6
	267.4	− 3.4	+ 14	+ 7		285.8	− 4.3	− 12	− 2
	295.0	− 5.4	+ 6	+ 10		313.6	− 6.6	− 1	0
	322.4	− 6.1	+ 3	+ 6		343.4	− 7.4	− 16	− 7
	349.2	− 5.3	− 12	6	76	184.4	+ 7.6	+ 29	+ 15
						205.6	+ 6.4	+ 5	+ 2
68	343.2	− 6.2	− 13	− 3		230.8	+ 4.1	− 5	− 1
	314.9	− 6.1	+ 18	+ 10		257.2	+ 0.8	− 8	− 10
	287.2	− 4.4	− 6	+ 2		285.5	− 2.9	− 12	− 1
						315.4	− 5.9	+ 14	(+ 24)

	269.2	− 1.8	+ 29	(+ 19)					
	233.9	+ 1.2	− 15	− 3					
	209.5	+ 3.9	+ 4	+ 4	77	315.7	− 2.7	+ 16	+ 9
	188.9	+ 5.6	+ 18	+ 6		286.5	+ 0.5	+ 6	+ 6
						254.8	+ 3.6	+ 15	+ 8
						232.4	+ 5.3	+ 3	+ 7
69	325.7	− 6.2	− 19	− 16		208.0	+ 6.5	+ 20	+ 16
	296.7	− 6.6	+ 8	+ 7		185.2	+ 6.7	+ 16	+ 3
	268.6	− 5.3	− 1	− 2		156.6	+ 5.1	+ 22	+ 8
	241.6	− 2.8	− 9	− 3		131.1	+ 2.8	+ 23	+ 11
	269.8	+ 1.5	− 10	− 6					
					78	184.1	+ 7.2	+ 29	+ 6
70	283.4	+ 6.8	+ 29	(+ 20)		211.1	+ 5.0	− 14	− 16
	227.2	+ 4.9	+ 8	+ 12		236.5	+ 1.8	− 38	(− 26)
	252.9	+ 2.0	+ 21	+ 15		264.2	− 2.1	− 31	(− 28)
	302.9	− 4.7	+ 3	+ 6		293.8	− 5.6	− 7	− 1
	328.5	− 6.1	− 2	+ 10		324.3	− 7.0	− 28	(− 30)
	(159.5)	(+ 7.5)	− 2	− 14					
					79	320.4	− 5.8	− 18	− 13
71	27.7	− 6.8	− 8	− 4		299.2	− 4.6	+ 16	+ 13
	54.9	− 5.5	− 29	− 17		269.8	− 2.2	− 11	− 1
	81.1	− 3.0	− 1	− 1		242.6	+ 0.8	− 8	− 6
	105.5	− 0.2	− 35	− 17		216.1	+ 3.4	+ 10	+ 6
	128.2	+ 2.6	+ 15	− 1		192.5	+ 5.3	+ 20	+ 8
	149.4	+ 4.9	+ 15	+ 5					
	169.4	+ 7.3	+ 33	+ 11	80	193.6	+ 5.3	+ 29	+ 7
						217.8	+ 2.4	− 19	− 8
72	348.0	− 6.6	− 19	− 7		273.6	− 4.8	− 3	+ 7
	318.1	− 7.5	− 6	− 4		335.3	− 7.4	− 10	− 4
	289.9	− 7.0	+ 11	+ 7		347.2	− 6.9	+ 1	+ 3
	263.5	− 4.6	+ 12	+ 10		304.4	− 7.1	+ 21	+ 18
	239.4	− 1.0	− 8	+ 3		247.3	− 1.6	+ 7	+ 7
	213.0	+ 2.6	− 3	+ 1					
	202.1	+ 4.0	+ 15	+ 14	81	162.3	− 6.7	− 30	− 10
						136.4	− 7.4	− 1	− 1
73	266.2	+ 3.3	+ 1	0		110.6	− 6.5	− 46	(− 39)
	229.3	+ 0.3	− 13	− 8		85.5	− 4.3	+ 18	+ 14
	254.8	− 2.6	+ 15	+ 9		60.9	− 1.3	− 6	+ 1
	282.0	− 5.6	− 15	− 5		36.3	+ 1.9	+ 3	+ 3
	312.0	− 7.3	− 18	− 14		1.0	+ 6.0	− 3	0
	338.8	− 7.2	− 12	− 7					
	348.0	− 6.7	− 23	− 11	82	339.9	+ 7.2	− 4	− 2
						4.0	+ 5.6	− 12	− 4
74	342.8	− 7.0	− 13	− 4		27.9	+ 3.1	− 8	− 1
	318.5	− 7.4	− 1	− 2		51.6	+ 0.1	− 14	− 2
	292.6	− 6.4	− 4	+ 4		75.9	− 2.9	− 7	− 3
	269.4	− 4.1	+ 7	+ 1		101.8	− 5.7	− 21	− 4

83	162°7	− 6°1	− 35	− 15		99°5	− 6°6	+ 15	+ 9
	137.2	− 6.4	− 1	+ 4		66.5	+ 0.2	− 9	− 3
	111.9	− 5.4	− 48	(− 22)		42.7	+ 1.0	− 3	+ 1
	87.2	− 3.4	+ 15	+ 12		2.8	+ 2.6	+ 1	+ 8
	63.9	− 0.3	− 14	− 7					
	39.2	+ 2.0	+ 11	+ 10	92	4.6	+ 1.9	0	+ 4
	0.2	+ 5.7	+ 5	+ 4		32.5	+ 1.2	− 10	− 6
						59.6	+ 0.3	− 6	− 1
84	2.9	+ 5.5	0	+ 8		86.6	− 0.6	+ 14	+ 10
	28.8	+ 3.1	+ 9	+ 16		111.9	− 1.2	− 37	(− 20)
	54.4	+ 0.1	− 1	+ 8		137.8	− 1.6	− 20	− 6
	80.4	− 2.9	+ 24	(+ 24)		169.8	− 1.6	− 15	− 8
	107.0	− 2.7	− 34	− 11					
					93	170.2	+ 8.6	+ 30	(+ 24)
85	11.7	+ 4.8	+ 3	0		146.6	+ 10.3	+ 6	+ 3
	347.6	+ 7.0	− 7	− 3		124.4	+ 10.3	+ 1	+ 1
	323.4	+ 8.1	− 13	− 5		101.9	+ 8.8	+ 21	(+ 20)
	299.0	+ 7.8	− 5	− 4		77.4	+ 5.7	− 5	+ 1
	274.2	+ 6.1	+ 1	+ 7		48.8	+ 0.9	− 30	− 14
	249.1	+ 3.3	− 1	− 1		15.5	− 4.9	0	+ 6
	203.4	− 2.8	− 2	− 3					
86	201.7	− 3.0	+ 13	+ 10	95	341.1	− 7.5	− 18	− 10
	230.3	+ 0.9	− 11	− 2		313.9	− 6.8	− 5	− 5
	258.5	+ 4.6	+ 12	+ 10		287.0	− 4.6	− 18	− 10
	286.4	+ 7.3	− 24	− 16		261.2	− 1.5	+ 22	+ 15
	313.9	+ 8.3	+ 4	− 1		237.0	+ 1.8	− 23	− 11
	341.0	+ 7.5	0	0		214.6	+ 4.6	− 10	− 10
	367.7	+ 5.2	− 4	− 2		20.9	+ 6.0	− 6	− 9
87	166.1	+ 1.1	0	− 16	96	348.9	− 7.7	− 20	− 8
	143.6	+ 1.7	− 5	− 6		321.7	− 6.9	+ 5	+ 10
	121.8	+ 2.0	− 14	− 8		294.3	− 6.4	0	+ 6
	99.3	+ 2.1	− 7	− 4		264.3	− 3.0	− 12	− 10
	78.0	− 1.9	− 12	− 10		242.9	+ 0.1	− 10	− 8
	54.8	+ 1.5	− 12	− 2		219.6	+ 3.4	− 24	(− 20)
	11.1	+ 0.2	− 9	− 8		193.6	+ 6.5	+ 28	+ 14
88	282.4	− 2.6	+ 10	+ 7	97	195.6	+ 6.5	+ 12	+ 1
	227.7	+ 0.8	− 6	− 3		217.4	+ 4.0	− 8	− 5
	252.9	+ 4.0	+ 23	+ 14		241.4	+ 0.6	− 13	− 10
	277.8	+ 6.5	+ 7	+ 5		267.4	− 3.1	+ 1	− 5
	302.6	+ 7.6	− 2	+ 1		295.1	− 6.2	− 6	− 2
	327.0	+ 7.8	− 28	− 15		323.5	− 7.9	− 9	− 1
	0.9	+ 5.6	− 8	− 5		348.3	− 7.8	− 20	− 8
89	5.7	+ 5.2	− 12	− 4	98	349.0	− 7.8	− 29	− 17
	333.6	+ 7.4	− 3	− 1		294.4	− 7.0	− 9	− 4
	313.4	+ 8.1	+ 5	+ 1		267.7	− 4.1	0	− 7
	286.8	+ 7.3	− 15	− 7		242.5	− 0.4	− 16	− 14

	261.0	+ 5.0	+ 15	+ 7		219.1	+ 3.1	− 22	− 18
	233.0	+ 1.5	− 24	− 15					
	201.6	− 2.6	+ 18	+ 9	99	345.4	− 7.1	− 10	+ 1
						313.7	− 7.9	+ 1	+ 1
90	202.7	− 2.6	+ 9	+ 6		282.7	− 3.0	+ 16	+ 17
	230.5	+ 1.3	− 6	+ 2		225.6	+ 0.9	+ 2	+ 4
	257.2	+ 4.3	+ 12	(+ 19)		199.7	+ 4.3	+ 8	+ 6
	283.9	+ 7.3	− 12	− 3		183.1	+ 6.2	+ 30	(+ 26)
	310.4	+ 6..	+ 4	+ 5					
	336.7	+ 7.7	+ 10	+ 14					
	2.0	+ 5.6	0	+ 6	100	20.5	− 2.9	− 3	− 1
						46.7	− 0.2	− 8	− 1
91	169.6	− 1.6	− 15	− 9		70.5	+ 1.3	+ 1	+ 7
	143.6	− 1.6	− 22	− 14		92.3	+ 4.3	− 12	− 4
	118.4	− 1.3	+ 4	+ 4		112.6	+ 5.7	− 3	− 2
	132.5	+ 6.4	+ 21	+ 14	109	1154	+ 39.6	+ 2	− 1
	152.7	+ 6.3	+ 4	− 5		344.0	+ 5.9	+ 2	0
	169.1	+ 4.4	+ 8	− 2		316.3	+ 6.9	+ 11	+ 5
						284.3	+ 6.4	− 12	− 4
101	193.6	+ 2.5	+ 11	+ 5		260.1	+ 4.4	+ 22	+ 14
	168.1	+ 4.9	− 11	− 7		232.0	+ 1.5	− 18	− 9
	142.4	+ 6.1	+ 20	+ 12		201.5	− 2.0	+ 16	+ 12
	116.9	+ 6.0	+ 3	+ 4					
					110	346.2	+ 3.2	+ 1	+ 4
102	348.4	− 8.3	− 13	− 1		14.6	+ 1.0	+ 1	0
	313.7	− 9.9	+ 9	+ 8		42.8	− 1.4	− 2	− 4
	278.7	− 6.5	+ 2	+ 10		70.8	− 3.3	0	0
	247.6	− 2.0	− 2	0		96.9	− 4.1	− 3	− 4
	218.4	+ 2.8	− 2	+ 2		126.2	− 4.4	+ 16	+ 8
	200.7	+ 5.4	+ 13	+ 10		170.3	− 2.4	− 30	(− 19)
					111	354.9	+ 2.6	− 1	+ 1
103	197.9	+ 5.9	+ 14	0		329.7	+ 5.2	− 39	− 15
	218.0	+ 3.0	− 10	− 7		304.5	+ 6.8	+ 4	+ 2
	240.4	− 0.7	− 19	− 12		279.7	+ 7.2	+ 2	+ 6
	264.6	− 4.4	− 6	− 11		255.2	+ 6.3	− 4	− 4
	290.3	− 7.5	− 15	− 5		231.1	+ 4.4	− 5	− 1
	316.4	− 9.0	+ 3	+ 1		199.0	+ 0.8	+ 12	+ 2
	350.2	− 8.2	− 9	+ 1					
					112	199.1	+ 0.9	+ 31	(+ 21)
104	188.6	+ 3.6	+ 6	− 2		221.4	+ 3.9	− 2	0
	211.2	+ 1.4	− 4	− 3		250.3	+ 6.2	+ 39	+ 5
	236.0	− 1.4	− 28	− 12		278.6	+ 7.4	+ 5	+ 4
	262.5	− 4.7	+ 11	+ 6		303.2	+ 7.0	+ 3	+ 7
	290.3	− 5.8	− 12	− 3		330.5	+ 5.2	− 9	− 5
	316.5	− 6.2	− 2	− 5		350.0	+ 3.2	− 8	− 2
	349.0	− 5.0	− 20	− 8					
					113	354.6	− 0.8	+ 19	(+ 25)
105	163.5	− 6.6	− 19	− 7		297.2	+ 3.9	− 1	+ 5
	137.2	− 7.0	− 12	− 6		269.3	+ 5.2	− 46	(− 24)
	111.7	− 6.0	− 44	(− 18)					

	86.7	3.9	+ 10	+ 6		244.2	+ 5.4	− 16	− 12
	62.3	− 1.0	− 17	− 19		215.6	+ 4.5	− 10	− 6
	38.5	+ 2.1	− 2	− 1		189.6	+ 2.6	+ 2	− 9
	354.9	+ 6.5	+ 10	+ 10					
					114	149.8	+ 2.3	− 6	− 6
						226.3	+ 5.5	− 14	− 11
106	157.2	− 6.5	− 3	− 1		252.7	+ 7.6	+ 12	+ 5
	126.4	− 6.4	+ 13	+ 8		279.5	+ 8.2	+ 9	+ 4
	96.3	− 4.4	− 5	− 1		307.1	+ 7.1	+ 2	− 1
	67.1	− 1.2	− 3	− 2		315.2	+ 4.3	− 19	− 11
	38.6	+ 3.4	− 4	− 1		351.1	− 2.2	− 12	− 7
	10.1	+ 5.2	0	+ 1		261.2	+ 8.0	+ 9	+ 3
	341.2	+ 6.9	+ 5	+ 4					
					115	342.6	− 4.2	− 11	− 4
107	357.6	+ 6.2	+ 14	(+ 18)		312.2	− 1.9	+ 8	+ 4
	26.9	+ 3.0	6	+ 2		283.4	+ 1.6	− 13	− 6
	51.7	− 0.7	− 7	+ 1		229.9	+ 5.8	− 7	− 3
	84.1	− 4.2	+ 18	+ 14		205.7	+ 6.4	− 2	− 5
	114.3	− 6.5	− 11	0		170.9	+ 5.2	− 4	0
	145.2	− 7.0	− 10	− 2		139.4	+ 6.1	+ 27	+ 13
	162.4	− 6.4	− 32	− 11					
					116	194.2	+ 4.3	+ 18	+ 10
108	200.8	− 2.2	+ 12	+ 8		218.7	+ 7.7	− 13	− 10
	225.6	+ 0.6	− 9	− 4		243.4	+ 8.3	− 13	− 7
	251.0	+ 3.3	+ 18	(+ 19)		268.9	+ 8.2	− 29	− 13
	272.2	+ 5.2	− 32	− 16		295.6	+ 6.5	− 4	− 2
	301.3	+ 6.6	− 4	0		323.4	+ 3.3	− 12	− 11
	326.2	+ 6.6	− 25	− 12		350.6	− 0.6	− 12	− 6
	10.4	+ 3.7	− 1	− 4					
					126	154.7	− 2.7	+ 28	+ 7
117	189.0	+ 7.1	+ 27	+ 5		130.7	− 3.6	+ 8	+ 6
	211.6	+ 6.0	− 3	− 7		106.5	− 3.9	− 43	− 17
	236.1	+ 3.8	− 16	− 11		62.0	− 3.4	+ 5	+ 4
	262.5	+ 6.8	− 2	± 1		57.2	− 2.3	− 12	− 6
	288.9	− 2.6	− 7	− 2		32.0	− 0.6	− 1	0
	319.5	− 5.3	− 4	− 6		6.5	+ 1.2	+ 3	+ 3
	348.6	− 6.6	− 23	− 11		347.0	+ 2.5	− 7	− 1
118	351.9	− 6.7	− 15	− 6	127	155.1	+ 5.1	+ 26	+ 16
	317.7	− 5.1	+ 4	+ 4		179.0	+ 7.3	+ 13	+ 6
	282.3	− 2.3	± 2	+ 4		206.2	+ 8.3	+ 14	+ 7
	253.1	+ 1.3	+ 1	+ 6		228.7	+ 8.0	− 14	− 12
	210.6	+ 6.2	± 4	− 1		253.6	+ 6.1	+ 23	+ 18
	188.9	+ 7.2	+ 31	+ 9		282.9	+ 2.6	− 11	− 6
						326.3	− 3.6	− 20	− 6
119	189.2	+ 6.6	+ 8	− 10					
	211.9	+ 5.2	− 1	− 6					
	236.8	+ 2.7	− 12	− 2	128	327.4	− 3.6	− 16	− 1
	263.4	− 6.9	+ 6	+ 4		293.4	+ 1.2	− 2	0
	292.6	− 5.1	− 1	+ 4		260.8	+ 5.4	+ 20	+ 12

	322.6	−5.9	−6	−2
	343.2	−6.5	−18	−10
120	190.0	+2.5	+14	0
	211.9	+0.4	−8	−3
	235.6	−1.9	−26	−10
	261.7	−4.2	−2	2
	346.9	−3.9	−18	−9
121	345.2	−2.5	−12	−8
	319.6	−4.1	+2	0
	293.4	−4.9	10	−7
	267.1	−4.6	+4	−4
	241.5	−3.4	−21	13
	217.2	−1.5	−5	−2
	190.2	+0.9	+19	+2
122	188.7	−0.5	−1	−8
	212.0	−2.4	0	+4
	237.5	−4.0	52	(−40)
	264.4	−4.7	3	−3
	291.7	−4.4	−7	−1
	318.9	−3.6	+12	+5
	356.1	0.0	−11	−5
123	29.8	+4.8	−18	−13
	4.3	+5.1	−15	−7
	339.1	+5.1	2	3
	308.2	+4.6	0	0
	280.4	+1.2	−14	−3
	251.0	−1.4	+10	+8
	220.9	−3.8	−4	−2
124	313.1	+4.3	+10	+3
	340.2	+4.9	+8	+7
	4.0	+4.6	7	+1
	28.1	+3.6	0	+6
	51.6	+2.0	−14	−3
	74.7	+0.2	−8	−4
	98.0	−1.6	[illegible]	+1
	122.5	3.2	+5	−3
	138.5	−4.0	−33	−17
134	354°2	−2°4	−10	−6
	325.8	−1.2	−28	−17
	296.6	+0.3	+13	+10
	268.2	+1.8	−37	−18
	241.0	+2.9	−3	−4
	214.2	+3.4	−2	−2
	189.0	+3.3	+2	−8
	232.0	+7.8	0	+2
	205.0	+8.4	0	−2
	179.7	+7.4	+6	−2
	155.1	+5.0	+29	+17
129	335.3	−3.3	−2	+2
	305.0	−2.1	+25	(+27)
	371.4	0.0	−33	−15
	241.2	+1.9	+9	+10
	212.9	+3.3	0	+1
	188.3	+4.0	+20	+10
	155.9	+3.8	+42	(+24)
130	155.8	+3.7	+36	+17
	181.1	+4.0	+60	(+35)
	208.1	+3.5	0	0
	237.0	+2.2	−8	+3
	267.9	+0.3	−31	−15
	300.5	−1.8	+7	+10
	339.3	−3.3	−6	−2
131	184.0	+6.2	+1	−1
	212.9	−2.5	+5	+6
	243.6	−2.9	−7	−4
	275.2	−2.3	−23	−12
	307.2	−1.0	−5	−1
	338.4	+1.8	−15	−12
	332.5	+0.4	−42	(−20)
132	8.6	−6.5	−17	−11
	38.9	−8.0	−3	−1
	68.0	−7.3	−19	−11
	164.2	+4.4	+10	+3
	119.0	−1.9	−2	−4
	142.8	+1.5	−18	−10
	96.5	−4.8	−4	0
133	188.7	+3.2	+5	−4
	213.0	+3.1	−4	−2
	266.2	+1.4	−31	−12
	294.7	−0.2	+16	+16
	323.9	−1.5	−17	−7
	354.7	−2.4	0	+4
	270°2	+4°3	−40	−18
	290.1	+0.9	+6	+9
	347.1	−4.6	−15	−3
	322.5	−2.0	−14	−3
143	346.3	−4.5	−14	−2
	312.5	−0.6	+11	+6

135	187.9	+ 3.4	+ 18	+ 8
	212.4	+ 3.7	− 4	− 4
	237.3	+ 3.4	− 4	+ 1
	262.8	+ 6.2	+ 16	(+ 20)
136	181.0	+ 8.1	+ 23	+ 11
	161.2	+ 5.2	+ 18	+ 8
	137.7	+ 2.1	− 4	0
	114.2	− 1.3	− 18	− 2
	88.7	− 4.7	+ 11	+ 7
	60.9	− 7.3	− 13	− 7
	18.0	− 7.8	− 38	(− 33)
137	8.0	− 7.3	− 5	− 3
	40.6	− 8.2	− 7	− 6
	72.1	− 7.1	− 1	+ 3
	103.1	− 3.6	− 21	− 12
	127.9	+ 0.1	+ 26	+ 11
	152.5	+ 3.8	+ 20	+ 8
	165.0	+ 5.5	+ 23	+ 11
138	164.6	+ 5.5	+ 16	+ 4
	141.6	+ 2.1	− 22	− 12
	119.4	− 1.3	+ 4	− 2
	93.0	− 5.1	+ 13	+ 4
	66.2	− 7.7	− 15	− 7
	36.6	− 8.7	− 6	− 4
	11.2	− 7.5	− 15	− 7
139	10.8	− 7.6	− 18	− 10
	40.8	− 8.8	+ 1	+ 2
	69.7	− 7.7	− 9	− 3
	95.9	− 4.8	− 3	+ 1
	121.8	− 1.1	− 8	− 6
	144.8	+ 2.5	− 13	11
	162.6	+ 3.1	+ 20	+ 6
140	161.0	+ 4.9	+ 20	+ 11
	141.3	+ 2.0	− 12	− 2
	117.0	− 1.4	− 9	− 5
	88.8	− 5.0	+ 5	+ 1
	61.8	− 7.2	+ 4	− 11
	31.2	− 7.7	− 6	− 2
	10.5	− 6.8	− 18	− 10
141	154.8	+ 2.8	+ 34	(+ 22)
	130.3	− 0.3	+ 7	+ 7
	104.9	− 3.4	− 32	− 14
	77.5	− 5.8	− 6	− 4

	280.4	+ 3.4	+ 20	(+ 22)
	250.2	+ 6.3	+ 16	+ 11
	222.1	+ 7.5	− 10	− 7
	195.0	+ 7.2	+ 23	+ 11
	173.8	+ 7.2	− 6	− 5
144	181.0	+ 7.5	+ 18	+ 6
	204.7	+ 9.0	+ 6	+ 6
	229.2	+ 8.9	− 19	− 15
	256.0	+ 7.1	− 4	− 1
	284.9	+ 3.5	− 19	− 7
	315.5	− 1.2	+ 18	+ 11
	352.7	− 6.2	− 26	− 14
145	352.1	− 6.2	− 24	− 12
	319.4	− 1.7	+ 3	+ 2
	287.9	+ 3.3	26	+ 12
	259.5	+ 7.1	− 2	− 4
	231.4	+ 9.0	− 6	− 4
	206.3	+ 9.2	− 3	− 7
	181.3	+ 8.5	+ 17	+ 4
	206.3	+ 9.1	− 9	− 13
146	317.5	− 1.3	+ 13	+ 4
	285.7	+ 3.5	− 30	− 19
	255.8	+ 7.0	− 3	0
	171.5	+ 6.3	− 4	− 4
147	349.0	− 4.8	− 9	+ 3
	321.5	− 0.6	− 9	+ 2
	289.0	+ 4.5	− 6	+ 2
	261.4	+ 7.8	+ 24	(+ 20)
	236.0	+ 9.4	− 6	+ 4
	211.4	+ 9.2	+ 7	+ 1
	183.5	+ 7.1	+ 42	(+ 24)
148	171.0	+ 6.6	+ 8	+ 3
	148.4	+ 5.4	+ 12	+ 4
	126.1	+ 3.4	+ 15	+ 13
	102.4	+ 0.9	+ 1	+ 9
	76.8	− 2.1	+ 4	+ 6
	45.4	− 4.9	+ 8	+ 14
	8.0	− 6.3	+ 11	+ 16
149	5.8	− 6.3	− 5	0
	38.4	− 5.5	+ 4	+ 4
	69.4	− 3.1	− 3	0
	97.6	0.0	− 16	− 12

	46.2	− 7.0	+ 1	+ 1		122.6	+ 2.8	+ 5	+ 6
	0.1	− 4.9	+ 1	+ 3		170.7	+ 6.5	+ 13	+ 8
	21.4	− 6.5	− 10	− 6		146.2	+ 5.0	+ 2	+ 2
142	171.0	+ 5.5	− 2	+ 1	150	330.8	− 3.8	− 22	− 12
	193.8	+ 7.0	+ 27	+ 13		294.5	− 4.0	− 2	0
	217.6	+ 7.4	+ 12	+ 14		259.6	− 2.6	+ 26	(+ 19)
	243.0	+ 6.6	0	+ 3		226.5	− 4.9	+ 2	+ 1
	197.2	+ 1.9	+ 28	+ 16	159	185.9	− 2.4	− 24	− 10
	168.2	+ 3.7	− 7	+ 2		238.9	+ 4.9	− 1	− 3
	142.5	+ 4.5	+ 3	+ 1		265.9	+ 7.4	− 30	− 13
						295.7	+ 8.4	+ 1	+ 2
						320.5	+ 7.6	− 36	− 16
151	193.6	+ 3.2	+ 9	+ 2		354.6	+ 4.3	− 10	− 9
	167.1	+ 4.8	+ 4	+ 2					
	141.8	+ 4.9	+ 10	+ 9					
	118.4	+ 4.2	− 8	− 8	160	356.6	+ 6.3	+ 15	(+ 21)
	91.6	+ 2.7	− 7	+ 1		330.4	+ 6.9	− 14	+ 2
	63.8	+ 0.5	− 15	− 6		306.3	+ 6.0	− 2	+ 2
	38.3	− 1.9	+ 4	+ 6		269.5	+ 3.4	− 33	− 11
						227.6	− 1.3	− 8	− 4
152	6.9	− 5.9	− 9	− 4		195.6	− 4.5	+ 26	(+ 19)
	41.9	− 3.5	− 4	− 1					
	72.4	− 1.2	− 1	+ 1					
	99.4	+ 1.4	+ 6	+ 3	161	9.4	− 5.1	− 15	− 9
	125.6	+ 3.6	+ 15	+ 10		42.8	− 0.6	+ 8	+ 6
	150.1	+ 4.9	+ 17	+ 6		72.2	+ 3.6	0	+ 6
	185.4	+ 5.5	+ 19	+ 7		98.2	+ 6.7	+ 10	+ 13
						121.8	+ 8.3	+ 12	+ 12
153	19.9	− 5.8	− 14	− 6		144.8	+ 8.6	+ 15	+ 9
	42.9	− 4.3	− 3	+ 1		174.5	+ 7.1	− 8	− 5
	101.8	+ 1.5	− 5	− 1					
	125.6	− 3.8	+ 14	+ 8	162	170.9	+ 7.4	+ 20	+ 8
	149.7	+ 5.6	+ 26	+ 16		146.3	+ 8.5	− 5	− 8
	178.5	+ 6.4	+ 5	− 1		123.1	+ 8.2	− 2	− 4
						99.7	+ 6.6	− 11	− 6
154	10.3	− 7.0	− 2	+ 6		44.5	− 0.5	− 2	0
	42.7	− 7.0	+ 13	+ 16		9.4	− 5.1	− 15	− 9
	73.2	− 4.9	+ 27	(+ 29)					
	104.3	− 1.3	− 12	+ 4	163	9.0	− 6.0	− 11	− 5
						42.7	− 1.5	+ 2	0
155	31.4	− 0.4	+ 9	+ 11		72.5	+ 0.5	− 4	− 2
	6.4	+ 1.7	+ 6	+ 5		98.6	+ 6.5	− 5	− 1
	340.8	+ 3.6	+ 19	+ 8		122.4	+ 8.4	+ 8	+ 7
	315.1	+ 4.6	+ 31	(+ 23)		145.3	+ 9.1	+ 9	+ 3
	284.5	+ 5.1	+ 4	+ 12		170.6	+ 8.1	+ 30	+ 14
	265.2	+ 4.6	− 25	− 3					
	198.7	+ 0.7	+ 16	+ 4					

156	183.7	+ 1.0	+ 28	(+ 22)	164	180.1	+ 7.3	+ 12	+ 4
	209.1	+ 4.1	+ 6	+ 5		155.3	+ 8.8	− 23	− 16
	234.2	+ 6.4	+ 16	(+ 19)		131.1	+ 8.7	− 2	− 2
	259.9	+ 7.5	+ 28	(+ 20)		109.1	+ 8.2	− 12	− 10
	286.3	+ 7.2	+ 1	+ 9		84.9	+ 4.6	− 12	− 6
	313.5	+ 5.4	+ 19	+ 13		55.7	+ 0.4	− 15	− 12
	355.4	+ 0.6	− 6	0		14.2	− 5.4	− 8	− 2
	338.8	+ 2.7	+ 1	+ 3	165	171.3	+ 8.3	+ 28	+ 14
						147.4	+ 8.5	+ 4	+ 3
157	352.5	+ 1.0	− 32	(− 25)		124.2	+ 7.3	+ 13	+ 7
	321.4	+ 4.7	− 23	− 14		99.8	+ 4.9	− 12	− 8
	291.3	+ 7.1	− 19	− 13		72.7	+ 1.2	− 10	− 8
	189.7	+ 1.7	+ 1	− 9		42.0	− 3.2	− 7	− 4
	263.8	+ 7.7	− 26	(− 19)		9.6	− 6.7	− 15	− 8
158	351.2	+ 3.5	− 6	0	166	11.4	− 6.5	− 9	− 1
	322.2	+ 6.7	− 16	+ 2		44.9	− 2.9	+ 1	+ 6
	295.3	+ 8.2	0	− 1		75.3	+ 1.4	+ 1	+ 5
	265.5	+ 7.9	− 27	− 14		102.1	+ 4.9	+ 6	+ 7
	237.8	+ 5.8	− 7	− 5		126.4	+ 7.3	+ 9	+ 9
	210.2	+ 2.4	− 9	− 5		149.7	+ 8.4	+ 13	+ 12
	184.8	− 1.1	− 14	− 6		167.3	+ 8.3	+ 13	+ 5
167	189°2	− 0°2	+ 19	+ 9	176	184°8	− 2°1	− 12	+ 1
	249.6	− 2.9	+ 34	(+ 30)		212.9	+ 1.1	− 9	− 5
	281.6	− 3.1	− 6	+ 13		240.5	+ 4.1	− 7	− 11
	353.3	− 0.3	− 6	0		268.0	+ 6.2	− 22	0
	318.8	− 2.1	− 15	(− 21)		295.9	+ 7.0	− 14	− 13
						323.4	+ 6.2	− 26	− 18
168	188.7	+ 1.4	+ 20	+ 10		354.7	+ 3.7	− 10	− 10
	215.5	− 0.6	+ 8	+ 9					
	246.9	− 3.0	+ 4	+ 6	177	351.8	+ 4.1	− 9	− 3
	276.9	− 3.9	− 15	− 8		324.6	+ 6.3	− 13	− 4
	308.0	− 4.0	+ 11	+ 13		296.6	+ 7.2	− 10	− 6
	339.7	− 2.8	− 14	− 10		268.9	+ 6.5	− 26	− 4
	361.4	− 1.4	− 7	− 5		241.3	− 4.4	+ 7	+ 5
						214.1	+ 1.4	− 3	− 2
169	377.6	− 3.9	− 5	− 1		185.7	− 2.0	− 11	− 1
	49.8	− 0.2	− 5	− 1					
					179	142.5	− 4.8	− 22	− 13
170	186.6	+ 5.4	− 14	+ 2		119.0	− 3.7	− 14	− 15
	161.6	+ 7.3	− 10	− 10		61.8	+ 0.6	− 12	0
	137.0	+ 7.7	− 1	0		35.4	+ 2.9	− 9	− 7
	112.8	+ 6.8	− 17	− 15		352.4	− 5.3	0	+ 6
	87.1	+ 4.6	− 9	− 11					
	57.5	− 1.0	− 10	− 4	180	2.3	+ 5.6	− 22	− 14
	16.3	− 4.1	− 8	− 4		336.2	+ 8.2	− 2	+ 2
						309.3	+ 9.1	− 2	+ 2

171	170.7	+ 7.7	+ 25	+ 13		282.1	+ 8.0	— 26	(— 29)
	147.0	+ 8.4	— 1	— 1		254.7	+ 5.3	— 13	— 15
	123.9	+ 7.8	+ 7	+ 4		226.9	+ 1.3	0	0
	100.0	+ 6.0	— 4	0		191.1	— 3.1	— 8	— 6
	73.7	+ 2.8	— 5	— 1					
	74.3	+ 0.1	— 19	— 9	181	359.9	+ 6.2	+ 1	— 1
	13.4	— 5.3	— 2	+ 6		332.6	+ 5.8	— 23	— 15
						306.0	+ 3.6	— 9	— 5
172	12.3	— 6.4	— 6	+ 2		279.2	+ 0.4	+ 2	+ 8
	46.5	— 2.6	— 6	+ 2		251.8	+ 5.4	+ 40	(+ 30)
	76.6	+ 1.5	— 1	+ 1		224.3	+ 1.2	0	— 1
	103.3	+ 5.0	+ 4	+ 6		191.2	— 1.1	— 9	— 1
	127.0	+ 7.2	— 1	— 3					
	151.0	+ 8.2	+ 36	(+ 27)	182	0.9	+ 0.5	+ 5	+ 4
	164.7	+ 8.2	+ 21	(+ 18)		31.3	+ 0.8	— 3	+ 1
						60.5	+ 0.9	— 8	— 9
173	191.3	— 2.8	+ 18	+ 9		88.2	+ 0.8	+ 14	+ 11
	220.7	+ 0.5	— 2	0		115.2	+ 0.7	+ 5	+ 16
	248.8	+ 3.7	— 6	+ 2		142.1	+ 0.4	— 19	— 10
	276.8	+ 6.1	+ 1	+ 2		169.8	+ 0.1	— 31	— 19
	306.7	+ 7.1	+ 5	+ 2					
	334.6	+ 6.4	— 24	— 15	183	171.5	+ 2.1	— 31	(— 28)
	5.0	+ 4.0	— 12	— 6		144.5	+ 3.0	— 12	— 13
						119.0	+ 3.2	4	— 4
174	356.2	+ 2.2	— 6	— 2		91.2	+ 2.9	— 7	— 3
	327.4	+ 4.5	— 39	(— 26)		66.4	+ 2.0	— 40	(— 37)
	298.8	+ 5.8	— 8	— 3		37.3	+ 0.6	— 1	+ 3
	270.8	+ 4.6	— 37	— 15		5.9	— 1.0	— 8	— 3
	241.5	+ 4.8	+ 12	+ 2					
	212.1	— 2.3	— 6	4	184	10.0	— 2.3	— 10	— 6
	185.9	— 0.8	— 18	— 15		42.1	+ 0.6	— 10	— 6
						69.7	+ 3.0	— 2	+ 4
175	186.3	— 0.3	+ 25	+ 16		95.0	+ 4.7	— 1	+ 1
	217.2	+ 2.4	+ 8	+ 6		119.0	+ 5.5	— 5	— 5
	244.5	+ 4.7	+ 2	+ 5		142.6	+ 5.4	0	— 4
	272.3	+ 6.9	— 7	— 6		166.7	+ 4.4	— 2	— 5
	300.5	+ 6.0	— 2	— 2					
	317.8	+ 5.3	+ 11	+ 9	185	10.0	— 4.6	— 7	0
	351.2	+ 2.7	+ 4	+ 11		42.8	+ 0.4	— 9	— 7
						71.8	+ 4.8	— 10	— 4
185	97.3	+ 7.7	+ 3	+ 1	191	187.8	— 4.5	— 26	— 11
	120.4	+ 9.1	+ 9	+ 7		213.6	— 2.5	0	+ 2
	143.1	+ 9.1	+ 18	+ 9		239.8	+ 0.3	— 15	— 8
	170.3	+ 9.1	+ 15	+ 5		265.8	+ 3.6	— 41	(— 19)
						291.7	+ 5.1	— 6	— 2
186	179.4	+ 7.4	+ 8	+ 1		317.1	+ 6.2	+ 5	+ 2
	154.8	+ 9.8	— 14	— 5		336.0	+ 5.7	— 2	+ 4
	132.4	+ 10.4	+ 1	+ 1					

	110.1	+ 9.6	+ 7	+ 6
	86.3	+ 7.3	− 15	− 11
	59.3	+ 3.1	− 15	− 11
	12.3	− 5.0	− 14	− 6
187	7.8	− 6.2	− 10	− 5
	43.0	− 0.1	0	− 1
	73.2	+ 5.4	− 8	− 5
	90.2	+ 9.0	− 7	− 3
	122.6	+ 10.7	− 2	− 2
	145.3	+ 10.8	+ 4	+ 4
	170.4	+ 9.0	+ 24	+ 12
188	191.9	− 1.7	+ 35	(+ 20)
	219.5	+ 0.6	+ 1	+ 3
	247.9	+ 2.8	+ 10	+ 13
	1.4	+ 3.0	− 1	+ 5
	306.6	+ 5.0	+ 27	+ 19
189	0.2	+ 1.4	+ 1	+ 3
	328.4	+ 2.3	− 19	+ 5
	296.3	+ 2.7	− 16	(+ 22)
	263.2	+ 2.3	− 37	(− 19)
	233.1	− 1.3	− 30	− 10
	199.0	− 0.5	+ 20	+ 7
190	6.3	− 0.5	− 6	− 2
	334.6	− 0.2	− 21	− 12
	302.3	+ 0.1	− 8	+ 1
	270.1	+ 0.5	− 52	(− 32)
	238.0	+ 0.8	− 9	− 1
191	204.0	+ 1.8	− 8	− 4
	171.8	+ 3.0	− 21	− 9
	140.9	− 3.3	− 2	0
	123.8	+ 3.0	+ 15	+ 13
	94.6	+ 2.2	+ 14	+ 16
	70.8	+ 1.0	+ 6	+ 12
	12.6	− 1.8	− 9	− 3
	42.6	− 0.4	+ 3	+ 1
192	191.0	− 0.8	+ 18	+ 8
	219.5	+ 1.2	4	− 2
	249.7	+ 3.1	+ 6	+ 2
	280.6	+ 4.3	− 6	0
	312.0	+ 4.2	+ 14	+ 9
	335.8	+ 3.1	− 1	+ 5

195	189.0	− 4.6	− 22	− 4
	218.[illegible]	− 1.6	− 1	+ 3
	247.2	+ 1.7	− [illegible]	+ 1
	275.9	+ 4.6	− 6	+ 14
	304.3	+ 6.8	+ 7	+ 6
	332.0	+ 7.2	− 15	− 2
	359.8	+ 7.2	+ 5	+ 3
196	5.5	+ 5.4	− 2	+ 6
	338.4	+ 7.4	+ 3	+ 3
	311.5	+ 7.8	+ 3	+ 3
	233.7	+ 6.5	− 6	− 2
	255.6	+ 3.8	− 7	− 3
	227.2	+ 0.2	− 6	− 3
	196.1	− 3.8	+ 18	+ 12
197	25.0	+ 2.2	− 5	+ 2
	357.7	+ 4.6	3	0
	330.2	+ 6.4	− 38	− 17
	302.2	+ 6.7	− 5	− 1
	274.1	+ 5.4	− 2	+ 7
	245.9	+ 2.9	+	+ 2
	223.6	+ 0.5	+ 10	+ 4
	204.0	− 1.7	− 11	− 10
198	208.2	− 1.0	− 6	− 2
	238.1	+ 2.5	− 14	− 7
	2[illegible].0	+ 2.1	− 16	− 13
199	347.6	+ 4.2	0	+ 4
	17.3	+ 1.7	+ 6	+ 6
	47.0	− 1.1	12	− 4
	76.9	− 3.6	0	− 2
	106.9	− 5.1	− 45	− 19
	136.8	− 5.1	− 13	− 10
	156.3	− 4.4	− 3	− 5
200	203.3	− 4.5	+ 3	+ 2
	178.6	+ 4.1	− 8	0
	154.0	+ 3.0	+ 18	+ 8
	129.7	+ 1.4	− 18	+ 2
	104.5	− 0.5	− 6	+ 10
	77.0	− 2.3	+ 3	+ 3
	25.9	− 0.0	0	+ 1
	52.4	− 3.5	− 12	− 5
201	339.1	− 3.2	0	+ 4
	305.8	− 0.4	0	+ 4

193	183.3	− 1.5	− 3	+ 5		272.8	+ 2.6	− 18	+ 4		
	214.2	− 2.1	− 2	− 1		241.7	+ 4.7	+ 20	+ 18		
	242.2	− 2.1	− 16	− 10		212.9	+ 5.5	+ 13	+ 21		
	274.5	− 1.4	− 29	− 16		185.3	+ 5.2	− 5	− 5		
	304.8	− 0.2	4	+ 1		157.0	+ 3.6	+ 26	+ 16		
	325.6	+ 1.0	3	+ 1							
	357.0	+ 1.8	3	+ 1	202	171.3	− 0.9	− 8	− 3		
						147.6	+ 2.5	0	+ 1		
						118.6	+ 5.2	− 6	− 6		
	289.2	+ 6.7	− 1	− 1		307.2	+ 1.1	+ 12	+ 14		
	60.7	+ 6.6	− 16	− 6		331.2	+ 3.7	− 7	+ 15		
	31.4	+ 4.9	− 14	− 10		356.0	+ 5.7	+ 6	+ 12		
	356.7	+ 1.4	− 4	0							
203	265.7	+ 7.7	− 6	− 9	211	355.1	+ 6.0	− 7	− 4		
	233.4	+ 6.4	− 8	− 5		330.0	+ 5.1	− 27	− 3		
	262.9	+ 3.4	− 8	0		304.1	+ 3.2	− 5	− 4		
	301.7	− 1.6	0	+ 5		276.7	+ 0.5	− 17	− 7		
	326.6	− 4.5	− 19	− 9		249.7	− 2.2	− 8	− 6		
	351.8	− 6.5	− 16	− 4		223.2	− 4.3	− 6	− 6		
						195.6	− 5.5	+ 4	− 2		
204	186.4	+ 2.5	+ 11	+ 1	212	199.6	− 4.7	+ 2	+ 4		
	215.5	− 0.8	− 4	− 2		226.4	− 3.1	0	0		
	245.7	− 4.2	− 15	− 13		253.5	− 0.7	− 3	− 5		
	275.6	− 6.3	− 14	− 8		278.5	+ 1.7	− 1	+ 4		
	307.0	− 6.7	− 12	− 12		306.8	+ 4.1	+ 15	+ 7		
	328.1	− 5.0	− 12	− 7		330.0	+ 5.3	− 10	+ 14		
	350.1	− 3.7	− 8	− 6		1.2	+ 5.7	− 4	0		
	259.4	− 5.3	+ 3	− 2		294.2	+ 3.1	+ 1	+ 6		
205	2.3	+ 6.2	− 7	− 1	213	12.4	+ 3.6	− 14	(− 18)		
	335.2	+ 4.5	− 3	+ 4		347.4	+ 1.7	− 6	− 4		
	308.6	+ 1.9	+ 8	+ 9		328.0	+ 5.1	− 15	− 7		
	279.9	+ 0.9	− 7	+ 5		295.7	+ 4.4	− 3	+ 2		
	250.6	− 4.1	+ 6	+ 16		269.9	+ 3.0	− 25	− 3		
	222.1	− 5.8	+ 3	+ 4		244.4	+ 1.0	− 9	− 7		
	193.5	− 6.0	+ 7	+ 2		222.9	− 0.8	− 11	− 13		
						200.1	− 2.6	− 2	− 6		
206	194.6	− 5.8	− 3	− 11							
	221.3	− 5.5	− 12	− 12							
	249.9	− 3.8	− 14	− 6	215	196.4	− 4.3	+ 8	+ 4		
	274.8	− 1.5	− 33	(− 19)		225.9	− 2.4	− 29	− 17		
	301.9	+ 1.4	− 19	− 9		255.8	+ 0.2	− 8	− 4		
	328.1	+ 4.0	− 18	+ 6		285.6	+ 2.9	0	+ 8		
	357.9	+ 5.9	− 14	− 10		314.9	− 4.8	+ 8	0		
						357.4	+ 5.5	− 5	− 4		
207	193.4	− 6.1	+ 31	(+ 27)		1.4	+ 5.4	− 4	+ 2		
	222.9	− 5.6	− 4	− 3							
	252.1	− 3.7	− 2	+ 2	216	334.9	+ 4.9	− 12	− 3		
	281.0	− 0.7	− 17	+ 1		305.3	+ 4.6	+ 3	− 5		

	335.2	+ 4.6	− 16	− 10
	8.0	+ 6.5	0	+ 4
	325.3	+ 4.0	− 22	− 6
208	217.5	− 3.0	+ 9	+ 13
	283.7	− 0.6	+ 8	+ 10
	326.3	+ 5.5	− 11	+ 3
	352.2	+ 5.7	+ 9	+ 15
	17.1	+ 4.9	+ 14	+ 10
	68.4	+ 0.6	+ 11	+ 17
	42.5	+ 3.2	− 24	− 20
209	357.6	+ 4.2	− 1	− 1
	24.2	+ 2.2	− 16	− 9
	50.8	− 0.2	− 14	− 9
	77.2	− 2.4	− 10	− 10
	103.5	− 4.1	− 10	+ 2
	131.0	− 4.9	+ 4	+ 1
	160.7	− 4.1	− 19	0
210	189.1	− 5.9	− 17	+ 3
	218.3	− 6.3	+ 6	+ 8
	249.6	− 4.8	+ 7	+ 15
	278.1	− 2.2	− 7	+ 6
221	250.5	− 6.3	+ 9	+ 5
	0.4	+ 5.8	− 4	− 4
	340.7	+ 3.7	+ 8	+ 6
222	202.5	− 8.3	− 4	+ 2
	224.1	− 8.4	0	+ 1
	253.3	− 6.7	− 4	− 2
	282.6	− 3.1	− 19	+ 1
	341.4	+ 5.5	− 7	− 9
	6.4	+ 7.6	− 12	− 6
223	14.2	+ 6.9	+ 1	0
	349.0	+ 5.1	− 11	− 6
	321.5	+ 2.1	− 15	− 2
	295.4	− 1.2	0	− 4
	271.2	− 3.9	− 8	0
	245.8	− 6.9	+ 9	+ 10
	198.4	− 6.5	+ 5	+ 11
	230.6	− 6.3	− 2	+ 10
224	189.0	− 6.6	14	+ 5
	217.8	− 8.4	0	0
	277.8	− 5.4	− 7	+ 2
	305.8	− 1.4	− 11	− 7
	329.7	+ 2.1	− 28	− 4
	356.4	+ 5.7	+ 4	+ 10

	278.2	+ 2.9	− 5	− 3
	249.9	+ 0.6	0	− 2
	224.3	− 1.6	+ 5	+ 7
	198.9	− 3.4	− 1	+ 1
217	201.3	− 1.9	+ 12	+ 7
	228.0	+ 0.3	+ 3	+ 7
	255.2	+ 2.6	− 2	+ 2
	282.4	+ 4.3	+ 3	+ 13
	309.5	+ 5.1	+ 12	+ 12
	335.6	+ 4.1	+ 6	+ 9
	332.0	+ 5.0	− 12	+ 5
218	167.5	+ 7.5	+ 10	0
	145.4	+ 6.3	+ 3	− 1
	123.4	+ 4.3	+ 4	+ 2
	98.5	+ 1.2	− 6	− 2
	74.4	− 1.9	− 5	− 3
	45.9	− 5.1	− 10	− 4
	12.0	− 7.1	− 10	− 2
221	183.5	− 6.2	− 11	+ 8
	212.9	− 7.5	+ 1	+ 2
	235.8	− 7.5	− 16	− 4
231	172.7	+ 0.2	− 2	+ 3
	145.3	+ 1.3	− 20	− 14
	120.4	+ 2.0	− 14	− 11
	93.1	+ 2.5	− 16	− 12
	66.6	+ 2.5	− 10	− 6
	38.3	+ 1.9	0	0
	9.8	+ 2.0	+ 3	0
232	189.6	+ 5.7	+ 8	− 4
	218.7	+ 7.2	− 20	− 18
	246.6	+ 7.6	+ 5	+ 6
	274.5	+ 5.3	− 11	− 1
	305.0	+ 2.1	− 2	0
	328.1	+ 1.3	− 19	0
	352.2	+ 4.1	− 5	+ 1
233	351.5	− 2.7	− 1	+ 5
	321.0	+ 1.0	− 11	+ 2
	292.1	+ 4.3	+ 6	+ 12
	236.2	+ 7.3	+ 6	+ 8
	211.7	+ 6.6	+ 6	+ 2
	189.4	+ 5.0	+ 9	− 2

226	194.9	− 6.9	− 15	− 19
	223.3	− 8.6	− 17	− 16
	253.6	− 7.8	− 5	− 3
	284.7	− 3.9	− 34	(− 22)
	313.3	+ 0.1	− 13	(− 20)
	339.6	+ 3.8	− 5	− 7
	366.3	+ 5.9	+ 2	+ 8
227	190.4	− 1.4	+ 14	+ 2
	247.2	− 1.4	− 7	− 7
	277.0	− 0.8	− 11	− 6
	307.0	+ 0.2	+ 2	+ 6
	335.4	+ 1.6	− 1	+ 3
	366.6	+ 1.1	− 15	− 6
228	267.4	+ 1.7	− 2	+ 1
	237.5	+ 8.8	− 3	− 4
	209.8	+ 9.2	− 4	− 10
	184.5	+ 8.0	+ 15	+ 2
	161.6	+ 5.5	+ 17	+ 3
229	181.8	+ 6.8	+ 18	+ 1
	161.8	+ 4.9	+ 23	+ 14
	140.3	+ 2.2	+ 7	+ 16
	116.1	− 1.1	+ 2	+ 12
	89.6	− 4.4	+ 5	+ 2
	71.8	− 7.1	+ 1	+ 8
	52.2	− 7.3	+ 5	+ 10
230	3.3	− 2.6	0	+ 2
	33.0	− 2.1	− 6	− 4
	59.1	− 1.2	− 7	+ 3
	86.3	+ 0.1	+ 5	+ 1
	108.7	+ 1.3	− 14	− 4
	134.2	+ 2.3	+ 4	+ 2
	162.8	+ 3.1	+ 12	+ 10
	186.3	+ 2.7	− 1	+ 2
239	355°7	+ 4°8	− 20	− 16
	330.3	+ 1.3	− 28	− 4
	301.2	− 2.6	− 14	− 11
	271.3	− 6.0	− 27	− 18
	241.2	− 7.7	− 22	− 11
	216.0	− 7.5	− 12	− 12
	189.5	− 6.7	− 15	− 9

234	354.5	+ 1.6	− 9	− 4
	325.7	+ 2.6	− 32	− 13
	296.9	+ 4.0	− 4	+ 1
	268.5	+ 2.8	− 21	0
	241.2	+ 2.1	− 4	− 2
	213.2	+ 0.7	− 7	− 4
	131.2	− 0.7	− 2	+ 1
235	190.7	− 0.3	+ 16	0
	217.1	+ 1.1	+ 1	+ 1
	244.4	+ 2.3	+ 4	+ 5
	272.3	+ 3.1	− 20	+ 2
	300.8	+ 3.2	− 1	+ 5
	329.2	+ 2.7	− 22	+ 2
	356.6	+ 1.5	− 4	0
236	355.2	+ 2.8	+ 3	+ 5
	327.0	+ 2.9	− 12	+ 12
	298.6	+ 2.3	− 1	+ 5
	270.1	+ 1.2	− 12	+ 9
	241.9	− 0.1	+ 9	+ 12
	216.8	− 1.2	+ 16	+ 19
	185.8	− 2.1	+ 2	+ 12
237	214.3	− 1.4	− 10	− 7
	245.6	+ 0.1	− 10	− 9
	271.6	+ 1.4	− 38	− 17
	300.9	+ 2.6	− 18	− 9
	329.7	+ 3.1	− 42	− 18
	356.7	+ 3.0	− 14	− 11
238	264.2	+ 4.9	+ 6	(+ 24)
	300.5	− 3.0	+ 14	+ 13
	333.7	− 0.5	+ 1	+ 14
	6.0	+ 2.2	+ 8	+ 8
	35.9	+ 4.0	+ 12	+ 11
	63.4	+ 4.9	+ 9	+ 14
	89.1	+ 4.8	+ 18	(+ 18)
	270°6	+ 0°6	− 23	− 4
	299.1	+ 3.4	− 13	− 6
	327.2	+ 5.3	− 38	(− 20)
	356.9	+ 6.1	+ 7	+ 13

241	352.5	− 1.2	− 8	− 3
	323.9	− 3.1	− 4	+ 5
	294.4	− 4.2	− 6	− 3
	264.9	− 4.1	0	− 7
	226.3	− 3.0	− 17	− 1
	198.9	+ 0.5	+ 10	0
	211.3	− 1.3	+ 12	+ 12
243	239.7	− 2.4	− 8	+ 4
	272.2	+ 0.9	− 23	− 4
	304.1	+ 3.8	+ 1	+ 1
	334.7	+ 5.7	− 13	− 4
	4.8	+ 6.0	− 1	+ 7
	32.8	+ 5.0	− 9	− 5
	60.1	+ 2.9	− 2	+ 4
244	185.8	− 5.6	− 21	− 12
	211.2	− 4.1	− 24	(− 24)
	237.0	− 1.6	− 23	− 7
	263.3	+ 1.3	− 22	− 11
	290.6	+ 4.0	− 6	+ 1
	317.9	+ 5.9	0	− 2
	356.7	+ 6.4	− 11	− 7
246	157.6	+ 6.0	− 1	− 13
	214.3	− 4.3	− 2	0
	242.3	− 2.2	+ 1	+ 6

247	135.8	− 6.4	− 10	− 12
	110.5	− 5.7	− 31	− 5
	85.7	− 3.8	− 18	(− 22)
	61.3	− 1.3	− 28	(− 21)
	37.2	+ 1.5	− 16	− 14
	17.9	+ 3.6	− 10	− 14
	354.5	+ 5.6	− 22	(− 22)
248	355.6	+ 4.6	− 3	0
	22.6	+ 2.0	− 7	− 1
	49.7	− 1.1	0	+ 1
	77.0	− 3.9	− 15	− 13
	106.2	− 5.8	− 23	+ 3
	133.4	− 6.2	− 1	− 4
	161.2	− 5.2	− 15	− 8
249	349.5	− 1.6	− 4	0
	325.3	− 2.1	− 10	0
	298.4	− 2.0	+ 1	
	276.9	− 1.0	− 6	+ 2
	247.9	− 0.6	+ 9	+ 9
	222.9	+ 0.3	+ 8	+ 2
	212.2	+ 0.8	0	− 1
250	185.4	+ 3.3	+ 11	+ 11
	211.4	+ 1.7	+ 5	+ 7
	235.6	− 0.2	− 10	+ 2
	261.2	− 2.2	+ 14	+ 7
	288.3	− 3.8	− 5	+ 1
	315.5	− 4.4	+ 16	+ 8
	350.0	− 3.8	− 34	(− 23)

Table 22

Bel'kovich's Observations

№№ набл.	P	D	II	$II - II'$
6	208°6	− 19.1	− 3	− 4
	249.3	+ 3.3	− 6	− 1
	256.4	+ 6.9	− 2	+ 2
	262.3	+ 9.1	− 11	− 6
	268.2	+ 9.5	− 5	− 1
	334.0	+ 8.2	− 12	− 5
	355.0	+ 3.9	− 1	+ 2
7	354.6	+ 5.7	− 3	− 2
	329.6	+ 8.4	− 13	− 3
	322.7	+ 9.6	+ 1	+ 1
	275.8	+ 9.0	+ 6	0
	254.9	+ 6.9	+ 1	0
	223.8	+ 3.4	− 3	− 4
	264.3	− 0.7	− 4	− 1
8	354.3	+ 4.9	− 3	− 5
	328.8	+ 7.5	− 14	+ 1
	303.5	+ 8.6	− 1	− 1
	278.3	+ 8.3	+ 2	+ 1
	253.2	+ 6.4	+ 4	+ 3
	228.1	+ 3.3	+ 2	+ 0
	202.7	− 0.4	+ 4	+ 5
9	346.1	+ 2.9	− 2	+ 2
	320.0	+ 5.6	− 26	− 3
	294.0	+ 7.2	− 3	− 4
	268.3	+ 7.4	+ 2	0
	242.3	+ 6.2	+ 6	− 3
	217.9	+ 3.9	− 3	0
	198.3	+ 0.3	+ 10	+ 1
11	159.2	+ 2.7	− 2	− 3
	135.9	+ 4.2	− 7	− 6
	113.6	+ 5.0	− 4	− 3
	91.4	+ 5.1	− 16	− 6
	68.2	+ 4.4	− 18	− 8
	43.3	+ 3.0	− 30	(− 26)
	16.2	+ 0.9	− 1	− 1

12	5.5	+ 2.6	+ 5	+ 6
	33.2	+ 3.6	+ 2	+ 5
	59.2	+ 3.8	+ 1	+ 6
	83.8	+ 3.4	+ 10	+ 11
	107.8	+ 2.4	− 1	+ 2
	132.3	+ 1.0	+ 10	+ 8
	154.8	− 0.4	+ 23	+ 2
13	1.4	+ 0.7	0	+ 2
	29.2	+ 2.4	− 4	+ 3
	55.8	+ 3.6	− 9	− 4
	81.6	+ 4.1	− 6	− 2
	108.4	+ 3.9	+ 10	+ 4
	129.0	+ 3.0	+ 22	+ 2
	153.5	+ 1.7	+ 15	+ 5
14	3.1	+ 3.5	− 2	+ 4
	31.5	+ 3.9	− 3	0
	58.3	+ 3.4	− 4	− 1
	84.1	+ 2.4	+ 3	+ 4
	111.0	+ 0.8	− 7	+ 2
	135.8	− 0.7	+ 2	+ 1
	162.0	− 2.2	− 14	+ 1
15	2.1	+ 4.4	− 6	+ 2
	29.2	+ 4.3	− 7	− 3
	55.0	+ 3.3	− 16	0
	85.2	+ 1.8	+ 3	+ 4
	105.3	− 0.1	− 16	+ 1
	131.0	− 1.9	+ 1	− 1
	161.8	− 3.4	− 20	0
16	170.0	− 0.3	− 11	+ 1
	144.2	+ 1.3	− 8	− 1
	119.7	+ 2.5	− 1	+ 2
	95.9	+ 3.5	+ 11	+ 4
	71.8	+ 3.9	− 6	0
	49.2	+ 2.5	0	+ 3
	353.4	+ 1.1	0	+ 6
17	189.0	+ 1.6	+ 9	− 3
	219.8	− 1.7	+ 4	+ 6
	252.6	− 4.8	− 1	+ 2
	285.7	− 6.2	− 7	+ 1
	322.7	− 5.2	− 6	− 2
	352.4	− 2.8	− 3	+ 3

18	352.1	− 1.2	−	8	−	3	
	321.0	− 3.6	−	2	−	2	
	288.8	− 4.9	−	8	−	2	
	256.7	− 4.6	+	3	+	1	
	225.9	− 3.0	−	5	+	3	
	197.3	− 0.6		0	−	2	
	168.6	+ 0.2	+	8		0	
19	345.4	+ 2.9	−	5	−	3	
	325.4	+ 0.6	−	9	+	4	
	293.9	− 1.9	+	12	+	9	
	261.6	− 3.6	+	14	+	9	
	229.6	− 4.4	+	2	+	6	
	198.4	− 3.2	−	12	+	1	
20	151.5	− 5.9	−	9	+	2	
	132.9	− 6.2	+	5	+	2	
	104.6	− 4.9	+	8	+	11	
	77.5	− 2.5	+	9	+	9	
	50.5	+ 0.5	+	2	+	4	
	23.7	+ 3.4	−	1	+	5	
	351.5	+ 5.8	+	7	+	7	
21	198.7	− 5.9	−	13	+	7	
	218.1	− 4.6	+	3	+	7	
	247.9	− 2.1	+	5	+	7	
	277.3	+ 1.0	−	1	−	9	
	305.1	+ 3.3	+	10	+	3	
	333.8	+ 5.8	+	2	+	3	
	0.4	+ 6.4	+	8	+	7	
22	0.2	+ 6.4	+	3	+	2	
	333.6	+ 5.9	−	11	−	1	
	305.8	+ 4.1	+	9	+	3	
	277.1	+ 1.3	+	0	+	6	
	247.6	− 1.9	−	6	−	6	
	218.2	− 4.5	+	1	+	5	
	189.0	− 5.8	−	14	+	6	
23	193	+ 6.0	−	12	−	0	
	336.9	+ 6.5	−	11	−	5	
	309.9	+ 5.8	−	6	−	4	
	283.2	+ 4.0	−	15	−	4	
	256.6	+ 1.3	−	12	−	8	
	228.6	− 1.7	−	12	−	7	
	201.1	− 4.2	−	1	−	3	

24	356.3	+ 6.4	− 2	+ 4
	330.0	+ 6.9	− 13	+ 3
	302.9	+ 6.0	− 6	− 2
	275.2	+ 3.7	− 6	+ 7
	247.1	+ 0.6	0	+ 1
	218.7	− 2.6	− 4	− 1
	190.2	− 5.2	− 13	0
25	356.9	+ 3.9	0	− 2
	329.1	+ 6.3	− 18	+ 5
	301.3	+ 7.3	− 5	− 1
	273.6	+ 6.6	− 5	0
	246.0	+ 4.6	− 10	− 4
	218.5	+ 1.6	− 3	+ 1
	190.9	− 1.8	+ 10	+ 3
26	186.2	+ 3.5	0	0
	212.4	+ 5.5	− 2	− 5
	239.5	+ 6.4	+ 2	− 3
	267.9	+ 6.0	− 26	− 4
	297.6	+ 4.0	− 3	+ 3
	328.5	+ 0.9	− 17	+ 3
27	182.9	+ 7.2	+ 20	0
	159.8	+ 6.2	− 4	+ 1
	137.0	+ 4.3	+ 2	+ 4
	113.0	+ 1.6	− 5	− 1
	87.9	− 1.6	− 1	− 5
	56.2	− 4.6	− 12	− 4
	27.1	− 6.5	− 3	+ 1
28	196.0	− 1.4	+ 4	+ 7
	223.6	− 0.6	+ 4	+ 2
	252.0	+ 0.5	+ 14	+ 5
	281.9	+ 1.6	− 5	+ 3
	311.0	+ 2.3	+ 7	+ 3
	339.6	+ 2.[illegible]	− 4	− 2
	359.8	+ 2.3	− 1	+ 2
29	359.6	+ 2.2	− 7	− 1
	332.3	+ 2.5	− 13	+ 4
	304.7	+ 2.2	− 4	− 1
	276.8	+ 1.6	− 8	+ 1
	249.0	+ 0.6	[illegible]	3
	221.8	− 0.5	+ [illegible]	+ 5
	195.3	1.3	0	− 1
30	357.8	− 0.2	− 1	+ 4
	328.8	+ 1.2	− 17	+ 6
	299.8	+ 2.3	+ 3	+ 13
	271.1	+ 3.0	− 17	+ 5
	243.1	+ 2.9	− 3	+ 1
	216.2	+ 2.3	+ 15	+ 11
	187.7	+ 1.6	+ 16	+ 1
31	189°.3	+ 0°.7	+ 10	− 3
	216.5	+ 1.7	+ 2	− 1
	244.7	+ 2.4	+ 4	+ 4
	273.9	+ 2.6	− 19	0
	303.6	+ 2.2	− 2	+ 2
	333.6	+ 1.3	− 6	+ 7
	356.5	+ 0.3	− 7	− 1
32	356.3	+ 0.3	− 8	− 2
	327.5	+ 1.5	− 19	− 1
	298.5	+ 2.4	− 4	+ 2
	269.9	+ 2.8	− 22	0
	241.9	+ 2.6	+ 1	+ 1
	214.9	+ 1.8	+ 2	+ 2
	188.5	+ 0.6	+ 8	− 1
33	355.0	− 1.3	− 9	− 4
	325.6	+ 0.9	− 16	− 1
	296.6	+ 3.0	− 6	0
	268.4	+ 4.3	− 19	+ 3
	241.2	+ 4.7	0	− 5
	215.1	+ 4.2	0	0
35	189.9	+ 2.3	+ 8	− 8
	214.3	+ 3.5	0	0
	239.5	+ 4.2	− 2	− 4
	265.7	+ 4.1	− 22	0
	292.8	+ 3.2	− 5	− 3
	320.6	+ 1.6	− 17	− 6
	353.7	− 0.7	0	+ 6
36	349.9	− 0.6	− 6	+ 1
	321.8	+ 1.5	− 3	+ 15
	294.1	+ 3.3	− 7	− 1
	266.9	+ 4.4	− 17	+ 5
	240.8	+ 4.5	+ 10	+ 6
	215.7	+ 3.9	+ 8	+ 5
	189.6	+ 2.4	+ 9	− 5

37	352.7	−3.2	−10	−4
	321.7	+0.8	−19	−1
	291.7	+4.4	−8	−2
	263.2	+6.9	−11	−4
	236.2	−7.7	−7	−7
	210.8	+7.1	−1	−5
	186.3	+5.2	−8	10
38	187.6	+8.4	+15	+1
	211.1	+9.6	+2	−4
	236.0	+9.2	−2	−4
	263.0	+7.6	−5	+2
	323.2	2.2	−15	−5
	345.7	−5.6	−10	+2
39	2.5	+0.6	7	−2
	29.2	+2.4	−15	−10
	54.1	+3.6	−27	−7
	77.3	+4.2	−11	−3
	99.4	+4.2	−21	−15
	121.2	+3.7	−18	−12
	161.0	+1.4	−7	−6
40	171.5	+2.7	−20	−9
	146.3	+3.0	−5	−2
	121.5	+2.7	−6	−1
	96.3	+2.0	−9	−7
	69.8	+0.9	−9	−4
	41.5	−0.4	−10	−7
	6.8	−1.8	−4	0
41	353.0	−0.6	−7	−1
	323.6	+0.4	−9	+1
	294.1	+1.3	−5	−3
	264.9	+2.0	−30	−10
	235.6	+2.2	−11	0
	209.8	+2.0	−6	−2
	184.1	+1.4	+9	+2
42	188.2	+1.4	0	−9
	214.2	+2.0	−9	−8
	241.4	+2.2	−7	−7
	269.8	+2.0	−33	−12
	299.0	+1.3	−9	−5
	328.6	+0.4	−24	−4
	352.7	−0.4	−11	−4
43	355.6	+1.0	−6	−1
	325.7	+0.9	−14	+1
	297.1	+0.7	+8	+7
	267.5	+0.3	−16	−1
	238.4	0.0	−1	+10
	210.4	−0.3	+9	+10
	186.4	−0.4	+5	−2
44	185.5	−0.6	−13	−8
	212.4	−0.4	+2	+3
	240.6	0.0	−11	−6
	269.7	+0.4	−27	−8
	299.2	+0.8	−5	−2
	329.7	+1.1	−21	+1
	356.8	+1.1	−10	−6
45	1.2	+6.3	−11	−8
	331.5	+2.9	−29	+1
	303.6	−1.0	−9	−2
	272.2	−5.0	−13	−5
	240.0	−7.5	−10	+2
	208.2	−7.6	−6	0
	197.6	−7.1	−6	0
46	195.0	−6.9	0	−8
	223.9	−7.7	−3	−2
	253.6	−6.6	+8	+9
	283.1	−3.6	−25	−8
	311.7	+0.2	−9	−10
	339.8	+3.9	−6	−4
	4.0	+6.6	−10	−4
47	1.7	+6.4	−16	−11
	336.2	+3.6	−19	−15
	309.0	−0.1	−6	−3
	280.3	−3.9	−23	−7
	250.6	−6.7	−11	−9
	221.1	−7.7	−3	−3
	192.9	−6.7	−17	−12
48	189.3	−6.9	−25	−5
	222.0	−8.8	−9	−9
	256.0	−7.8	+1	+1
	289.7	−4.1	−20	−14
	321.8	+0.9	−22	−4
	355.8	+5.9	−17	−12

49	189.3	+ 0.9	+ 9	− 4
	217.7	− 0.8	+ 6	+ 8
	248.2	− 2.3	− 2	0
	280.2	− 3.1	− 11	+ 6
	312.6	− 2.8	− 3	− 3
	344.6	− 1.7	− 8	− 2
	354.6	− 1.2	+ 2	+ 7
50	352.5	− 1.3	− 6	− 1
	324.3	− 2.5	− 22	− 12
	295.3	− 3.0	− 8	− 7
	266.4	− 2.7	− 6	− 15
	238.3	− 1.6	− 13	0
	211.7	− 0.3	− 2	− 1
	197.8	+ 0.5	+ 4	− 4
51	15.7	− 7.8	− 6	0
	47.1	− 7.6	− 3	− 1
	77.9	− 5.3	− 7	− 2
	106.0	− 1.7	− 26	− 5
	131.6	+ 2.0	+ 6	− 1
	155.3	+ 5.1	+ 16	+ 2
	193.8	+ 8.2	+ 14	+ 1
52	195.2	+ 8.4	+ 19	+ 2
	169.6	+ 6.7	+ 17	+ 11
	144.0	+ 3.7	+ 5	+ 4
	116.7	− 0.3	0	+ 6
	88.6	− 4.4	+ 5	+ 4
	52.0	− 7.6	− 5	0
	17.2	− 7.9	− 1	+ 4
53	189.4	+ 6.5	+ 10	− 7
	213.5	+ 6.3	+ 7	+ 4
	239.5	+ 4.9	+ 6	0
	267.5	+ 2.3	− 24	− 4
	297.3	− 1.6	+ 4	0
	328.4	− 4.0	− 16	0
	345.3	− 5.2	− 9	+ 3
55	189.6	+ 8.1	+ 20	+ 1
	167.7	+ 6.4	+ 10	+ 3
	145.2	+ 3.6	− 4	− 5
	121.7	+ 0.2	− 5	+ 1
	96.0	− 3.5	− 6	− 2
	67.8	− 6.7	− 8	0
	37.1	− 8.2	− 2	+ 2

56	350.9	− 4.6	− 1	+11
	319.4	− 3.4	+ 8	+ 3
	293.3	− 1.2	+ 5	+ 3
	265.4	+ 1.4	+ 12	+ 3
	240.3	+ 3.6	+ 3	+13
	214.3	+ 4.9	+ 7	+ 5
57	193.5	+ 2.0	+ 4	+ 5
	221.9	+ 4.0	+ 2	+ 4
	251.1	+ 5.1	+ 8	− 1
	281.5	+ 5.0	− 4	+ 4
	312.8	+ 3.5	− 4	−11
	344.4	+ 1.0	+ 6	+12
	355.4	+ 0.1	− 10	− 4
58	349.0	+ 0.8	− 7	+ 1
	320.4	+ 3.1	− 16	− 7
	292.2	+ 4.8	− 1	+ 5
	264.5	+ 5.3	− 17	+ 1
	239.0	+ 4.8	− 4	− 4
	213.2	+ 3.3	− 4	− 2
	189.9	+ 1.3	+ 13	+ 5
59	2.0	+ 3.7	− 2	+ 5
	27.6	+ 6.2	− 9	− 5
	51.8	+ 5.6	− 15	− 2
	75.2	+ 4.2	+ 4	+ 4
	98.5	+ 2.1	− 1	+ 4
	122.5	− 0.4	− 3	+ 1
	156.0	− 3.5	− 2	− 8
60	154.7	− 3.5	+ 16	+ 3
	127.8	− 1.0	+ 14	+ 1
	102.6	+ 1.6	− 6	+ 2
	78.3	+ 3.8	− 2	+ 2
	54.1	+ 5.5	− 13	+ 1
	29.0	+ 6.2	− 9	− 5
	2.6	+ 5.8	− 2	+ 6
61	3.0	+ 6.4	+ 5	+11
	29.3	+ 7.5	+ 4	+ 8
	53.8	+ 7.4	+ 1	+10
	77.2	+ 6.0	+ 5	+10
	100.5	+ 3.6	+ 15	+10
	124.9	+ 0.6	+ 24	(+22)
	151.3	− 2.8	+ 26	+ 9

62	283.4	− 0.1	−	1	+	1			
	231.2	+ 2.2	−	1	+	5			
	259.4	+ 4.1	+	9	+	2			
	288.0	+ 5.0	−	2	+	9			
	316.7	+ 4.9	+	15	+	9			
	345.4	+ 3.6	+	2	+	1			
	358.6	+ 2.7	−	3	+	0			
63	261.6	− 0.3	+	8	+	2			
	290.8	+ 2.2	+	2	+	5			
	319.3	+ 4.1	−	6	−	3			
	347.0	+ 5.1	−	5	−	2			
	13.4	+ 5.1	+	4	−	1			
	38.8	+ 4.1	−	6	−	4			
64	2.1	+ 6.2	−	8	−	2			
	30.4	+ 8.2	−	8	+	2			
	56.2	+ 8.5	−	7	+	2			
	80.6	+ 7.2	−	12	−	2			
	105.0	+ 4.7	+	11	+	1			
	130.9	+ 1.1	+	3	−	6			
	158.3	− 3.0	+	14	−	6			
65	155.9	− 0.1	+	7	−	3			
	129.7	+ 4.0	+	12	−	3			
	106.0	+ 7.1	−	0	+	2			
	83.4	+ 8.9	−	12	−	2			
	60.5	+ 9.4	−	13	−	0			
	35.8	+ 8.4	−	8	−	2			
	2.8	+ 4.5	−	10	−	2			
66	6.4	+ 5.3	−	11	−	5			
	34.0	+ 8.3	−	13	−	7			
	58.9	+ 9.4	−	17	−	1			
	82.0	+ 9.0	−	13	−	3			
	104.6	+ 7.2	−	7	−	3			
	126.2	+ 4.2	+	10	−	0			
	134.2	+ 0.1	+	6	+	4			
67	191.0	− 2.1	+	14	+	10			
	216.0	+ 0.5	+	4	+	5			
	245.1	+ 3.1	+	6	+	6			
	272.3	+ 5.1	−	16	−	11			
	299.7	+ 6.0	+	6	+	10			
	327.1	+ 5.6	−	17		0			
	354.2	+ 4.1		0	−	2			

68	352.3	+ 4.3	− 6	0
	325.2	+ 5.8	− 16	− 4
	297.9	+ 6.0	− 6	0
	270.6	+ 5.0	− 19	+ 3
	243.4	+ 2.9	− 5	− 3
	216.3	+ 0.3	+ 6	+ 7
	195.1	− 1.9	+ 6	+ 3
69	180.0	− 1.6	+ 15	+ 4
	152.1	+ 2.2	− 19	(−24)
	106.7	+ 5.2	− 17	− 13
	82.5	+ 7.2	− 29	(−19)
	58.0	− 8.0	− 30	− 16
	22.5	+ 6.6	− 10	− 8
70	346.6	+ 4.3	− 5	− 2
	321.4	+ 5.7	− 18	− 3
	296.1	+ 6.0	− 8	− 5
	270.8	+ 5.2	− 25	− 3
	245.7	+ 3.5	− 8	− 7
	220.8	+ 1.2	− 4	− 2
	196.0	− 1.2	− 6	− 2
71	192.9	− 1.6	+ 16	− 0
	218.7	+ 1.0	− 7	− 5
	244.6	+ 3.5	− 2	− 3
	270.7	+ 5.3	− 26	− 4
	296.9	+ 6.1	− 7	− 3
	323.2	+ 5.7	− 12	− 3
72	335.7	+ 5.9	+ 2	+ 6
	331.1	+ 6.3	− 14	+ 5
	305.9	+ 5.6	+ 8	+ 1
	280.1	+ 3.8	− 3	− 1
	254.1	+ 1.3	− 1	− 2
	227.9	− 1.5	− 5	− 2
	201.6	− 3.9	+ 4	+ 4
73	196.5	− 5.4	− 8	− 2
	228.9	− 5.8	− 12	− 9
	260.2	− 4.5	+ 4	− 1
	291.4	− 1.8	− 8	− 4
	321.4	+ 1.4	− 19	− 2
	350.2	+ 4.2	− 9	− 2
	358.4	+ 4.8	− 13	−10

74	352.8	+ 1.9	0	+ 6
	326.5	− 0.9	− 1	− 9
	298.7	− 3.6	+ 3	+ 3
	270.2	− 5.4	+ 15	+ 16
	241.7	− 5.9	+ 7	+ 14
	214.2	− 4.9	+ 4	+ 6
	189.0	− 3.0	+ 6	+ 17
76	21.3	− 4.2	− 6	− 4
	53.5	− 1.8	− 13	− 4
	82.5	+ 2.3	− 4	− 1
	108.6	+ 4.8	+ 2	+ 3
	132.9	+ 6.2	+ 8	+ 2
	157.0	+ 6.7	+ 2	0
	182.8	+ 5.9	+ 27	+ 3
77	177.9	+ 6.2	+ 1	− 4
	153.4	+ 6.7	+ 19	+ 11
	130.2	+ 6.0	+ 19	+ 6
	105.6	+ 4.5	+ 3	+ 7
	81.2	+ 2.0	+ 2	+ 3
	53.0	− 1.2	− 7	+ 2
	21.7	− 4.2	+ 1	+ 3
78	357.3	− 3.4	− 4	0
	327.6	− 6.0	− 14	− 3
	296.8	− 7.0	− 2	− 3
	266.0	− 6.0	+ 2	− 2
	236.7	− 3.3	− 19	− 4
	209.3	0.0	+ 1	+ 4
	184.5	+ 3.1	+ 14	+ 3
79	187.4	+ 2.9	+ 8	0
	212.5	− 0.2	− 4	− 3
	240.1	− 3.5	− 12	− 1
	269.6	− 6.0	− 8	− 4
	300.4	− 6.9	− 10	− 10
	331.0	− 5.8	− 25	− 9
	358.0	− 3.4	− 2	+ 2
80	359.2	− 3.3	− 3	0
	328.4	− 5.9	− 24	− 9
	298.8	− 5.8	− 1	− 5
	268.0	− 5.9	− 15	− 16
	238.6	− 3.3	− 12	+ 2
	211.3	0.0	− 8	− 3

81	353.7	−5.0	−5	+2
	323.5	−6.8	−9	−1
	292.6	−6.7	−10	−2
	263.3	−4.8	−1	−3
	233.6	−1.5	−12	−1
	207.1	+1.8	−2	+2
	183.2	+4.6	+26	+2
82	18676	+4.4	+5	0
	210.9	+1.5	0	+2
	237.7	−1.8	−12	+2
	266.6	−4.9	+9	+2
	297.1	−6.7	+2	+11
	327.9	−6.6	−10	−1
	353.9	−5.0	−5	+2
83	62.7	−4.1	−3	+4
	92.8	−0.7	+4	0
	119.9	+2.6	+1	+4
	145.0	+5.2	+10	+7
	169.5	+6.3	+4	0
	194.7	+7.2	+16	+2
84	351.4	−7.6	−12	−1
	316.3	−7.1	+10	+5
	287.6	−4.6	−14	−7
	263.5	−1.6	+3	+6
	237.6	+2.1	+1	+10
	213.8	+5.1	−1	−2
	192.1	+7.1	+22	+3
85	179.5	+6.3	+20	(+23)
	199.3	+6.7	+18	+4
	220.3	+6.3	+17	+19
	242.7	+5.0	+12	+13
	266.7	+2.9	−10	+12
	291.9	0.0	+12	+11
	318.1	−2.8	+16	+7
	342.6	−4.9	0	+8
86	359.4	+5.0	+2	0
	27.4	+2.3	−13	−5
	55.5	−0.9	−6	0
	83.9	−3.8	+6	+2
	112.9	−5.8	−27	−4
	142.3	−6.2	−9	−3
	172.0	−5.0	−24	−2

87	169.6	− 5.2	− 15	+ 6
	140.5	− 6.4	− 12	− 2
	111.5	− 5.8	− 29	− 3
	83.1	− 3.8	− 4	− 7
	55.2	− 0.9	− 10	− 4
	27.6	+ 2.3	− 9	− 1
	0.0	+ 5.0	− 1	− 1
88	346.6	− 5.6	− 5	+ 7
	319.3	− 3.4	+ 3	+ 0
	290.7	− 0.2	+ 3	+ 2
	263.1	+ 2.9	− 4	+ 3
	237.1	+ 5.3	+ 1	+ 4
89	353.2	+ 2.2	− 1	+ 5
	322.4	+ 4.7	− 10	0
	291.8	+ 6.0	+ 3	+ 9
	261.6	+ 5.7	− 1	− 1
	232.1	+ 4.0	+ 3	+ 6
	203.2	+ 1.3	− 6	− 2
	180.6	− 0.1	+ 7	− 1
90	190.5	0.0	+ 29	+ 12
	216.4	+ 2.6	+ 12	+ 8
	242.6	+ 4.8	+ 14	+ 16
	269.3	+ 6.0	− 9	+ 15
	295.6	+ 6.0	+ 7	+ 10
	324.1	+ 4.8	+ 5	+ 14
	351.8	+ 2.4	+ 5	+ 12
91	4.4	+ 6.0	0	+ 8
	30.7	+ 5.1	− 1	+ 3
	56.2	+ 3.3	− 2	+ 3
	81.4	+ 0.9	+ 9	+ 8
	107.1	− 1.6	− 15	− 13
	133.8	− 3.9	+ 7	+ 5
	151.9	− 5.3	− 12	+ 1
92	160.3	− 5.3	+ 4	+ 1
	132.2	− 3.8	+ 1	− 1
	105.6	− 1.5	− 18	+ 3
	79.9	+ 1.0	+ 4	+ 2
	54.7	+ 3.4	− 10	+ 10
	29.1	+ 5.2	+ 4	+ 7
	2.6	+ 6.1	− 9	− 3

93	3.4	+ 6.1	− 7	+ 1
	29.8	+ 5.2	− 10	− 7
	55.2	+ 3.4	− 8	+ 5
	80.5	+ 1.0	+ 3	+ 1
	106.2	− 1.6	− 26	− 5
	132.9	− 4.0	+ 1	− 1
	161.0	− 5.4	− 9	− 6
94	191.3	− 1.3	+ 3	− 9
	218.5	+ 2.5	− 17	− 13
	245.5	+ 5.8	− 16	− 10
	272.6	+ 7.9	− 20	− 14
	299.9	+ 8.3	− 12	− 8
	327.3	+ 6.9	− 27	− 10
	355.0	+ 4.0	− 16	− 14
95	193.9	− 3.7	+ 20	+ 6
	222.5	+ 0.2	+ 12	+ 7
	250.6	+ 3.9	+ 3	− 5
	278.5	+ 6.9	+ 6	+ 2
	306.0	+ 8.2	+ 5	+ 3
	333.3	+ 7.7	− 2	+ 7
	6.3	+ 5.7	+ 2	+ 2
96	9.7	− 0.8	+ 3	+ 2
	40.3	+ 2.7	+ 2	+ 4
	68.7	+ 5.3	− 8	+ 2
	94.0	+ 6.7	− 7	− 2
	117.5	+ 6.8	0	0
	141.7	+ 5.9	+ 1	− 4
	167.3	+ 3.8	− 10	− 6
97	168.9	+ 3.6	+ 4	+ 15
	143.2	+ 5.8	+ 7	0
	127.1	+ 6.6	+ 9	+ 4
	95.4	+ 6.7	+ 5	+ 8
	70.3	+ 5.4	+ 5	+ 10
	42.6	+ 2.9	− 5	− 1
	11.6	− 0.6	+ 1	+ 4
98	192°8	− 3°3	+ 11	+ 3
	223.1	− 1.8	+ 2	+ 4
	253.9	+ 0.3	− 1	0
	284.8	+ 2.4	− 1	+ 5
	315.4	+ 3.9	+ 4	− 4
	345.2	+ 4.4	+ 2	0

99	332.2	−4.0	− 4	+ 4
	323.9	−5.1	+ 4	+ 2
	295.0	−4.9	0	+ 4
	266.6	−3.4	+ 8	0
	239.4	−1.2	− 7	+ 4
	214.0	+1.2	+10	+11
	190.4	+3.2	+10	− 3
100	187.6	+6.9	+16	0
	163.2	+8.5	− 5	− 6
	140.6	+8.8	+ 5	− 1
	118.4	+7.8	− 2	− 2
	95.6	+5.6	− 9	− 5
	69.0	+2.0	− 9	− 3
	39.5	−2.4	− 11	− 8
101	345.9	−5.7	− 8	+ 4
	319.6	−6.9	− 4	− 3
	292.8	−6.6	− 5	+ 3
	266.0	−4.9	+ 7	0
	240.5	−2.1	− 3	+ 6
	216.6	+0.9	+ 11	+11
	194.7	+3.5	+ 12	+ [illegible]
102	191.7	+4.0	+ 11	0
	213.4	+1.4	− 4	0
	237.0	−1.6	−18	− 2
	262.2	−4.4	+ 6	+ 1
	288.8	−6.4	− 9	− 1
	316.0	−7.0	− 6	−12
	342.8	−6.0	− 12	− 3
103	89.8	+3.9	−26	(−23)
	114.2	+6.6	−11	− 9
	136.9	+8.0	− 6	− 4
	152.4	+8.2	−14	− 5
	183.4	+7.2	+12	− 8
	210.0	+4.5	0	− 2
	240.9	+0.5	− 1	+ 2
104	284.1	−2.5	− 6	− 1
	232.0	+1.9	− 7	0
	203.0	+5.5	+ 3	+ 2
	177.2	+7.6	+ 12	+ 9
	153.8	+8.2	+ 8	+ 7
	131.3	+7.6	+16	+ 2
	104.2	+5.9	+ 7	+ 2

105	22.1	— 4.3	— 5	— 2
	32.3	— 1.6	— 4	+ 4
	79.8	+ 1.2	— 7	— 5
	104.8	+ 3.7	+ 2	+ 3
	126.0	+ 5.4	+ 15	+ 3
	150.6	+ 6.2	+ 15	+ 4
	173.7	+ 6.2	— 5	— 1
106	15.5	— 4.1	— 8	— 2
	46.0	— 2.6	— 4	+ 4
	74.3	— 0.5	— 5	— 2
	100.3	+ 1.7	+ 1	0
	124.4	+ 3.4	+ 6	+ 2
	147.7	+ 4.6	+ 10	+ 6
	164.8	+ 5.0	+ 9	— 2
107	339.0	— 8.5	— 7	— 2
	314.8	— 9.2	— 1	— 3
	290.5	— 8.3	— 7	+ 8
	266.8	— 6.0	+ 12	+ 7
	244.3	— 2.7	+ 9	+ 12
	223.2	+ 0.7	+ 10	+ 4
	203.8	+ 3.9	+ 5	+ 4
	197.8	+ 4.8	+ 17	+ 3
	217.7	+ 1.7	+ 11	+ 12
	239.4	— 2.0	— 6	+ 5
108	345.4	— 8.2	— 11	+ 1
	320.4	— 9.4	— 4	+ 1
	292.2	— 8.4	— 9	— 1
	264.9	— 5.4	+ 8	+ 5
	239.2	— 1.5	— 7	+ 4
	215.5	+ 2.5	+ 4	0
	196.0	+ 5.8	+ 21	+ 5
109	341.9	— 8.2	— 8	0
	313.1	— 8.2	— 9	— 8
	284.4	— 6.2	— 7	+ 1
	256.9	— 2.7	— 10	— 9
	231.2	+ 1.2	— 7	+ 3
	207.8	+ 4.6	— 1	— 2
	182.9	+ 7.4	+ 20	+ 2
110	212.8	+ 3.5	+ 7	+ 7
	186.6	+ 5.0	+ 9	+ 3
	162.6	+ 5.5	+ 21	+ 5
	139.1	+ 5.0	+ 2	— 1
	116.4	+ 3.9	+ 9	+ 11
	92.1	+ 2.0	+ 5	+ 10
	66.1	— 0.4	+ 1	+ 1
	39.6	— 2.6	— 3	0

111	347.4	−8.7	−18	−6
	319.3	−9.9	−9	−5
	290.6	−8.7	−17	−7
	263.3	−5.4	−3	−5
	237.6	−1.2	−13	+2
	214.0	+3.0	−7	−7
	192.7	+6.4	+7	−5
112	346.3	−8.6	−14	−2
	319.0	−10.2	−5	−5
	289.5	−9.2	−14	−4
	261.8	−5.8	+6	+2
	234.5	−1.4	−12	0
	210.3	+3.1	+1	+4
	188.6	+6.6	+15	−3
113	191.0	+6.3	+11	−4
	213.0	+2.7	−2	+2
	237.4	−1.8	−16	0
	264.1	−6.2	−1	−1
	292.7	−9.4	−10	−3
	322.3	−10.1	−8	−8
	347.6	−8.7	−15	−4
114	7.3	+0.6	−4	−4
	35.7	+1.1	−4	−1
	64.6	+1.3	−8	−2
	91.1	+1.3	−6	0
	116.7	+1.1	−3	+2
	142.5	+0.7	−7	+3
	169.6	+0.2	−16	+1
115	167.8	+0.3	−5	−5
	141.3	+0.7	−10	−1
	115.6	+1.1	−10	0
	89.9	+1.2	−5	−5
	63.4	+1.2	−13	−5
	35.4	+1.0	−12	−6
	5.6	+0.6	−5	−2
116	3.7	+0.5	−7	−1
	33.6	+0.9	−13	−9
	61.7	+1.2	−18	−4
	88.4	+1.2	−9	−10
	114.4	+1.0	−16	−7
	139.9	+0.7	−12	−6
	166.3	+0.3	−1	−3

117	11.3	−0.6	−11	−8	
	41.3	+0.8	0	0	
	69.1	+2.0	−1	+5	
	94.9	+2.8	−4	−2	
	119.7	+3.0	−6	−3	
	145.4	+2.8	−1	−1	
	170.1	+2.1	−10	−4	
118	166.9	+2.2	−1	−3	
	140.5	+2.9	−12	−2	
	115.8	+3.0	−13	−10	
	90.9	+2.6	−12	−3	
	64.8	+1.3	−16	−10	
	36.7	+0.5	−10	−5	
	6.4	−0.9	−12	−7	
120	165.6	+5.7	+12	0	
	141.7	+6.7	+6	−2	
	118.9	+6.7	+2	+1	
	95.4	+5.6	+3	+5	
	70.2	+3.5	−8	−2	
	42.3	+0.4	−8	−5	
121	359.1	+6.5	−3	−5	
	332.1	+9.4	+7	+1	
	305.1	+10.2	+1	+1	
	278.0	+9.0	0	−1	
	250.7	+5.6	−1	−3	
	222.8	+1.2	+4	−1	
	194.0	−3.8	+17	+3	
122	191.0	−3.8	−7	0	
	219.3	+0.6	+8	+9	
	247.0	+4.0	−6	−2	
	274.3	+7.9	+1	+1	
	301.3	+9.3	−13	−9	
	328.1	+8.8	−14	−2	
	354.9	+6.4	+2	+2	
123	1293	−3?7	−6	0	
	43.7	+0.3	−3	+2	
	71.7	+3.9	+4	0	
	98.7	+6.4	+3	+5	
	119.6	+7.6	+6	+3	
	142.1	+7.8	+14	+19	
	165.5	+6.7	+21		

124	2.9	−3.4	−10	−8
	37.7	+0.6	−10	−8
	68.8	+4.0	−17	−7
	96.3	+6.2	−9	−11
	121.7	+7.0	−10	−4
	147.0	+6.5	+3	+3
	174.0	+4.7	−2	+2
125	175.1	+4.6	−2	−1
	149.0	+6.4	+11	+5
	122.7	+6.9	+1	+1
	97.2	+6.1	+1	−2
	69.7	+4.0	−1	+5
	35.8	+0.6	+2	+1
	4.2	−3.2	+2	+1
126	344.5	−8.0	−11	−2
	315.5	−8.9	+10	+7
	286.3	−7.5	−2	+5
	258.2	−4.3	+5	0
	231.9	−0.3	−3	+8
	207.9	+3.5	+7	+7
	185.1	+6.5	+16	+4
127	351.6	−4.5	−4	+6
	323.9	−6.5	−1	+6
	295.4	−7.0	−5	−3
	267.2	−5.8	+6	+1
	240.0	−3.2	−6	+6
	214.7	−0.1	+5	+6
	191.4	+2.6	+14	−1
128	353.2	−1.2	+4	+9
	327.1	−2.9	−8	+6
	300.2	−3.9	−8	−10
	273.0	−4.0	−8	0
	245.3	−3.2	+4	+6
	220.7	−1.7	+2	+4
	196.8	0.0	−2	−4
129	359.9	+4.8	+7	+6
	333.7	+4.3	+4	+16
	305.4	+2.9	−2	−5
	278.4	+0.9	−4	+6
	250.0	−1.4	+3	+3
	221.8	−3.2	+2	+3
	194.0	−4.2	+9	−5

130	192.9	−4.2	+9	+4
	220.6	−3.2	+10	+10
	248.8	−1.3	0	0
	277.1	+1.0	−1	−9
	305.1	+3.0	+5	+3
	332.3	+4.4	−11	+5
	359.5	+4.9	+2	+5
131	28.7	+6.1	−2	+3
	5.0	+5.6	+6	+14
	340.7	+6.3	+4	+3
	315.7	+5.9	+15	+7
	290.1	+4.4	+4	+12
	263.9	+2.0	−10	+4
	237.5	−0.8	−5	+6
132	327.0	+6.9	−15	0
	356.3	+6.2	+2	+8
	25.7	+3.9	−4	+1
	55.9	+0.7	−1	+2
	85.4	−2.7	+4	0
	115.6	−5.3	−2	+3
	147.3	−6.4	+4	−1
133	0.3	+5.2	+8	+8
	25.4	+2.7	+2	+9
	50.3	−0.3	+1	+2
	75.8	−3.2	−2	+3
	101.7	−5.5	+12	+16
	128.1	−5.6	+20	+1
	162.0	−6.0	−19	−4
134	0.0	+4.5	−2	−2
	26.4	+1.6	−2	+5
	53.6	−1.6	−2	+6
	79.8	−1.4	+3	+7
	107.1	−6.2	−27	−1
	134.6	−6.6	−2	−3
	162.2	−5.4	−16	−11
135	3.1	−1.0	−3	5
	33.4	−2.9	−2	+2
	63.1	−4.0	−10	−4
	91.8	−4.0	+9	+5
	119.5	−2.9	0	+1
	146.3	−1.2	−6	0
	172.6	+0.7	−4	+1

136	173.4	+ 0.8	− 6	− 2
	156.4	− 0.5	+ 2	+ 8
	120.4	− 2.9	+ 6	+ 5
	93.3	− 4.0	+ 2	− 2
	63.9	− 4.1	− 6	+ 1
	34.2	− 3.0	− 4	0
	3.9	− 1.1	− 6	− 6
137	351.4	− 6.3	− 8	+ 4
	320.9	− 3.1	− 1	− 1
	291.5	+ 0.9	+ 6	+ 4
	263.6	+ 3.5	− 17	− 1
	237.6	+ 7.0	+ 5	+ 7
	213.5	+ 8.1	− 1	− 4
	191.7	+ 7.9	+ 20	+ 1
138	192.4	+ 8.0	+ 11	− 4
	215.0	+ 8.2	0	0
	239.2	+ 7.0	+ 8	+ 8
	265.2	+ 4.4	− 23	− 2
	293.2	+ 0.7	− 5	− 3
	322.7	− 3.3	− 8	− 1
	351.7	− 6.3	− 6	+ 6
139	354°3	− 4°4	− 8	− 1
	320.8	+ 1.0	− 11	+ 1
	289.1	+ 5.9	− 7	+ 1
	259.3	+ 8.9	+ 2	− 3
	231.6	+ 9.8	− 5	− 4
	205.4	+ 8.5	+ 1	− 2
	182.2	+ 6.1	+ 27	+ 7
140	4.3	+ 4.8	− 9	− 1
	33.0	+ 7.8	− 6	− 1
	59.0	+ 8.9	− 17	− 1
	83.2	+ 8.4	− 9	+ 1
	106.9	+ 6.5	− 6	− 3
	131.7	+ 3.4	+ 8	+ 1
	159.0	− 0.6	+ 20	+ 2
	169.4	− 2.2	− 9	− 1
141	9.5	+ 4.5	− 4	− 5
	340.7	+ 4.5	+ 4	+ 2
	310.6	+ 3.4	+ 7	+ 4
	279.6	+ 1.4	− 3	+ 6
	248.2	− 1.0	0	0
	216.9	− 3.0	0	+ 4

					+	2
					+	7
					+	2
					+	4
					−	1
					−	4
142	215.3	− 3.1	−	2		
	245.6	− 1.1	+	7		
	278.0	+ 1.3	−	5		
	309.1	+ 3.4	+	5		
	339.2	+ 5.5	−	1		
	8.0	+ 4.6	−	4		
					(+	27)
143	13.8	+ 6.6	+	29		0
	40.4	+ 8.1	−	4	+	5
	65.0	+ 8.0	−	4	+	10
	88.6	+ 6.7	+	10	+	10
	112.4	+ 4.2	+	11	+	13
	137.6	+ 0.8	+	9	+	9
	169.3	− 3.5	−	4		
144	189.7	− 1.9	+	12	+	14
	220.1	− 4.9	+	6	+	8
	252.9	− 5.5	+	10	+	12
	285.8	− 5.9	−	5	+	3
	320.3	− 3.3	+	17	+	15
	350.5	+ 0.9	−	3	+	1
	357.3	+ 1.0	+	1	+	5
	340.5	− 2.2	−	13	+	1
	302.2	− 4.9	+	10	+	6
					−	7
145	161.7	− 5.2	−	10	+	1
	134.6	− 4.3	+	2	−	1
	108.7	− 2.5	−	22	−	2
	83.5	− 0.3	−	5	0	
	58.7	+ 2.2	−	1	0	
	33.7	+ 4.2	−	4	0	
	8.3	+ 5.5	−	3	0	
	343.0	+ 5.7	+	2	0	
146	241.1	+ 5.7	−	1	−	3
	7.5	+ 5.4	−	1	+	3
	33.0	+ 4.2	−	7	−	3
	58.0	+ 2.2	−	3	−	1
	82.8	− 0.2	−	5	−	2
	108.0	− 2.4	−	24	−	2
	134.6	− 4.3	+	2	0	
	162.0	− 5.2	−	14	0	

147	4.2	+4.8	−15	−8
	338.2	+7.2	−8	−4
	307.9	+8.0	−8	0
	279.3	+6.9	−14	−12
	250.4	+4.2	−3	−10
	221.4	+0.5	−4	−3
	192.1	−2.4	−5	−7
148	9.3	+5.4	−8	−7
	342.3	+6.3	+1	−1
	314.3	+5.6	+5	−2
	285.5	+4.0	−6	+3
	256.1	+1.2	−13	−9
	226.4	−1.9	−11	−8
	196.8	−4.4	+6	+5
149	3.1	+1.2	+2	+8
	34.4	+3.4	−7	+1
	62.1	+4.6	−6	0
	89.8	+4.8	0	+2
	115.6	+4.0	−2	0
	142.0	+2.5	−5	+2
	170.2	+0.3	−15	−3
151	357.2	+5.6	−12	−7
	329.4	+5.6	−31	−10
	300.6	+4.2	−17	−12
	271.0	+1.9	−31	−12
	241.2	−1.0	−23	−15
	211.4	−3.4	−14	−16
	193.6	−4.5	−3	−14

Table 23

Nefed'yev's Observations

Meteor No.	P	D	H	H − H'
3	163.2	− 3.5	− 16	0
	134.6	− 6.7	+ 4	+ 2
	107.0	− 6.3	− 24	+ 2
	79.7	− 4.5	+ 5	+ 9
	52.8	− 1.6	+ 1	+ 9
	25.2	+ 1.6	− 0	− 7
	358.7	+ 4.5	+ 3	+ 3
4	152.3	− 4.5	− 11	+ 3
	128.1	− 6.0	− 3	+ 6
	113.8	− 6.3	− 5	+ 10
	98.4	− 5.5	+ 18	+ 11
	63.2	− 3.7	− 2	+ 4
	41.0	− 1.2	+ 9	+ 12
	17.0	+ 1.6	+ 12	+ 12
5	68.1	− 2.6	− 16	− 12
	143.6	− 4.7	− 4	+ 1
	117.7	− 5.8	− 5	− 6
	91.3	− 5.7	− 1	− 3
	64.8	− 4.4	− 15	− 5
	38.4	− 2.0	− 9	− 6
	11.6	+ 0.8	− 3	− 4
6	161.7	− 1.9	− 10	+ 1
	131.8	− 4.3	− 7	− 9
	101.0	− 5.5	− 10	− 7
	69.4	− 5.0	− 9	− 6
	37.2	− 3.0	− 6	− 4
	1.7	+ 0.1	− 9	− 3
7	7.2	− 5.7	− 8	− 3
	341.1	+ 6.7	− 1	− 2
	314.2	+ 6.4	− 2	− 6
	286.8	+ 4.7	− 6	+ 5
	258.9	+ 1.9	− 0	− 8
	230.5	− 1.3	− 12	− 2
	201.9	− 4.1	− 2	− 0

8	13.4	− 3.2	− 6	+ 1
	41.5	− 4.2	− 16	− 12
	68.8	− 4.2	− 6	− 2
	95.2	− 3.3	− 1	+ 1
	119.7	− 1.7	+ 2	− 2
	143.6	+ 0.2	− 12	− 2
	166.6	+ 2.0	+ 2	0
9	166.4	+ 6.2	+ 4	− 4
	144.3	+ 6.2	+ 3	+ 3
	122.6	+ 7.1	+ 1	+ 1
	99.9	+ 4.9	− 5	− 1
	74.7	+ 1.6	− 13	− 10
	45.8	− 2.3	− 16	− 8
	15.4	− 5.9	− 2	+ 4
10	1.6	− 0.8	+ 12	+ 12
	333.9	+ 1.8	− 13	− 1
	306.6	+ 4.0	− 38	(− 26)
	279.7	+ 5.4	+ 4	+ 6
	252.8	+ 5.6	+ 12	+ 7
	226.4	+ 4.9	+ 4	+ 8
	203.9	+ 3.3	− 2	− 2
11	201.2	+ 3.1	− 2	0
	225.5	+ 4.6	− 5	− 3
	250.5	+ 5.7	+ 2	− 5
	276.5	+ 5.5	− 5	0
	303.2	+ 4.3	− 14	− 10
	330.4	+ 2.1	− 20	+ 4
	358.0	− 0.5	− 16	− 12
12	347.7	− 2.5	− 2	+ 3
	321.2	+ 1.3	− 6	+ 9
	295.8	+ 4.8	+ 5	+ 9
	271.4	+ 7.3	+ 33	(+ 44)
	248.3	+ 8.4	+ 9	+ 7
	225.1	+ 8.4	+ 2	+ 4
	204.9	+ 7.2	+ 11	+ 9
13	205.5	+ 7.4	− 6	− 8
	226.7	+ 8.5	− 12	− 10
	248.3	+ 8.6	− 7	− 9
	272.1	+ 7.4	0	+ 8
	296.4	+ 4.8	− 8	− 3
	321.8	+ 1.2	− 25	− 7
	348.2	− 2.7	− 17	− 12

14	345.6	−5.8	− 8	+ 4
	315.5	−5.6	+ 8	− 2
	285.7	−3.9	− 2	+ 9
	256.8	−1.2	− 4	− 2
	229.5	+1.7	+ 1	+ 9
	204.8	+4.1	+ 5	+ 3
15	175.2	+6.0	+ 3	+ 5
	197.6	+4.8	+ 17	+ 3
	221.9	+2.6	+ 3	+ 5
	248.4	−0.2	+ 4	+ 4
	276.7	−3.1	− 3	+ 5
	305.5	−5.2	+ 10	+ 8
	336.6	−5.9	− 9	− 3
17	19.5	−0.4	+ 4	+ 6
	49.0	+2.6	− 10	− 4
	75.4	+4.8	+ 3	+ 4
	92.8	+6.0	+ 1	+ 5
	123.1	+6.2	+ 5	+ 4
	145.4	+5.4	+ 7	+ 7
	171.5	+3.6	− 4	− 7
18	260.9	+7.4	+ 1	− 5
	220.4	+6.3	+ 3	+ 5
	241.0	+4.3	+ 4	0
	263.2	+1.6	− 6	+ 2
	286.4	−1.4	− 10	0
	311.2	−4.4	− 9	− 6
	336.1	−6.4	− 11	− 5
19	338.6	−6.5	+ 5	+ 10
	310.9	−4.9	− 2	+ 1
	283.4	−2.2	− 4	+ 15
	257.7	+0.9	+ 9	+ 3
	233.4	+3.8	+ 10	+ 15
	210.7	+5.8	+ 17	+ 13
	190.2	+7.0	+ 22	+ 6
20	349.3	− 6.0	− 7	+ 3
	318.4	− 5.4	+ 15	+ 5
	287.8	− 3.4	+ 3	+ 10
	261.6	− 0.8	+ 15	+ 8
	235.7	+ 1.9	− 6	+ 6
	213.5	+ 4.2	+ 10	+ 9
	192.6	+ 5.7	+ 21	+ 9

22	12.2	+ 1.6	− 2	− 5
	37.3	− 0.9	− 12	− 10
	62.3	− 3.1	− 16	− 10
	87.4	− 4.8	+ 1	− 1
	112.3	− 5.4	− 29	− 3
	137.3	− 5.0	− 14	− 8
	162.1	− 3.7	− 22	− 2
23	357.3	+ 5.5	− 6	− 1
	332.2	+ 4.4	− 18	− 2
	305.6	+ 2.3	− 6	− 6
	278.5	− 0.3	− 18	− 4
	250.7	− 2.8	+ 2	+ 6
	223.0	− 4.6	− 9	− 8
	195.5	− 5.2	+ 3	+ 6
24	196.6	− 5.2	− 3	+ 3
	226.3	− 4.3	− 7	− 7
	254.1	− 2.4	+ 12	+ 6
	281.8	+ 0.2	− 13	+ 2
	308.9	+ 2.8	− 2	− 3
	335.2	+ 4.6	− 6	+ 2
	0.0	+ 5.6	− 3	− 4
25	358.7	+ 2.7	− 2	+ 1
	330.7	+ 3.4	− 13	+ 11
	302.1	+ 3.3	+ 6	+ 10
	273.7	+ 2.5	− 21	− 2
	245.6	+ 1.2	+ 16	+ 10
	217.6	− 0.4	+ 10	+ 10
	190.4	− 1.7	+ 9	+ 6
26	195.0	− 1.5	+ 2	− 1
	222.5	0.0	+ 9	+ 4
	250.7	+ 1.6	+ 6	0
	278.9	+ 2.9	− 2	0
	307.2	+ 3.5	+ 5	− 1
	334.3	+ 3.4	0	+ 7
	2.8	+ 2.6	− 3	+ 3
27	17.3	− 1.4	− 9	− 6
	345.5	+ 0.6	− 6	0
	313.2	+ 2.8	+ 5	0
	282.2	+ 4.0	− 13	− 5
	251.4	+ 4.2	+ 3	− 7
	221.8	+ 3.3	− 6	− 4
	193.2	+ 1.6	+ 6	+ 2

25	346.0	—	3.8	—	6	+ 4
	316.9	+	0.8	+	4	— 2
	289.2	+	5.1	—	2	+ 7
	262.8	+	8.0	+	1	+ 4
	238.1	+	9.4	+	9	+ 6
	215.6	+	9.1	—	2	— 1
	192.9	+	7.6	+	13	0
29	331.4	—	4.1	—	3	+ 2
	302.5	+	0.5	+	14	(+ 24)
	272.2	+	4.8	—	12	+ 3
	246.6	+	7.4	+	10	+ 11
	220.8	+	9.7	+	5	+ 9
	196.6	+	8.4	+	16	+ 5
	173.1	+	6.7	+	15	(+ 17)
30	295.2	+	0.1	+	9	+ 11
	253.4	+	4.9	—	15	— 2
	235.2	+	6.6	+	10	+ 3
	209.2	+	7.8	+	5	0
	185.2	+	7.5	+	26	+ 7
	162.1	+	6.1	+	23	+ 7
	138.9	+	3.7	+	5	+ 6
31	341.4	—	3.4	—	8	— 3
	313.0	+	1.7	—	1	— 1
	286.6	+	6.2	—	19	— 5
	261.7	+	9.2	+	4	— 3
	238.5	+	10.6	—	6	— 6
	215.7	+	10.4	—	11	— 7
	193.5	+	8.8	+	12	— 2
32	194.4	+	9.0	+	10	— 4
	215.3	+	10.3	—	9	— 6
	237.3	+	10.3	+	1	— 1
	260.9	+	8.6	+	1	— 5
	285.8	+	5.4	—	19	+ 4
	312.5	+	0.8	—	7	+ 7
	340.7	—	4.2	—	7	— 2
33	339.5	—	4.9	+	2	+ 7
	312.6	—	1.1	+	19	+ 11
	287.9	+	2.9	—	2	0
	264.0	+	6.1	+	18	+ 13
	241.8	+	7.9	+	10	+ 13
	220.5	+	8.3	+	13	+ 10
	191.8	+	8.0	+	36	(+ 17)
	183.6	+	7.5	+	29	+ 10

34	340.4	− 4.5	− 3	+ 2
	312.3	− 0.8	+ 7	+ 2
	285.0	+ 3.1	− 2	+ 7
	258.8	+ 6.2	+ 11	+ 6
	234.5	+ 8.0	+ 2	+ 1
	211.3	+ 8.4	+ 6	+ 1
	190.7	+ 7.7	+ 24	+ 6
35	194.4	+ 5.6	+ 18	+ 4
	215.7	+ 2.9	− 3	− 7
	237.9	− 0.3	− 1	+ 12
	262.0	− 3.7	+ 1	− 4
	288.6	− 6.5	− 11	− 3
	316.8	− 8.0	+ 5	+ 2
	345.7	− 7.5	− 9	+ 2
36	328.5	− 4.0	+ 7	+ 12
	309.9	− 1.2	+ 19	+ 11
	282.2	+ 2.0	+ 8	+ 13
	255.6	+ 4.6	+ 14	+ 16
	231.0	+ 6.2	+ 8	+ 12
	207.8	+ 6.8	+ 17	+ 14
	189.3	+ 6.5	+ 38	(+ 23)
38	337.5	− 3.2	− 8	− 3
	310.5	− 0.7	+ 12	+ 4
	284.0	+ 2.0	− 2	+ 4
	258.9	+ 4.3	+ 7	+ 1
	235.1	+ 5.7	0	+ 3
	212.4	+ 6.2	+ 4	0
	196.2	+ 6.0	+ 22	+ 14
39	340.8	− 2.9	− 4	+ 1
	314.5	− 1.1	+ 8	+ 3
	288.8	+ 1.0	− 2	+ 4
	266.8	+ 2.6	− 14	+ 7
	243.5	+ 4.9	0	+ 1
	220.9	+ 4.7	+ 10	+ 8
	199.1	+ 4.8	+ 10	+ 2
40	344.0	− 0.7	− 8	− 1
	318.7	− 0.7	+ 2	− 1
	292.5	− 0.6	− 1	+ 1
	271.0	− 0.4	− 20	− 3
	245.5	0.0	0	0
	222.1	+ 0.4	+ 6	+ 3
	198.2	+ 0.8	+ 14	+ 3

41	338.2	+ 2.2	+ 14	+ 14
	8.5	+ 4.7	+ 13	+ 12
	36.2	+ 6.0	+ 7	+ 5
	61.7	+ 6.0	− 11	+ 2
	85.2	+ 5.0	+ 13	+ 12
	110.3	+ 3.1	+ 4	+ 1
	135.7	+ 0.6	+ 8	+ 7
42	353.5	+ 4.9	0	+ 1
	329.2	+ 1.8	− 23	+ 1
	308.6	− 1.8	− 7	− 2
	276.7	− 5.1	− 8	− 1
	249.3	− 7.2	+ 7	+ 7
	221.9	− 7.7	0	0
	195.2	− 6.5	+ 9	+ 1
43	349.4	+ 3.2	− 7	0
	325.4	+ 0.6	− 21	− 9
	300.6	− 2.2	− 3	0
	275.1	− 4.5	− 11	− 5
	249.1	− 5.9	+ 4	+ 7
	223.4	− 6.1	− 3	− 2
	198.7	− 5.0	− 4	− 2
44	351.4	− 1.9	− 2	+ 2
	324.7	− 1.3	− 13	− 3
	298.0	− 0.3	+ 12	+ 6
	271.2	+ 0.8	− 22	− 3
	245.7	+ 1.6	+ 6	+ 9
	220.9	+ 2.4	0	+ 2
	197.7	+ 2.7	+ 12	+ 3
45	355.9	+ 0.2	− 3	+ 3
	336.7	+ 1.6	− 22	− 3
	317.4	+ 2.8	+ 9	+ 14
	299.1	+ 3.2	− 19	+ 3
	281.5	+ 3.0	+ 3	+ 2
	264.6	+ 2.2	+ 9	+ 8
	249.1	+ 1.0	+ 13	+ 1
46	195	+ 5.4	+ 2	+ 9
	30.4	+ 7.7	+ 6	+ 11
	58.4	+ 8.1	− 6	+ 3
	80.9	+ 7.1	+ 2	+ 12
	105.2	+ 4.9	+ 19	+ 13
	130.9	+ 1.7	+ 14	+ 5
	158.9	− 2.2	+ 26	+ 9

	47	163.7	− 2.6	+ 10	+ 16	
		125.2	+ 1.7	+ 19	(+ 19)	
		109.5	+ 5.3	+ 8	+ 2	
		85.1	+ 7.7	+ 2	+ 6	
		60.6	+ 8.8	− 4	+ 8	
		34.8	+ 9.4	+ 8	+ 14	
		6.4	+ 6.0	+ 19	(+ 17)	
	48	159.5	− 1.2	+ 34	+ 9	
		131.8	+ 2.7	+ 10	+ 2	
		106.8	+ 5.7	+ 1	+ 5	
		82.6	+ 7.6	− 2	+ 8	
		58.4	+ 8.3	− 16	+ 1	
		32.2	+ 7.4	− 3	− 1	
		3.2	+ 4.8	− 1	+ 7	
	49	35.3	+ 7.6	− 4	0	
		61.0	+ 8.2	− 22	− 10	
		85.3	+ 7.4	− 13	− 6	
		109.5	+ 5.4	− 3	− 3	
		134.9	+ 2.2	− 7	− 6	
		163.0	− 1.7	− 16	− 7	
	50	9.9	+ 4.5	− 2	− 4	
		39.0	+ 7.2	− 11	− 7	
		64.8	+ 8.0	− 17	− 8	
		88.8	+ 7.5	− 9	− 8	
		112.7	+ 5.8	+ 2	+ 1	
		137.7	+ 2.9	− 6	− 3	
		165.5	− 0.8	− 2	0	
	51	354.1	+ 5.5	+ 1	− 1	
		328.4	+ 4.2	− 24	0	
		303.8	+ 2.0	− 4	0	
		277.6	− 0.6	− 11	0	
		251.0	− 3.0	+ 2	+ 7	
		223.9	− 4.8	− 2	+ 1	
		197.7	− 5.4	− 7	− 2	
	52	353.3	+ 4.0	+ 9	+ 12	
		25.4	+ 6.4	− 12	− 8	
		54.0	+ 7.0	− 13	− 4	
		80.9	+ 6.1	− 4	+ 6	
		107.1	+ 4.0	+ 4	+ 7	
		134.8	+ 0.9	+ 4	+ 2	
		165.1	− 2.6	− 12	− 9	

53	163.9	0.0	0	+	1	+	1				
	135.5	+ 3.0	+ 6	+	6	+	6				
	103.7	+ 5.3	+ 11	+	5	+	5				
	84.6	+ 6.5	+ 2	+	6	+	6				
	59.0	+ 6.5	− 11	−	9	−	9				
	39.8	+ 5.1	− 4	−	2	−	2				
	5.9	+ 2.9	+ 6	+	6	+	6				
54	139.9	+ 2.2	+ 9	+	4	+	4				
	41.7	+ 4.6	− 3	+	1	+	1				
	67.7	+ 5.8	− 5	+	2	+	2				
	92.1	+ 6.0	+ 6	+	12	+	12				
	115.4	+ 5.2	+ 3	+	5	+	5				
	138.7	+ 3.5	+ 5	+	6	+	6				
	165.4	+ 1.1	+ 14	+	12	+	12				
55	349.0	− 3.7	− 10	−	1	−	1				
	321.3	− 4.8	− 6	−	1	−	1				
	294.0	− 4.8	− 6	−	3	−	3				
	266.6	− 3.6	+ 10	+	1	+	1				
	249.9	− 1.7	− 7	+	6	+	6				
	216.0	+ 0.5	0	+	5	+	5				
	193.4	+ 2.5	+ 7	+	5	+	5				
56	346.4	− 3.9	− 13	−	4	−	4				
	318.1	− 5.0	+ 12	+	6	+	6				
	291.4	− 5.9	+ 11	+	2	+	2				
	263.1	− 4.8	+ 4	+	6	+	6				
	236.5	− 2.6	− 8	+	6	+	6				
	211.4	0.0	− 2	−	1	−	1				
	186.3	+ 1.6	+ 11	+	6	+	6				
57	200.0	+ 1.2	− 9	−	12	−	12				
	223.2	− 1.3	− 11	−	10	−	10				
	248.0	− 3.6	− 12	−	7	−	7				
	273.5	− 5.3	− 13	−	3	−	3				
	300.6	− 5.9	− 12	−	8	−	8				
	326.8	− 5.2	− 30	(−	21)	(−	21)				
	352.9	− 3.4	− 9	−	2	−	2				
58	12.5	− 6.1	− 17	−	9	−	9				
	39.2	− 7.0	− 5	−	4	−	4				
	65.8	− 6.4	− 13	−	5	−	5				
	91.1	− 4.5	− 2	−	4	−	4				
	114.6	− 1.9	− 18	−	3	−	3				
	134.7	+ 0.8	− 6	−	8	−	8				
	155.6	+ 3.3	+ 14	+	2	+	2				

59	4.3	+ 1.2	— 2	+ 4
	333.4	+ 3.7	+ 1	+ 13
	302.9	+ 5.2	— 7	— 3
	272.1	+ 5.3	— 17	— 1
	242.3	+ 4.1	0	+ 1
	212.8	+ 1.8	— 4	0
	183.8	0.8	0	+ 3
60	185.4	— 0.6	— 7	— 2
	214.5	+ 2.0	+ 3	+ 4
	243.9	+ 4.2	— 1	— 1
	273.9	+ 5.4	— 9	+ 1
	304.4	+ 5.2	0	— 2
	335.2	+ 3.6	— 9	— 1
	6.0	+ 1.1	0	+ 1
61	13.2	+ 6.2	— 7	— 10
	42.5	+ 6.3	— 7	— 3
	70.0	+ 5.0	— 20	— 14
	97.0	+ 2.7	— 13	— 10
	124.3	— 0.2	— 2	— 4
	141.6	— 2.3	— 14	— 5
	160.3	— 3.8	— 13	— 7
62	316.9	— 0.4	— 9	— 2
	320.4	+ 2.9	— 10	(— 39)
	294.0	+ 5.7	— 2	+ 1
	269.1	+ 7.3	— 18	+ 1
	245.3	+ 7.6	+ 4	+ 7
	222.0	+ 6.7	— 8	— 6
	199.6	+ 4.9	+ 9	+ 4
63	195.6	+ 4.5	+ 14	+ 7
	218.5	+ 6.6	— 2	0
	241.4	+ 7.6	+ 4	+ 4
	265.3	+ 7.6	0	+ 13
	293.3	+ 6.1	+ 2	+ 8
	316.0	+ 3.5	+ 9	+ 2
	342.5	+ 0.2	0	+ 4
64	347.2	+ 2.3	— 10	— 3
	320.4	+ 5.6	— 8	+ 3
	294.5	+ 7.6	— 1	— 3
	241.3	+ 7.2	— 5	+ 1
	220.0	+ 5.1	— 5	— 2
	195.9	+ 2.2	— 2	— 7

65	198.4	+ 2.5	+ 6	0
	222.7	+ 5.4	− 8	− 6
	247.4	+ 7.4	− 2	− 3
	271.9	+ 8.2	− 2	+ 5
	297.4	+ 7.4	− 13	− 8
	323.6	+ 5.2	− 10	− 2
	349.8	+ 2.0	− 7	0
66	356.3	+ 5.0	− 21	(− 19)
	329.5	+ 6.8	− 31	− 14
	302.8	+ 7.2	− 15	− 12
	275.7	+ 6.2	− 16	− 11
	248.7	+ 3.8	− 23	(− 22)
	221.8	+ 0.7	− 19	(− 19)
	191.7	− 2.5	− 1	− 10
67	197.0	− 2.2	+ 3	+ 8
	224.1	+ 1.0	+ 7	+ 4
	240.7	+ 3.6	+ 2	+ 1
	268.0	+ 5.6	− 26	− 4
	294.8	+ 7.1	+ 12	+ 10
	321.9	+ 7.0	− 7	+ 13
	348.2	+ 5.6	− 3	+ 2
68	6.7	+ 4.8	− 5	0
	37.2	+ 6.2	− 10	− 9
	63.6	+ 6.0	− 16	− 5
	88.8	+ 4.8	0	− 1
	114.3	+ 2.7	− 8	− 5
	140.6	0.0	− 8	− 1
	169.5	− 2.9	− 11	− 1
69	349.3	+ 6.5	− 2	+ 3
	329.6	+ 7.2	− 17	− 2
	309.8	+ 7.1	− 7	− 3
	288.8	+ 6.1	− 10	− 1
	268.8	+ 4.5	− 24	− 2
	248.7	+ 2.3	+ 2	+ 4
	228.1	− 0.2	− 8	− 3
	199.4	− 3.6	− 7	− 1
70	344°7	+ 4°0	+ 11	+ 9
	21.5	+ 5.1	+ 18	(+ 19)
	55.6	+ 4.3	− 2	+ 7
	88.1	+ 2.3	+ 15	+ 12
	120.9	− 0.4	+ 13	+ 12

73	8.8	+ 0.2	− 4	− 5
	39.9	+ 3.2	− 6	− 2
	68.7	+ 5.2	− 13	− 3
	91.6	+ 5.9	− 10	− 4
	119.6	+ 5.6	0	+ 1
	145.0	+ 4.2	− 17	(− 18)
74	170.4	+ 2.2	− 3	+ 3
	143.6	+ 4.4	+ 9	+ 6
	118.1	+ 5.7	+ 4	+ 4
	93.0	+ 5.9	+ 2	+ 5
	65.9	+ 5.1	− 3	+ 4
	38.2	+ 3.0	− 2	0
	6.2	− 0.1	+ 8	+ 13
75	0.0	+ 0.1	− 1	+ 1
	331.0	− 1.7	− 25	− 8
	300.9	− 3.1	− 6	− 5
	270.6	− 3.5	− 7	+ 2
	240.8	− 3.0	− 5	+ 4
	212.3	− 1.7	+ 5	+ 6
	188.0	− 0.1	+ 2	− 4
76	183.6	+ 0.2	+ 13	+ 10
	210.4	− 1.5	+ 5	+ 6
	239.7	− 2.9	− 8	+ 4
	268.2	− 3.5	+ 1	− 5
	298.2	− 3.2	− 2	+ 1
	328.5	− 1.9	− 5	+ 5
	357.8	− 0.1	− 6	− 1
77	13.6	− 1.8	+ 1	+ 6
	47.3	+ 2.1	− 8	− 2
	76.7	+ 5.0	− 7	0
	103.4	+ 6.5	− 5	− 2
	128.8	+ 6.8	+ 15	+ 1
	154.7	+ 5.8	+ 6	− 2
	179.3	+ 3.6	+ 14	+ 5
78	173.1	+ 4.3	− 8	− 3
	146.2	+ 6.1	+ 7	+ 6
	121.6	+ 6.7	− 8	− 2
	97.0	+ 6.1	+ 6	+ 2
	70.5	+ 4.3	− 4	+ 1
	41.0	+ 1.3	0	− 1
	14.1	− 1.7	+ 1	+ 6

79	13.7	−6.2	−13	−6	
	45.6	−2.2	−16	−8	
	74.9	+2.1	−14	−11	
	100.6	+5.6	−7	−4	
	123.7	+7.7	−11	−14	
	146.1	+8.7	−3	−6	
	168.9	+8.4	−3	−5	
80	189.9	+8.4	0	+7	
	143.2	+8.5	+4	−3	
	120.7	+7.4	−8	−3	
	97.6	+5.0	−9	−12	
	71.2	+1.5	−20	−14	
	41.4	−2.8	−22	(−19)	
	12.0	−6.3	−16	−8	
81	351.0	−1.4	−8	−3	
	324.0	−2.8	−10	0	
	296.1	−3.4	−16	−11	
	268.1	−3.2	+1	−1	
	240.7	−2.2	−4	+5	
	190.4	+0.8	+16	−3	
82	15.6	−4.6	−11	−6	
	52.7	+0.3	−13	0	
	84.6	+4.5	+7	+12	
	112.7	+7.2	−14	−12	
	139.2	+8.2	+6	0	
	165.0	+7.6	+12	+3	
	182.0	+6.5	+15	−4	
83	179.5	+6.8	+7	−2	
	152.9	+8.2	+16	+13	
	128.3	+8.1	+3	0	
	103.1	+6.5	−4	0	
	75.8	+3.4	−4	−1	
	44.3	−1.0	0	0	
	14.6	−4.8	−1	0	
84	15.7	−5.6	−10	−5	
	48.4	−1.8	−13	−8	
	82.5	+3.1	−11	−7	
	105.7	+5.9	−2	−1	
	127.3	+7.8	−6	−5	
	148.5	+6.5	−1	−3	
	162.8	+8.4	−2	−3	

85	166.1	+ 8.3	+ 10	+ 3	
	145.8	+ 8.4	− 4	− 10	
	124.2	+ 7.4	0	− 6	
	102.3	+ 5.4	− 15	− 13	
	78.8	+ 2.5	− 16	− 13	
	52.6	− 1.3	− 8	+ 1	
	22.9	− 5.1	− 14	− 11	
86	15.1	− 6.2	− 12	− 6	
	45.7	− 2.8	− 14	− 7	
	73.0	+ 0.9	− 19	(− 18)	
	97.5	+ 4.2	− 12	− 9	
	120.0	+ 6.6	− 7	− 4	
	141.9	+ 7.9	+ 7	0	
	164.1	+ 8.2	+ 3	− 4	
87	159.4	+ 8.2	− 20	− 11	
	137.9	+ 7.6	+ 8	+ 5	
	116.7	+ 6.2	− 6	− 5	
	94.1	+ 3.7	− 12	− 6	
	69.4	+ 0.3	− 8	− 4	
	41.5	− 3.3	− 13	− 9	
	16.6	− 6.5	− 18	− 10	
88	169.0	− 5.9	+ 8	+ 13	
	48.6	− 2.2	+ 3	+ 6	
	77.2	+ 1.8	+ 1	+ 2	
	102.7	+ 5.0	− 5	− 2	
	126.5	+ 7.2	− 8	− 10	
	172.2	+ 8.0	− 2	− 2	
	148.8	+ 8.2	− 13	− 13	
89	170.2	+ 8.0	+ 11	+ 6	
	147.1	+ 8.0	+ 6	+ 5	
	124.8	+ 7.0	+ 10	0	
	101.1	+ 4.7	+ 1	0	
	75.0	+ 1.4	− 10	− 7	
	45.9	− 2.6	− 6	+ 2	
	13.3	− 6.1	− 5	+ 2	
90	16.3	− 5.9	− 4	+ 1	
	47.3	− 2.8	− 4	+ 2	
	75.8	+ 0.6	− 2	+ 1	
	101.1	+ 3.9	+ 2	− 4	
	124.3	+ 6.1	+ 12	+ 2	
	146.2	+ 7.4	+ 2	− 2	
	167.3	+ 7.6	− 9	− 2	

91	164.8	+7.6	+12	+ 3
	142.2	+7.2	+23	+11
	120.2	+5.7	− 4	− 2
	98.6	+3.3	+ 2	0
	76.5	0.0	6	+ 5
	41.6	−3.6	− 7	− 4
	13.5	−6.1	− 1	− 6
92	12.2	−6.2	− 8	0
	44.4	−3.5	−10	− 5
	74.1	+0.1	− 4	0
	101.2	+3.4	+ 1	− 4
	125.1	+5.3	+ 2	− 3
	149.8	+7.2	+ 8	+ 1
	164.6	+7.5	+14	+ 5
95	165.2	+4.4	+ 1	− 6
	141.2	+2.9	−13	− 3
	116.9	+6.9	−14	− 9
	90.9	−1.3	−16	−15
	63.2	−3.4	−16	−11
	33.7	−4.6	−12	− 8
	2.1	−4.5	−12	−16
96	8.9	−3.7	− 8	− 5
	38.1	−4.2	− 8	− 7
	66.7	−3.7	− 8	− 2
	92.6	−2.3	−17	(−22)
	117.8	−0.5	−11	−10
	165.3	+3.9	+ 6	+ 4
	141.8	+1.4	− 6	+ 4
97	343.8	−2.1	−24	(−19)
	322.1	+1.1	−23	− 5
	294.1	+4.2	−36	(−31)
	266.3	+6.3	−20	+ 1
	190.4	+4.8	−19	0
98	346.4	−8.1	−21	−16
	317.8	−8.9	− 3	− 2
	289.5	−7.5	−10	− 1
	260.5	−4.3	− 3	− 2
	234.6	−0.3	−14	− 2
	210.2	+3.6	− 8	− 5
	188.3	+6.5	+17	0

99	190.0	+6.4	+16	+ 1
	212.1	+3.3	+ 5	+ 6
	236.5	−0.6	− 1	+12
	262.9	−4.6	+ 4	− 1
	290.6	−7.7	−10	0
	320.4	−8.9	− 2	+ 4
	349.2	−7.9	− 8	+ 3
100	3.9	−2.5	+ 6	+ 5
	33.1	−3.2	− 8	− 3
	62.9	−3.0	− 3	+ 2
	93.4	−2.1	+ 7	+ 3
	113.8	−0.8	− 1	+14
	138.1	+0.7	− 4	+ 1
	162.1	+2.0	+ 7	+ 6
101	345.4	−4.8	+22	− 10
	316.7	−4.3	−14	(−22)
	288.3	−2.6	−18	− 13
	261.0	−0.4	+ 7	0
	235.0	+1.9	−20	− 8
	211.1	+3.8	− 3	− 1
	188.6	+4.9	− 4	− 15
102	191.1	+4.8	− 4	− 14
	213.8	+3.6	−15	− 15
	238.5	+1.7	−14	− 7
	264.3	−0.5	−23	− 12
	291.5	−2.7	−24	(−20)
	319.6	−4.2	−12	− 15
	347.7	−4.7	−25	− 13
103	349.3	−0.3	− 5	+ 2
	321.3	−0.9	−23	− 8
	293.2	+1.9	−10	− 6
	265.1	+2.5	−25	− 4
	236.3	+2.6	− 1	+ 4
	212.7	+2.3	− 7	− 3
	187.8	+1.5	+ 8	− 1
104	189.2	+1.6	+10	− 3
	214.3	+2.4	− 4	− 3
	240.5	+2.8	− 2	− 1
	267.6	+2.7	−17	− 4
	295.1	+2.0	− 6	− 2
	323.2	+0.9	−10	− 1
	351.0	−0.3	− 8	− 1

105	343.2	−0.3	−18	−12
	316.7	+0.9	−8	−15
	290.7	+2.0	−7	−4
	265.3	−2.2	−22	(−20)
	240.3	+3.0	−7	−7
	216.5	+2.7	−4	−8
	193.8	+2.1	−5	−4
106	196.0	+ 2.2	+ 2	0
	219.1	+ 2.8	−13	−10
	242.4	+ 3.1	+ 1	+ 2
	265.9	+ 2.8	−25	− 4
	292.5	+ 2.0	− 7	− 5
	318.4	+ 0.9	−10	−11
	344.4	− 0.3	−10	− 2
107	348.8	+ 4.9	− 2	+ 3
	323.1	+ 6.9	− 5	+ 5
	297.4	+ 7.7	−17	−12
	271.9	+ 7.0	−12	− 1
	246.4	+ 4.9	+ 4	+ 9
	220.9	+ 2.0	− 1	+ 1
	195.3	− 1.3	− 3	− 4
108	193.6	− 1.5	+11	+ 2
	219.1	+ 1.8	− 4	0
	244.6	+ 4.8	− 4	− 1
	270.1	+ 6.9	−22	− 1
	295.3	+ 7.6	+ 4	+ 4
	321.1	+ 7.0	−23	− 3
	346.8	+ 5.1	− 1	+ 2
109	352.0	+ 6.4	−13	− 7
	326.2	+ 8.5	−21	−11
	300.1	+ 9.0	−12	− 8
	274.0	+ 7.8	− 7	− 7
	247.[illegible]	+ 5.0	−14	−11
	221.1	+ 1.1	−12	−11
	194.3	− 3.0	+ 9	− 2
110	352.8	+ 6.7	0	+ 3
	328.0	+ 8.6	−13	0
	302.9	+ 9.0	+ 3	+ 4
	277.7	+ 7.7	+ 3	0
	252.1	+ 5.0	+13	+ 3
	200.2	− 2.7	+12	+ 9

111	12.9										
	42.4										
	70.9										
	95.5										
	119.7										
	143.8										
	168.7										
112	358.0										
	330.3										
	301.9										
	273.5										
	245.6										
	216.1										
	191.4										
113	12.2										
	45.1										
	74.4										
	98.2										
	121.8										
	143.6										
	166.6										
114	157.7										
	137.6										
	118.0										
	98.1										
	76.6										
	53.5										
	16.2										
115	354.5										
	327.0										
	296.9										
	271.4										
	244.9										
	219.7										
	195.5										
116	18.5										
	49.0										
	76.0										
	99.8										
	121.5										
	142.2										
	160.1										

117	4.7	-	1.0	—	6	—	1		
	35.2	+	0.6	—	18	—	11		
	63.4	+	2.0	—	16	—	2		
	89.6	+	2.9	—	3	—	9		
	114.4	+	3.2	—	10	—	8		
	138.9	+	3.1	—	13	—	10		
	164.3	+	2.4	—	6	—	8		
118	37.7	+	0.4	+	2	+	1		
	65.8	+	0.5	+	0	+	1		
	92.6	+	0.6	+	7	+	9		
	118.6	+	0.5	+	10	+	4		
	141.5	+	0.4	+	0	+	9		
	169.5	+	0.3	—	5	+	7		
119	346.0	—	7.4	—	13	—	2		
	315.3	—	6.8	—	6	—	4		
	290.5	—	5.2	—	21	—	11		
	263.3	—	5.7	+	6	+	4		
	237.2	—	2.1	—	22	—	6		
	213.5	+	1.7	—	9	—	7		
	191.6	+	4.9	+	10	—	1		
120	352.2	+	3.5	—	7	—	3		
	21.2	+	2.8	—	9	—	4		
	49.2	+	1.5	—	12	—	6		
	69.8	+	0.4	—	28	(—	23)		
	96.8	—	1.2	—	10	—	4		
	123.9	—	2.4	—	2	—	4		
	151.6	—	3.0	+	13	—	3		
121	350.4	+	6.6	—	20	—	14		
	324.9	+	7.3	—	19	—	10		
	298.1	+	6.5	—	16	—	12		
	272.8	+	4.5	—	33	(—	20)		
	246.1	+	1.5	—	19	—	9		
	219.2	—	1.9	—	2	—	8		
	194.8	-	4.4	—	1	—	14		
122	197.2	—	4.2	—	1	—	1		
	224.7	—	1.0	—	11	—	9		
	251.6	+	2.4	+	1	—	9		
	278.1	+	5.2	—	9	+	4		
	304.3	+	7.0	+	8	—	7		
	330.0	+	7.4	—	13	—	2		
	355.0	+	6.5	—	19	—	9		

123	347.6	+ 5.1	− 6	− 1	
	322.9	+ 7.1	− 9	+ 3	
	298.2	+ 7.8	− 12	− 7	
	273.6	+ 7.3	− 10	− 7	
	249.0	+ 5.4	+ 1	− 6	
	224.8	+ 2.7	− 8	− 6	
	200.4	− 0.6	+ 3	− 2	
125	346.5	+ 4.5	− 10	− 9	
	321.7	+ 6.9	− 24	− 4	
	297.0	+ 8.1	− 13	− 9	
	272.5	+ 7.9	− 17	− 12	
	248.2	+ 6.3	− 11	− 12	
	199.6	+ 0.8	− 5	− 8	
126	351.4	− 0.6	− 15	− 8	
	323.1	+ 3.5	− 32	(− 23)	
	295.2	+ 5.5	− 17	− 14	
	268.0	+ 6.4	− 24	− 2	
	241.6	+ 6.0	− 5	− 4	
	216.0	+ 4.4	− 12	− 10	
	200.3	+ 3.0	− 9	− 8	
127	195.4	+ 2.6	+ 8	+ 3	
	220.2	+ 4.9	− 13	− 10	
	245.9	+ 6.3	− 14	− 11	
	272.3	+ 6.6	− 8	+ 3	
	299.4	+ 5.5	− 3	− 6	
	327.5	− 3.2	− 37	− 13	
	355.9	+ 0.1	− 15	− 8	
128	28.2	− 5.1	− 5	+ 3	
	61.5	− 2.0	− 9	− 4	
	91.5	+ 1.4	− 6	− 0	
	116.5	+ 4.3	+ 3	+ 3	
	143.8	+ 6.2	+ 4	− 4	
	170.0	+ 7.0	+ 9	+ 2	
	195.6	+ 6.4	+ 13	+ 2	
129	196.8	+ 6.8	+ 6	− 2	
	170.4	+ 6.6	+ 15	+ 9	
	145.3	+ 5.1	+ 12	+ 9	
	120.2	+ 2.8	− 12	− 9	
	93.4	− 0.3	− 3	− 5	
	63.4	− 3.5	− 3	+ 4	
	24.5	− 6.1	− 8	− 4	

130	16.7	−5.4	− 8	− 3
	48.7	−0.9	−10	− 4
	77.1	+3.5	−14	− 8
	102.1	+6.7	− 9	− 6
	124.9	+8.6	+ 4	+ 3
	146.9	+9.2	− 5	− 8
	169.8	+8.4	+11	+ 8
131	170.6	+8.4	+17	+ 2
	147.6	+9.2	− 1	− 2
	125.6	+8.6	− 3	− 1
	102.8	+6.8	−10	− 8
	77.9	+3.6	−10	− 4
	49.6	−0.8	− 4	− 1
	17.7	−5.3	−11	− 6
132	11.2	+3.5	− 4	− 7
	38.4	+5.0	− 9	− 5
	63.6	+5.5	−12	− 3
	87.2	+5.0	− 4	− 4
	110.7	+3.8	−11	− 9
	134.6	+1.9	− 4	− 6
	160.1	−0.4	+19	+10
133	156.9	−0.1	+ 2	− 9
	130.2	+2.4	+ 5	−12
	106.5	+4.1	− 6	− 2
	59.3	+5.6	−26	−17
	33.8	+4.9	−10	− 6
	6.3	+3.2	−10	−16
134	349.7	−5.3	−18	− 5
	322.0	−6.3	−11	− 6
	293.9	−5.8	− 8	0
	265.2	−3.8	+28	(+ 19)
	239.0	−1.1	−14	− 3
	214.6	+1.7	− 6	− 6
	192.1	+4.1	+ 6	− 4
135	190.0	+4.2	− 3	−13
	212.4	+2.0	− 8	− 4
	236.7	−0.8	−17	− 2
	262.7	−3.5	− 6	−11
	288.9	−5.4	+ 2	+ 8
	316.8	−6.2	−12	− 5
	344.6	−5.5	−18	− 6

136	350.0	−3.2	−5	−1
	323.8	−5.3	−8	−7
	296.8	−6.3	+3	+2
	270.1	−5.9	−8	−2
	243.9	−4.3	+1	+4
	219.3	−1.8	+4	+5
	196.2	+0.8	−1	−2
137	352.8	+4.7	−13	−8
	328.5	+2.3	−40	−16
	303.0	−0.7	−11	−4
	276.7	−3.5	−22	−14
	249.9	−5.6	−18	−10
	223.1	−6.4	−10	−9
	197.1	−5.9	−10	−8
138	194.2	−5.7	−4	−12
	219.7	−6.3	−6	−6
	245.4	−5.7	−10	−6
	272.2	−3.8	−17	−5
	298.6	−1.0	−11	−8
	325.1	+1.9	−29	−14
	349.4	+4.4	−13	−8
139	347.6	+4.8	−8	−3
	17.5	+3.2	+8	+5
	46.9	+0.8	−9	−4
	75.3	−1.6	−6	−3
	104.3	−3.6	−20	−5
	133.7	−4.7	+1	−1
	163.7	−4.4	−5	+2
140	15.4	−5.9	−9	−4
	48.8	−3.2	−1	0
	79.2	+0.2	−10	−9
	106.2	+3.4	−13	−10
	131.2	+5.6	+14	+4
	155.3	+6.9	0	−2
	179.9	+6.9	+6	−3
141	181.7	+6.9	+15	−2
	155.8	+6.9	−2	−3
	108.2	+2.5	−2	−4
	90.8	+0.4	−5	−4
	51.1	−3.0	−9	−3
	17.6	−5.7	−5	0

142	8?1	−5?2	−13	−	8
	41.9	−2.0	−19	−	9
	71.9	+1.5	−15	−	10
	98.7	+4.4	−11	−	8
	123.3	+6.3	+1		0
	147.1	+7.0	+6		6
	171.4	+6.6	+2		1
143	170.4	+6.5	+6	+	1
	145.7	+6.8	+1	−	2
	121.6	+6.0	−6	−	2
	96.7	+4.1	−1	−	5
	69.3	+1.2	−5	−	0
	39.1	−2.2	−14	−	12
	5.7	−5.2	−	−	3

1107

E N D